Metal Nanoparticles Catalyzed Oxidation of Amino Acids in Aqueous Solutions : A Kinetic Study

A THESIS

Submitted to the

University of Kota, Kota

for the Degree of

Doctor of Philosophy

In Chemistry

(Faculty of Science)

Submitted by

SHIKHA JAIN

Under the Supervision of

Dr. (Mrs.) Vijay Devra

Department of Chemistry

J. D. B. Govt. P.G. Girls College

Kota (Rajasthan)

2016

Dedicated to
My Parents
&
My Husband
Ankur

UNIVERSITY OF KOTA, KOTA

M. B. S. Marg, Near Kabir Circle, Rawatbhata Road, Kota (Raj.)

Certificate

It is to certify that,

(i) The thesis entitled ***"Metal Nanoparticles Catalyzed Oxidation of Amino Acids in Aqueous Solutions : A Kinetic Study"*** submitted by ***Shikha Jain*** is an original piece of research work carried out under my supervision.

(ii) Literary presentation is satisfactory and the thesis is in a form suitable for publication.

(iii) Work evidences the capacity of the candidate for critical examination and independent judgment.

(iv) Fulfills the requirement of the ordinance relating to the Ph.D. degree of the university.

(v) Candidate has put in at least 200 days of attendance every year.

Dr. (Mrs.) Vijay Devra
Department of Chemistry,
J. D. B. Govt. P. G. Girls College,
Kota (Raj.)

WORD OF GRATITUDE

A great teacher is simply one, who not only imparts knowledge to their students, but who awakens their in it and makes them eager to pursue it for themselves. Words shall fail to express the deep sense of gratitude and regards to my respected teacher and guide. I cannot forget the joy, the zeal, the zest, the pride and the privilege I always felt working under my guide ***Dr. (Mrs.) Vijay Devra, Senior Lecturer, J.D. B. Govt. Girls College, Kota, (Raj.).*** *She entrusted and instructed at every stage of my study. It is only because of her keen interest, scholarly guidance, perpetual encouragement and constant inspiration, alleviation of the practical difficulties at every step that the present work has been initiated, conducted and completed. I have only to say fortunate are those who get the opportunity to work under the guidance of such a learned guide and I have been so fortunate, I shall never be able to thank her adequately for all her co-operation and ineffable support.*

Shikha Jain

Acknowledgement

*I am grateful to numerous local and global **'Peers'** who have contributed towards the shaping of thesis. At the outset, I glorify and praise the Almighty **God** for his countless blessing which enabled me to complete this endeavor fruitfully and **Vandami to Shri 105 Gometeshwari Mataji** who poured her benediction on me. No words can express my profound and deep sense of gratitude to my supervisor **Dr. (Mrs.) Vijay Devra**, Department of Chemistry, J. D. B. Govt. Girls College, Kota for her exuberant knowledge, ungrudging guidance, consistent encouragement, eloquent talks and criticism throughout the period of my research work.*

*I am highly indebted to **Mrs. Jagriti Sharma,** Principal and **Dr. (Mrs.) Uma Sharma,** Head, Department of Chemistry, J. D. B. Govt. Girls College, Kota for encouragement, motivation, precious blessing and for extending facilities available in the college during the research work.*

*Heartfelt thanks are extended to **Dr. Naveen Mittal**, **Dr. Manju Bala Yadav** and **Dr. Shweta Saxena** and **all faculty members of J. D. B. Govt. Girls College, Kota,** whom have been very kind enough to extend their help at various phases of this research, whenever I approached them, and I do hereby acknowledge all of them. I am extremely grateful to **Prof. Ashu Rani** for their never ending enthusiasm, continuous flow of suggestions, excellent time management and constant encouragement throughout the course of this investigation. At this moment of accomplishment, I take this opportunity to sincerely acknowledge **Dr. Pankaj Kachhawah** for encouragement and support.*

*I am beholden to my seniors **Mrs. Shanu Mathur, Dr. Khusboo Shrivastava, Dr. Renu Hada, Dr. Stuti Katara** for their valuable suggestion in the experimental work and help during the entire research work. It gives me immense pleasure to acknowledge the affection, moral support, forbearance and all assistance rendered to me by my research Colleagues and friends **Ankita Jain, Niharika Nagar, Gajala Tazwer, Dhanraj Meena, Rajesh Meena, Priya Vijayvergiya, Lokesh Agarwal, Neha Jain.***

*I pay special thanks to my husband **Mr. Ankur Jain** (Senior Data Analyst) for his valuable suggestions, constant support and help during the research*

period. It is once against the mater of expressing emotions, feeling gratitude in available few limited words.

Inspiration always works behind every achievement. And I was blessed with a special guardian ***Angel-Mother (Late) Smt. Anita Jain,*** *who continuously inspired me in my memories with her moral, intellectual and physical education which resulted in form of my present success. There are no words for the painstaking efforts of my beloved father* ***Shri Gyan Chand Jain*** *and Grandmother* ***Smt. Shanti Jain*** *who has always remained the most prominent figure of inspiration at every step of my life. Their continuous encouragement, grace, love and blessing have inspired and sustained me throughout the period of my research. If my deeds could bring a little smile on his face it would be the precious moment for me. Words won't be enough to thank my Father-in-law* ***Shri Subhash Chand Jain,*** *mother-in-law* ***Smt. Suman lata Jain*** *for their unconditional support, love, blessings and prayers which made me tougher times to easier and are acts that could not be thanked by mere words. Their moral and friendly support brought this process of studies to culminate successfully.*

It is hard to find words acknowledge to my brother ***Arihant Jain****, sister* ***Mrs. Parul Jain*** *and jijosa* ***Mr. Parag Jain*** *and niece* ***Ridhi Jain*** *and I am deeply thankful to Sister-in law* ***Mrs. Neha Jain,*** *jijosa* ***Mr. Mandeep Jain****, nephews* ***Deval Jain****,* ***Aditya Jain*** *for their hearted Cooperation and love patience and constant encouragement which made it possible to reach my goal. I want to mention the affectionate and caring nature of my Bhuaji* ***Mrs. Renu Jain, Mrs. Pramila Jain, Mrs. Kusum Jain,*** *Nanaji* ***Sh. Rajendra Jain,*** *Naniji* ***Smt. Kiran Jain****, Mausiji* ***Smt. Sarita Jain, Smt. Krishna Jain, Smt. Garima Jain,*** *In-laws Nanaji* ***Sh. J. D. Jain****, Mausiji* ***Smt. Kusum Jain, Smt. Saroj Jain, Smt. Sudha Jain, Smt. Renu Jain****, which enabled me to complete this work and bringing happiness in our home and life.*

I wish to express my sincere thanks to ***USIC Department****,* ***University of Rajasthan, Jaipur and Dr. Banwari*** *for providing instrumentation facilities for sample analysis and also to* ***University Grant Commission, New Delhi through a Junior Research Fellowship*** *for financial support.*

Shikha Jain

CONTENTS

Chapter-1

Introduction

Abstract

The present chapter gives a review on the kinetics of the oxidation of amino acids in the presence of metal nanoparticles as catalyst. This review reports a brief discussion of mainly various transition metal nanoparticles and their applications in different reactions. A collection of several references is presented a general overview of amino acids and oxidants. The present introductory chapter is not intended to give a complete survey of all published work on oxidation catalysis but rather to gives a background and summary of recent important development in catalytic oxidation reactions in the presence of nanoparticles. The scope of the present work has been outlined at the end of this chapter.

1.1. Chemical Kinetics

Chemical Kinetics is a very important tool to better understand and describe a chemical process and its complexity. Now-a-days mathematical models developed from kinetic results are being used to describe the characteristics of a chemical reaction, in the design and modification of chemical reactors to optimize reaction conditions, product yield in low cost and more efficient environmental friendly pathways.Therefore, Chemical kinetics is not just an aspect of physical chemistry but it is a unifying topic covering the whole of chemistry, many aspects of biochemistry and pharmaceutical industries.

The present research describes the application of chemical kinetics to study the complex chemistry of biological systems. Emphasis is given on extensive experimental data collection, determination of standard kinetic quantities relating to rate of reaction, development of the mechanism describing the chemical steps in solution phase. The systems are catalytic as well as non-catalytic. Catalytic reactions proceeded by an alternative pathway of lower activation energy whereas non-catalytic reactions adopted ordinary oxidation – reduction pathways.

On the basis of the observation within the experimental limits, a suitable mechanism is proposed for every reaction. However a revision in the light of new data or other related information can further modify the presented mechanism [1]. Further product analysis and the stoichiometry under conditions as close as possible to those of the rate measurements are explored. The effect of pH and salt effects can further be investigated for extension of the present work.The present research study broadly includes oxidation of amino acid, a biologically important reaction in the synthesis of polypeptides, proteins and nucleotides [2]. Oxidation of neutral amino acids viz. serine, threonine, alanine and glycine is studied by peroxomonosulphate and peroxodisulphate in the presence of copper nanoparticles as a catalyst in acidic or aqueous medium. A Review of peroxomonosulphate and peroxodisulphate as oxidants, copper nanoparticles as a catalyst and oxidation of amino acids is presented in this chapter.

1.2. Metal Nanoparticles

Nanostructured materials derived from nanoparticles have evolved as a separate class of materials over the past decade. Metal nanoparticles have received a great scientific interest because of their high conductivity as compared to metal oxides. Metal nanoparticles [3] are defined as isolated particles between 1-100 nm diameters that do not represent a chemical compound with a metal-metal bond and a particular nuclearism. Due to this small size, nanoparticles have a large fraction of surface atoms, i.e. a high surface-to-volume ratio. This increases the surface energy compared with that of bulk material. The high surface-to-volume ratio together with size effects (quantum effects) gives nanoparticles distinctively different properties (chemical, electronic, optical, magnetic and mechanical) from those of bulk material [4-8]. Since nanoparticles have a large surface-to-volume ratio compared to bulk materials, they are attractive to use as catalysts [9, 10].

Research in nanomaterials has achieved considerable attention because of their unique properties and numerous applications in different areas [11, 12]. In past two decades, nanoparticles exhibit unique optical, electronic, photonic and catalytic properties [13-23] and explore their applications in electronics [24–26], catalysis [27, 28], sensors [29], optical and biological devices [30-33]. Major scientific interest targeting fabrication of metal nanoparticles of distinct shape and diminutive size has been developed in the recent years because of their exclusive properties as compared to their bulk materials [34-36]. Metal nanoparticles with variety of shape and size allow exploring their fascination applications in fields like catalysis, electronics, sensor, and optical device [37-39].The ability to synthesize metal nanoparticles with different shapes and sizes is important to explore their applications in electronics [40–42], optical and biological devices [43–46]. They have an ideal size for use as nanotechnologicalbuilding blocks [47].

1.3. Remarkable Properties of Nanoparticles

Nanoparticles exhibit following many unique properties, for which they are intensely being studied in a number of research fields[48]. The remarkable properties of nanoparticles describe in the brief by the following flow chart **(Figure 1.1).**

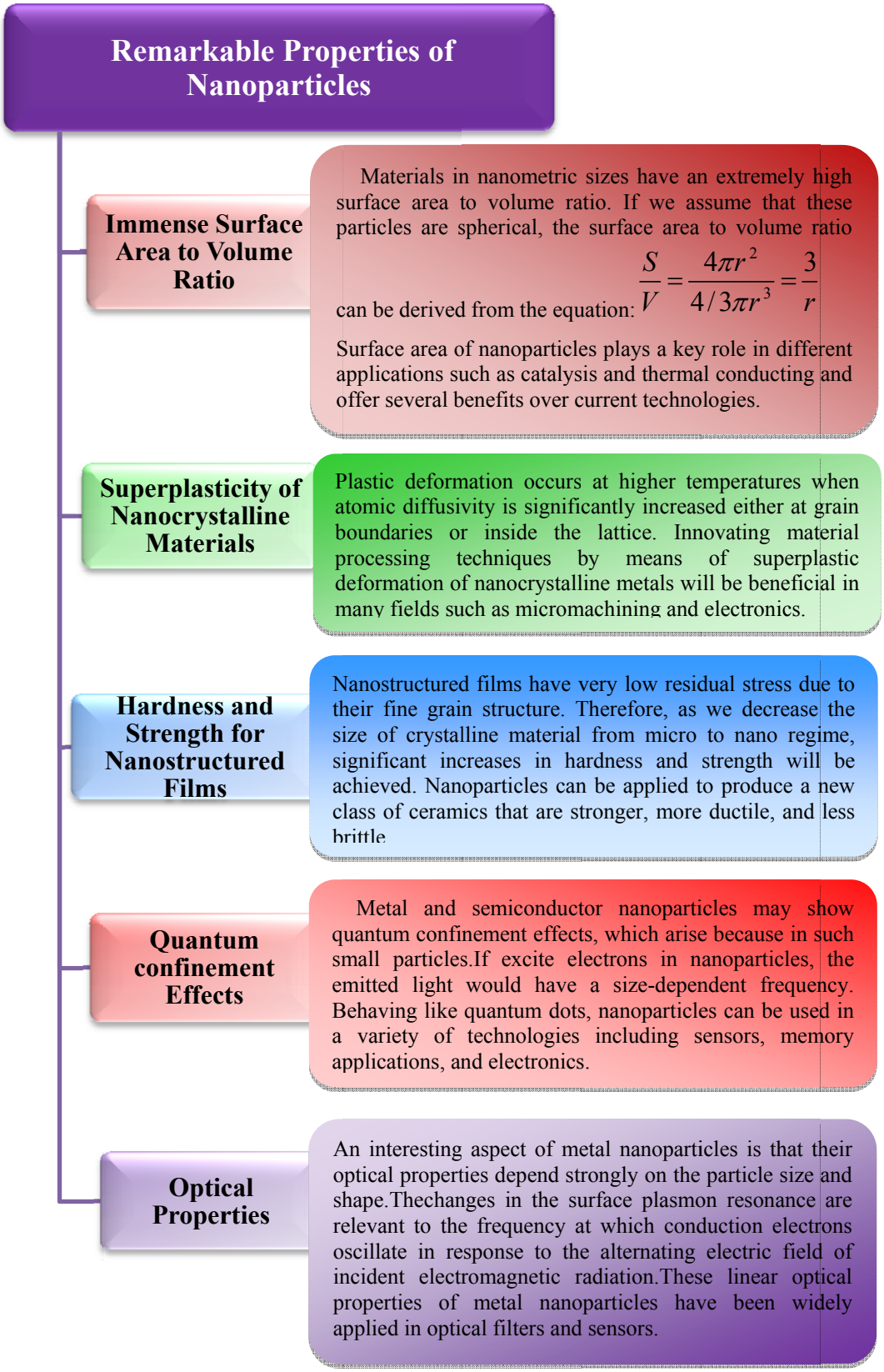

Figure 1.1: Flowchart of remarkable properties of metal nanoparticles

1.4. Classification of Nanocatalysis

The field of nanocatalysis has undergone an explosive growth during the past decade [49-52], two types of nanocatalysis can be distinguished, the homogeneous type with catalysis in colloidal solution [53-60] and the heterogeneous type in which the nanoparticles are supported on solid surfaces catalyzing gas-phase reactions [22, 61-72]. A heterogeneous catalyst in a solution-phase reaction may very well serveas a catalytic reservoir or 'resting state', from which molecular catalytic species are liberated for catalysis, and re-deposited after the completion of a catalytic cycle [73]."Naked" metal nanoparticles are unstable and tend to aggregate, agglomerate, and even precipitate out of solution and lose their catalytic activities. Therefore metal nanoparticles traditionally need to be supported on solid surfaces (*e.g.* oxide, carbon) [74] to form heterogeneous catalysts. However, they often have poor catalytic activity and selectivity compared to many homogeneous catalysts [75-77].

In homogeneous catalysis, transition metal nanoparticles in colloidal solutions are used as catalysts. In this type of catalysis, the colloidal transition metal nanoparticles are finely dispersed in an organic or aqueous solution, or a solvent mixture. The colloidal nanoparticle solutions must be stabilized in order to prevent aggregation of the nanoparticles and also to be good potential recyclable catalysts. Metal colloids are very efficient catalysts because a large number of atoms are present on the surface of the nanoparticles. Such catalytic systems are often called "quasi-homogeneous" nanoparticle catalysts. Quasi-homogeneous catalysts can have high catalytic activities and selectivities. They combine both the advantages and the challenges of homogeneous and heterogeneous catalysts as shown in **figure 1.2.** 'Quasi-homogeneous catalysis', a classification that has largely been accepted by the catalysis community, is used to describe catalytic processes that reside at the interface between the traditional protocols of homogeneous and heterogeneous catalysis [73]. This category of catalysts consists almost entirely of macroscopically homogeneous but microscopically heterogeneous dispersions of nanoparticles in fluids [78-80]. The catalytic studies reported in the present work can all be classified under the category of 'quasi-homogeneous nanocatalysis' i.e., they take place on metal nanoparticles surfaces in a solvated phase.

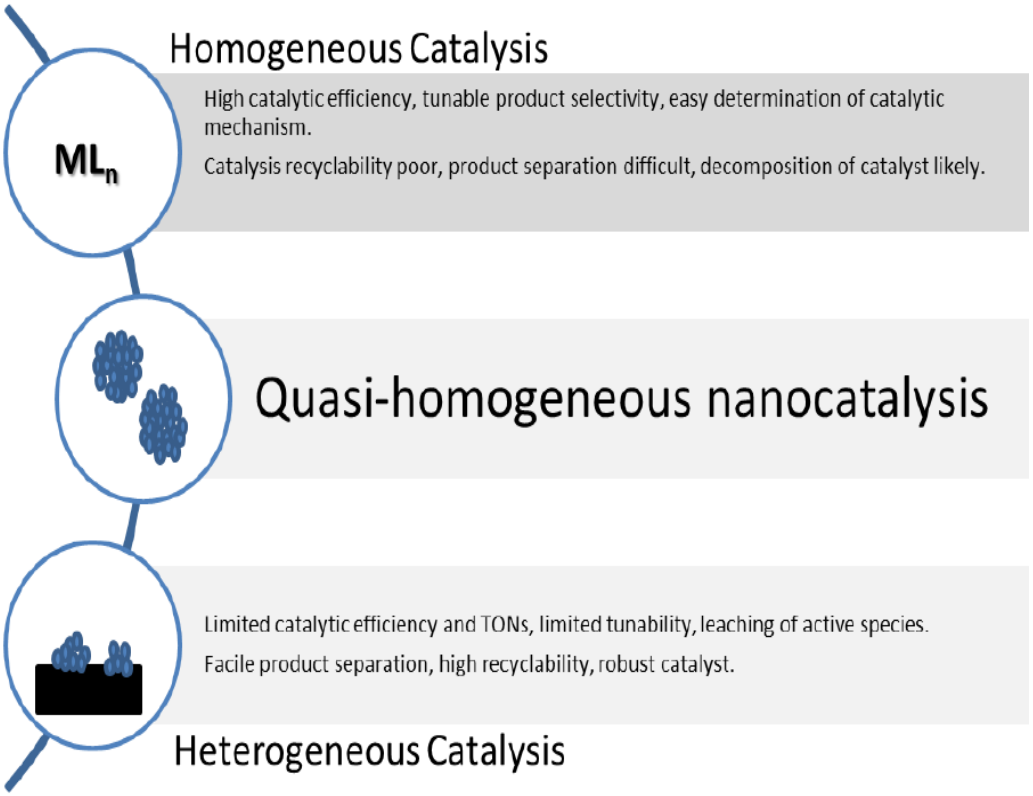

Figure 1.2: Homogeneous, heterogeneous, and quasi-homogeneous catalysis: a comparison

1.5. Role of the Transition Metal Nanoparticles in Catalysis

The catalytic activity of transition metals is mainly decided by their d-orbital properties and therefore metal type selection is the first choice for selectivity control. Mainly according to their catalytic behavior, we divided the frequently encountered metals nanoparticles in catalysis into five categories: (1) Ti, Zr, Nb, Mn, V, Cr, Mo and W; (2) Fe, Co and Ni; (3) Ru, Rh, Pt and Ir; (4) Pd; (5) Ag, Au and Cu.

1.5.1. Ti, V, Cr, Mn, Zr, Nb, Mo and W as Nanocatalyst

A major advantage of these early transition metal nanoparticles in catalysis is their cheap price. They exhibit weak hydrogenation ability and sometimes can be used in hydrogenation reactions. For example, Ti, Zr, Nb and Mn nanoparticles prepared in THF by K[BEt_3H] reduction from metal halide precursors [56]. The oxides of Mn, V, Cr and Mo are extensively used as nanocatalyst in the selective

oxidation of alkanes. Titanium nanoparticles have also been successfully utilized in catalyzing McMurry coupling reaction **(scheme 1.1).** For other substrates, such as benzaldehyde and acetophenone, similar activities and selectivities were observed [81].

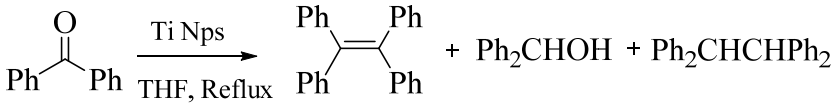

***Scheme 1.1: McMurry coupling reaction catalyzed by Ti nanoparticles* [81]**

1.5.2. Fe, Co and Ni as Nanocatalyst

Fe, Co and Ni are abundant and cheap elements, and are of great significance in catalysis. Recently, the potential of their metal nanoparticles as catalysts in quasi-homogenous mode has attracted increased attention. The catalysts are currently applied in reactions including hydrogenation, hydrosilation, and C–C coupling and oxidation reactions. Iron nanoparticles prepared by reducing iron ions with $LiBH_4$ in reverse micelle solutions. These Fe nanoparticles were active catalysts in the hydrogenolysis of Naphthyl bibenzyl methane [82]. Nickel nanoparticles with a size of about 45 nm were prepared from $Ni(CH_3COO)_2$ via hydrazine reduction in solvothermal process, which exhibit excellent activity and selectivity in the hydrogenation of nitrobenzene [83]. The Ni nanoparticles were also synthesized in ionic liquid phase through the decomposition of [bis(1,5-cyclooctadiene) nickel(0)] organometallic precursor. When applied in cyclohexene hydrogenation, the nanoparticles exhibit two orders of magnitude higher activities than traditional heterogeneous Ni-based catalyst [84]. Ni nanoparticles readily prepared by reduction of Nickel (II) chloride with lithium. These synthesized nanoparticles have been used in the transfer hydrogenation of carbonyl compounds. The reaction rate of the transfer hydrogenation was found to be dependent on the acetophenone and isopropanol concentration but independent on the amount of lithium chloride **(scheme 1.2).**

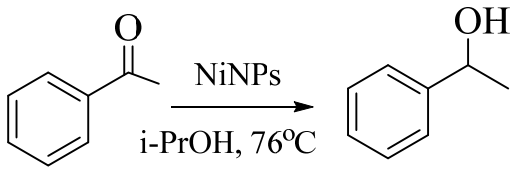

Scheme 1.2: Transfer Hydrogenation of Acetophenone in the presence of Ni nanoparticles **[85]**

Fe, Co and Ni based catalysts are widely used in oxidation reactions in industry. A simple example is the production of adipic acid, an indispensable intermediate compound for the synthesis of nylon-6 and nylon-66 from the oxidation of cyclohexane via Fe catalyst **(scheme 1.3).** On the contrary, Fe, Co or Ni based soluble nanoparticles under quasi-homogenous mode for oxidation reactions are seldom reported. The only available report came from Patin et al., who found that Fe nanoparticles prepared by reverse micro emulsion can catalyze the oxidation of cyclooctane with acceptable activity under mild conditions [86].

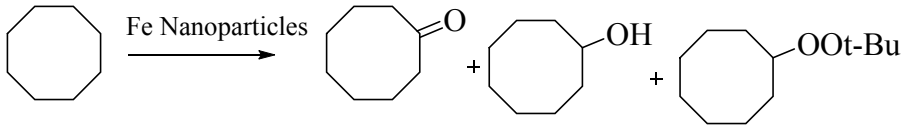

Scheme 1.3: Oxidation of Cyclooctane Catalyzed by Fe Nanoparticles in Reverse Microemulsions **[86]**

To conclude, Fe, Co and Ni nanoparticles are widely used in many kinds of reactions. Being paid much attention, these nanoparticles promises a lot for the catalytic reactions in solution phase in the future.

1.5.3. Ru, Rh, Pt and Ir as Nanocatalyst

These noble metals are typical catalysts with excellent hydrogenation ability. For the hydrogenation of C=C bonds, the activity of their metal nanoparticles usually follows the trend of Rh > Ru > Pt > Ir. This trend is similar to that observed in traditional heterogeneous catalysis. The hydrogenation of C=C bonds using these soluble nanoparticles is comparatively easy and there are numerous studies on this topic [87]. Rhodium (Rh) and Ruthenium (Ru) are the most active metals towards benzene hydrogenation [88, 89]. For the

hydrogenation of C=O bonds, Iridium (Ir), Platinum (Pt) and Ru exhibit excellent activity. Ozkar and Finke prepared Ir nanoparticles and used them for the hydrogenation of acetones [90] **(Scheme 1.4).** The authors pointed out that the typical temperature applied for this reaction under traditional supported catalyst is much higher, between 100 and 300^{o}C.

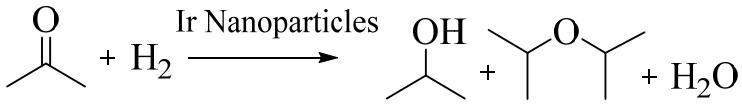

***Scheme 1.4: Selective hydrogenation of acetone catalyzed by Ir nanoparticles* [90]**

Oxidation reactions using these nanoparticles as catalysts have also been reported. For example, soluble Pt nanoparticles prepared in glycol, which displays good performance in the oxidation of both activated and non-activated alcohols including a wide range of aromatic alcohols, allylic alcohols, alicyclic alcohols, and primary and secondary aliphatic alcohols in water under aerobic conditions without using any bases [91]. Ru nanoparticles can also be utilized in oxidation reactions and under water/cyclooctene biphasic conditions; cyclohexane can be converted into cyclooctanone and cyclooctanol under mild conditions [92].

1.5.4. Pd as Nanocatalyst

Palladium (Pd) nanoparticles have excellent catalytic activity toward hydrogenation/dehydrogenation. The most intriguing aspect of Pd nanoparticles in hydrogenation reactions is its unique selectivity. It is well known that Pd can selectively catalyze the hydrogenation of alkynes and diene compounds into alkenes. For example, PVP stabilized Pd nanoparticles can catalyze the production of cyclopentene and cyclooctene from cyclopenta-1,3-diene and cycloocta-1,5-diene, respectively is reported [93]. The first Pd nanoparticles catalyzed Heck reaction was reported by Belleret et al. [94]. They prepared tetraoctylammonium bromide protected Pd nanoparticles which can catalyze the Heck type cross coupling reaction between ethyl acrylate and benzyl halides, as demonstrated **(Scheme 1.5).**

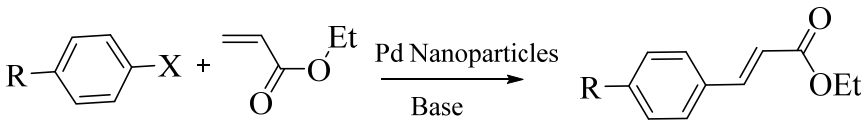

***Scheme 1.5: Heck reaction catalyzed by Pd nanoparticles* [94]**

1.5.5. Ag, Au and Cu as Nanocatalyst

Silver (Ag) nanoparticles are mainly used in oxidation / dehydrogenation reactions. Ag catalyzed epoxidation reaction is well known and widely applied in ethylene oxide production. Soluble Ag nanoparticles in ethanol/water mixture are superior catalysts relative to a conventional heterogeneous Ag catalyst **(Scheme 1.6)** [95]. Research concerning the catalytic properties of Gold (Au) nanoparticles is also focused on oxidation reactions. Current applications include oxidation of carbon monoxide into carbon dioxide and glucose into gluconic acid [96].

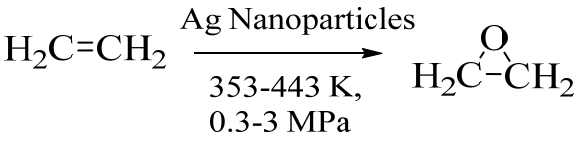

***Scheme 1.6: Epoxidation reaction of ethylene catalyzed by Ag nanoparticles* [95]**

Au and Ag nanoparticles can also effectively decompose $NaBH_4$, a potential hydrogen storage material, into H_2 and $NaBO_2$ [97, 98]. The Diels-Alder Ag nanoparticles catalyzed reaction supported the used of metal nanoparticles as catalyst. The use of the silver nanoparticle catalyst to form panduratin A is desirable because of the medicinal aspects as a drug, and reproducibility for further reactions [99].

Interest in **copper (Cu)** nanoparticles arises from the useful properties of this metal such as the good thermal and electrical conductivity at a cost much less than noble metals. This leads to potential application in cooling fluids for electronic systems [100] and conductive inks [101]. Due to plasmon surface resonance, copper nanoparticles exhibit enhanced nonlinear optical properties, which could result in many applications in optical devices and nonlinear optical materials, such as optical switches or photochromic glasses [21, 102-104].

Furthermore, in this last case, it is possible to expect an interesting effect coming from the depression of the melting temperature of a metal when it has the form of nanoparticles [105].

The catalytic activity of prepared **Cu** nanomaterials was tested in Ullman reaction for the synthesis of biphenyl from iodobenzene [106]. The morphology of prepared nanoparticles was investigated by analysis which clearly shows the spherical morphology of prepared **Cu** nanomaterials having a size around 50 nm **(Figure 1.3).**

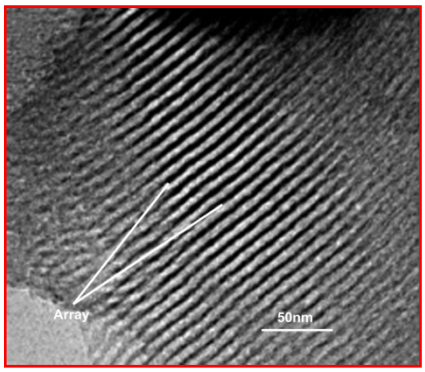

***Figure 1.3: TEM image of Cu nanoparticles* [106]**

The high surface area of small copper nanoparticles is effective in order to improve the rate of reaction. The study reports that the size as well as exposed surface area of the copper nanoparticles is responsible for the increase in yield of biphenyl up to 92%. This is higher compare to the 40% yield with the normal size copper powder under the same reaction condition [106-111] **(scheme 1.7).**

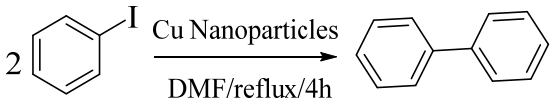

***Scheme 1.7: Synthesis of biphenyl from condensation of iodobenzene* [106]**

Copper (Cu) nanoparticles are usually used for redox reactions. For example, Vukojevic et al. found that **Cu** nanoparticles synthesized by the reduction of copper acetylacetonate with trialkylaluminum in THF were highly

active in methanol synthesis [112]. The copper nanoparticles have a narrow size distribution, and the size can be tuned in the range of 3–5 nm. When applied to methanol synthesis, the **Cu** nanoparticles exhibited notable activity at temperatures above 130^{o}C.

Under similar reaction conditions, their catalytic activity was comparable to that of commercialized Cu/ZnO catalyst. The author claimed that **Cu** nanoparticles are remarkably active catalysts in the quasi-homogeneous phase for methanol synthesis, considering that traditional catalyst requires a second component, generally zinc, to be active. However, this conclusion may not be convincing since it is highly possible that the copper nanoparticles incorporated with Al during the reduction process, as suggested by other researchers [113].

In industry, methyl formate (MF) is produced from methanol by carbonylation reaction catalyzed by a strong base such as CH_3ONa which is highly efficient but obviously not green. It leads to inevitable problems such as corrosion, byproduct formation and the possible deactivation of catalyst by CO_2 and H_2O impurities. Recently the **Cu** nanoparticles catalyzed synthesis of methyl formate in the absence of any base is discovered [114]. Three nanometer Cu nanoparticles is prepared from $NaBH_4$ reduction in methanol **(Scheme 1.8).** Further advances in improving MF productivity will potentially lead to a green substitute for the current industrial process that requires environmental unfriendly alkaline metal alkoxides as catalysts.

$$CO + CH_3OH \xrightarrow[353\text{-}443\ K,\ 0.3\text{-}3\ MPa]{Cu\ Nanoparticles} HCOOCH_3$$

***Scheme 1.8: Production of methyl formate from methanol carbonylation catalyzed by Cu nanoparticles* [114]**

Air-stable **copper** nanoclusters are good catalysts in the CuI-catalyzed cycloaddition of azides with terminal alkynes to give 1, 4-disubstituted 1, 2, 3-triazoles. No additional base or reducing agent is required **(scheme 1.9)** [115].

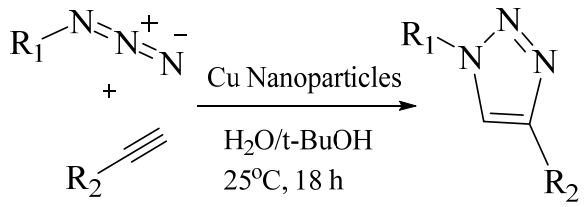

***Scheme 1.9: Copper clusters catalyze the cycloaddition of azides with terminal Alkynes* [115]**

Copper nanoparticles are known to act as excellent catalysts in reduction reactions [116-118]. For this purpose of testing the catalytic activity, chose an easy-to-follow model reaction, the reduction of p-nitrophenol to p-aminophenol using sodium borohydride as reducing agent, which has been employed before for evaluating the catalytic performance of noble-metal nanoparticles [119-124]. The copper nanoparticles showed excellent catalytic activity in the reductive degradation of Eosin B (EB) dye in just 16 sec of reaction time and maintained their catalytic activity when reused multiple times. Copper was found an attractive catalyst in the nanosize regimes. The copper nanoparticles are expected to be suitable alternative and play an imperative role in the fields of catalysis and environmental remediation [125].

For detailed information of current status of metal nanoparticles catalyzed reaction in aqueous medium is illustrated in **Table 1.1.**

1.6. Peroxo Oxidants

Peroxooxidants such as peroxomonosulphate (PMS), peroxomono-phosphate (PMP), peroxydisulphate (PDS) and peroxomonocarbonate (PMC) have gained paramount importance due to their utilization as auxiliary reagents in organic synthesis [150-153]. These peroxo oxidants are considered as the derivatives of hydrogen peroxide (H-O-O-H), formed by replacement of hydrogen atom by groups such as sulphate, phosphate and carbonate. There is a great variety of inorganic peroxo compounds possessing O–O group. The weak peroxide bond (–O-O-) makes the peroxides highly reactive with easily oxidizable molecules. The –O-O- linkage undergoes cleavage during the reaction and makes sensitive towards trace amount of catalysts and promoters, which can accelerate the decomposition.

Table 1.1

Metal Nanoparticles catalyzed Reactions in Aqueous Medium

S. No.	Nanocatalyst (Size)	Type of Reaction	Substrate	Product	Reaction Conditions	References
1.	Ni (1.75±1nm)	Hydrogenation	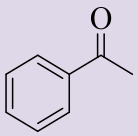	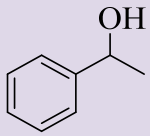	76°C	[85]
2.	Ni (45 nm)	Hydrogenation	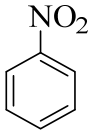	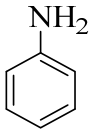	-	[83]
3.	Ru (~4nm)	Hydrogenation (Arene)	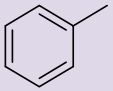	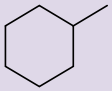	20°C, 1 atm., 24 h	[126]
4.	Ru (~4nm)	Oxidation		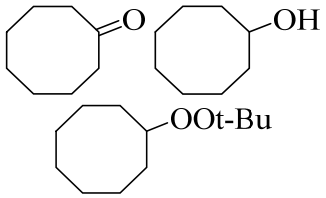	Mild condition	[92]
5.	Rh (2.0 nm)	Hydrogenation (C=C bond)	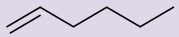		20°C, 20 atm.,	[127]

Table 1.1 Continued…

S. No.	Nanocatalyst (Size)	Type of Reaction	Substrate	Product	Reaction Conditions	References
6.	Rh (2.7 nm)	Dehalogenation /Hydrogenation	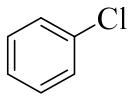		20°C, 10 atm., 1.7 h	[128]
7.	Pt (1.4±0.2 nm)	Hydrogenation (C=C bond)		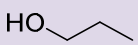	20±2°C	[129]
8.	Pt (1.8±0.6 nm)	Selective Hydrogenation	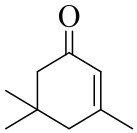	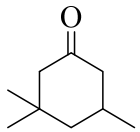	r.t., 2 atm., 8h	[130]
9.	Pt (2-8 nm)	Enantioselective Hydrogenation	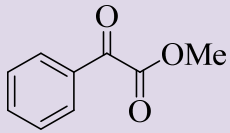	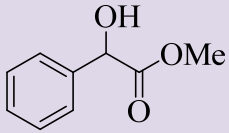	Mild condition	[131]
10.	Pt (1.5±0.2 nm)	Oxidation	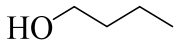	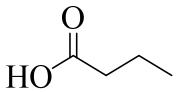	80°C, 1.0 atm., 24 h	[132]
11.	Pt (2-8 nm)	Oxidation	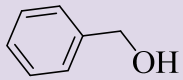	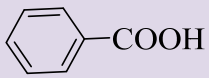	80°C, O_2 as Oxidant, 8 h	[133]
12.	Ir (10 nm)	Oxidation	H_2NCH_2COOH	HCOCOOH	35±0.1°C	[227]

Table 1.1 Continued…

S. No.	Nanocatalyst (Size)	Type of Reaction	Substrate	Product	Reaction Conditions	References
13.	Pd (2-8 nm)	Hydrogenation (C=O bond)	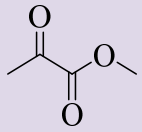	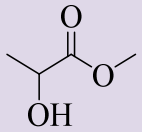	27°C, 50 atm., 12 h	[134]
14.	Pd (2-6 nm)	Heck C-C Coupling	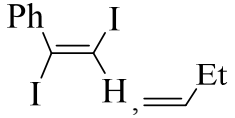	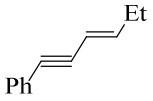	80°C, 6 h	[135]
15.	Pd (7-10 nm)	Still Coupling	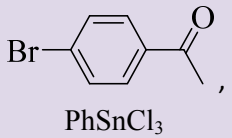 $PhSnCl_3$	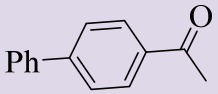	80°C, 2 h	[136, 137]
16.	Pd (15-20 nm)	Sonogashira C-C Coupling	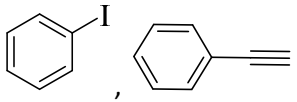		80°C, 2 h	[138]
17.	Pd (2.3±0.2 nm)	Suzuki C-C Coupling	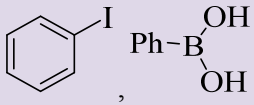		25°C, 6 h	[139]
18.	Pd (9.7 nm)	Hiyama C-C Coupling	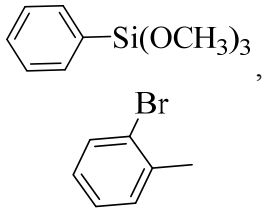	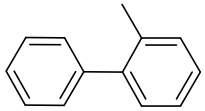	90°C, 3 h	[140]

Table 1.1 Continued…

S. No.	Nanocatalyst (Size)	Type of Reaction	Substrate	Product	Reaction Conditions	References
19.	Pd (2.3±0.7 nm)	Oxidation	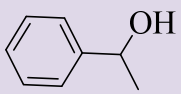	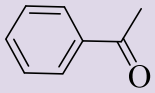	pH=7, 100°C, 1 atm. O_2, 2 h	[141]
20.	Au (6.7±0.9 nm)	Hydrogenation (nitro group)	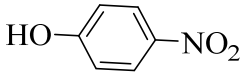	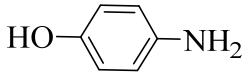	20 min.	[142]
21.	Au (1.0 nm)	Suzuki C-C Coupling	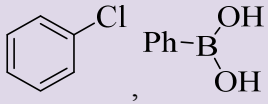	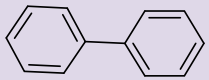	80°C, air, 4 h	[143]
22.	Au (1.1±0.2 nm)	Oxidation	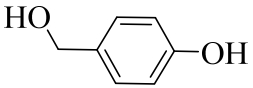	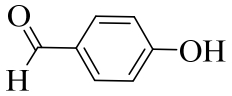	27°C, air, 6 h	[144]
23.	Ag (2-4 nm)	Hydrogenation (nitro group)	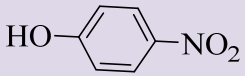	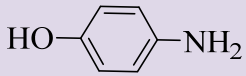	23-24°C, air, 0. 1 h	[145]
24.	Ag (25 nm)	Oxidation	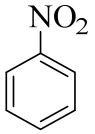	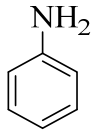	-	[146]
25.	Ag (10-20 nm)	Polymerization	$C_{18}H_{37}SiH_3.H_2O$	Polymer microspheres	90 min., 1 atm.	[147]

Table 1.1 Continued…

S. No.	Nanocatalyst (Size)	Type of Reaction	Substrate	Product	Reaction Conditions	References
26.	Cu (4-6 nm)	Other coupling	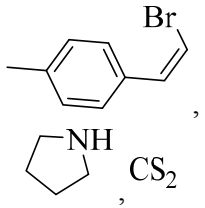	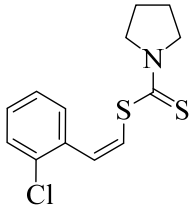	100°C, reflux, 7 h	[148]
27.	Cu (4.3±0.6 nm)	Phenyl-Selenylation	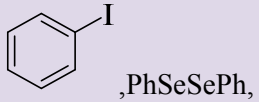	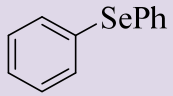	100°C, 10 h	[149]
28.	Cu (8 nm)	Ullman Reaction	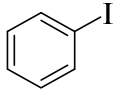	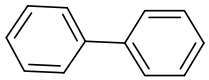	200°C, 5h	[108]
29.	Cu (50 nm)	Ullman Reaction	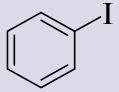	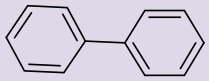	200°C	[106]
30.	Cu (4.15 nm)	Cycloaddition	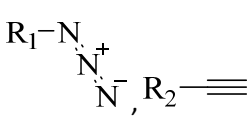	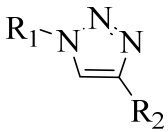	25°C, 18 h	[115]
31.	Cu (30-80 nm)	reduction	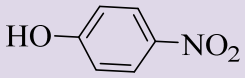	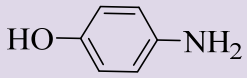	Room temp.	[124]
32.	Cu (6 nm)	Oxidation	Amino Acids	Hydroxyl Amine	30°C	[235]

1.6.1. Peroxomonosulphate (PMS)

Peroxomonosulphate (PMS) is a derivative of hydrogen peroxide, replacing one of the hydrogen atoms in H_2O_2 by sulphate group. Peroxomonosulphuric acid is commonly known as Caro's acid. Peroxomonosulphuric acid is a dibasic acid having two ionisable protons in which one proton is highly acidic and the second is weakly acidic. Its first pKa value is equivalent to that of sulphuric acid (3 ± 0.1) and the second pKa value is 9.4 ± 0.2 [154]. IR studies revealed that the O-O stretching frequency is higher than that of H_2O_2 and the two OH groups are structurally different [155]. Hence, PMS will exist as HSO_5^- at pH 4.0. The structure of HSO_5^- is shown by **figure 1.4.**

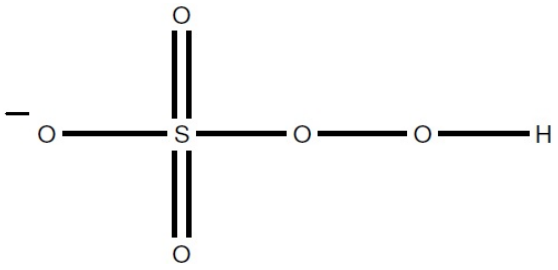

Figure 1.4: Molecular structure of HSO_5^-

Peroxomonosulphate has high oxidation potential (-1.8 V) [156-158] and propensity to react through oxygen transfer [159-161] make this molecule as a favourable one for the oxidation of various organic compounds in aqueous solution. Hence, it has gained importance as one of the potential oxidants for organic compounds. It has also been proved to be a strong oxidizing agent compared to other peroxo oxidants like peroxodisulphate and peroxomono-phosphoric acid [162-164].

The potentiality of PMS as a powerful oxidant is brought by its ability to oxidize many organic and inorganic compounds [165]. The use of PMS is very common in organic reactions [166, 167] **(scheme 1.10).** There are several interesting reactions of PMS for example oxidation of alkanes [168], phase-transfer catalysis in the free-radical polymerization of acrylonitrile [169] and catalytic oxidations of amino acids [170] and citrate ion [171].

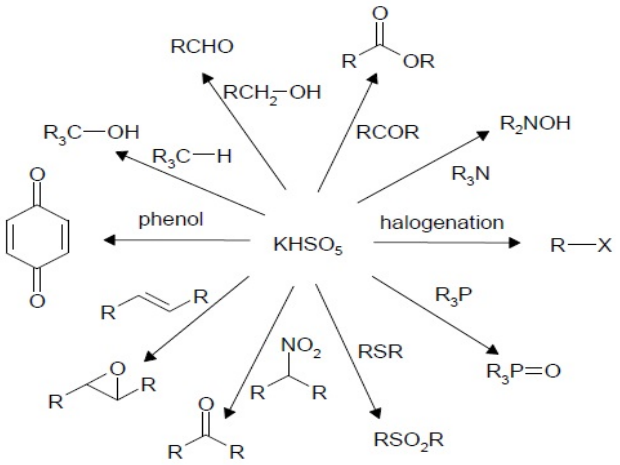

***Scheme 1.10: Examples of the organic oxidation reactions with PMS* [172]**

The predominant reactive species of PMS in acidic medium is HSO_5^- and it is more reactive than SO_5^{2-}. The higher reactivity of HSO_5^- is due to both electrostatic effect and weakening of peroxide bond by the proton. The HSO_5^- frequently acts as a two electron oxidant in redox reactions that involve heterolytic cleavage of peroxo bond [173, 174].

1.6.2. Peroxodisulphate (PDS)

Peroxodisulphate are the most chemically active of the peroxygens, with great utility in a variety of chemical processes. The term peroxydisulphate is used by chemical abstract although the international union of pure and applied chemistry (IUPAC) has recommended the name Peroxodisulphate, the trivial names; persulphate, peroxodisulphate and peroxydisulphate were used in the literature [175-178]. The Peroxodisulphate group consists of two sulphate groups linked by a covalent bond between two oxygen atoms, the distance between these two oxygen atoms is 1.46A^o, the distance S-O is 1.50A^o, while S-O-O inter bond angle is 128^o and the axis of symmetry is pass through the mid-point between the central oxygen atoms. This was approved by the results of Raman spectra of sodium and ammonium peroxodisulphate [179] **(Figure 1.5).**

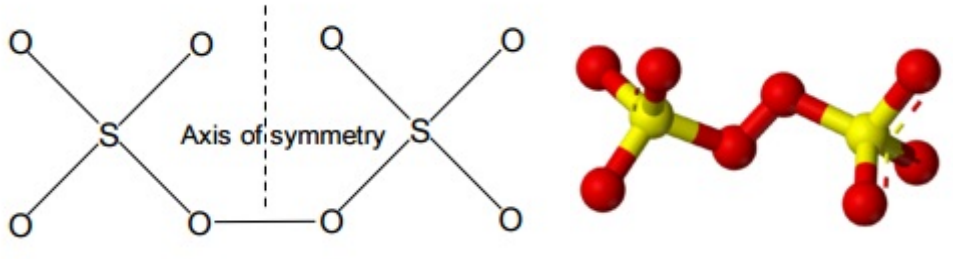

Figure 1.5: Structure of peroxodisulphate group

Peroxydisulphuric acid is also considered as an oxidizing agent, peroxodisulphate ion, ($S_2O_8^{2-}$) is an excellent and versatile oxidant for a variety of organic and inorganic compounds. The peroxodisulphate ion is one of the strongest oxidizing agents known in aqueous solution. The standard oxidation reduction potential for the following reaction is estimated to be - 2.01 volts **(equation 1)** [180].

$$2\ SO_4^{2-} \longrightarrow S_2O_8^{2-} + 2e^- \qquad (1)$$

Many peroxodisulphate oxidations have been studied kinetically [181]. The reaction between the peroxodisulphate ion [182] and the formate ion has been previously investigated [183-185]. Its utility as an oxidizing agent for various substrates is derived from its ability to oxidize in acidic, neutral, and alkaline media [181]. It has industrial importance as a polymerization activator, e.g., in production of polystyrene [186]. The decomposition of persulphate in aqueous solution involves the reactions **(Equation 2, 3, 4)** [187].

Neutral solution,

$$S_2O_8^{2-} + H_2O \longrightarrow 2HSO_4^- + \tfrac{1}{2}\ O_2 \qquad (2)$$

Alkaline solution,

$$S_2O_8^{2-} + H_2O \longrightarrow HSO_4^- + \tfrac{1}{2}\ O_2 \qquad (3)$$

Dilute acid solution,

$$S_2O_8^{2-} + 2H_2O \longrightarrow 2HSO_4^- + H_2O_2 \qquad (4)$$

The following equations represent the hydrolysis of peroxodisulphate ion in neutral solution, alkaline solution, and acidic solution, respectively. An acid catalyzed reaction is involving the unsymmetrical rupture of the O-O bond of the $H_2S_2O_8$ ion to form oxygen and sulfur tetroxide.

Reactions involving this ion are however, generally slow at ordinary temperatures, but are catalysed by adding transition metal ions [188-199] and catalytic effects of both cupric and silver ions were examined. The kinetics and mechanism of the oxidation of inorganic and organic substrates by peroxodisulphate under both catalysed and uncatalyzed conditions have received considerable attention in recent years [175, 180]. Peroxodisulphate are desirable oxidizing agent because their products pose little or no threat to human or animal life [200], and are nontoxic to the environment.

1.7. Amino Acids

Amino acids exhibit acidic as well as basic properties, i.e., they are amphoteric in character. It has been shown that neutral amino acids exist as inner salts with the dipolar structure as $RCHH_3^+NCOO^-$. These are called "Zwitter ions". This is the form that amino acids exist in even in the solid state. If we dissolve the amino acid in water, a simple solution also contains this ion. Amino acids are known to exist in the following equilibrium in aqueous solutions **(equation 5, 6).**

$$RCHNH_2COOH \rightleftharpoons RCHNH_2COO^- + H^+ \rightleftharpoons RCH\overset{+}{N}H_3COO^- \qquad (5)$$

The dissociation of these acids is pH dependent

$$RCH\overset{+}{N}H_3COOH \underset{+H^+}{\overset{-H^+}{\rightleftharpoons}} RCH\overset{+}{N}H_3COO^- \underset{+H^+}{\overset{-H^+}{\rightleftharpoons}} RCHNH_2COO^- \qquad (6)$$

Cation Zwitter ion Anion

In pure water, amino acid exists as zwitter ions but in more acidic solutions it behaves as a base and in alkaline solutions zwitter ions behaves as a

weak acid. The pH of the dilute solution of zwitter ions is determined by its basic strength and acidic strengths as in **equation 7.**

$$pH = \frac{pK_{a1} + pK_{a2}}{2} \quad (7)$$

Where pK_{a1} and pK_{a2} are the acid dissociation constant of its basic and acidic groups respectively. For alanine pKa_1 and pKa_2 are 2.35 and 9.78 respectively, the pH of the dilute solution of alanine comes out to be 6.11.This pH 6.11 is the isoionic point of alanine where the number of negative charges on the molecule produced by protolysis equals the number of positive charges required by the gain of protons. Since the alanine molecule at this pH does not carry any net charge and is electrophoretically mobile, this point is also known as isoelectric point.

Amino acids not only act as the building blocks in protein synthesis, but they also play a significant role in metabolism. Amino acids can undergo many types of reaction depending on whether a particular amino acid contains nonpolar groups or polar substituents. The oxidation of amino acids is of interest as the oxidation products differ for different oxidants [201]. Thus, the study of amino acids becomes important because of their biological significance and selectivity toward the oxidant.

1.8. Oxidation of Amino Acids

Oxidation reactions of α-amino acids (AA) are one of the most relevant biochemical reactions because such reactions serve as models for protein oxidations [202-204]. Also, uncharacterized oxidation reactions of α-amino acids involving a wide range of oxidants are of particular concern in biotechnology and medicine. Simple amino acids present in municipal waste waters cause serious eutrophication in water bodies. Pharm industries dealing with biochemical and tanneries are some of the major sources of waste waters containing amino acids [205]. It is essential to remove or oxidatively degrade the dissolved amino acids from waste waters. Non enzymatic model oxidation reactions involving α – amino acids and a wide variety of oxidants are reported plenty in literature [206-209]. Kinetics and mechanism of decarboxylation of α-amino acids by peroxo oxidants

is an area of intensive research because peroxo oxidants are environmentally benign oxidants and do not produce toxic compounds during their reduction.

The kinetics of the silver ion catalyzed oxidation of dl(α) alanine and glycine [210, 211] by peroxodisulphate was studied. The reaction was first order with respect to peroxodisulphate and silver ion concentration and was almost independent of alanine and glycine concentration. In addition, neutral salt effect is investigated which shows a negative salt effect. Aldehyde was formed through radical intermediates during oxidative decarboxylation of amino acids by peroxodisulphate is reported in literature [212, 213]. This reaction was considered as a model system to understand the catalysis by monoamine oxidase [214, 215].

In the study of kinetics and mechanism of the oxidation of α-amino acids by peroxomonosulphate in acetic acid/sodium acetate buffered medium (pH 3.6 – 5.2) [216-218] and observed that SO_5^{2-} was more reactive (six orders of magnitude higher than HSO_5^-) and this higher reactivity was attributed to nucleophilic attack of peroxide on the amino group. In spite of, the kinetics of oxidation of amino acids by peroxomonosulphate in aqueous alkaline medium and observed that the electrophilic attack on HSO_5^- occurred at the amino acid nitrogen is reported [219]. The breakdown of the intermediate was influenced by the nature of the substituent on the amino carbon atom. The intermediate disintegrated to give either imine or imino acids, which hydrolyzed to the corresponding aldehyde. A systematic kinetic study on the copper (II) catalyzed oxidation of histidine by peroxomonosulphate (PMS) in acetic acid sodium acetate buffered medium (pH 3.6-4.8) and the catalytic effect of copper(II) was investigated [220, 221]. Some selective oxidation reactions are reported involving transition metal ions of Cr, Ag, Rh, etc. are reported to act as catalyst for amino acids oxidation [207, 222, 223]. With the emergence of metal nanoparticles possessing appreciable stability and high surface area per particle, their potential use as catalyst for organic biochemical relevant reactions [224, 225].

Noble metal nanoparticles with high specific catalytic activity are ubiquitous in modern synthetic organic chemistry during the recent decades.

However how to reduce their dosage is one of the most exiting challenges due to the limited reserves of noble metals. The catalytic activity of colloidal iridium nanoparticles was evaluated in some oxidation reactions like amino acids-hexacyanoferrate (III) redox system in alkaline medium **(scheme 1.6).** These iridium nanoparticles show a better catalytic activity than an equal amount of iridium precursor. Easy recovery of the catalyst from the reaction mixture shows another positive significance [226, 227]. Superior catalytic activities of nanoparticle-based catalytic systems than the corresponding bulk materials and recycling of metal nanoparticles are helpful in reducing the raw material costs and engineering a greener process via limiting the amount of waste chemicals for disposal.

The catalytic activity of surfactant stabilized Au and Ag nanoparticles for the oxidation of an amino acid, L-leucine, was studied using hydrogen peroxide as the oxidant [228]. The Au and Ag nanoparticle catalysts exhibited very good catalytic activity and the kinetics of the reaction was found to be pseudo-first order with respect to the amino acid. In particular, optimal oxidant and catalyst concentrations were determined. Very high concentrations of the metal nano-catalysts or the oxidant led to a dramatic increase in reaction rate. Moreover, bimetallic Au-Ag catalysts provided higher selectivity than pure Au or Ag.

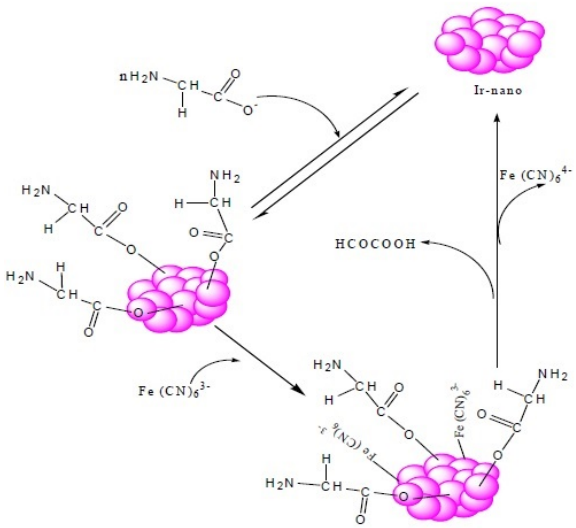

***Scheme 1.6: Proposed catalytic cycle of the oxidation of glycine in the presence of iridium nanoparticles* [227]**

For the exposure of metal nanoparticles possessing appreciable stability and high surface area per particle, their prospective use as catalyst for organic biochemical relevant reactions stands well documented in recent years [225, 229]. The metal nanoparticles of cheap, cost effective and abundant transition metals like Cu, when used as catalysts are expected to produce ecofriendly process enroutes [230-234]. The synthesized copper nanoparticles are used as catalyst for the oxidation of free α-amino acids by peroxomonosulphate (PMS) in aqueous medium [235]. The products N-hydroxylated amino acids are identified using TLC and FT-IR spectra. For constant concentration of copper nanoparticles catalyst constant the trend in the oxidation of free α-amino acids is alanine> glycine>leucine>valine> phenylalanine>serine. Pseudo first order rate coefficient values are used to investigate the catalytic activity of copper nanoparticles.

In the light of all reported observations on amino acid oxidation, very few attempts have been made so far on the oxidative deamination of amino acid in presence of metal nanoparticles [227]. Copper is particularly an interesting transition metal catalyst. It is well known for promoting organic transformation [236-241]. But in literature the use of copper nanoparticles in the oxidations reaction of amino acid by peroxo oxidants is scanty. Thus an attempt has been made to study the catalytic effect of colloidal copper nanoparticles in the oxidation of amino acids by peroxo oxidants in aqueous/acidic medium. The colloidal dispersion of copper nanoparticles was synthesized by chemical reduction method. The synthesis of size controlled copper nanoparticles through a simple one phase aqueous route using ascorbic acid as reducing and capping agent and evaluate the catalytic activity of the synthesized copper nanoparticles on the oxidation of amino acid by peroxomonosulphate and peroxodisulphate (abbreviated as PMS and PDS). The catalytic activities of these particles at different sizes have been investigated on the oxidation of amino acids. The present study aims at further exploring the oxidation of few neutral amino acids by peroxomonosulphate or peroxodisulphate in catalytic and non-catalytic pathways as well as plausible oxidative mechanism in the presence of copper nanoparticles. This work an attempt has been made to construct a model.

1.9. Scope of the Work

Research involving metal nanoparticle catalysts has attracted a great deal of attention and gained numerous achievements in the past years. This study has revealed that at a certain point of their growth the particles become catalytic and the growing particles are more catalytic than bulk metal. In order to maximize their usefulness, reliable synthesis are required that can generate well-defined nanoparticles with a high degree of monodispersity. The synthesis of copper nanoparticles was carried out with specific attention to their future use. This aim is being achieved in the synthesis of copper nanoparticles by using green chemical reduction method with control the synthesis. The aqueous reduction method is widely selected for the synthesis of copper nanoparticles because it is robust, cost effective, and efficient in yield. This enables properties such as the size, shape, solubility and surface functionality of the resulting nanoparticles to be carefully tuned. The diameter of the relatively monodisperse copper nanoparticles could be controlled in the range of approximately 12–55 nm by varying the concentration of reducing agent, with smaller nanoparticles obtained for higher L-ascorbic acid content, because in this case more small nuclei can apparently become stabilized. This means that this method allows for the formation of copper nanoparticles of variable size that are stable under ambient conditions, something that is typically not achieved by simple chemical approaches. Such materials are being explored for many different applications, especially in catalysis.

The current research work represents the development of innovative methodology of synthesis of stable metal nanoparticles and their application in the oxidation reactions of amino acids with the detail study of quasi homogeneous catalytic oxidation kinetics. Oxidation of amino acids is of great importance both from the chemical point of view and its bearing on the mechanism of amino acids metabolism. The influence of various operating conditions viz. concentration variation of amino acid, oxidants, catalyst and the size of nanocatalyst, temperature etc. are investigated during the reaction. Surpassing catalytic activities of nanoparticle-based catalytic systems than the corresponding bulk materials are helpful in reducing the raw material costs and engineering a greener process via limiting the amount of waste chemicals for disposal.

Thus precise understanding of mechanism of such biological redox reaction is important as it helps in the synthesis of specific reaction products. Hence, in the case of highly active and selective synthesized catalysts towards oxidation reactions, the optimal conditions of experimental parameters are essential. This catalyst can replace industrial scale conventional, costly catalysts such as other noble metals. The metal nanoparticles field is presently burgeoning, and it is anticipated that these key challenges will be met in the close future, and that this area of nanoscience will be much more applied in tomorrow's laboratory and industry.

1.10. References

[1] J. H. Espenson, ***Chem. Kinetics and Reaction Mechanism, Mcgraw-Hill Book Company, 1981;*** K. J. Laidler, ***Chemical Kinetics, 2nd edn., Mcgraw-Hill Book Company, New York, 1965;*** C. H. Bamford and C. H. F. Tipper, ***Comprehensive Chem. Kinetics, Elsevier Scientific Publishing Co. Inc, New York, 1965;*** R. G. Wilkins, ***The study of Kinetics and Mechanism of Reactions of Transition Metal Complexes, Allyn and Bacon, Inc. Boston, 1974;*** S. W. Benson, ***The Foundations of Chemical Kinetics, Mcgraw-Hill Book Company, NewYork, 1960.***

[2] H. D. Jakubke and H. Jersehkeit, ***Amino acids, Peptides and Proteins***, ***Wiley, New York, 1977;*** H. C. Freeman, ***Adu. Protein Chem.,*** 22 (1967) 258.

[3] L. N. Lewis, ***Chem. Rev.,*** 93 (1993) 2693.

[4] M. A. El-Sayed, ***Accounts of Chemical Research,*** 34 (2001) 257.

[5] M. C. Daniel, D. Astruc, ***Chemical Reviews***, 104 (2004) 293.

[6] C. Burda, X. B. Chen, R. Narayanan, M. A. El-Sayed, ***Chemical Reviews***, 105 (2005)1025.

[7] M. A. El-Sayed, ***Accounts of Chemical Research,*** 37 (2004) 326.

[8] A. P. Alivisatos, ***Journal of Physical Chemistry***, 100 (1996) 13226.

[9] A. S. Bruss, M. A. Gelesky, G. Machado, J. Dupont, ***J. of Molecular Catalysis A***, 252 (2006) 212.

[10] A. A. Firooz, A. R. Mahjoub, and A. A. Khodadadi, ***World Academy of Science, Engineering and Technology,*** 76 (2011) 138.

[11] A. Tiwari, S. K. Shukla, (Ed.), ***In Advanced Carbon Materials and Technology, WILEY-Scrivener Publishing LLC, USA, 2014;*** A. Tiwari, ***Adv. Mat. Lett.,*** 3 (2012) 1.

[12] P. Singh, A. Katyal, R. Kalra, R. Chandra, ***Tetrahedron Lett.,*** 49 (2008) 727; A. Tiwari, A. K. Mishra, H. Kobayashi, A. P. F. Turner, ***In Intelligent Nanomaterials, WILEY-Scrivener Publishing LLC, USA, 2012.***

[13] X. Liu, B. Geng, Q. Du, J. Ma, X. Liu, ***Material science and engineering A,*** 448 (2007) 7.

[14] S. Sun, C. B. Murry, D. Weller, L. Folks, A. Moster, ***Science,*** 287 (2000) 1989.

[15] J. F. Wang, M. S. Gudiksen, X. F. Duan, Cui, Y.C.M. Lieber, ***Science,*** 293 (2001) 1455.

[16] L. L. Beecroft, C. K. Ober, ***Chem. Mater.***, 9 (1997) 1302.

[17] J. H. Fendler, ***Chem. Rev.,*** 87 (1987) 877.

[18] B. C. Gates, ***Chem. Rev.,*** 95 (1995) 511.

[19] P. V. Kamat, ***Chem. Rev.,*** 93 (1993) 267.

[20] L. N. Lewis, ***Chem. Rev.,*** 93 (1993) 2693.

[21] G. Schmid, ***Chem. Rev.,*** 92 (1992) 1709.

[22] N. Toshima, T. Yonezawa, ***New J. Chem.***, 22 (1998) 1179.

[23] T. M. D. Dang, T. T. T. Le, E. Fribourg-Blanc, M. C. Dang, ***Adv. Nat. Sci: Nanosci. Nanotechnol.,*** 2 (2011) 015009.

[24] B. K. Park, D. Kim, S. Jeong, J. Moon, J. S. Kim, ***Thin Solid Films,*** 515 (2007) 7706.

[25] N. A. Luechinger, E. K. Athanassiou, W. J. Stark, ***Nanotechnology,*** 19 (2008) 445201.

[26] Y. Lee, J. Choi, K. J. Lee, N. E. Stott, D. Kim, ***Nanotechnology,*** 19 (2008) 415604.

[27] A. Sarkar, T. Mukherjee, S. Kapoor, ***J. Phys. Chem. C,*** 112 (2008) 3334.

[28] B. C. Ranu, A. Saha, R. Jana, ***Adv. Synth. Catal.,*** 349 (2007) 2690.

[29] E. K. Athanassiou, R. N. Grass, W. J. Stark, ***Nanotechnology,*** 17 (2006) 1668.

[30] Y. Leroux, J. C. Lacroix, C. Fave, G. Trippe, N. Felidj, J. Aubard, A. Hohenau, J. R. Krenn, ***ACS Nano,*** 2 (2008) 728.

[31] N. Cioffi, L. Torsi, N. Ditaranto, G. Tantillo, L. Ghibelli, L. Sabbatini, T. B. Zacheo, M.D. Alessio, P. G. Zambonin, E. Traversa, ***Chem. Mater.,*** 17 (2005) 5255.

[32] X. Zhang, G. Wang, X. Liu, H. Wu, B. Fang, ***Cryst. Growth Des.,*** 8 (2008) 1430.

[33] P. S. Ghosh, C. K. Kim, G. Han, N. S. Forbes, V. M. Rotello, ***ACS Nano,*** 2 (2008) 2213.

[34] K. Mallick, M. J. Witcomb, M. S. Scurrell, ***Materials Science and Engineering: B***, 123 (2005) 181.

[35] R. Das, S. S. Nath, R. Bhattacharjee, ***Journal of Luminescence***, 131 (2011) 2703.

[36] M. Abdulla-al-mamun, Y. Kusumoto, M. Muruganandham, ***Materials Letters,*** 63 (2009) 2007.

[37] B. R.Cuenya, ***Thin Solid Films,*** 518 (2010) 3127.

[38] Y. Li, F. Qian, J. Xiang and M. L. Charles, ***Material Today,*** 9 (2006) 18.

[39] D. L. Feldheim, C. A. Foss, ***Marcel Dekker Incorporated, New York, USA, 2002.***

[40] B. K. Park, D. Kim, S. Jeong, J. Moon, J. S. Kim, ***Thin Solid Films,*** 515 (2007) 7706; N. A. Luechinger, E. K. Athanassiou, W. J. Stark, ***Nanotechnology***, 19 (2008) 445201.

[41] Y. Lee, J. Choi, K. J. Lee, N. E. Stott, D. Kim, ***Nanotechnology,*** 19 (2008) 415604.

[42] Y. Leroux, J. C. Lacroix, C. Fave, G. Trippe, N. Felidj, J. Aubard, A. Hohenau, J. R. Krenn, ***ACS Nano,*** 2 (2008) 728.

[43] N. Cioffi, L. Torsi, N. Ditaranto, G. Tantillo, L. Ghibelli, L. Sabbatini, T. B. Zacheo, M. D. Alessio, P. G. Zambonin, E. Traversa, ***Chem. Mater.,*** 17 (2005) 5255.

[44] X. Zhang, G. Wang, X. Liu, H. Wu, B. Fang, ***Cryst. Growth Des.***, 8 (2008) 1430.

[45] P. S. Ghosh, C. K. Kim, G. Han, N. S. Forbes, V. M. Rotello, ***ACS Nano,*** 2 (2008) 2213.

[46] S. Chen, J. M. Sommers, ***J. Phys. Chem. B***, 105 (2001) 8816.

[47] C. Petit, A. Taleb, M. P. Pileni, ***Adv. Mater,*** 10 (1998) 259.

[48] N. Dadgostar, ***Ph.D. Thesis, Investigations on Colloidal Synthesis of Copper Nanoparticles in a Two-phase Liquid-liquid System, Waterloo, Ontario, Canada, 2008.***

[49] E. Bayram, J. C. Linehan, J. L. Fulton, J. A. S. Roberts, N. K. Szymczak, T. D. Smurthwaite, S. Ozkar, M. Balasubramanian, R. G. Finke, ***J. Am. Chem. Soc.,*** 133 (2011) 18889.

[50] V. Artero, M. Fontecave, ***Chem. Soc. Rev.*****,** 42 (2013) 2338.

[51] N. Yan, Y. Yuan, P. J. Dyson, ***Dalton Trans.,*** 42 (2013) 13294.

[52] R. H. Crabtree, ***Chem. Rev.*****,** 112 (2012) 1536.

[53] J. S. Bradley, ***Cluster Colloids*****,** 00 (1994) 459.

[54] D. G. Duff, A. Baiker, ***Stud. Surf. Sci. Catal.*****,** 91 (1995) 505.

[55] N. Toshima, ***NATO ASI Ser.*****,** 12 (1996) 371.

[56] H. Boennermann, G. Braun, G. B. Brijoux, R. Brinkman, A. S. Tilling, S. K. Schulze, K. Siepen, ***J. Organomet. Chem.*****,** 520 (1996) 143.

[57] K. Fugami, ***Organomet. News,*** 1 (2000) 25.

[58] A. B. R. Mayer, ***Polym. AdV. Technol.***, 12 (2001) 96.

[59] H. Bonnemann, R. Richards, ***Synth. Methods Organomet. Inorg. Chem.***, 10 (2002) 209.

[60] I. I. Moiseev, M. N. Vargaftik, ***Russ. J. Chem.,*** 72 (2002) 512.

[61] A. Eppler, G. Rupprechter, L. Guczi, G. A. Somorjai, ***J. Phys. Chem. B,*** , 101 (1997) 9973.

[62] G. Schmid, ***Met. Cluster Chem.*****,** 3 (1999) 1325.

[63] R. J. Puddephatt, ***Met. Cluster Chem.,*** 2 (1999) 605.

[64] C. R. Henry***, Appl. Surf. Sci.*****,** 164 (2000) 252.

[65] T. P. St. Clair, D. W. Goodman, ***Top. Catal.*****,** 13 (2000) 5.

[66] M. Kralik, B. Corain, M. Zecca, ***Chem. Pap.,*** 54 (2000) 254.

[67] C. C. Chusuei, X. Lai, K. Luo, D. W. Goodman, ***Top. Catal.,*** 14 (2001) 71.

[68] M. Bowker, R. A. Bennett, A. Dickinson, D. James,; R. D. Smith, P. Stone, ***Stud. Surf. Sci. Catal.,*** 133 (2001) 3.

[69] M. Kralik, A. Biffis, ***J. Mol. Catal. A: Chem.,*** 177 (2001)113.

[70] J. M. Thomas, R. Raja, ***Chem. Rec.,*** 1 (2001) 448.

[71] C. Mohr, P. Claus, ***Sci. Prog.*****,** 84 (2001) 311.

[72] J. M. Thomas, B. F. G. Johnson, R. Raja, G. Sankar, P. A. Midgley, ***Acc. Chem. Res.,*** 36 (2003) 20.

[73] J. F. Sonnenberg, R. H. Morris, ***Catal. Sci. Technol.,*** 4 (2014) 3426.

[74] D. Astruc, F. Lu, and J.R. Aranzaes, ***Angew. Chem. Int. Ed.,*** 44 (2005) 7852.

[75] R. Nishio, M. Sugiura, and S. Kobayashi, ***Org. Lett.,*** 7 (2005) 4831.

[76] S. Gloggler, A. M. Grunfeld, Y. N. Ertas,; J. McCormick, S. Wagner, P. P. M. Schleker, L. S. Bouchard, ***Angew. Chem. Int. Ed.,*** 54 (2015) 2452.

[77] B. Yoon, H. Kim, and C. M. Wai, ***Chem. Comm.,*** 00 (2003) 1040.

[78] R. Xu, T. Xie, Y. Zhao, Y. Li, ***Nanotechnology,*** 18 (2007) 055602.

[79] W. A. Herrmann, C. W. Kohlpaintner, ***Angew. Chem. Int. Ed.,*** 32 (1993) 1524.

[80] C. Coperet, M. Chabanas, R. Petroff Saint-Arroman, J. M. Basset, ***Angew. Chem. Int. Ed.***, 42 (2003) 156.

[81] M. T. Reetz, S. A. Quaiser, C. Merk, ***Chem. Ber.,*** 129 (1996) 741.

[82] A. Martino, M. Stoker, M. Hicks, C. H. Bartholomew, A. G. Sault, J. S. Kawola, ***Appl. Catal. A,*** 161 (1997) 235.

[83] R. Xu, T. Xie, Y. Zhao, Y. Li, ***Nanotechnology*,** 18 (2007) 055602.

[84] P. Migowski, G. Machado, S. R. Texeira, M. C. M. Alves, J. Morais, A. Traverse, J. Dupont, ***Phys. Chem. Chem. Phys.,*** 9 (2007) 4814.

[85] F. Alonso, P. Riente, J. A. Sirvent, M. Yus, ***Applied Catalysis A: General*,** 378 (2010) 42.

[86] F. Launay, H. Patin, ***New J. Chem.,*** 21 (1997) 247.

[87] (a) J. A. Widegren, R. G. Finke, ***J. Mol. Catal. A,*** 191 (2003) 187; (b) A. Roucoux, J. Schulz, H. Patin, ***Chem. Rev.,*** 102 (2002) 3757.

[88] K. R. Januszkiewicz, H. Alper, ***Organometallics***, 2 (1983) 1055.

[89] X. Mu, J. Meng, Z. Li, Y. Kou, ***J. Am. Chem. Soc.***, 127 (2005) 9694.

[90] S. Ozkar, R. G. Finke, ***J. Am. Chem. Soc.,*** 127 (2005) 4800.

[91] (a) T. Wang, C. X. Xiao, L. Yan, L. Xu, J. Luo, H. Shou, Y. Kou, H. Liu, ***Chem. Commun.*,** 00 (2007) 437; (b) T. Wang, H. Shou, Y. Kou, H. Liu, ***Green Chem.,*** 11 (2009) 562.

[92] F. Launay, A. Roucoux, H. Patin, ***Tetrahedron Lett.,*** 39 (1998) 1353.

[93] (a) H. Hirai, S. Komatsuzaki, N. Toshima, ***Bull. Chem. Soc. Jpn,*** 57 (1984) 488; (b) H. Hirai, H. Chawanya, H. Toshima, ***React. Polym.***, 3 (1985) 127.

[94] (a) M. Fernandez-Garcia, A. Martinez-Arias, L. N. Salamanca, J. M. Coronado, J. A. Anderson, J. C. Conesa, J. Soria, ***J. Catal.*,** 187 (1999)

474. (b) Y. Nishihata, J. Mizuki, T. Akao, H. Tanaka, M. Uenishi, M. Kimura, T. Okamoto, N. Hamada, ***Nature,*** 418 (2002) 164.

[95] (a) Y. Shiraishi, N. Toshima, ***J. Mol. Catal. A***, 141 (1999) 187; (b) Y. Shiraishi, N. Toshima, ***Colloid Surf. A,*** 169 (2000) 59.

[96] P. G. N. Mertens, M. Bulut, L. E. M. Gevers, I. F. J. Vankelecom, P. A. Jacobs, D. E. De Vos, ***Catal. Lett.,*** 102 (2005) 57.

[97] Y. Lu, Y. Mei, M. Drechsler, M. Ballauff, ***Angew. Chem. Int. Ed.,*** 45 (2006) 813.

[98] (a) Y. Wang, G. Wei, W. Zhang, X. Jiang, P. Zheng, L. Shi, A. Dong, ***J. Mol. Catal. A: Chem.,*** 266 (2007) 233; (b) Y. Wang, G. Wei, F. Wen, X. Zhang, W. Zhang, L. Shi, ***J. Mol. Catal. A: Chem.,*** 280 (2008) 1.

[99] H. Cong, C. F. Becker, S. J. Elliott, M. W. Grinstaff, J. A. Porco, ***Journal of the American Chemical Society,*** 132 (2010) 7514.

[100] H. S. Kim, S. R. Dhage, D. E. Shim and H. T. Hahn, ***Appl. Phys. A,*** 97 (2009) 791.

[101] Y. Lee, J. R. Choi, K. R. Lee, N. E. Stott and D. Kim, ***Nanotechnology,*** 19 **(**2008) 415604.

[102] C. Wu, B. P. Mosher and T. Zeng, ***Mater. Res. Soc. Symp. Proc. 879E Z6.3 (2005) 1***.

[103] M. J. G. Pacheco, J. E. M. Sanchez, G. Hernandez, F. Ruiz, ***Mater. Lett.,*** 64 (2010) 1361.

[104] M. Vaseema, K. M. Leeb, D. Y. Kima, Y. B. Hahna, ***Mater. Chem. Phys.,*** 125 (2011) 334.

[105] S. Y. Xie, Z. J. Ma, C. F. Wang, S. C. Lin, Z. Y. Jiang, R. B. Huang and L. S. Zheng ***J. Solid State Chem.,*** 177 (2004) 3743.

[106] N. V. Suramwar, S. R. Thakare, N. T. Khaty, ***Arabian Journal of Chemistry,*** 5 (2012) 1.

[107] H. Ohde, F. Hunt, C. M. Wai, ***Chem. Mater,*** 13 (2001) 4130.

[108] M. Samim, N. K. Kaushik and A. Maitra, ***Bull. Mater. Sci.,*** 30 (2007) 535.

[109] A. A. Ponce and K. J. Klabunde, ***J. Molecular catalysis A*: Chemical,** 255 (2005) 1.

[110] J. Hassan, V. Penalva, L. Lavenot, C. Gozzi, M. Lemaire, ***Tetrahedron*****,** 54 (1998) 13793.

[111] A. Nasirian, ***Int. J. Nano Dim.,*** 2 (2012) 3159.

[112] S. Vukojevic, O. Trapp, J. D. Grunwaldt, C. Kiener, F. Schuth, ***Angew. Chem. Int. Ed.***, 44 (2005) 7978.

[113] M. K. Schroter, L. Khodeir, M.W. E. van den Berg, T. Hikov, M. Cokoja, S. J. Miao, W. Grunert, M. Muhler, R. A. Fischer, ***Chem. Commun.,*** 00 (2006) 2498.

[114] L. He, H. Liu, C. Xiao, Y. Kou, ***Green Chem.*****,** 10 (2008) 619.

[115] L. D. Pachon, J. H. Maarseveen and G. Rothenberg, ***Adv. Synth. Catal.,*** 347 (2005) 811.

[116] A. K. Patra, A. Dutta, A. Bhaumik, ***Catal. Commun.,*** 11 (2010) 651.

[117] E. A. Karakhanov, A. L. Maximov, Y. S. Kardasheva, V. A. Skorkin, S. V. Kardashev, V. V. Predeina, M. Y. Talanova, E. Lurie-Luke, J. A. Seeley, S. L. Cron, ***Appl. Catal. A*****,** 385 (2010) 62.

[118] F. Benaskar, V. Engels, E. V. Rebrov, N. G. Patil, J. Meuldijk, P. C. Thune, P. C. M. M. Magusin, B. Mezari, V. Hessel, L. A. Hulshof, E. J. M. Hensen, A. E. H. Wheatley, J. C. Schouten, ***Chem. Eur. J.*****,** 18 (2012) 1800.

[119] S. Wunder, Y. Lu, M. Albrecht, M. Ballauff, ***ACS Catal.*****,** 1 (2011) 908.

[120] K. Esumi, K. Miyamoto, T. Yoshimura, ***J. Colloid Interface Sci.,*** 254 (2002) 402.

[121] K. Hayakawa, T. Yoshimura, K. Esumi, ***Langmuir***, 19 (2003) 5517.

[122] Y. Lu, Y. Mei, M. Drechsler, M. Ballauff, ***Angew. Chem.,*** 118 (2006) 827; Y. Lu, Y. Mei, M. Drechsler, M. Ballauff, ***Angew. Chem. Int. Ed.,*** 45 (2006) 813.

[123] J. Lee, J. C. Park, H. Song, ***Adv. Mater.***, 20 (2008) 1523.

[124] R. Kaur, C. Giordano, M. Gradzielski, and S. K. Mehta, ***Chem. Asian J.,*** 9 (2014) 189.

[125] R. A. Soomro, S. T. H. Sherazi1, Sirajuddin, N. Memon, M. R. Shah, N. H. Kalwar, K. R. Hallam, A. Shah, ***Adv. Mat. Lett.,*** 5 (2014) 191.

[126] C. Hubert, A. Denicourt-Nowicki, A. Roucoux, D. Landy, B. Leger, G. Crowync, E. Monflier, ***Chem. Commun.,*** 00 (2009) 1228.

[127] C. Xiao, Z. Cai, T. Wang, Y. Kou, N. Yan, ***Angew. Chem. Int. Ed.***, 47 (2008) 746.

[128] J. Liu, F. He, E. Durham, D. Zhao, C.B. Roberts, ***Langmuir***, 24 (2008) 328.

[129] M. Zhao, R. M. Crooks, ***Angew. Chem. Int. Ed.,*** 38 (1999) 364.

[130] J. D. Marty, E. Martinez-Aripe, A. F. Mingotaud, C. Mingotaud, ***J. Colloid Interface Sci.,*** 326 (2008) 51.

[131] M. J. Beier, J. M. Andanson, T. Mallat, F. Krumeich, A. Baiker, ***ACS Catal.,*** 2 (2012) 337.

[132] T. Wang, H. Shou, Y. Kou, H. Liu, ***Green Chem.,*** 11 (2009) 562.

[133] P. Maity, C.S. Gopinath, S. Bhaduri, G. K. Lahiri, ***Green Chem.,*** 11 (2009) 554.

[134] P. Maity, S. Basu, S. Bhaduri, G. K. Lahiri, ***Adv. Synth. Catal.,*** 349 (2007) 1955.

[135] B. C. Ranu, K. Chattopadhyay, ***Org. Lett.,*** 9 (2007) 2409.

[136] (a) M. T. Reetz, E. Westermann, ***Angew. Chem.***, ***Int. Ed.***, 39 (2000) 165. (b) S. W. Kim, M. Kim, W. Y. Lee, T. Hyeon***, J. Am. Chem. Soc.***, 124 (2002) 7642. (c) S. U. Son, Y. Jang, J. Park, H. B. Na, H. M. Park, H. J. Yun, J. Lee, T. Hyeon, ***J. Am. Chem. Soc.,***126 (2004) 5026. (d) R. Franzen, ***Can. J. Chem.,*** 78 (2000) 957. (e) Y. Li, X. M. Hong, D. M. Collard, M. A. El-Sayed, ***Org. Lett.,*** 2 (2000) 2385.

[137] S. Sawoo, D. Srimani, P. Dutta, R. Lahiri, A. Sarkar, ***Tetrahedron,*** 65 (2009) 4367.

[138] J. Z. Jiang, Y. A. Wei, C. Cai, ***J. Colloid Interface Sci.,*** 312 (2007) 439.

[139] U. Laska, C. G. Frost, P. K. Plucinski, G. J. Price, ***Catal. Lett.,*** 122 (2008) 68.

[140] D. Srimani, S. Sawoo, A. Sarkar, ***Org. Lett.,*** 9 (2007) 3639.

[141] A. Biffis, L. Minati, ***J. Catal.,*** 236 (2005) 405.

[142] S. Kundu, K. Wang, H. Liang, ***J. Phys. Chem. C,*** 113 (2009) 5157.

[143] J. Han, Y. Liu, R. Guo, ***J. Am. Chem. Soc.,*** 131 (2009) 2060

[144] (a) L. M. Molina, B. Hammer, ***Appl. Catal. A,*** 291 (2005) 21; (b) T. V. W. Janssens, A. Carlsson, A. Puig-Molina, B. S. Clausen, ***J. Catal.***, 240 (2006) 108.

[145] A. Murugadoss, A. Chattopadhyay, ***Nanotechnology,*** 19 (2008) 015603.

[146] R. Kaur, C. Giordano, M. Gradzielski, S. K. Mehta, ***Chem. Asian J.,*** 9 (2014) 189.

[147] Q. Wei, B. Li, C. Li, J. Wang, W. Wang, X. Yang, ***J. Mater. Chem.,*** 16 (2006) 3606.

[148] S. Bhadra, A. Saha, B.C. Ranu, ***Green Chem.,*** 10 (2008) 1224.

[149] A. Saha, D. Saha, B. C. Ranu, ***Org. Biomol. Chem.,*** 7 (2009) 1652.

[150] D. Swern***, Organic peroxides, Interscience, New York, 1971***.

[151] G. Sosnovsky and D. J. Rawlison, ***Organic peroxide, (Ed. By Swern, D.), Interscience, New York, 1971.***

[152] W. Adam, R. Hadjiarapoglou, R. Curci, and R. Mello, **Organic peroxides, (ed. by Ando, E. J.) Wiley and Sons, New York, 1992.**

[153] K. Anand kumar, P. Sivasaroop and P. V. Krishna Rao, ***Indian J. Chem.,*** 30A (1991) 966.

[154] D. L. Ball, and J. O. Edwards, ***J. Am. Chem. Soc.,*** 78 (1956) 1125.

[155] J. L. Arnau and P. A. Giguere, ***Can. J. Chem.,*** 48 (1970) 3903.

[156] T. Hu, G. J. Dryhurst, ***Electroanal. Chem.,*** 362 (1993) 237.

[157] M. Spiro, ***Electrochim. Acta,*** 24 (1979) 313.

[158] W. V. Steele and E. H. Appelman, ***J.Chem. Thermodynam.,*** 14 (1982) 337.

[159] B. Trost and D. Curran, ***Tetrahedron Lett.,*** 22 (1981) 1287.

[160] M. D. Johnson and R. J. Balahura, ***Inorg. Chem.,*** 27(1987) 3104.

[161] J. O. Edwards and C. Marsh, ***Progress in reaction kinetics, Pergamon Press, New York, 1989.***

[162] M. Sundar, D. Easwaramoorthy, S. Kutti Rani, I. M. Bilal, ***Cat. Comm.,*** 9 (2008) 2340.

[163] S. M. Sundaram, and V. Sathiyendran, ***J. Chem. Res.,*** 10 (2000) 1118.

[164] S. Shailaja, and M. S. Ramachandran, ***Inter. J. Chem. Kinet.,*** 43(2011) 620.

[165] R. J. Kennedy and A. M. Stock, ***J. Org. Chem.,*** 25 (1960) 1901.

[166] H. Hussain, I. R. Green, I. Ahmed, ***Chem. Rev.,*** 113 (2013) 3329.

[167] F. Epifano, M. C. Marcotullio, M. Curini, ***Trends Org. Chem.,*** 10 (2003) 21.

[168] W. Zhu, W. T. Ford, ***J. Org. Chem.,*** 56 (1991) 7022.

[169] T. Balakrishnan, S. Damodarkumar, ***J. Appl. Polym. Sci.,*** 76 (2000) 1564.

[170] R. S. Kannas, M. S. Ramachandran, ***Int. J. Chem. Kinet.,*** 35 (2003) 475.

[171] G. Ragukumar, P. Andal, M. Murugavelu, C. Lavanya, M. S. Ramachandran, ***J. Mol. Cat. A-Chem.,*** 390 (2014) 22.

[172] G. Beller, ***The oxidation of tris(phenanthroline)iron(II) and bis(terpyridine)iron(II) complexes and the corresponding ligands by peroxomonosulfate ion: kinetics and mechanism, Ph. D. thesis***, ***Debrecen, 2015 .***

[173] R. C. Thompson, ***Inorg. Chem.,*** 20 (1981) 1005.

[174] B. C. Gilbert and J. K. Stell, ***J. Chem. Soc. Perkin Trans,*** 2 (1990) 1281.

[175] M. Ahmad, A. L. Teel, R. J. Watts, ***Journal of Contaminant Hydrology,*** 115 (2010) 34.

[176] D. A. House, ***Chemical Review,*** 62 (1962) 185.

[177] C. J. Liang, C. J. Bruell, M. C. Marley, K. L. Sperry, ***Chemosphere,*** 55 (2004) 1213.

[178] K. C. Huang, R. A. Couttenye, G. E. Hoag, ***Chemosphere,*** 49 (2002) 413.

[179] P. Durrant, B. Durrent, ***Introduction to Inorganic Chemistry, Longman, 1962***.

[180] W. M. Latimert, ***The oxidation states of the elements and their potentials in aqueous solution, Prentice Hall, Englewood Cliffs, New York. N.Y. 1952.***

[181] W. K. Wilmarth, A. Haim, ***Peroxide reaction mechanisms. Edited by J. 0. Edwards. Wiley Inter-Science, New York, 1962.***

[182] International Union of Pure and Applied Chemistry: Reports on Symbolism and Nomenclature**, *J. Am. Chern. Soc.,*** 82 (1960) 5535.

[183] S. Srivastava, S. Ghosh, ***Z. Physik. Chern.,*** 202 (1953) 198.

[184] S. Srivastava, S. Ghosh, ***Z. Physik. Chem.,*** 207 (1957) 161.

[185] A. N. Kappana, ***Z. Physik. Chem.,*** 20 (1956) 4.

[186] R. B. Seymouri, ***An introduction to polymer chemistry, International student edition. McGraw-Hill, Kogukusha, Ltd-Tokyo. 1956***.

[187] M. A. A. Khalid, ***Kinetics and Mechanism of Peroxodisulphate Oxidation of Certain Amino Acids in Acidic Aqueous Solution, Ph.D. Thesis, University of Khartoum, 2006.***

[188] J. M. Anderson, J. K. Kochi, ***J. Am. Chem. Soc.,*** 92 (1970) 1651.

[189] C. Walling, D. M. Camaioni, ***J. Org. Chem.,*** 43 (1978) 3266.

[190] C. Arnoldi, A. Citterio, F. Minisci, ***J. Chem. Soc., Perkin Trans.,*** 2 (1983) 531.

[191] A. Citterio, C. Arnoldi***, J. Chem. Soc. Perkin Trans.,*** 1 (1983) 891.

[192] C. Giordano, A. Belli, A. Citterio, F. Minisci, ***J. Org. Chem.,*** 44 (1979) 2314.

[193] C. Giordano, A. Belli, A. Citterio, F. Minisci, ***J. Chem. Soc., Perkin Trans.,*** 1 (1981) 1574.

[194] S. Yamazaki, Y. Yamazaki, ***Chem. Lett.,*** 00 (1989) 1361.

[195] C. I. Nikishin, I. E. Troyansky, I. Lazareva, ***Tetrahedron Lett.,*** 25 (1984) 4987.

[196] S. Tyrlik, I. Woiochowicz, ***Bull. Soc. Chim. Fr.,*** 00 (1973) 2147.

[197] J. E. McMurry, M. P. Fleming, ***J. Am. Chem. Soc.,*** 96 (1974) 4708.

[198] H. Wynberg, K. Lammertsma, L. A. Hulshof, ***Tetrahedron Lett.,*** 16 (1975) 3749.

[199] R. F. Langler, T. T. Tidwell, ***Tetrahedron Lett.,*** 16 (1975) 777.

[200] Usepa, ***Fed. Reg.,*** 63 (1998) 69389.

[201] D. Laloo and M. M. Mahanti, ***J. Chem. Soc., Dalton Trans.,*** 1 (1990) 311.

[202] C. L. Hawkins, D. I. Pattison, M. J. Davies, ***Amino Acids,*** 25 (2003) 259.

[203] E. R. Stadtman, ***Annual Review of Biochemistry,*** 62 (1993) 797.

[204] E. R. Stadtman, R. L. Levine, ***Amino Acids,*** 25 (2003) 207.

[205] J. Rodriguez-Martinez, A. Silvia, Y. Martinez-Amador, Y. Garza-Garcia, ***J. Ind. Microbiol. Biotechnol.,*** 32 (2005) 691.

[206] C. V. Hiremath, S. D. Kulkarni, S. T. Nandibewoor, ***Ind. Eng. Chem. Res.***, 45 (2006) 8029.

[207] D. Bilehal, R. Kulkarni, S. Nandibewoor, ***J. Mole Catal A: Chem.,*** 232 (2005) 21.

[208] T. Sumathi, P. Shanmuga Sundaram, G. Chandramohan, ***Arabian Journal of Chemistry,*** 4 (2011) 427.

[209] M. B. Yadav, V. Devra and A. Rani, ***Indian Journal of Chemistry,*** 49A (2010) 442.

[210] G. Chandra, and S. N. Srivastava, ***J. Inorg. Nucl. Chem.,*** 34 (1972) 197.

[211] G. Chandra, and S. N. Srivastava, ***Bull. Chem. Soc.,*** 44 (1971) 3000.

[212] F. Minisci, A. Citterio, and A. Giordano, ***Acc. Chem. Res.,*** 16 (1983) 27.

[213] Y. Zelechonok, R. B. Silverman, ***J. Org. Chem.,*** 57 (1992) 5787.

[214] K. S. Gates, and R. B., Silverman, ***J. Am. Chem. Soc.,*** 112 (1990) 9364.

[215] R. B. Silverman, ***Advances in Electron Transfer Chemistry, (ed. by P. S. Mariano) JAI Press, Greenwich, CT, 1992.***

[216] M. S. Ramachandran, T. S. Vivekanandan, ***Tetrahedron,*** 40 (1984) 4929.

[217] M. S. Ramachandran, T. S. Vivekanandan, ***Ind. J. Chem.,*** 27A (1988) 498.

[218] M. S. Ramachandran, T. S. Vivekanandan, ***Tetrahedron,*** 40 (1984b) 4929.

[219] M. S. Ramachandran, D. Eswaramoorthy, D. Sureshkumar, ***Tetrahedron,*** 50 (1994) 9495.

[220] Suresh Kumar, ***Kinetics and Mechanism of Copper(II) Catalyzed Oxidative Deamination of Basic Amino Acids by Peroxomonosulphate, Ph.D. Thesis, Anna University, Chennai, 2012***.

[221] P. Suresh Kumar, R. Mohan Raj, S. Kutti Rani, D. Easwaramoorthy, ***Ind. Engg. Chem. Res,*** 51 (2012) 6310.

[222] V. Devra, M. B. Yadav, ***Rasayan J. Chem.,*** 5 (2012) 67.

[223] B. K. Singh, R. P. Singh, ***Asian J. of Chem.,*** 4 (1992) 508.

[224] J. Sanathanlakshmi, P. Vankatesan, ***Chinese Journal of Catalysis,*** 33 (2012) 1306.

[225] X. Huang, I. H. El-Sayed, X. Yi, M. A. El-Sayed, ***J. Photochem. Photobiol. B,*** 81 (2005) 76.

[226] A. Goel, R. Bhatt, Neetu, ***Int. J. Res. Chem. Environ.,*** 00 (2012) 210.

[227] A. Goel, S. Sharma, ***J. Chem. Bio. Phy. Sci. Sec. A***, 2 (2012) 628.

[228] P. Venkatesan, J. Santhanalakshmi, ***Chinese Journal of Catalysis*****,** 33 (2012) 1306.

[229] J. Santhanalakshmi, P. Venkatesan, ***J. Nanopart. Res.*****,** 13 (2011) 479.

[230] Q. Wang, H. Qian, Y. Yang, Z. Zhang, C. Naman, X. Xu, ***J. Contam. Hydrol.,*** 114 (2010) 35.

[231] A. Wang, H. Yin, H. Lu, J. Xue, M. Ren, T. Jiang, ***Langmuir,*** 25 (2009) 12736.

[232] A. Wang, H. Yin, H. Lu, J. Xue, M. Ren, T. Jiang, ***Catalysis Communications*****,** 10 (2009) 2060.

[233] S. Sundar, J. Kundu and S. C. Kundu, ***Sci. Technol. Adv. Mater.*****,** 11 (2010) 014104.

[234] J. Cao, R. Xu, H. Tang, S. Tang, M. Cao, ***Science of the Total Environment,*** 409 (2011) 2336.

[235] L. Parimala and J. Santhanalakshmi, ***Nanoscience and Nanotechnology: An International Journal*****,** 3 (2013) 4.

[236] E. Eiser, F. Bouchama, M. B. Thathagar, G. Rothenberg, ***Chem. Phys. Chem.*****,** 4 (2003) 526.

[237] F. Bouchama, M. B. Thathagar, G. Rothenberg, D. H. Turkenburg, E. Eiser, ***Langmuir*****,** 20 (2004) 477.

[238] C. J. Zhong, M. M. Maye, ***Adv. Mater.,*** 13 (2001)1507.

[239] G. Schmid, ***Adv. Eng. Mater.,*** 3 (2001) 737.

[240] M. T. Reetz, M. Winter, R. Breinbauer, T. Thurn-Albrecht, W. Vogel, ***Chem. Eur. J.,*** 7 (2001) 1084.

[241] P. Lu, T. Teranishi, K. Asakura, M. Miyake, N. Toshima, ***J. Phys. Chem. B*****,** 103 (1999) 9673.

Chapter-2

Instrumentation and Materials

Abstract

The current chapter describes the fundamental experimental details of the studies conducted in this thesis. The first part of this chapter deals with the description of various characterization techniques which are most important to characterize the synthesized nanocatalyst. This part also describes the basic theories and principles of the main analytical methods, electron microscopy and description of instrument which are used for analysis. The second part is deals with the details of the reagents, chemicals and their solutions with other specifications employed in kinetic study of various reactions.

The present chapter describes the instrumental details of all the characterization tools, details of the reagents, chemicals and their solutions with other specifications employed in kinetic study of various reactions. This chapter is divided into two following parts:

PART A

2.1. Instrumental Techniques

This part describes the basic theories and principles of the main analytical methods and electron microscopy. Electron microscopy is extremely versatile for providing structural information over a wide range of resolution from 10 μm to 2Å. Particularly in the range where the specimen is so small (<1μm) that optical microscopes are not able to image it anymore. Electron microscopes operate in either transmission (TEM) or scanning (SEM) mode. This part describes the details of various instrumental techniques such as SEM, TEM, FTIR spectroscopy, UV-VIS spectrophotometer, etc. adopted to study the oxidation of amino acids in the presence of nanocatalysts.

2.1.1. Transmission Electron Microscopy

Transmission Electron Microscopy (TEM) is one of the most important tools of nanotechnology for imaging nanomaterial with sub-nanometer resolution (High –resolution TEM). In this technique, a thin specimen is imaged by an electron beam, which is irradiated through the sample at uniform current density [1]. The typical acceleration voltage in an operational TEM is 80-200 KV. The electrons are emitted from a thermionic (tungsten or lanthanum hexaboride filament) or field emission (tungsten filament) electron guns. The illumination aperture and the area of specimen illuminated are controlled by a set of condenser lenses (see **figure 2.1** for ray diagram). The function of the objective lens is either image or diffraction pattern formation of the specimen. Electron diffraction patterns are used to identify the crystallographic structure of the material. In our case, to investigate the size and distribution of metal nanoparticles the image mode is used, while the crystalline structure is studied by the diffraction mode.

The electron intensity distribution behind the specimen is magnified with a three or four stage lens system and viewed on a fluorescent screen [1]. The image is captured on a photographic plate or CCD camera. A full detailed description about the TEM can be found elsewhere [2]. The analysis capacity of TEM has been significantly enhanced by integration of several advanced techniques into the instrument.

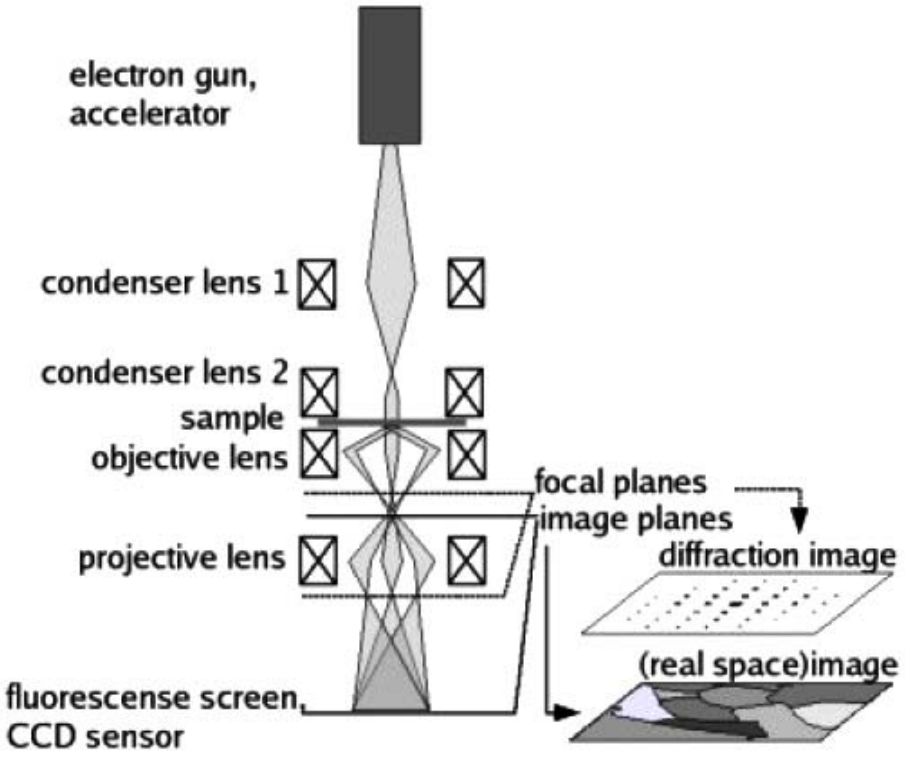

***Figure 2.1: Ray diagram of a Transmission Electron Microscope for imaging and diffraction modes* [3]**

Nowadays, there is increasing demand to produce images with atomic resolution, so that the lattice arrangements within crystalline materials can be visualized. One well known technique for this is high resolution TEM (HRTEM). A very high magnification is necessary in order to obtain a high-resolution atomic image.

In addition to a high-voltage magnification, several other factors must be controlled in order to acquire a good quality HRTEM image. First, TEM column

alignment needs to be carried out as accurately as possible, which includes electron gun and condenser lens alignment, plus astigmatism correction of condenser lenses and objective lens. Secondly, in a HRTEM, an atomic image of a crystal is only possible if certain conditions are satisfied, one of which, choosing the optimum focus, is crucial.

For the work presented in this thesis, transmission electron microscope Model- FEI Techni G2S2 Twin with CCD camera and plate film camera instrument, which is located at University of Rajasthan, Jaipur (Raj.) has been used to get information regarding particle size, shape and determining the size distribution of copper particles. Electron diffraction patterns from a TEM field emission gun were used to study the composition and morphology of the metallic particles. It has a maximum operating voltage of 20 to 200kv. For this, Samples were prepared by taking small quantities of copper nanoparticles separated by centrifugation then ultrasonicated dispersed suspensions were mounted on carbon coated copper grids.

2.1.2. Scanning Electron Microscopy (SEM)

The Scanning electron microscope (SEM) is a type of electron microscope capable of producing high resolution images of a sample surface. It was developed to overcome the limitations of optical microscopy and provide increased magnification and resolution, far superior to optical systems. SEM is powerful tool for examining and interpreting microstructure of materials, and is widely used in the field of material science. The principle of SEM is based on the interaction of an incident electron beam and the specimen [4]. Due to the manner in which the image is created, SEM images have a characteristic three-dimensional appearance and are useful for judging the surface structure of the sample. By correlating the sample scan position with the resulting signal, a black and white image can be formed that is absolutely similar to what would be seen through an optical microscope. A schematic diagram of an SEM apparatus is given below in **figure 2.2.**

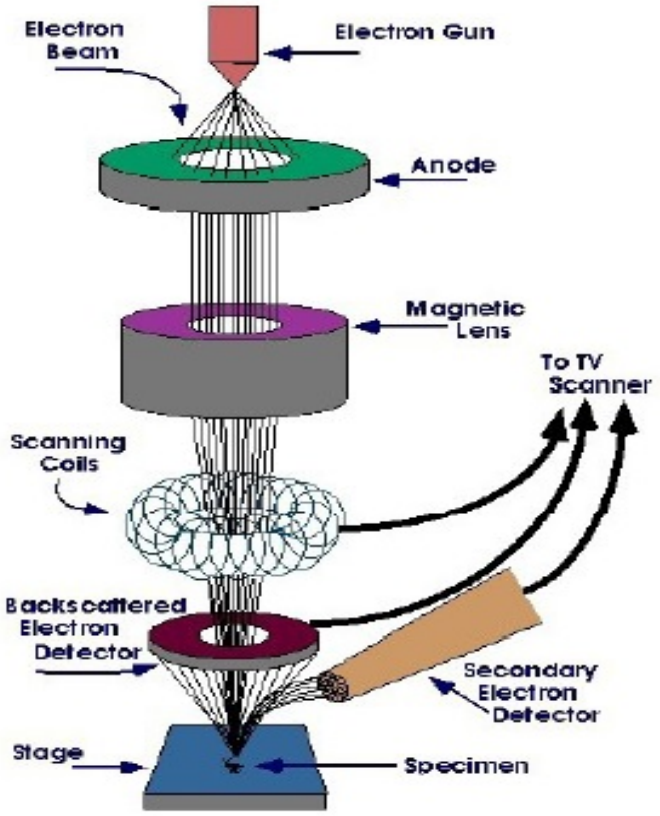

Figure 2.2: Schematic diagram of Scanning Electron Microscope **[5]**

SEM is a very versatile tool due to the several complementary imaging modes available such as: 1) Specimen current imaging mode, using the intensity of the electrical current induced in the specimen by the illuminating electron beam to produce an image. It can often be used to show subsurface defects, 2) Backscatter imaging mode, using high-energy electrons that emerge nearly 180 degrees from the illuminating beam direction. The backscatter electron yield is a function of the average atomic number of each point on the sample, and thus can give compositional information. A detailed description of the technique and background theory can be found elsewhere [6].

SEM analyses for our samples were performed with an EVO 18 carlzeiss instrument, which is located at University of Rajasthan, Jaipur (Raj.). This microscope is equipped with a field emission gun, operating at an accelerating voltage variable from 0.2 to 30kV, with a claimed resolution images of 2 nm. For this, dispersed nanoparticles were centrifuged and ultrasonicated by probe

sonicator for 40 minutes. 30µl aliquots were then extracted and deposited on stub for SEM analysis.

2.1.3. Fourier Transform Infrared (FTIR) Spectrophotometer

Fourier transform infrared (FTIR) spectrometers have replaced dispersive instruments for most applications due to their superior speed and sensitivity. They have greatly extended the capabilities of infrared (IR) spectroscopy and have been applied to many areas that are very difficult or nearly impossible to analyze by dispersive instruments [7]. FTIR is a technique based on the vibrations of the atoms within a molecule. An infrared spectrum is obtained by passing IR radiation through a sample and determining what fraction of the incident radiation is observed at a particular energy. The energy at which any peak in an absorption spectrum appears corresponds to the frequency of a vibration of a part of a sample molecule [8]. Moreover, chemical bonds in different environments will absorb at varying intensities and at varying frequencies. Thus, IR spectroscopy involves collecting absorption information and analyzing it in the form of a spectrum. In this spectrum, the frequencies of infrared radiation absorbed (peaks or signals) can be correlated directly to bonds within the compound in question. Because each interatomic bond may vibrate in several different motions (stretching or bending) individual bonds may absorb at more than one IR frequency. Stretching absorptions usually produce stronger peaks than bending, however the weaker bending absorptions can be useful in differentiating similar types of bonds (e.g. aromatic substitution).

One of the great advantages of infrared spectroscopy using various sampling accessories, IR spectrometers can accept a wide range of sample types such as gases, liquid, pastes, powders, films, fibers and surfaces can all be examined by a judicious choice of sampling technique. The latter, which is the technique used in this research work, is often termed as attenuated total reflectance (ATR).

Attenuated total Reflectance FTIR (ATR-FTIR) is a modified version of FTIR, in which IR radiation is not transmitted through the sample but reflected by

the sample. Consequently, a specimen is not placed between two IR windows, but onto an IR crystal. It is used for analysis of the surface of materials. It is also especially useful for obtaining IR spectra of difficult samples that cannot be readily examined by the normal transmission method, such as thick or highly absorbing solid and liquid materials, including films, coatings, powders, threads, adhesive, polymers and aqueous samples. ATR requires little or no sample preparation for most samples and is one of the most versatile sampling techniques [7]. The sampling surface is pressed into intimate optical contact with the top surface of the crystal such as ZnSe, diamond or Ge.

In this work, FTIR spectra were recorded using model ALPHA-T model, Bruker, Germany spectrometer with a universal Attenuated Total Reflectance (ATR) sampling accessory supplied with a top plate ZnSe. For ATR data acquisition, with no need for sample preparation, the sample was placed onto the crystal and its spectrum was recorded while record the FT-IR spectra in the range of 400-4000 cm^{-1} by mixing the sample with dried KBr (in 1: 20 weight ratio) with a resolution of 4 cm^{-1}.

2.1.4. Ultraviolet -Visible Spectrophotometer

Ultraviolet-visible (UV-Vis) Spectroscopy offers a relatively straight forward and effective way for quantitatively characterizing both organic and inorganic compounds. Furthermore, as it operates on the principle of absorption of photons that promotes the molecule to an excited state it is an ideal technique for determining the electronic properties such as the band gap of a material. UV-Vis analysis can be performed on metal nanoparticles dispersed in a solvent or embedded in the insulator matrix. In such cases, absorption of incident radiation takes place due to surface plasmon resonance (SPR) of the metal nanoparticles. Surface plasmon resonance is essentially the light waves that are trapped on the surface because of their interaction with the free electrons of the metal [9].

The UV-Vis spectrum of metal nanoparticles embedded in dielectric media shows a characteristic absorption band at a specific wavelength depending upon the nature of metal, matrix, shape of the particles and distribution [10, 11, 12]. It

should be noted that the strong UV-visible absorption band observed for metal nanoparticles and known as localized surface plasmon surface is not present in the spectrum of their bulk metal counterparts [13]. Furthermore, size-depending optical properties can also be observed in a UV-visible spectrum, particularly in the nano and atomic scales. These include peak broadening or shifts of the absorption wavelength. The excitation of such higher order modes can be explained in terms of an in homogeneous polarization of the nanoparticles by the electromagnetic field as the particle size becomes comparable to the wavelength of the incoming radiation [14]. The size dependence resonance is a useful phenomenon for sensing application [15].

As a part of this research work, a double beam 3000+ LABINDIA, UV-Vis spectrophotometer with U.V. path length 1.0 cm in the spectral range 200-800 nm, was used for optical characterization of the synthesized metallic nanoparticles and analyses the reaction.

2.1.5. Ultrasonic Processor

Ultrasonic processor model EI-250UP which has 250 watts (average) and 20+/-3 KHz frequency and microprocessor based timer 0 to 30 minutes was used to prepare the sample for analysis the synthesized copper nanoparticles by using electron microscopy TEM and SEM.

2.1.6. Centrifuge

Centrifuge with 8X15 swings out heads was used to obtained supernatant liquid from colloidal solution of synthesized nanoparticles and separate out the two months stabilized copper nanoparticles.

2.1.7. Electronic Balance

Citizon electronic balance, CX 220 was used for weighing purposes. The maximum count of balance is 220 g.

2.1.8. pH-Meter

Systronic digital pH meter, model MAC (MSW-552) was used for the determination of pH of the synthesized nanoparticles and the reaction mixtures with the maximum uncertainty in pH of ±0.01 unit.

2.1.9. Magnetic Stirrer with Hot Plate

Remi 2 LH stirrer was used for stirring the reaction mixture at a fixed and suitable rpm and temperature. It was used in the synthesis of copper nanoparticles. The size of copper nanoparticles is also sensitive by stirring with suitable rpm and temperature.

2.1.10. Thermostat

Fabricated thermostat model MAC (MSW-273) with electronic relay, mechanical stirrer and heating rod was used for kinetic measurement of the catalytic oxidation reaction of amino acids by peroxomonosulphate or peroxodisulphate in aqueous medium.

PART B

2.2. Materials

The kinetics of the oxidative decarboxylation of amino acid by peroxomonosulphate / peroxodisulphate in acidic / aqueous medium has been studied. The effect of copper nanoparticles as a catalyst on the oxidation kinetics was also investigated. The details regarding methods of preparation of various solution and the details of all reagents employed in these studies have been given in this part of the chapter. Glassware used for handling reagents were cleaned with chromic acid, rinsed thoroughly with doubly distilled water and then air dried at room temperature. All the solutions used in this study were prepared by using double distilled water. The solutions of the reagents used in this study were prepared a fresh every day before starting the experiments.

2.2.1. Copper Chloride Dihydrate ($CuCl_2.2H_2O$)

A fresh solution of copper chloride dihydrate, (E. Merck) was prepared by dissolving an appropriate amount of $CuCl_2.2H_2O$ with the addition of double distilled water, made up to required volume in a standard measuring flask.

2.2.2. L-Ascorbic Acid ($C_6H_8O_4$)

A fresh solution of L-ascorbic acid (E. Merck) was prepared by dissolving an relevant amount of ascorbic acid with the addition of double distilled water, made up to required volume in a standard measuring flask.

2.2.3. Serine [$CH_2OH.CH(NH_2).COOH$]

The solutions of required concentration of this amino acid were prepared by dissolving the requisite amount of serine (E. Merck) in the known volume of distilled water.

2.2.4. L-Threonine [$CH_3.CH(OH).CH(NH_2).COOH$]

The solution of L-Threonine was prepared by dissolving the requisite amount of threonine (E. Merck) in the known volume of distilled water. The solution being quite stable does not show any kind of photodecomposition.

2.2.5. Glycine [$H.CH(NH_2).COOH$]

Solutions of required concentration of glycine were prepared by dissolving the requisite amount of glycine (E. Merck) in a known volume of distilled water.

2.2.6. Alanine [$CH_3.CH(NH_2).COOH$]

The solutions of required concentration of this amino acid were prepared by dissolving the requisite amount of alanine (E. Merck) in the known volume of distilled water.

2.2.7. Peroxomonosulphate Solution (HSO_5^-)

Peroxomonosulphate (PMS) from Sigma Aldrich by the trade name "Oxone" was the source of PMS ion. The solution of peroxomonosulphate (Aldrich) was prepared by dissolving the requisite amount of its potassium salt in doubly distilled water and was kept in the flask painted black from the outside to avoid its decomposition from photo light. Potassium peroxomonosulphate is a triple salt with the composition of $2KHSO_5 \cdot KHSO_4 \cdot K_2SO_4$ and is found to be 96% pure when analyzed both ceremetrically and iodometrically. Tests with permanganate showed the absence of free hydrogen peroxide and hence this reagent was used without further purification. However, tests for free H_2O_2 were negative. The concentration was checked both ceremetrically and iodometrically [16] as when desired. A fresh solution of the peracid was employed. Whenever required in kinetics as well as analytical studies.

2.2.8. Peroxodisulphate Solution ($S_2O_8^{2-}$)

Potassium peroxodisulphate (A.R., Merck) was recrystallized from deionized water and was dried in a vacuum desiccator. It was standardized using a method modified by Rosin [17], 1.0g of dried recrystallized peroxodisulphate was added to a solution of 25 ml of 1.0M potassium iodide and followed by immediate addition of 0.5g of sodium bicarbonate and 10.0 ml of 10% sulfuric acid was added. During and after the liberation of carbon dioxide, which provide a convenient means of sweeping out the oxygen, the solution was left to stand in a glass-stoppered flask for thirty minutes in the dark at room temperature. The liberated iodine was titrated against standard thiosulphate solution.

2.2.9. Sodium Thiosulphate Solution ($Na_2S_2O_3.5H_2O$)

The solution of sodium thiosulphate (A.R.) was prepared by dissolving known quantities in appropriate volume of double distilled water. These were standardized against standard solution of copper sulphate pentahydrate iodometrically [18]. Freshly prepared solutions of sodium thiosulphate were always used as these were reportedly deteriorated on standing at ambient temperature.

2.2.10. Copper Sulphate Pentahydrate ($CuSO_4.5H_2O$)

Copper sulphate (A.R., E. Merck) solution was prepared by dissolving the requisite quantity of copper sulphate in doubly distilled water and sufficient acetic acid was added to check the hydrolysis of copper sulphate in the solution.

2.2.11. Potassium Iodide Solution (KI)

Potassium iodide (A.R.) was used as supplied in titrimetric analysis. 2g of potassium iodide was dissolved in 10 ml of deionized water to give 20% (w/v) solution.

2.2.12. Starch Indicator

Starch (A.R) was used as supplied. 1.0g of soluble starch (A.R.) was dissolved in 100ml deionized water and a freshly prepared solution was used every time.

2.2.13. Sulfuric Acid Solution (H_2SO_4)

Solution of sulfuric acid (A.R) was prepared by dissolving the requisite volume of sulfuric acid in doubly distilled water and then the solution was standardized against prestandardized solution of sodium hydroxide employing phenolphthalein as an indicator. This was kept stoppered as a stock solution.

2.2.14.Perchloric Acid ($HClO_4$)

Stock solution of perchloric acid was prepared by diluting 70% guaranteed reagent grade (E. Merck) perchloric acid. Perchloric acid solution was standardized by titrating a known aliquot of perchloric acid solution against sodium hydroxide solution using phenolphthalein as an indicator.

2.2.15. Sodium Hydroxide (NaOH)

The solution of sodium hydroxide was prepared by dissolving approximately weighed pellets of NaOH (BDH Analar) in doubly distilled water. The solution was standardized by titration the known aliquot sample against the standard oxalic acid solution to the phenolphthalein end point [19, 20]. However, sodium hydroxide solution was always used after standardizing as these solutions deteriorate on standing at ambient temperature.

2.2.16. Oxalic Acid [$(COOH)_2$]

Oxalic acid (A.R.) is a primary standard and its aqueous solution exhibits longer stability. The solution of oxalic acid was kept in the dark at ambient temperature to check any photo light decomposition.

2.2.17. Sodium Perchlorate ($NaClO_4$)

Sodium perchlorate solutions of required concentration were prepared by neutralizing perchloric acid with sodium carbonate (A.R.) to the pH ~6.8. The dissolved CO_2 in the solution was expelled on heating before making up the required volume.

2.2.18. Sodium Bicarbonate Solution (Na_2CO_3)

Stock solution of sodium bicarbonate was prepared by dissolving 4g of sodium bicarbonate (A.R) in 100 ml of deionized water.

2.2.19. Acetic Acid (CH_3-COOH)

Acetic acid was of (BDH, AnalaR) grade, its solution were prepared by diluting the acid and the solution was standardized by titrating it against the prestandardized solution of sodium hydroxide using phenolphthalein as an indicator [20].

2.2.20. Sodium Acetate (CH_3COONa)

Sodium Acetate was of G.R. grade (E. Merck) and its solution was prepared by dissolving the required quantity of the salt in doubly distilled water. The solution of acetates does not show any decomposition even in diffused light for a longer period.

2.2.21. 2, 4 –Dinitrophenylhydrazine Reagent

The reagent is prepared by means of Brady's method for aldehydes produced from amino acids, requisite amount of 2, 4-Dinitrophenylhydrazine was treated with 2.0 mol dm^{-3} HCl was added cautiously with cooling and 10 ml of deionized water was added.

2.2.22. Nessler's Reagent

100g of mercury (II) iodide and 70 g of potassium iodide were dissolved in100ml deionized water. The resulting solution was added with stirring to a solution of 160g of sodium hydroxide in 700 ml deionized water. This was then diluted to one liter with deionized water. The precipitate was allowed to settle for three days and the supernatant liquid was decanted and kept in a brown bottle.

All other reagent viz. hydrochloric acid, potassium sulphate, potassium chloride, ammonium chloride etc. were either of (BDH, AnalaR) grade or (E. Merck) guaranteed reagent grade. Their solutions were prepared by dissolving requisite quantities in known volumes of doubly distilled water and details regarding the preparation of their solutions are given in the respective chapters.

Kinetic procedure and methodology [21] adopted for the monitoring of kinetics and analysis of the kinetic results is given in concerned chapters. All glass vessels employed both for storing reagents solutions and also for kinetics were either of pyrex or coring make.

2.3. References

[1] L. Reimer, ***Transmission electron microscopy: physics of image formation and microanalysis; Springer–Verlag, Berlin: New York. 1989.***

[2] D. B. Williams, C. B. Carter, ***Transmission electron microscopy: A textbook for material science, Plenum Press, New York, 1996.***

[3] http://commons.wikipedia.org/wiki/File:TEM_ray_Diag.basic.en.png, visited **June, *2010.***

[4] P. J. Grundy, G. A. Jones, ***electron microscopy in the study of materials, Edward Arnold, London, 1976.***

[5] J. Goldstein, ***Scanning electron microscopy and X-ray microanalysis: A text book for biologist, material scientist, geologist, Plenum Press, New York, 1992.***

[6] http://www.purdue.edu/REM/rs/sem.htm, **visited June, *2010.***

[7] F. A. Settle, ***Handbook of instrumental techniques for analytical chemistry, Prentice Hall, Upper saddle River, N. J., 1997.***

[8] B. Stuart, D. J. Ando, ***Modern infrared spectroscopy, Wiley, Chichester, New York, 1996.***

[9] W. L. Brans, A. Dereux, T. W. Ebbesen, ***Nature***, 424 (2003) 824.

[10] F. Strelow, A. Fojtik, A. Henglein, ***J. Phys. Chem.,*** 98 (1994) 3032.

[11] A. C. Templeton, J. J. Pietron, R. W. Murray, P. Mulvaney, ***J. Phys. Chem. B,*** 104 (2000) 564.

[12] (a) C. Bullen, P. Mulvaney, ***Langmuir,*** 22 (2006) 3007. (b) A. Henglein, ***J. Phys. Chem. B,*** 103 (1999) 9302.

[13] J. J. Mock, D. R. Smith, S. Schultz, ***Nano Lett.,*** 3 (2003) 485.

[14] U. Kreibig, M. Vollmer, ***Optical properties of metal clusters, Springer, Berlin: New York, 1995.***

[15] A. D. Mcfarland, R. P. Van Duyne, ***Nano Lett.,*** 3 (2003) 1057.

[16] K. Bottger and W. Bottger, **Z. Anal. Chem,** 70 (1927) 225.

[17] Rosin, **Reagent Chemicals and Standards, 2nd Edition, 1946**.

[18] I. M. Kolthoff and R. Belcher, **Volumetric Analysis, inter science, New York, 1957.**

[19] A. I. Vogel, **A Text Book of Quantitative Inorganic Analysis, Longmans,** 2 (1961) 240**.**

[20] C. J. Battaglia and J. O. Edwards, **Inorg. Chem,** 4 (1965) 552.

[21] M. Latshaw**, J. Am. Chem. Soc,** 47(1925) 793.

Chapter-3

Experimental Investigation on the Synthesis of Copper Nanoparticles by Chemical Reduction Method

Abstract

The aim of this Chapter is to give an overview of the development and implications of nanoparticles synthesis which is an emerging field that covers a wide range of applications. It play a major role in the development of innovative methods to produce new products to suitable existing production equipment and to reformulate new material and chemicals with improved performance resulting in less consumption of energy and material and reduce harm to the environment as well as environmental remediation. Nanoparticles is an expected to be fruitful areas which are synthesized recently via various techniques, typically categorized as bottom up and top down methods mentioned in literature. The properties of copper nanoparticles (Cunps) depend largely on their synthesis procedures. This chapter describes the details of experimental work related to the synthesis of copper nanoparticles by chemical reduction method using L-ascorbic acid as reducing agent and antioxidant. Synthesized nanomaterials are characterized for morphological identification. Results based on different characterization techniques such as UV-Visible spectrophotometer, FT-IR spectroscopy, Transmission Electron Microscopy (TEM), Scanning Electron Microscopy (SEM) are discussed in this chapter.

3.1. Introduction

Nanotechnology is the most promising technology that can be applied almost all sphere of life, ranging from electronics, pharmaceuticals, defense, transportations heat transfer to sports and aesthetics. Major scientific interest targeting fabrication of metal nanoparticles of distinct shape and diminutive size has been developed in the recent years because of their exclusive properties as compared to their bulk materials [1-3]. Metal nanoparticles with variety of shape and size allow exploring their fascination applications in fields like catalysis, electronics, sensor, and optical device [4-6]. Most of the unique properties of metal nanoparticles are a consequence of their nano size scale regime. Metallic nanoparticles are of great interest due to their excellent physical, chemical and catalytic properties such as high surface to volume ratio and high thermal conductivity. The micro fabrication of conductive features like inkjet technology is common. So for electronics devices have utilized noble metal like gold and silver for printing highly conductive element while cost of noble metals are very high, copper is low cost, conductive material, therefore it is economically attractive. Copper nanoparticles have also been considered [7, 8] as an alternative for noble metals in many applications such as heat transfer and microelectronics [9] due to their low cost and easy availability.

Fabrication of nanomaterials with strict control over size, shape, and crystalline structure has become very important for the applications of nanotechnology in numerous fields including catalysis, medicine and electronics. From the present literature perspective development of suitable method for such nano materials and their uses in various practical applications is an important task. Synthesis methods for nanoparticles are typically grouped into two categories: “top-down” and “bottom-up” approach. The first involves the division of a massive solid into smaller and smaller portions, successively reaching to nanometer size. This approach may involve milling or attrition. The second, “bottom-up”, method of nanoparticle fabrication involves the condensation of atoms or molecular entities in a gas phase or in solution to form the material in the nanometer range.

The latter approach is far more popular in the synthesis of nanoparticles owing to several advantages associated with it. There are many bottom up methods of synthesizing metal nanomaterials, such as vacuum vapor deposition [10], pulsed laser ablation [11] and pulsed wire discharge [12] are physical techniques while chemical reduction [13-17], Micro emulsion techniques [18], sonochemical reduction [19], Electrochemical [20], Microwave assisted [21], and hydrothermal [22] are chemical approaches for the synthesis of nanoparticles.

Chemical reduction method usually employed for the synthesis of nanomaterial will be discussed in detail in this chapter because the materials reported in subsequent chapters was fabricated using this method. Chemical reduction method is widely selected for the synthesis of copper nanoparticles because it has simple control on the size and distribution of particles under controlled experimental parameters [23-26]. The parameters such as temperature, reaction time, reducing agent, precursor type, concentration and even mixing, effect on the nucleation, growth and agglomeration phenomena, consequently particle size distribution of nano materials. It is known that pure iron, cobalt and nickel nanoparticles are very difficult to synthesize due to their high chemical activity. Copper, which is less active than iron, cobalt and nickel, and more active than noble metals such as Ag and Au, is not easily produced via reduction of precursor salts, even in the presence of protecting/capping agents [15]. Although synthesis of copper nanoparticles has been carried via numerous routes is reported [27], very less is known about the size dependent performance of copper nanoparticles as a suitable catalyst.

The main difficulty lies in their preparation and preservation as they oxidized immediately when exposed in air. Scientists are using different inert media such as Argon, Nitrogen [6, 28, 29] to overcome this oxidation problem also using reducing, capping or protecting agents for the reduction of copper salt used. But the use of some hazardous reducing and protecting agent [30-36] are very expensive and makes the process toxic in some cases. To avoid the toxicity and to prepare copper nanoparticles in green environment, we have used ascorbic

acid in chemical reduction process. Ascorbic acid works both as reducing and protecting agent, which makes the process economical, nontoxic and environment friendly [27]. In this study, ascorbic acid (hydrogen potential of +0.08 V) can easily reduce metal ions with standard reduction potential higher than 0 V, such as Cu^{2+}, Ag^{+}, Au^{3+} and Pt^{4+} but cannot reduce these ions with potential less than 0 V such as Fe^{2+}, Co^{2+}, Ni^{2+}. Hydrogen free radicals released from ascorbic acid react rapidly with hydroxyl free radicals and oxygen, whose existence is usually related to the oxidation of the nanoparticles, so our experiment was performed without inert gas protection and pure copper nanoparticles were obtained.

Despite that oxidation resistance and dispersion are of immense importance in several applications but few studies have been carried out in this area. So in the present study, the influence of different concentration of L-ascorbic acid, precursor salt ($CuCl_2 \cdot 2H_2O$) and reaction temperature on the oxidation and dispersion of the aqueous copper nanoparticles were investigated. Copper nanoparticles were prepared with single reduction method without protective gas.

3.2. Chemical Reduction Method for Synthesis of Nanoparticles

Nowadays, the attention of many scientists is focused on the development of new methods for synthesis and stabilization of nanoparticles. Moreover, special attention is paid to monodispersed and stable particles formation. Different metals, metal oxide, sulfides, polymers, core-shell and composite nanoparticles can be prepared using a number of synthetic chemical methods are Microemulsion method, Electrochemical method, Sonochemical method, Photochemical method, Sol-gel method, Solvothermal decomposition method, Hydrothermal method, Microwave method, Chemical reduction method [37-45].

One of the most important methods for the synthesis of copper nanoparticles is the chemical reduction method. This method was presented by Faraday at 1857 [45] and has become the most effective methods in the nanomaterial field. This method is a simple one-pot solution-phase method for

synthesis of a variety of metal nanoparticles, including copper nano crystals. In this technique a copper salt is reduced by a reducing agent such as ascorbic acid, hypophosphite polyols, sodium borohydride, hydrazine, [15, 46-49]. In addition, it is used from capping agents such as Polyethylene glycol and poly (vinylpyrrolidone) [47, 50]. Some of the chemical reducing reactions can be carried out at room temperature. The latter prevent the undesired agglomeration and formation of metal nanoparticles **(Figure 3.1)** [51].

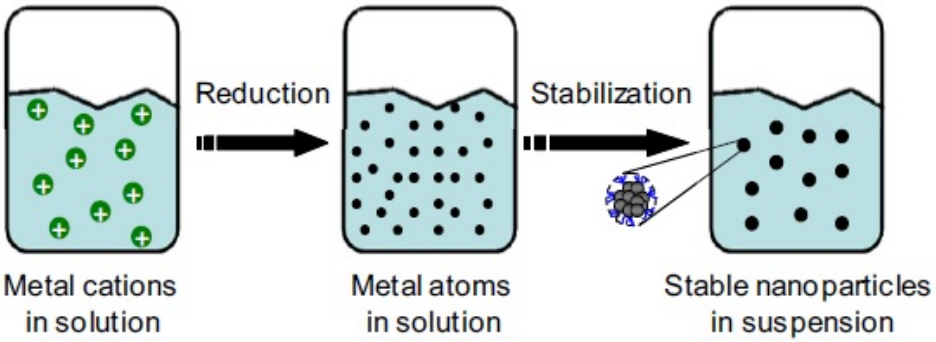

***Figure 3.1: Formation of nanoparticles via reduction of metal salt precursors* [51]**

Colloidal copper with particle sizes of 40–80 nm has been reported from reduction with sodium borohydride in aqueous solution at room temperature. The copper nanoparticles were stabilized by starch [52]. In 2008, copper nanoparticles were synthesized by the reduction of Cu^{2+}in solutions of poly(acrylic acid)-pluronic blends results in a stable sol of metallic copper with a particle size below 10 nm [53]. Reduction of copper ions by sodium borohydride in the presence of sodium polyacrylate was reported. Copper nanocrystals sizes were 14 nm [54]. A simple method for synthesis of metallic copper nanoparticles using $CuCl_2$ as reducing agent and gelatin as stabilizer with a size of 50-60 nm is presented in previous report [55].

Based on these studies, the salt reduction advantage in a liquid medium is our reproducibility and facility to produce nanoparticles with controlled size and large quantities **(Figure 3.2)**. Although, controlling the size and shape are still

being investigated. The actual size of the nanoparticles depends on many factors, including the type of reducing agent, metal precursor, solvent, concentration, temperature and reaction time [56].

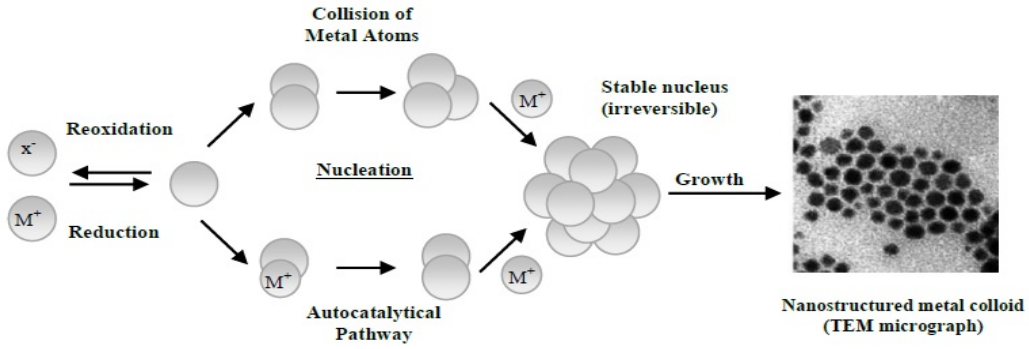

***Figure 3.2: Formation of nanostructured metal colloids by the ''Salt Reduction'' method* [56]**

The reaction temperature and additives are the factors affecting on the shape of copper nanoparticles. Copper nanoparticles were produced by the polyol method in ambient atmosphere. Synthesis of copper nanocubes with an edge length in the range of 100±25 nm is reported [57]. These particles were produced by using ascorbic acid as a reducing agent and poly(vinylpyrrolidone) (PVP) as a capping agent. In this procedure the ethylene glycol (EG) was used as a solvent because of its relatively high boiling point as the reaction temperature was set at 140°C. To avoid copper oxidation, a small amount of the ascorbic acid was added into the mixture, while cooling the final reddish brown solution to 80°C.

High reaction temperature is required to provide enough energy for the growth of nanocubes. Both the dissolution of small copper nanoparticles and the diffusion of Cu atoms on the surface of Cu nanoparticles call for a relatively high temperature. **Figure 3.3** shows Cu nanocubes fabricated at 140°C with a size of 100 ± 25 nm, while most of synthesized nanoparticles at 25°C were smaller than 30 nm **(Figure 3.4)**.

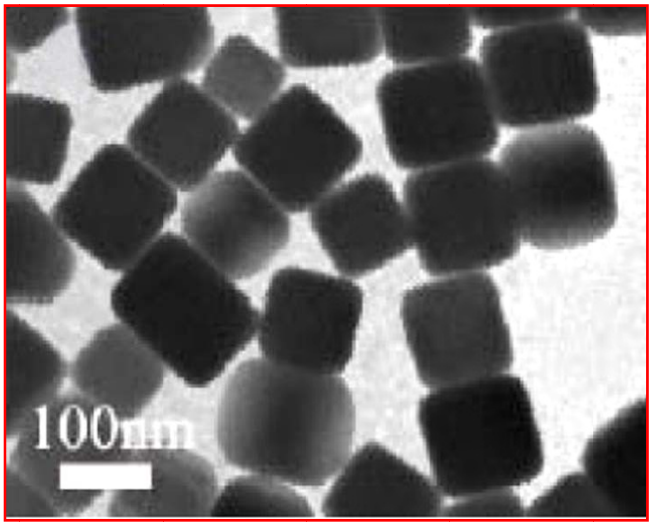

***Figure 3.3: TEM image of copper nanocubes synthesized by a simple one-pot solution-phase method at 140°C, in the presence of PVP and ascorbic acid* [57]**

The surface-regulating polymer (PVP) is considered not only as a stabilizer but also as the shape controller. The selective interaction of particles with PVP may lead to the formation of copper nanocubes. The introduction of PVP to the system could have enhanced the growth rate along the [001] direction and/or reduced the growth rate along the [111] direction so that PVP played a key role in nanocube formation [57]. Shape-controlled synthesis of copper nanoparticles in one-phase liquid systems can also be partially achieved by this method.

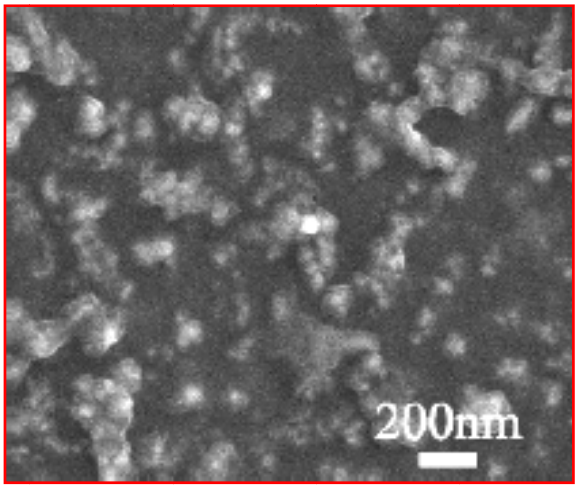

***Figure 3.4: SEM image of copper nanoparticles prepared using a procedure similar to that of Figure 3.6 except reaction system was kept at 25°C for 24h* [57]**

In the journey of the research work copper nanoparticles have been prepared by chemical reduction method. The synthesis route is robust, cost effective, efficient in yield, and requires limited equipment in ambient condition. So we have selected this method for the present work. The next section of this chapter deals with synthesizing of copper nanoparticles and investigates the effect of reactant concentration and reaction temperature on morphology of dispersed copper nanoparticles.

3.3. Experimental Investigation on the Synthesis of Copper Nanoparticles

We report a total ‘‘green’’ chemical method in aqueous solution for synthesizing the highly stable narrowly distributed copper nanoparticles without any inert gas protection. In this synthesis route, chemical reduction of copper salts by L-ascorbic acid is a new and green approach in which L-ascorbic acid, natural vitamin C (VC), an excellent oxygen scavenger, acts as both reducing agent and antioxidant, to reduce the metallic ion precursor, and to effectively prevent the common oxidation process of the new born pure copper nanoclusters. The formation of copper nanoparticles in dispersion was monitored through the analysis of absorbance spectra by UV-Visible Spectrophotometer which contributed towards the understanding of surface plasmon resonance (SPR) generation and optical behavior of copper nanoparticles at different stages during the process of synthesis. The morphology of copper nanoparticles was characterized by Scanning Electron Microscopy (SEM) and Transmission Electron Microscopy (TEM). The product of adding L-ascorbic acid in copper salt was characterized by Fourier Transform Infrared (FTIR) Spectrophotometer. The study revealed that L-ascorbic acid plays an important role of protecting the copper nanoparticles to prevent oxidation and agglomeration, so they have good stability for application.

3.3.1. Synthesis of Copper Nanoparticles

In the one step synthetic procedure, copper nanoparticles were obtained via a wet chemical reduction route. This new procedure for copper nanoparticles

fabrication was a simple process. $CuCl_2 \cdot 2H_2O$ aqueous solution was prepared by dissolving $CuCl_2 \cdot 2H_2O$ (0.02 mol dm^{-3}) in 50 ml deionized water and a blue color solution obtained. The flask containing aqueous solution of $CuCl_2 \cdot 2H_2O$ was heated to 80°C in an oil bath with magnetic stirring. 50 ml of L-ascorbic acid aqueous solution (0.10 mol dm^{-3}) was added to the aqueous solution of copper salt while vigorously stirring at 80°C in an oil bath. With the passage of time, the color of dispersion gradually changed from white, yellow, orange, brown, finally dark brown with a number of intermediate stages **(Figure 3.5).** The whole process of synthesis is given in a flowchart in **figure 3.6.** The appearance of yellow color followed by orange color indicated the formation of fine nanoscale copper particles from L-ascorbic acid assisted reduction. Schematic illustration of the synthesis of copper nanoparticles by the reduction of Cu^{2+} to zero-valent Cu particles with ascorbic acid is given in **scheme 1.**

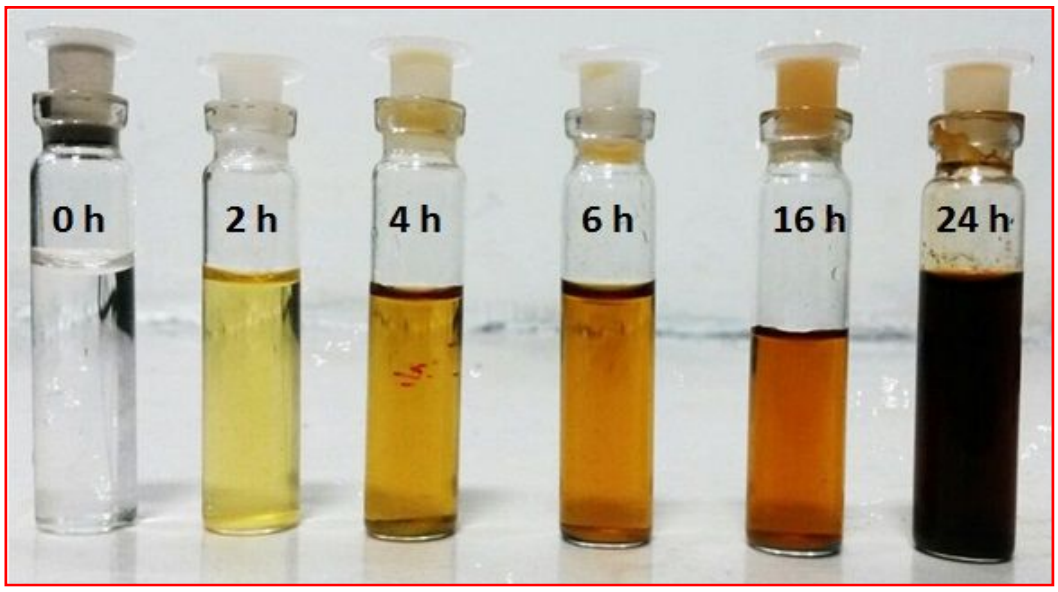

Figure 3.5: The time evolution photograph of copper nanoparticles formation

The resulting dispersion was centrifuged for 15 minutes. The supernatant was placed under ambient conditions for 2 months. Various optimization studies were performed to investigate the size and shapes of copper nanoparticles. We have performed several experiments with varying experimental parameters such as concentration of reducing agent (ascorbic acid), precursor salt concentration and reaction temperature to investigate the size and shapes of copper nanoparticles.

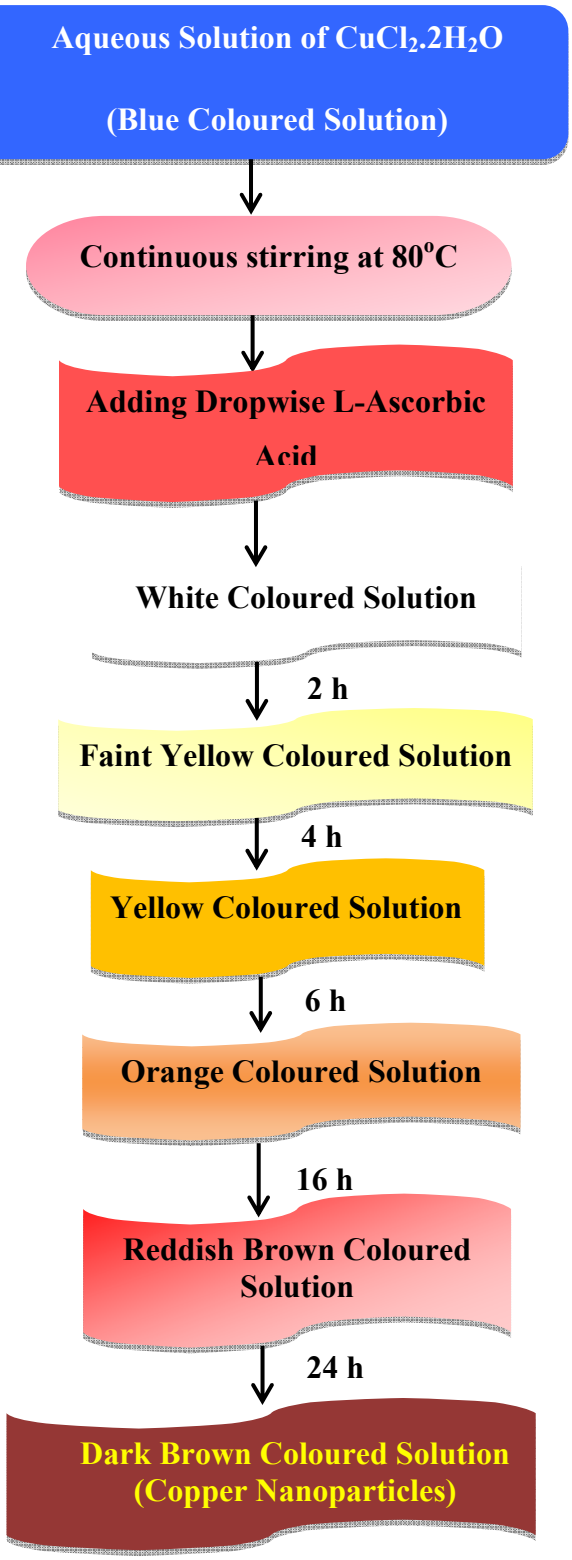

Figure 3.6: A Flow chart for the synthesis of copper nanoparticles by chemical reduction method

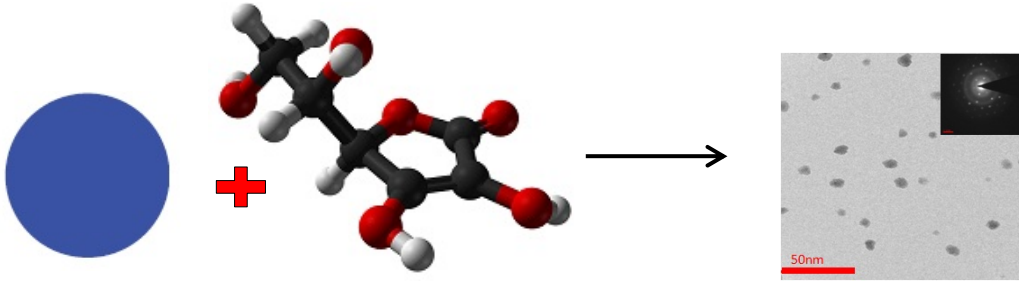

$CuCl_2.2H_2O$ Ascorbic Acid Copper nanoparticles

Scheme 1: Schematic illustration of synthesis of monodispersed highly stable copper nanoparticles

3.3.2. Characterization

The synthesized copper nanoparticles were characterized by SEM, TEM, FTIR and UV-Visible spectrophotometer analytical techniques. Details of these techniques are given in chapter 2 (Instrumentation and Materials).

3.4. Results and Discussion

3.4.1. Optical Characterization of Copper Nanoparticles

Unlike bulk gold metal, nanoscale gold spheres has red or violet color in aqueous solution, similarly silver and copper metal nanoparticles are yellow and brown respectively in aqueous solution. The bright colors possessed by noble metal nanoparticles are due to the collective oscillations of conduction band electrons that are excited by light of appropriate frequencies. The light scattering due to collective oscillation of the conduction electrons induced by the incident electric field in nanometer sized colloidal metal particles is known as localized surface plasmon resonance (SPR) and these are surface electromagnetic waves that propagate in a direction parallel to the metal/dielectric (or metal/vacuum) interface [58].

Figure 3.7 shows the displacement of the conduction electron charge cloud relative to the nuclei of spherical nanoparticle. The electric field of an incoming light wave induces a polarization of the conduction electrons with respect to the much heavier ionic core of a spherical copper nanoparticle. A net charge difference is only felt at the nanoparticle boundaries (surface), which in

turn acts as a restoring force. In this way a dipolar oscillation of the electrons is created with period. This is known as the surface plasmon absorption. This effect can be used to estimate the formation of nanoscale metal particles in the solution medium through simple UV-Vis spectrophotometry.

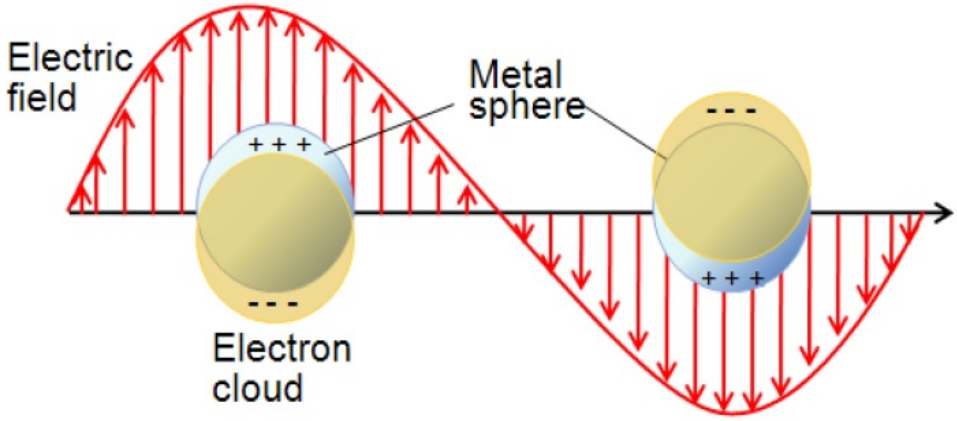

***Figure 3.7: Schematic illustration of the collective oscillation of free electrons under the effect of an electromagnetic wave* [59]**

It is worth mentioning that SPR of metal nanoparticles is greatly a size-dependent phenomenon. The electron scattering enhancement at the surfaces of nanoparticles increase bandwidth and decrease the particle size. Hence, variations in bandwidth and shifts in resonance are very important parameters in characterizing the nanosized regime metal particles [50].

UV-Visible absorbance spectroscopy has proved to be a very useful technique for studying metal nanoparticles because nanoparticles have a high surface area to volume ratio the surface plasmon resonance frequency is highly sensitive to the shape, size of nanoparticle and dielectric nature of its interface with the local environment [60-63]. During the synthesis of copper nanoparticles in aqueous solution, the UV-Visible spectra of samples were recorded at different time intervals for every color change presented in **figure 3.8.**

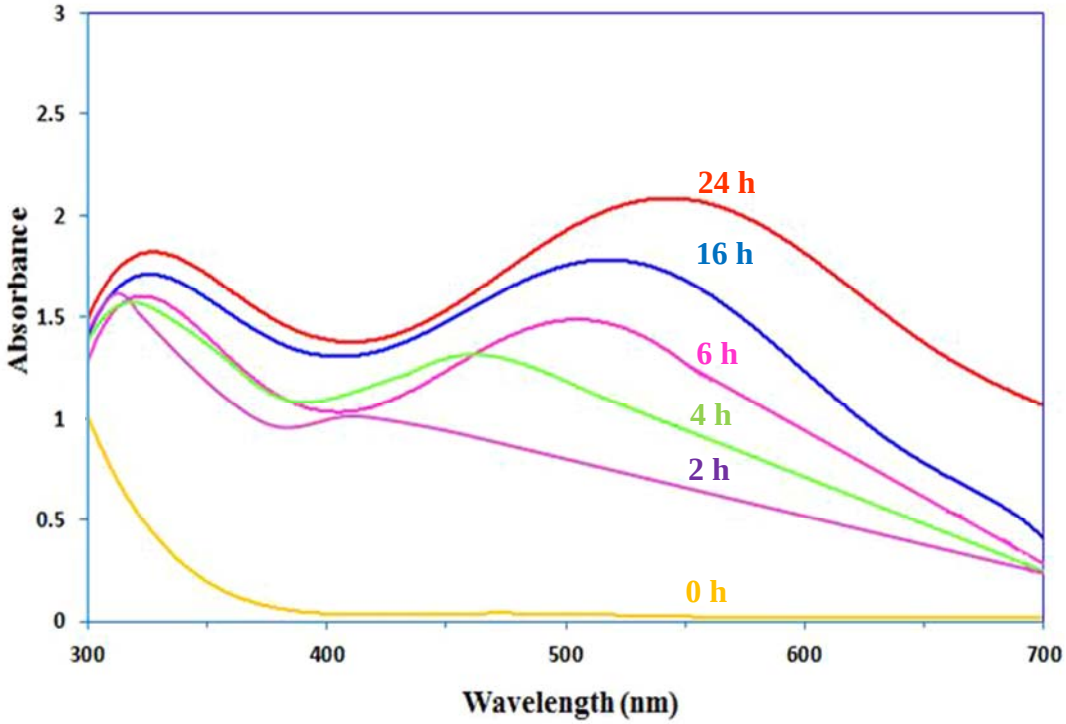

Figure 3.8: UV-Visible spectra of copper nanoparticles synthesized in an aqueous medium at different time intervals (Time 0-24 hours) during the reaction

The solution becomes colorless when L-ascorbic acid was added and turned to yellow, orange, brown and finally dark brown. Similar color changes have also been observed in previous studies [64]. However, initially there was no absorption peak, latter a broad SPR band was generated by the same sample within two hour of reaction time. There was an intensity increases with the reaction progressing, it was due to the growth of copper nanoparticles. The synthesis process was completed after 24 hour. A dark brown color appeared after 24 hour together with a highly SPR peak having maximum absorption at 550 nm which proves the formation of copper nanoparticles. In this work, the resulting copper nanoparticles displayed a broadened peak at the range 540-560 nm wavelength, indicating the presence of small separated copper nanoparticles. These experimental investigations were found to be in very good agreement with the results which is presented in the literature [65-67]. Moreover, UV-Vis spectral analysis was carried out for a number of samples prepared in the aqueous medium to optimize parameters such as different concentrations of reducing agent (L-ascorbic acid) on the synthesis of copper nanoparticles.

It is also evident that the small increase in absorbance turns orange color to red, which indicates the formation of nanoclustor of zero valent Cu under the influence of reduction reaction [68]. The solution was kept under an ambient atmosphere for two months.

3.4.2. Effect of Reducing Agent

3.4.2.1. Effect of Reducing Agent on SPR Peak Position

The formation of copper nanoparticles was confirmed by the generation SPR with a maximum absorbance at 550 nm. An excess of L-ascorbic acid was required to produce size homogeneity and well-dispersed copper nanoparticles in colloidal form. The effect of L-ascorbic acid concentrations on the SPR peak position of the synthesized copper nanoparticles was investigated with varying the ascorbic acid concentration from 0.07 to 0.10 mol dm^{-3} at constant other experimental parameters. The resulting UV-Vis spectra are shown in **figure 3.9.**

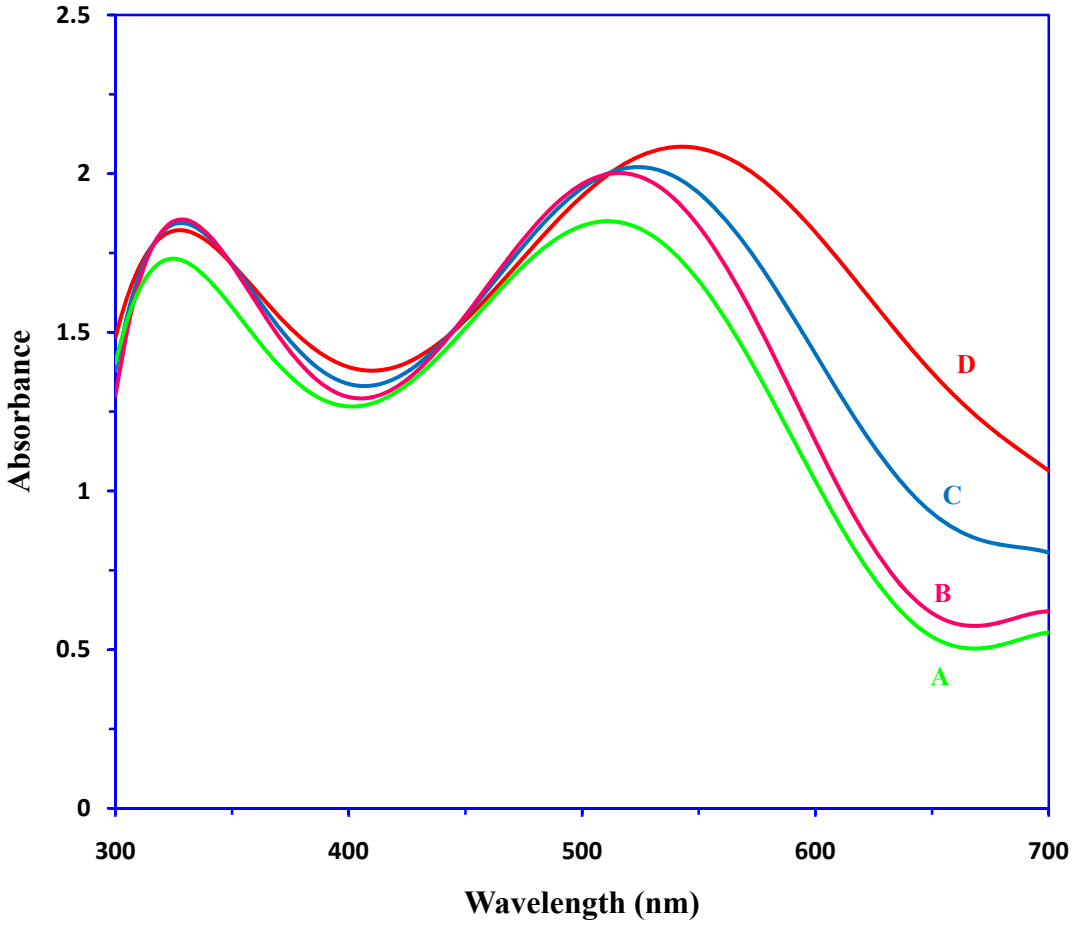

Figure 3.9: The UV-Visible absorption spectra of copper nanoparticles stabilized in L-Ascorbic acid with various concentrations: (A) 0.07 mol dm^{-3}, (B) 0.08 mol dm^{-3}, (C) 0.09 mol dm^{-3} and (D) 0.10 mol dm^{-3}

The first absorption peak of different curves is at 335 nm corresponding to oxidation product of L-ascorbic acid [67]. The second absorption peak is increasingly broadening with an increasing concentration of L-ascorbic acid. A broad and clear peak at 550 nm was observed when the color changed from yellow to orange and also when the reaction mixture gives a brown color **(Figure 3.5).** Moreover, with increasing the concentration of reducing agent higher nucleation rates resulted and consequently generated greater number of nanoparticles. Hence, the SPR peaks increasingly broadening with increase in absorbance as the increases the concentration of reducing agent, which is shown in the **figure 3.9**. Herein, **figure 3.9 D** shows maximum absorbance at the concentration of reducing agent (0.01 mol dm^{-3}). This phenomenon was also supported by previous studies [67]. The above result indicates that a higher L-ascorbic acid concentration leads to more effective capping capacity of L-ascorbic acid, suggestive of much smaller copper nanoparticles.

3.4.2.2. Effect of Reducing Agent on Particle Size

Particle size distribution and morphology are the most important parameters of characterization of nanoparticles. Morphology and size are measured by electron microscopy. Smaller particles offer larger surface area. As a drawback, smaller particles tend to aggregate during storage and transportation of nanoparticle dispersion. Hence, there is a compromise between a small size and maximum stability of nanoparticles [69]. There are several tools for determining nanoparticle morphology as discussed below.

Transmission Electron Microscope (TEM) Analysis

The effect of L-ascorbic acid concentrations on the morphology and size of the synthesized copper nanoparticles in the solution was investigated by TEM analysis with varying ascorbic acid concentration from 0.07 to 0.10 mol dm^{-3} at 0.02 mol dm^{-3} concentration of $CuCl_2 \cdot 2H_2O$ at 80^oC temperature. The TEM images with histograms of particle size distribution of synthesized copper nanoparticles presented in **figure 3.10** at different concentration of L-ascorbic acid. The HRTEM images clearly show that copper nanoparticles are well dispersed and that their shape is regularly spherical. The size of copper nanoparticles mainly ranges 12 nm to 55 nm at different concentration of L-ascorbic acid.

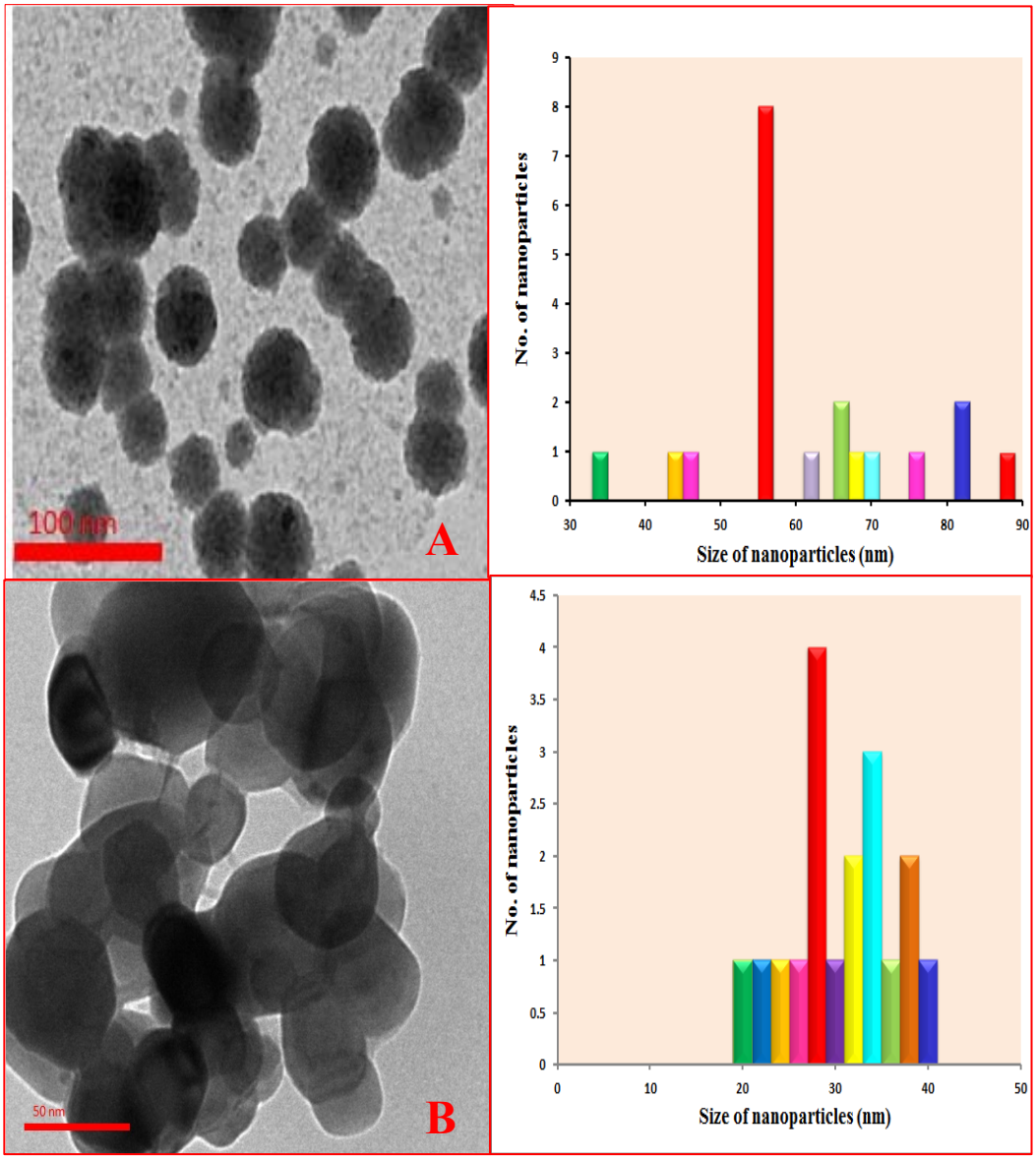
100 nm
A
No. of nanoparticles
Size of nanoparticles (nm)
50 nm
B
No. of nanoparticles
Size of nanoparticles (nm)

Continued…

Continued…

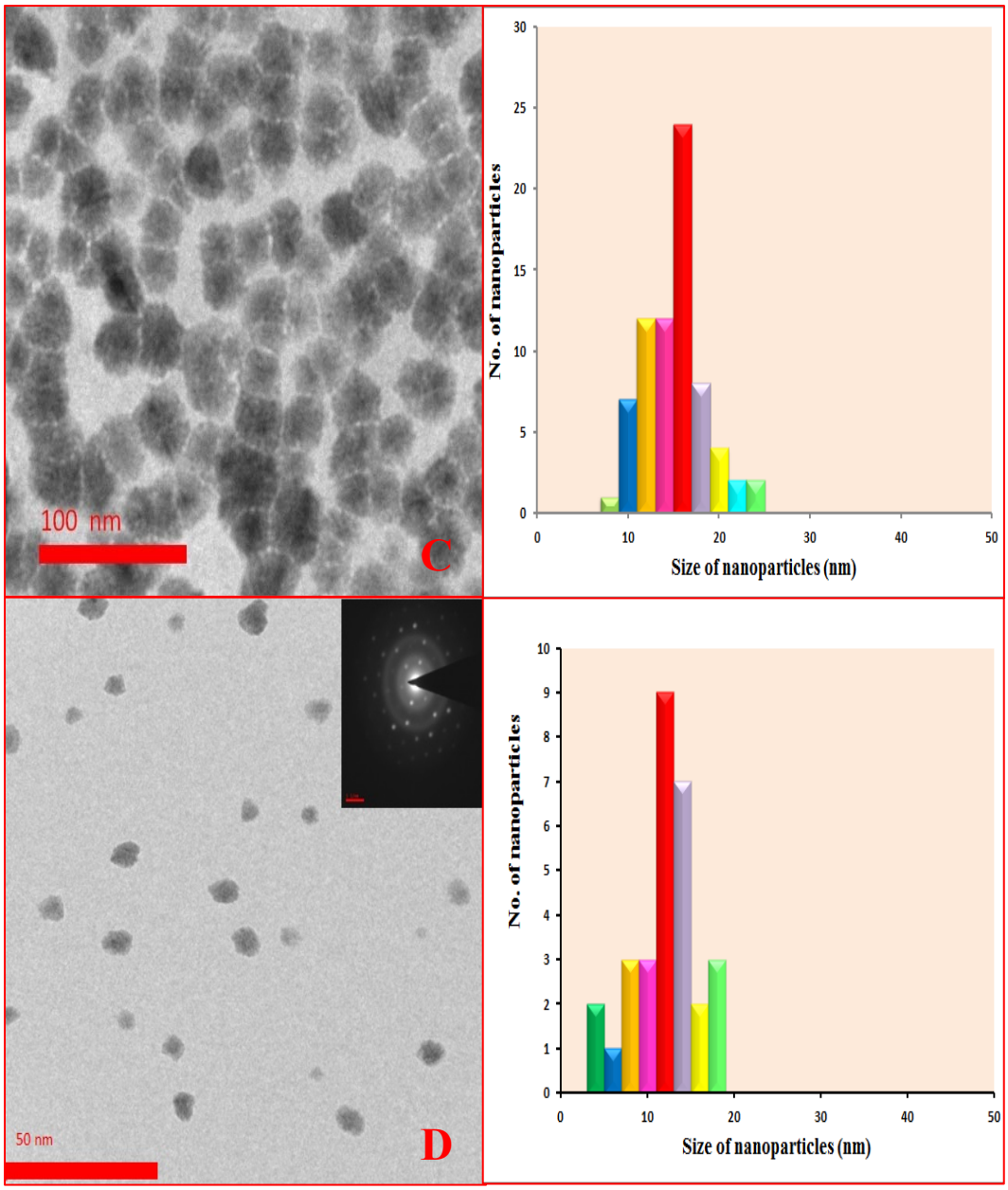

Figure 3.10: TEM images with histogram of the synthesized copper nanoparticles with various concentration of L-ascorbic acid: the average particle sizes (d) are: (A) 0.07 mol dm^{-3}. d = 55 nm (B) 0.08 mol dm^{-3}. d = 28 nm (C) 0.09 mol dm^{-3}. d = 16 nm (D) 0.10 mol dm^{-3}. d = 12 nm.

The crystalline phase of the synthesized nanoparticles was confirmed by selected area electron diffraction pattern (SAED). SAED pattern can clearly display the crystal structure. The inset of **figure 3.10D** shows the SAED pattern recorded from the copper nanoparticles. The ring like diffraction indicates that the particles are crystalline. The SAED pattern suggests that the metal nanoparticles are essentially crystalline and has characteristic face centered cubic structure [59]. The histogram reveals a decrease in particle size with increase of L-ascorbic acid concentration. The size of the copper nanoparticles with various concentration of L-ascorbic acid are (0.07 mol dm^{-3}, 0.08 mol dm^{-3}, 0.09 mol dm^{-3}, 0.10 mol dm^{-3}) 55 nm, 28 nm, 16 nm, 12 nm respectively.

At low reducing agent concentration (0.07 mol dm^{-3}), the reducing rate of the copper precursor is sluggish and consequently only a few nuclei are formed at the nucleation step. Precipitating copper atoms at the later period of the reaction are mostly involved in particle growth by collision with already generated nuclei rather than in the formation of new particles [47]. This reaction mechanism leads to the formation of larger sized particles, as shown in **figure 3.10 A**. With increasing reducing agent concentration, the enhanced reduction rate favors the generation of more nuclei, resulting in the formation of smaller copper particles (**Figure 3.10**).

At a higher reduction rate at 0.10 mol dm^{-3}, the number of precipitating metallic clusters steeply increases and considerably more nuclei are produced during a single event of the nucleation period. Eventually, the size of particles decreases because the amount of solute available for particle growth per growing particle decreases with the increasing number of nuclei. The reason is that L-ascorbic acid molecules encapsulate Cu^{2+} and reduce Cu^{2+} into Cu(0), then oxidation products absorbs on the resulting copper nanoparticles surface preventing the particles from growing further as a result smaller copper nanoparticles obtained. Thus, the number of Cu^{2+} encapsulated in ascorbic acid molecules decreases with increasing concentration of L-ascorbic acid, leading to the formation of smaller copper nanoparticles which is also confirmed by the SEM image of copper nanoparticles is shown in **figure 3.11 C**. SEM image

confirm that the nanoparticles are grown with well-defined morphology and are almost spherical in shape. The results show that more concentration of reducing agent reduces the size of the copper nanoparticles [70].

3.4.3. Effect of Initial Concentration of Precursor Salt

To evaluate the effect of initial concentration of precursor salt on synthesis of copper nanoparticles was studied at four different concentrations $CuCl_2 \cdot 2H_2O$ viz. 0.010, 0.015, 0.020, 0.030 mol dm^{-3} at constant 0.10 mol dm^{-3} concentration of L - ascorbic acid at 80^{o}C temperature. The SEM images of particle size distribution of synthesized copper nanoparticles presented in **figure 3.11** at different concentration of precursor salt ($CuCl_2 \cdot 2H_2O$). Scanning electron microscopy (SEM) is giving morphological examination with direct visualization. The surface characteristics of the sample are obtained from the secondary electrons emitted from the sample surface. SEM photographs shows that copper nanoparticles are nearly monodispersed and spherical in shape [71, 72].

At low precursor salt concentration (0.01 mol dm^{-3}), the generation rate of the copper nuclei is low so only a few nuclei are formed at the nucleation step. It can be seen that reaction rate increases with increases the concentration of Cu^{2+}. With the increasing reaction rate, the amount of copper nuclei rises and smaller particle size are obtained correspondingly which is shown in **SEM images A, B, C of figure 3.11**. It can be explained on the basis of increased nucleation rate due to greater amount of Cu^{2+} ions and generation of smaller nanoparticles in the solution [73]. However, with further increases the concentration of Cu^{2+}, the result is the agglomeration of the nuclei and growing the particle size as shown in **SEM image D of figure 3.11**. The results indicate that an excess number of nuclei will be generated when the Cu^{2+} ion concentration is too high i.e. 0.03 mol dm^{-3}. This may be due to collision between small particles, which leads to particle growth [50] The reason is that there are two stages in the synthesis of copper nanoparticles, the first stage is to generate copper nuclei and second stage is the growth of copper formed [74]. So it is important to control preparation process that copper nuclei must generate faster and grow up slower which require optimum concentration of the precursor salt.

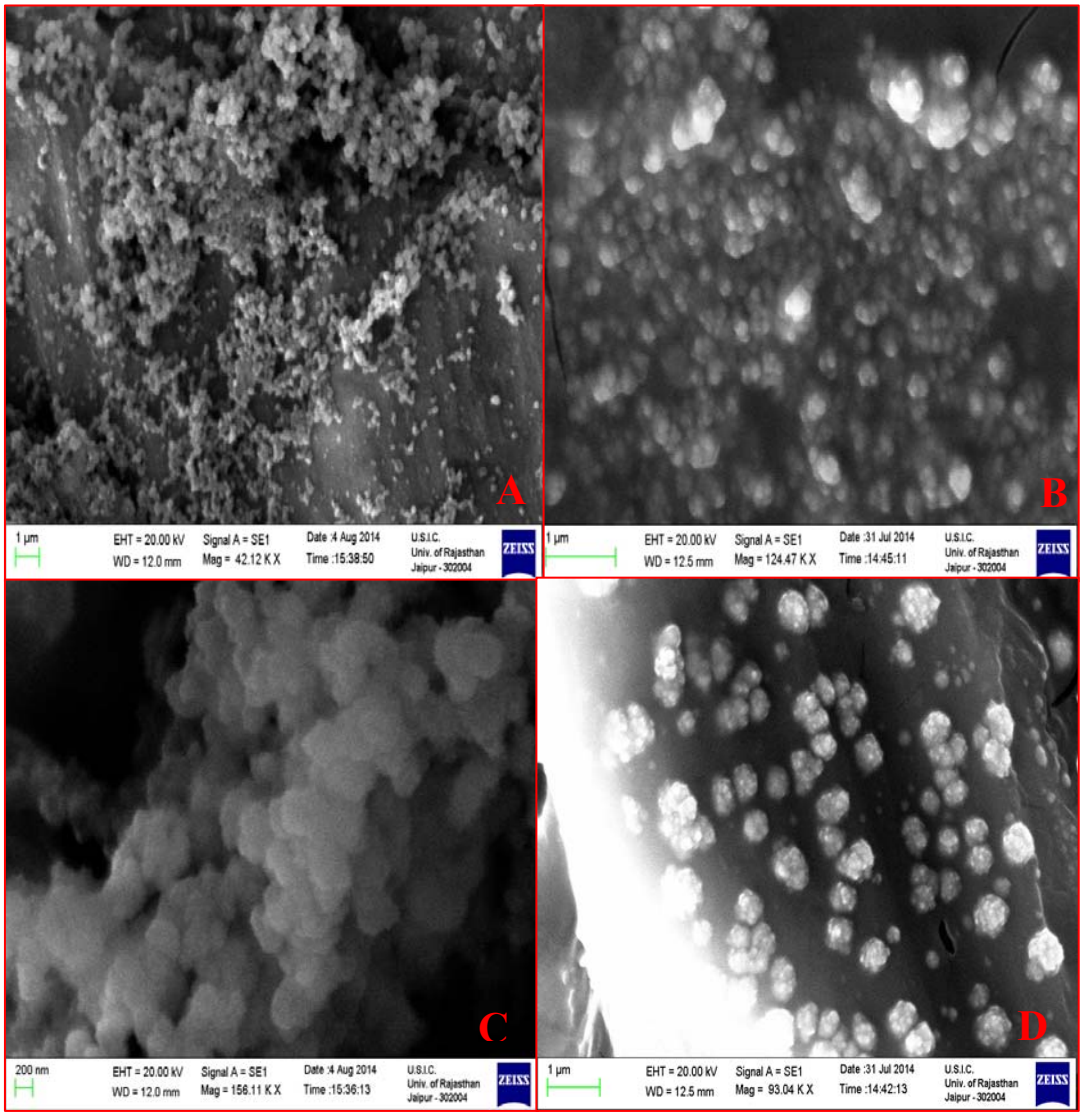

Figure 3.11: SEM images of the synthesized copper nanoparticles with various concentrations of the precursor salt ($CuCl_2 \cdot 2H_2O$) (A) 0.01 mol dm^{-3}, (B) 0.015 mol dm^{-3}, (C) 0.02 mol dm^{-3}, (D) 0.03 mol dm^{-3}

3.4.4. Effect of Reaction Temperature

The present investigation reveals that nanoparticles did not synthesize below the temperature 60^{o}C in any conditions. This shows that reaction constant at this temperature is too low to progress the reaction. Therefore reaction temperature higher than 60^{o}C with appropriate concentration of the reactants should be inserted to the progress of the reaction for synthesis of copper nanoparticles.

In **figure 3.12,** SEM images of copper nanoparticles synthesized at different temperatures (70^{o}C, 80^{o}C, 90^{o}C) respectively, indicates that at higher temperature (90^{o}C), the nanoparticles were agglomerated **(Figure 3.12 C),** while at 80^{o}C are well dispersed with an average size at about 12 nm **(Figure 3.12 B).** With decreasing reaction temperature, the size of the resulting particles becomes smaller and the size distribution is also narrowed [15].

Basically, the reduction of Cu^{+2} were increase by increasing the reaction temperature. A high reducing rate at the temperature of 90^{o}C allows instantaneous multiple nucleations to occur when the reducing solution is added drop wise. The resulting particles at this condition exhibit a relatively broad size distribution due to uneven particle growth and coagulation of the primary particles. Therefore the synthesis rate is too high to control particle size at high temperature. When reducing agent adds to precursor solution at 90^{o}C, rate of growth and agglomeration as well as nucleation of copper nanoparticles accelerated almost coincidently. This phenomena result in the formation of copper nanoparticles was precipitated. In contrast to the reaction at 90^{o}C, the color of dispersion gradually changed from white to brown finally dark brown with a number of intermediate stages **(Figure 3.5)** when the reducing solution is added at 80^{o}C. This indicates that there is no immediate reduction of copper ions upon addition to the reaction medium. Coagulation of the primary particles would be unlikely because the thermal energy is not sufficient for vigorous particle movement. Under these nucleation and growth conditions, as depicted in **figure 3.12 B,** the resulting particles are relatively monodisperse.

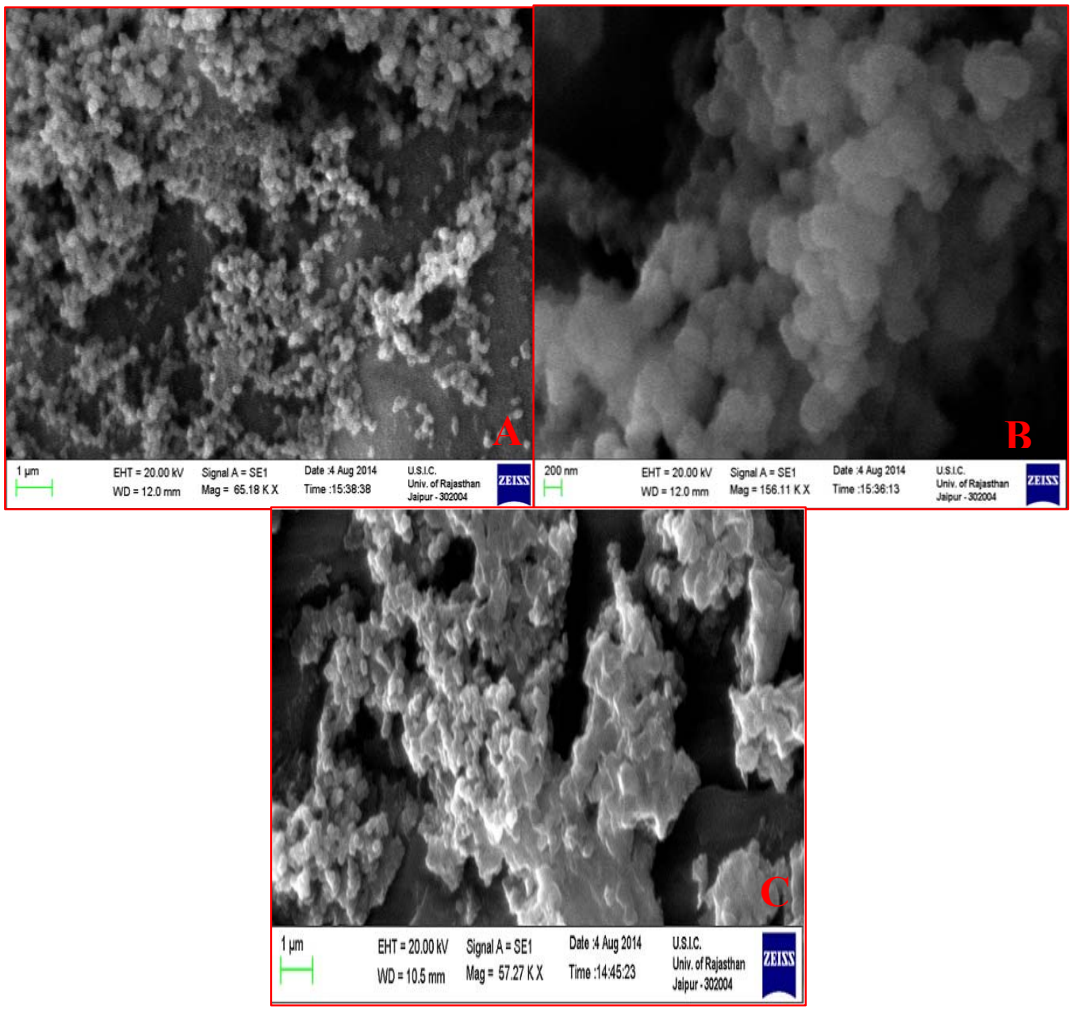

Figure 3.12: SEM images of synthesized copper nanoparticles with variation of temperature (A) 70^{o}C, (B) 80^{o}C, (C) 90^{o}C

At temperature lower than 80^{o}C, however, the reaction medium does not show gradually change in color, implying that the all copper ions do not undergo reduction to copper atoms, so the formation of copper nanoparticles were precipitated **(Figure 3.12 A).** So the optimal conditions for the synthesis of highly stable monodispersed copper nanoparticles are 0.02 mol dm^{-3} concentration of $CuCl_2 \cdot 2H_2O$ and 0.10 mol dm^{-3} concentration of L - ascorbic acid at 80^{o}C temperature.

3.4.5. Stabilization of Metal Nanoparticles

The nanoparticles having large surface energy coalesce to give thermodynamically favored bulk particle. In the absence of any counteractive repulsive forces the van der Waal forces between two metal nanoparticles would lead towards coagulation. Hence for spatial confinement of the particles in nano range it is essential to stabilize the particles. This can be achieved by either electrostatic or steric stabilization [75, 76] by using a capping agent such as polymer [77, 78], surfactant [79], solid support [80] or ligand [81] having suitable functional groups.

The stability of nanoparticles dispersion is key factor in their application including the extremely sensitive to oxygen and colloidal agglomeration. To prevent oxidation, the reaction solutions were carefully deoxygenated and the entire processes were performed under rigorous protection of inert gas in many reported studies [48] and many capping agents such as Polyvinyl Pyrrolidone (PVP) and Polyethylene glycol are used to prevent agglomeration. Some study reveals that to protect copper nanoparticles against oxidation during preparation and storage, ascorbic acid is utilized as reductant and antioxidant of nanostructured copper [82]. L-Ascorbic acid was used as reducing as well as capping agent without any other special capping agent in this work to avoid contamination of other organic compounds.

The aqueous L-ascorbic acid-stabilized copper nanoparticles dispersion was centrifuged for 15 min. A small amount of precipitate was obtained from the bottom of the centrifuge tube. The precipitate was found to be completely soluble

in aqueous solution again after the shaking of the centrifuge tube. In addition, the supernatant obtained by centrifuging was placed under ambient conditions and notably, no precipitation was observed and no sign of sedimentation was observed even after 2 months storage in a simply sealed container, suggestive of long-term stability of the as-prepared Cu colloids. The photographs of dispersion before and after the storage (2 months) are shown in **figure 3.13**. This indicates that the L-ascorbic acid-stabilized copper nanoparticles are highly stable due to the extreme capping effect of the L-ascorbic acid and the dispersion effect of the polyhydroxyl structure.

Figure 3.13: The photos of dispersion of copper nanoparticles (A) before and (B) after 2 months of storage

Mechanism

The above results show that well-dispersed copper nanoparticles can be obtained through the reduction of Cu^{2+} using L-ascorbic acid as both the reducing and capping agent. The structure of L-ascorbic acid is presented in **equation 3.1**. L-ascorbic acid is a highly water-soluble compound with strong polarity. As such, the structure of L-ascorbic acid gives enough reducibility to convert Cu^{2+} ions into Cu(0) nanoparticles. The redox equation of L-ascorbic acid and copper ions can be expressed in **equation 3.1**.

As illustrated in **equation 3.1**, L-ascorbic acid serves as a stable (electron + proton) donor in interactions, and is converted into the radical ion called semi-dehydroascorbate radical and then dehydroascorbic acid. Dehydroascorbic acid and L-ascorbic acid together constitute the redox system (reduction potential ~0.060 V *vs.* SCE) which is sufficient to reduce Cu^{2+} to Cu. Besides, it should be noted that L-ascorbic acid has also played the role of stabilizing agent during the reaction process. During the synthesis process, excessive L-ascorbic acid is essential to avoid the oxidation of copper nanoparticles.

The mechanism of L-ascorbic acid on the effective stability of copper nanoparticles can be explained from two aspects. One is the capping effect of L-ascorbic acid in the reduction process. The L-ascorbic acid is capped with copper ions, and then synthesizes Cu(0) nanoparticles through reduction of Cu^{2+} inside the nanoscopic templates. In the presence of nanoscopic templates, small copper nanoparticles are easily formed. The other explanation is the dispersion effect of the oxidation product of L-ascorbic acid on the copper nanoparticles after the completion of the reduction reaction. L-ascorbic acid is converted into dehydroascorbic acid through oxidation. The antioxidant properties of L-ascorbic acid come from its ability to scavenge free radicals and reactive oxygen molecules [15], accompanying the donation of electrons to give semi-dehydroascorbate radical and dehydroascorbic acid **(equation 3.2).**

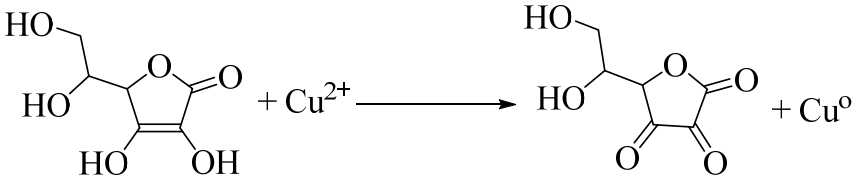

(3.1)

Ascorbic Acid Dehydroascorbic acid

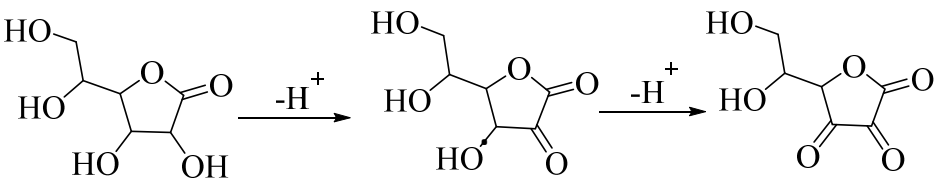

(3.2)

L-Ascorbic acid semi-dehydroascorbate radical dehydroascorbic acid

The dehydroascorbic acid has three carbonyls in its structure. The 1, 2, 3 tricarbonyl is too electrophilic to survive more than a few seconds in aqueous solution and the 6-OH and the 3-carbonyl groups form the hemiacetal rapidly. Hydration of 2-carbonyl is also reported [83]. Finally the polyhydroxyl structure is obtained through hydrolysis [67] **(equation-3.3).**

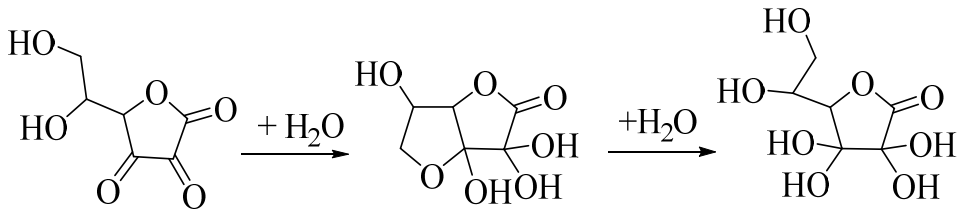

(3.3)

Hydrolysis of dehydroascorbic acid

The extensive number of hydroxyl group can be facilitated the complexation of copper nanoparticles to the number of matrix by inter–intramolecular hydrogen bond and thus prevent the agglomeration of copper nanoparticles. The result is confirmed with FT-IR Spectrophotometer **(Figure 3.14, 3.15).**

Pure L-ascorbic acid is represented in **figure 3.14.** The spectrum of pure L-ascorbic acid revealed that the stretching vibration of C-C double bond and the peak of enol-hydroxyl were observed at **1674.51 cm^{-1} and 1322.56 cm^{-1}**, respectively. These were replaced after the reaction with new peaks **3481.39 cm^{-1}, 1710.06 cm^{-1} and 1680.88 cm^{-1} (Figure 3.15).** These peaks correspond to the hydroxyl, oxidated carbonyl group and conjugated carbonyl group respectively. These results indicate the presence of polyhydroxyl structure on the surface of copper nanoparticles. Therefore L-ascorbic acid plays dual role as reducing agent and antioxidant of copper nanoparticles. Thus reaction can complete without any protective inert gas.

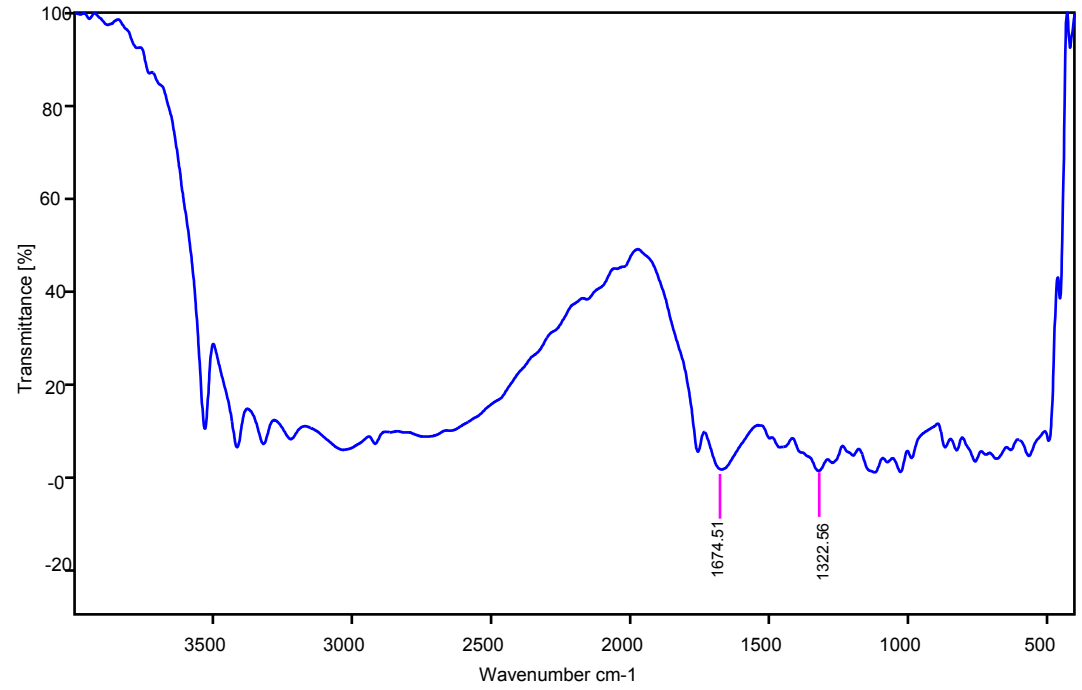

Figure 3.14: FT-IR spectra of pure L-Ascorbic Acid

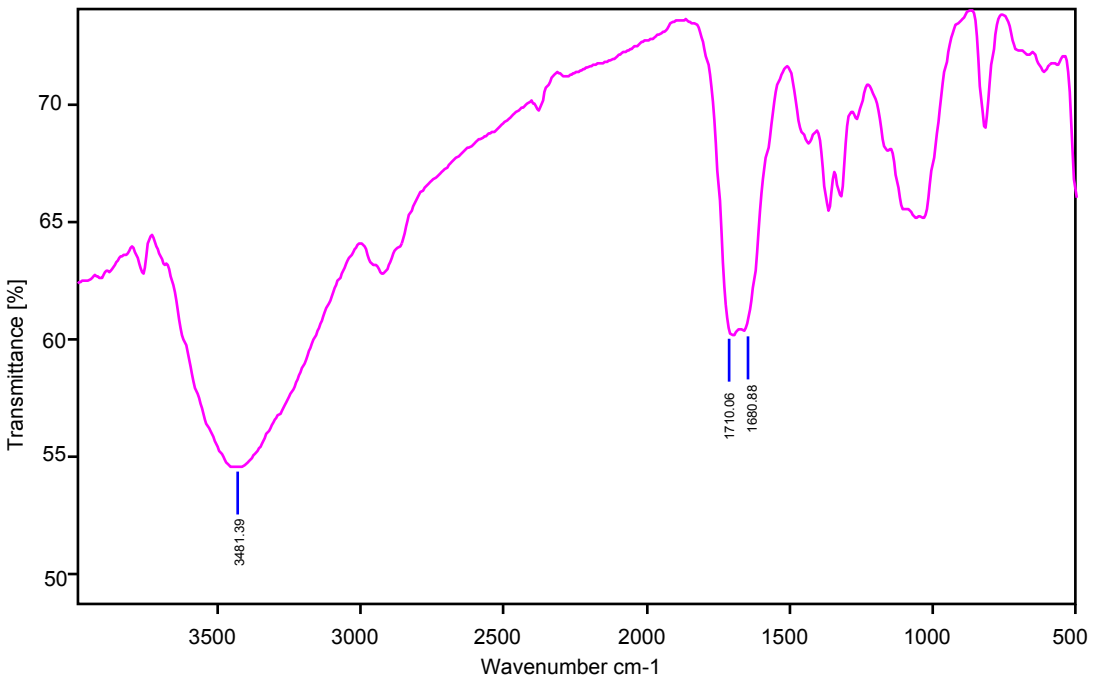

Figure 3.15: FT-IR spectra of L-ascorbic acid-stabilized copper nanoparticle

3.5. Conclusion

In the present study, highly stable copper nanoparticles with narrow and homogenous size distributions were synthesized by the chemical reduction method without employing any protective inert gas. By this green method synthesized copper nanoparticles (ranging from 12 nm to 55 nm) by employing different concentration of L-ascorbic acid as both reducing and capping agent. The characterization results indicate that a higher L-ascorbic acid concentration leads to more effective capping capacity and then forms smaller copper nanoparticles. FTIR spectra show the presence of polyhydroxyl structure on the surface of the copper nanoparticle that gives an excellent dispersion effect on copper nanoparticles.

The prepared copper nanoparticles are highly stable and do not show coagulation or agglomeration even after storage for two months. Moreover, it was clearly shown that the initial concentration of reactant and reaction temperature has an incredible effect on particle size and stability of the synthesized copper nanoparticles. The experimental investigation indicate the optimal conditions for the synthesis of copper nanoparticles are 0.02 mol dm^{-3} concentration of $CuCl_2 \cdot 2H_2O$ and 0.10 mol dm^{-3} concentration of L-ascorbic acid at 80^oC temperature. The obtained copper particles at optimal experimental conditions were confirmed to be crystalline copper with face centered cubic (FCC) structure on the basis of recorded selected area electron diffraction (SAED) spectra. Detailed surface analyses by HRTEM and SEM revealed that the synthesized particles is spherical and monodisperse with size 12 nm.

3.6 References

[1] K. Mallick, M. J. Witcomb, M. S. Scurrell, ***Materials Science and Engineering: B***, 123 (2005) 181.

[2] R. Das, S. S. Nath, R. Bhattacharjee, ***Journal of Luminescence,*** 131 (2011) 2703.

[3] M. Abdulla-al-Mamun, Y. Kusumoto, M. Muruganandham, ***Materials Letters,*** 63 (2009) 2007.

[4] B. R. Cuenya, ***Thin Solid Films,*** 518 (2010) 3127.

[5] Y. Li, F. Qian, J. Xiang and M. L. Charles, ***Material Today,*** 9 (2006)18.

[6] D. L. Feldheim, C. A. Foss, ***Marcel Dekker Incorporated, New York, USA, 2002***.

[7] N. N. Hoover, B. J. Auten and B. D. Chandler, ***J. Phys. Chem. B*****,** 110 (2006) 8606.

[8] Y. Niu and R. M. Crooks, ***Chem. Mater.*****,** 15 (2003) 3463.

[9] J. A. Eastman, S. U. S. Choi, S. Li, W. Yu, L. J. Thompson, ***Appl. Phys. Lett.*****,** 78 (2001) 718.

[10] M. S.Yeh, Y. S. Yang, Y. P. Lee, ***Journal of Physical Chemistry B,*** 103 (1999) 6851.

[11] Z. Liu, Y. Bando, ***Advanced Materials*****,** 15 (2003) 303.

[12] K. Yatsui, C.Grigoriu, H. Kubo, ***Applied Physics Letters*****,** 67 (1995) 1214.

[13] W. K. Han, J. W. Choi, G. H. Hwang, S. J. Hong, J. S. Lee and S. G. Kang, ***Appl. Surface Sci.*****,** 252 (2006) 2832.

[14] S. Sheibani, A. Ataie and S. Heshmati-Manesh, ***J. Alloys Compd.,*** 465 (2008) 78.

[15] C. Wu, B. P. Mosher and T. Zeng, ***J. Nanopart. Res.*****,** 8 (2006) 965.

[16] P. Pulkkinen, J. Shan, K. Leppanen, A. Kansakoshi, A. Laiho, M. Jarn and H. Tenhu, ***Appl. Mater. Interfaces,*** 2 (2009) 519.

[17] X. Cheng, X. Zhang, H. Yin, A. Wang and Y. Xu**,** ***Appl. Surface Sci.*****,** 253 (2006) 2727.

[18] M. P. Pileni, ***Journal of Physical Chemistry,*** 97 (1993) 6961.

[19] R. V. Kumar, Y. Mastai, Y. Diamant, ***Journal of Materials Chemistry*****,** 11 (2001) 1209.

[20] M. Molares, V. Buschmann, D. Dobrev, ***Advanced Materials***, 13 (2001) 62.

[21] S. Takayama, G. Link, M. Sato, ***Microwave and Radio Frequency Applications, In: Proceedings of the Fourth World Congress on Microwave and Radio Frequency Applications, Austin, Texas, USA, 2004.***

[22] L. Y. Chu, Y. Zhuo, L. Dong, ***Advanced Functional Materials*****,** 17 (2007) 933.

[23] Q. Liu, R. L.Yu, G. Z. Qiu, Z. Fang, A. L. Chen, Z.W. Zhao, ***Transac. Nonferr. Metal. Soc. China*****,** 18 (2008) 1258.

[24] H. T. Zhu, C. Y. Zhang, Y. S. Yin, ***J. Cryst. Growth*****,** 270 (2004) 722.

[25] O. Coussy, T.F. Chong, ***Comptes Rendus Mecanique,*** 333 (2005) 507.

[26] A. A. Athawale, P. P. Katre, M. Kumar, M.B. Majumdar, ***Mater. Chem. Phy.***, 91 (2005) 507.

[27] A. Umer, S.Naveed, N. Ramzan, M. S. Rafique, ***Nano,*** 7 (2012) 1230005.

[28] R. W. Siegel, E. Hu, M. C. Roco, ***Nanostructure Science and Technology: R & D Status and Trends in Nanoparticles, Nanostructured Materials, and Nano-devices, In: WTEC Panel Report, Kluwer Academic Press, Dordrecht, Netherland, ed. 1, 1999.***

[29] N. R. Jana, Z. L. Wang, T. K. Sau, ***Current Science,*** 79 (2000) 1367.

[30] F. Bonet, V. Delmas, S. Grugeon, ***Nano Structured Materials,*** 11 (1999) 1277.

[31] C. J. Murphy, T. K. San A, A. M. Gole, ***Journal of Physical Chemistry B****,* 109 (2005) 13857.

[32] I. P. Santos, L. M. Liz-Marzan, ***Langmuir*****,** 15 (1999) 948.

[33] Y. W. Tan, X. H. Dai, Y. F. Li, ***Journal of Materials Chemistry*****,** 13 (2003) 1069.

[34] K. S. Chou, C. Y. Ren, ***Materials Chemistry and Physics*****,** 64 (2000) 241.

[35] Y. Lee, J. R.Choi, K. J. Lee, ***Nanotechnology*****,** 19 (2008) 1.

[36] N. Leopold, B. Lendl, ***Journal of Physical Chemistry B,*** 107 (2003) 5723.

[37] T. Hirai, Y. Tsubaki, H. Sato and I. Komasawa, ***J. Chem. Eng. Japan***, 28 (1995) 468.

[38] M. Raja, J. Subha, F. Binti Ali and S. H. Ryu, ***Mater. Manuf. Process.,*** 23 (2008) 782.

[39] K. S. Suslick, S. B. Choe, A. A. Cichowlas and M. W. Grinsta, ***Nature***, 353 (1991) 414.

[40] G. G. Condorelli, L. L. Costanzo, I. L. Fragala, S. Giuffridaa, G. Ventimigliaa, ***J. Mater. Chem.***, 13 (2003)2409.

[41] C. J. Brinker, S. W. Scherer, ***Sol–Gel science: the physics and chemistry of sol–gel processing. Academic Press, New York, 1990.***

[42] S. H. Yu, ***J. Ceram. Soc. Jpn.,*** 109 (2001) 65.

[43] K. Byrappa, T. Adschiri, ***Progress in Crystal Growth and Characterization of Materials,*** 53 (2007) 117.

[44] K. J. Rao, B. Vaidhyanathan, M. Ganguli, P. A. Ramakrishnan, ***Chem. Mater.,*** 11 (1999) 882.

[45] M. Faraday, ***Philos. Trans. R. Soc., London,*** 147 (1857) 145.

[46] H.T. Zhu, Y.S. Lin, Y.S. Yin, ***J. Colloid. Interf. Sci.,*** 277 (2004**)** 100.

[47] B. K. Park, S. Jeong, D. Kim, J. Moon, S. Lim, J. S. Kim, ***J. Colloid. Interf. Sci.,*** 311 *(*2007) 417.

[48] X. Y. Song, S. X. Sun, W. M. Zhang, Z. L. Yin, ***J. Colloid. Interf. Sci.,*** 273 (2004) 463.

[49] X. D. Su, J. Z. Zhao, H. Bala, Y. C. Zhu, Y. Gao, S. S. Ma, Z. C. Wang, ***J. Phys. Chem. C****,*111 (2007) 14689.

[50] T. M. D. Dang, T. T. T. Le, E. Fribourg-Blanc, M. C. Dang, ***Adv. Nat. Sci. Nanosci. Nanotechnol.,*** 2 (2011) 15.

[51] R. G. Finke, D. L. Feldheim, C. A. Foss, ***Eds. Marcel Dekker, New York, 2002.***

[52] N.V. Suramwar, S. R. Thakare, N. T. Khaty, ***Arab. J. Chem.,*** 5 (2012) 1.

[53] G. Y. Ostaeva, E. D. Selishcheva, V. D. Pautov, I. M. Papisov, ***Polym. Sci. Ser. B.,*** 50 (2008) 147.

[54] R. Prucek, L. Kvitek, A. Panaek, L. Vanurova, J.Soukupova, D. Janik, R. ZboYil, ***J. Mater. Chem.,*** 19 (2009) 8463.

[55] A. K. Chatterjee, R. K. Sarkar, A. P. Chattopadhyay, P. Aich, R. Chakraborty, T. Basu, ***Nanotechnology,*** 23 (2012) 85103.

[56] H. Bonnemann, R. M. Richards, ***Eur. J. Inorg. Chem.,*** 245 (2001) 480.

[57] Y. H. Wang, P. L. Chen, M. H. Liu, ***Synthesis of Well-Defined Copper Nanocubes by a One-Pot Solution Process. Science Citation Index Expanded (2006).***

[58] P. K. Jain, X. Huang, I. H. El-Sayed, M. A. El-Sayed, ***Acc. Chem. Res.,*** 41 (2008) 1578.

[59] J. Biswal, ***A study on synthesis of silver and gold nanoparticles by employing gamma radiation, their characterization and application, Ph.D. Thesis, Bhabha Atomic Research Centre, Mumbai, India (2013).***

[60] E. C. Scher, L. Manna, A. P. Alivisatos, ***Phil. Trans. R. Soc. Lond. A***, 361 (2003) 241.

[61] A. P. Alivisatos, ***Science,*** 271 (1996) 933.

[62] A. P. Alivisatos, ***Endeavour,*** 21 (1997) 56.

[63] C. Chen, A. B. Herhold, C. S. Johnson, A. P. Alivisatos, ***Science,*** 276 (1997) 398.

[64] A. Umer, S. Naveed, N. Ramzan, M. S. Rafique, M. Imran, ***Materia-Rio De Janeiro,*** 19 (2014) 197.

[65] S. Kapoor, R. Joshi and T. Mukherjee, ***Chem. Phys. Lett.,*** 354 (2002) 443.

[66] H. X. Zhang, U. Siegert, R. Liu and W. B. Cai, ***Nanoscale Research Letter,*** 4 (2009) 705.

[67] J. Xiong, Y. Wang, Q. Xue and X. Wu, ***Green Chemistry,*** 13 (2011) 900.

[68] M. J. G. Pacheco, J. E. M. Sanchez, G. Hernandez, F. Ruiz, ***Mater. Lett.,*** 64 (2010) 1361.

[69] H. M. Redhead, S. S .Davis and L. Illum, ***J. Control. Release,*** 70 (2001) 353.

[70] S. Chandra, A. Kumar, P. Kumar, ***Tomar Journal of Saudi Chemical Society,*** 18 (2014) 149.

[71] S. L. Pal, U. Jana, P. K. Manna, G. P. Mohanta, R. Manavalan, ***Journal of Applied Pharmaceutical Science,*** 01 (2011) 228.

[72] K. Jores, W. Mehnert, M. Drecusler, H. Bunyes, C. Johan, K. Mader, ***J. Control Release,*** 17 (2004) 217.

[73] R. A. Soomro, S. T. H. Sherazi, Sirajuddin, N. Memon, M. R. Shah, N. H. Kalwar, K. R. Hallam, A. Shah, ***Adv. Mat. Lett.,*** 5 (2014) 191.

[74] Q. M. Liu, De-bi. Zhou, K. Nishio, R. I. chino, M. Okido, ***Materials Transactions,*** 51 (2010) 1386.

[75] G. Cao, ***Nanostructures and nanomaterials: synthesis, properties and applications, World scientific publishing Co. Pte. Ltd, 2004.***

[76] G. Schmid, ***Clusters and Colloids: From Theory to Application, Weinheim, VCH, 1994.***

[77] J. Shan, H. **Tenhu,** ***Chem. Commun. (Camb),*** 44 (2007) 4580.

[78] P. K. Khanna, R. Gokhale, V. V. V. S. Subbarao, ***J. Mater. Sci.,*** 39 (2004) 3773.

[79] N. R. Jana, ***Small,*** 1 (2005) 875.

[80] H. Yazid, R. Adnan, S. A. Hamid, M. A. Farrukh, ***Turk. J. Chem.,*** 34 (2010) 639.

[81] T. Yonezawa, T. Kunitake, ***Colloid. Surface. A,*** 149 (1999) 193.

[82] W. Yu, H. Xie, L. Chen, Y. Li and C. Zhang, ***Nanoscale Res. Lett.,***4 (2009) 465.

[83] R. C. Kerber, ***J. Chem. Educ.,*** 85 (2008) 1237.

Chapter-4

Kinetics of Copper Nanoparticles Catalyzed Oxidation of Serine by Peroxomonosulphate in Acidic Aqueous Medium

Abstract

Nanoparticles are now key species in the field of reaction catalysis. The relatively low cost and high efficiency has allowed different metal nanoparticles to be used as catalysts in numerous reaction schemes. The kinetics of colloidal copper nanoparticles catalyzed oxidation of serine by peroxomonosulphate (PMS) in acidic aqueous medium has been investigated by titrimetric techniques. The effect of copper nanoparticles on the rate of oxidation of serine has been studied at different concentration of copper nanoparticles at three different sizes of nanoparticles (28, 16 and 12 nm). The copper nanoparticles catalyst exhibited very good catalytic activity and the kinetics of the reaction was found to be first order with respect to serine and peroxomonosulphate concentration. Increase in [H^+] decreased the reaction rate. The main oxidation product of serine has been identified as the aldehyde which is confirmed by the FTIR spectrum of a corresponding hydrazone. The stoichiometry of the oxidation of serine by an oxygen transfer from peroxomonosulphate in the presence of copper nanoparticles was presented by equation (1)

$$HSO_5^- + R-\underset{NH_2}{\overset{H}{\underset{|}{\overset{|}{C}}}}-COOH \xrightarrow[308\ K,\ H^+]{\text{Copper Nanoparticles}} RCHO + NH_3 + HSO_4^- + CO_2 \quad \text{(1)}$$

The thermodynamic parameters viz. energy (Ea) and entropy ($\Delta S^{\neq}$) of activation has been calculated. The enthalpy of activation ($\Delta H^{\neq}$), free energy of activation ($\Delta G^{\neq}$) was also obtained 18.52 kJ mol^{-1} and 92.64 kJ mol^{-1} respectively.

4.1. Introduction

Amino acids act not only as the building blocks in the protein synthesis but they also play a significant role in metabolism. The specific metabolic role of amino acid includes the biosynthesis of polypeptides, proteins and synthesis of nucleotides [1]. The oxidation of serine has received much attention because of strengthening the immune system by providing antibodies and synthesize fatty acid sheath around nerve fibres [2, 3]. L-serine is an important non-essential amino acid with an –OH substituted side chain. It is required for the metabolism of fat, tissue growth and the immune system as it assists in the production of immunoglobulins and antibodies. It is a constituent of brain proteins, nerve coverings and is important in the formation of cell membranes. Serine is especially important to proper functioning of the brain and central nervous system. The study of amino acids thus becomes important of their biological significance and selectivity towards the oxidant to yield different product [4, 5]. However, metallic ions play a significant role in the oxidative decarboxylation of amino acids. Oxidation of amino acids by the more common oxidants such as MnO^{4-}, IO^{4-}, Mn(III) has been carried out, probably with an aim of investigating model systems for the enzymic oxidation of amino acids [6-10]. However, various types of the reaction models have been suggested by different researcher [11-15], the specific details are yet to be found out.

Kinetics and mechanistic aspects of the oxidation of neutral α-amino acids by oxone (PMS) have been reported [16–18]. Peroxomonosulphate is a derivative of hydrogen peroxide, replacing one of the hydrogen atoms in H_2O_2 by sulphate group. Peroxomonosulphate is one of the strong oxidizing agents compared to other peroxo oxidants [19, 20]. The predominant reactive species of peroxomonosulphate in acidic medium is HSO_5^-. The HSO_5^- frequently act as a one electron oxidant in redox reactions that involve heterolytic cleavage of peroxo bond [21, 22], oxidative decarboxylation of amino acids is a known and documented in biochemical reaction. Kinetics and mechanism of decarboxylation of amino acids by peroxo oxidants is an area of intensive research because peroxo oxidants are environmentally benign oxidants and do not produce toxic compounds during their reduction.

Some selective oxidation reactions are reported involving transition metal ions of Ag, Rh, Cr, Ru, Mn etc. are reported to act as catalyst for amino acids oxidation [23-27]. With the emergence of metal nanoparticles possessing appreciable stability and high surface area per particle, their potential use as catalyst for organic biochemical relevant reactions [28, 29]. Metal nanoparticles have been tested experimentally to display high catalytic properties in reactions for hydrogenation, hydroformylation, carbonylation [30], cycloadditions and numerous other reactions and mechanisms [31]. Copper nanoparticles are considered possible replacement for Ag and Au particles in some potential applications, such as in catalysis and conductive pastes [32-35]. Very few reports are available on the kinetics of oxidation of serine by peroxomonosulphate in the presence of metal nanoparticles in aqueous medium [36]. Therefore, it is of great interest to study metal nanoparticle catalyzed oxidation of serine using peroxomonosulphate. In this study, we demonstrate the efficiency of synthesized copper nanoparticles catalyst on the oxidation of serine under a range of different experimental conditions.

4.2. Experimental Details

4.2.1. Material and Reagents

Peroxomonosulphate (PMS) under the trade name "OXONE" (Aldrich) is a triple salt with the composition of $2KHSO_5 \cdot KHSO_4 \cdot K_2SO_4$. The purity of the sample was tested iodometrically [37] and also ceremetrically to 98%. Since earlier attempts failed to get a pure salt, no further attempts were, therefore, made. Thus $KHSO_4$ and K_2SO_4 together constituted 2% impurity which was either in the sample or was obtained in the solution. However, H_2O_2 was tested [38, 39] negative ruling out the possibility of any hydrolysis of peroxomonosulphate. The stability of peroxomonosulphate solution in moderate acid concentration is sufficiently high and the solution does not show any decomposition even on standing for Ca. 24 h under ambient conditions. A fresh solution was made before starting the experiment. All other reagents employed in this study were either of

AnalaR grade or guaranteed reagent grade and were used as supplied without undertaking any further treatment. Doubly distilled water was used throughout the study. The second distillation was from alkaline permanganate solution in an all glass apparatus.

4.2.2. Kinetic Measurements

Reaction mixture containing all other reagents except peroxomonosulphate were taken in glass stoppered Erlenmeyer flasks, the latter were suspended in water bath thermostated at $35^{o}\pm0.1^{o}C$ unless stated otherwise. Peroxomono-sulphate solution was taken in another flask and was immersed in the same water bath to attain the temperature of the reaction mixture. When these reaction solutions attained equilibrated temperature, an aliquot of requisite volume of concentration of peroxomonosulphate was taken out and immediately discharged into the reaction mixture, the time of initiation of the reaction was recorded when half of the contents from the pipette were released.

Kinetics was monitored by estimating peracid iodometrically at different time intervals. An aliquot (5 cm^3) was taken out of the reaction mixture periodically and then added to the solution of (10%) KI. The liberated iodine was titrated against thiosulphate solution using starch as an indicator without any interface from other components of the reaction mixture. The rate of reaction was studied under pseudo first order condition i.e. [Amino Acid]>> [PMS], the rate of reaction followed first order kinetics and rate constant (k_{obs}) was calculated from the linear plots of log [PMS] versus time.

4.3. Stoichiometry and Product Analysis

The stoichiometry of the reaction was determined for copper nanoparticles catalyzed reaction mixtures containing a large excess of [PMS] over [serine] by keeping all other condition of reaction is constant. The reaction mixtures were kept at $35^{o}C$ for 48 hours and the excess of peroxomonosulphate was estimated

iodometrically ensuring the completion of the reaction. The main reaction products are aldehyde, ammonia and CO_2.

The product of oxidation was corresponding aldehyde i.e. glycoldehyde was confirmed by FTIR spectrum of the corresponding hydrazone in **figure 4.1.** The reaction mixture was treated with acidified 2, 4-dinitrophenylhydrazine solution, which yielded a hydrazone. The IR peaks at **3367.24 cm^{-1}, 2936.98 cm^{-1} and 1618.76 cm^{-1}** are attributed to –NH, –CH, –C=N stretching respectively. The functional group–C=N was produced from the condensation reaction of aldehyde and hydrazine. Further, aldehyde group was confirmed by qualitative test such as tollen's reagent [40] and schiff's reagent.

Therefore, the stoichiometry of the oxidation of serine by an oxygen transfer from peroxomonosulphate in presence of copper nanoparticles with positive test of an aldehyde can be represented by **equation (4.1).**

$$HSO_5^- + R-\underset{NH_2}{\overset{H}{\underset{|}{\overset{|}{C}}}}-COOH \xrightarrow[308\ K,\ H^+]{\text{Copper Nanoparticles}} RCHO + NH_3 + HSO_4^- + CO_2 \quad \text{(4.1)}$$

Where R represents $-CH_2OH$

The reaction mixture containing peroxomonosulphate and serine in presence of copper nanoparticles at 35^oC was subjected to the UV-Visible absorption study which is presented in **figure 4.2**. The spectrum shows a peak at 206 nm of serine with maximum absorbance in the initial of reaction. The decrease peak in height with time indicates the deamination of L-serine. The ammonia evolved was confirmed by reaction with Nessler's test. The carbon dioxide evolved was confirmed by reaction with lime water.

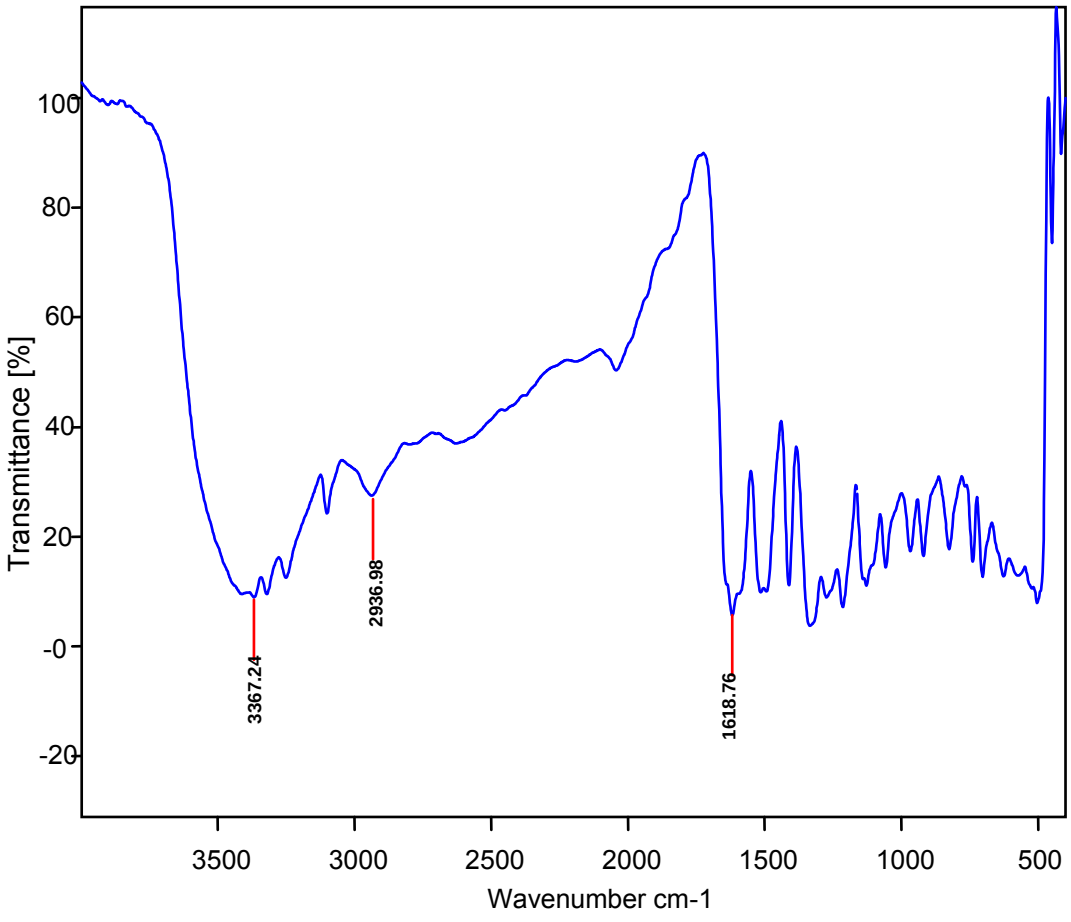

Figure 4.1: The FT-IR spectra of the hydrazone derivative from the reaction mixture of serine and peroxomonosulphate in the presence of copper nanoparticles

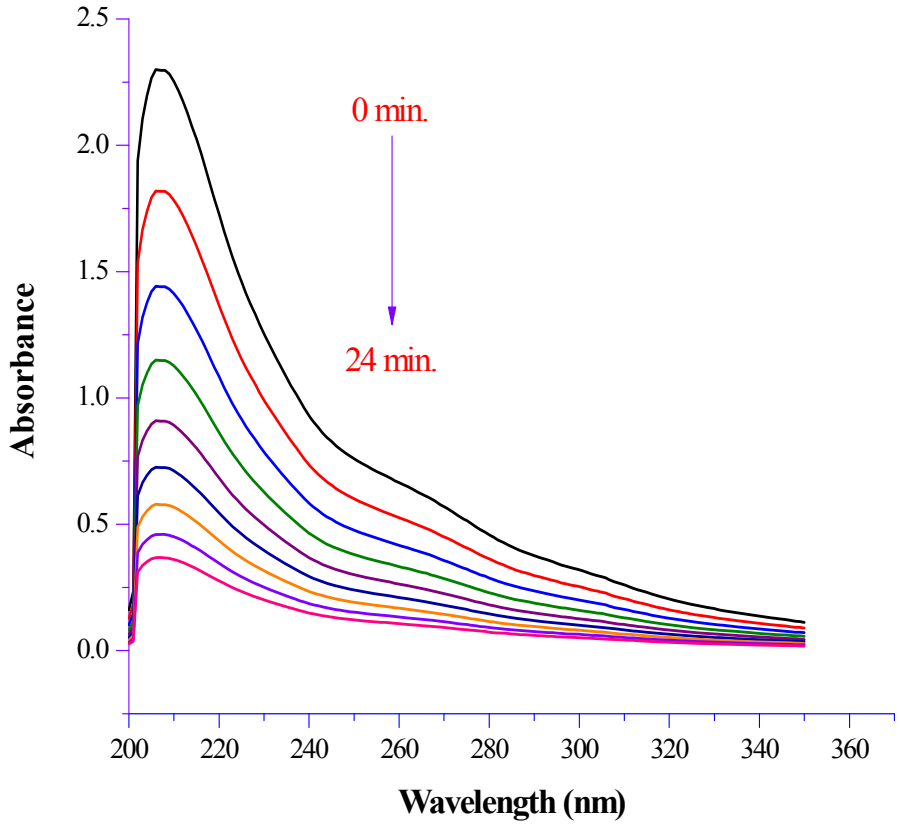

Figure 4.2: UV-Vis absorption spectra for the deamination of L-serine (0-24 min.) in the presence of the copper nanoparticles (size = 12 nm)

[PMS] = 5.0×10^{-3} mol dm^{-3}	[Serine] = 5.0×10^{-2} moldm^{-3}
[Cunps] = 5.0×10^{-6} mol dm^{-3}	$[H^+] = 1.0\times10^{-2}$ mol dm^{-3}
I = 2.0×10^{-2} mol dm^{-3}	Temp. = 35^oC

4.4. Results and Discussion

4.4.1. Effect of Peroxomonosulphate Concentration

The copper nanoparticles catalysed oxidation of serine was studied at different concentration of peroxomonosulphate varying from 1.0×10^{-3}– 7.0×10^{-3} mol dm^{-3} at three but constant concentration of serine 3.0×10^{-2}, 5.0×10^{-2}, 7.0×10^{-2} mol dm^{-3} respectively, keeping constant concentration of other reaction ingredients *viz.* $[H^+] = 1.0\times10^{-2}$ mol dm^{-3}, I =2.0×10^{-2} mol dm^{-3}, [Cunps] = 5.0×10^{-6} mol dm^{-3} at 35°C. The plot of log [PMS] (PMS, has been used in place of peroxomonosulphate heretofore) versus time was made that yielded linear plots which was shown in **figure 4.3,** indicating that the reaction is first order with respect to [PMS]. The pseudo first order rate constants calculated from these plots, the observed pseudo first order rate constant (k_{obs}) were independent of the concentration of peroxomonosulphate. Results are given in **Table-4.1, 4.2, 4.3.**

4.4.2. Effect of Serine Concentration

The effect of Serine concentration was studied by varying its concentration in the range of 1.0×10^{-2} – 7.0×10^{-2} mol dm^{-3} at three but constant concentration of peroxomonosulphate 3.0×10^{-3}, 5.0×10^{-3}, 7.0×10^{-3} mol dm^{-3} respectively, keeping all other reactant concentration and conditions constant *viz.* $[H^+] = 1.0\times10^{-2}$ mol dm^{-3}, I = 2.0×10^{-2} mol dm^{-3}, [Cunps] = 5.0×10^{-6} mol dm^{-3} at 35°C temperature. The pseudo first order rate constants calculated from these plots, the observed pseudo first order rate constant (k_{obs}) was found to increase proportionally with the increasing concentration of serine. Results are given in **Table-4.4, 4.5, 4.6**. A plot of first order rate constants (k_{obs}, sec^{-1}) against concentration of serine [Ser] (Ser, has been used in place of serine heretofore) were made, a straight line passing through the origin was obtained **(Figure 4.4)** confirming the first order dependence with respect to serine.

TABLE: 4.1

VARIATION OF PEROXOMONOSULPHATE

[Ser] = 3.0×10^{-2} mol dm^{-3} **Temp. = 35^{o}C**

[Cunps] = 5.0×10^{-6} mol dm^{-3} **Titrant [Hypo] = 1.0×10^{-3} mol dm^{-3}**

[H^{+}] = 1.0×10^{-2} mol dm^{-3} **Aliquot = 5.0 ml**

I= 2.0×10^{-2} mol dm^{-3}

10^3 [PMS], mol dm^{-3}	**1.0***	**2.0**	**3.0**	**4.0**	**5.0**	**6.0**	**7.0**
Time in minutes	**Volume of Titrant (ml)**						
0	10.0	10.0	15.0	20.0	25.0	30.0	35.0
4	8.3	8.3	12.2	16.5	20.6	24.9	28.7
8	6.9	6.8	10.1	13.6	17.1	20.6	23.8
12	5.7	5.6	8.4	11.3	14.1	17.1	19.7
16	4.8	4.7	7.0	9.3	11.7	14.2	16.4
20	4.0	3.9	5.8	7.7	9.7	11.8	13.6
24	3.3	3.2	4.8	6.4	8.0	9.8	11.3
28	2.7	2.6	4.0	5.3	6.6	8.1	9.3
32	2.3	2.2	3.3	4.4	5.5	6.7	7.7
10^3 (k_{obs}), sec^{-1}	**0.77**	**0.79**	**0.78**	**0.79**	**0.79**	**0.78**	**0.78**

*Hypo = 5.0×10^{-4} mol dm^{-3}

TABLE: 4.2

VARIATION OF PEROXOMONOSULPHATE

[Ser] = 5.0×10^{-2} mol dm^{-3} **Temp. = 35°C**
[Cunps] = 5.0×10^{-6} mol dm^{-3} **Titrant [Hypo] = 1.0×10^{-3} mol dm^{-3}**
[H^+] = 1.0×10^{-2} mol dm^{-3} **Aliquot = 5.0 ml**
I= 2.0×10^{-2} mol dm^{-3}

10^3 [PMS], mol dm^{-3}	**1.0***	**2.0**	**3.0**	**4.0**	**5.0**	**6.0**	**7.0**
Time in minutes	**Volume of Titrant (ml)**						
0	10.0	10.0	15.0	20.0	25.0	30.0	35.0
3	8.0	7.9	11.7	15.8	19.8	23.9	27.4
6	6.4	6.3	9.3	12.6	15.7	19.1	21.7
9	5.1	5.0	7.4	10.0	12.5	15.2	17.2
12	4.0	4.0	5.9	8.0	9.9	12.1	13.7
15	3.2	3.2	4.7	6.3	7.9	9.7	10.8
18	2.6	2.5	3.7	5.1	6.3	7.7	8.6
21	2.0	2.0	3.0	4.0	5.0	6.1	6.8
24	1.6	1.6	2.4	3.2	4.0	4.9	5.4
10^3 (k_{obs}), sec^{-1}	**1.26**	**1.28**	**1.27**	**1.27**	**1.28**	**1.26**	**1.29**

*Hypo = 5.0×10^{-4} mol dm^{-3}

TABLE: 4.3

VARIATION OF PEROXOMONOSULPHATE

[Ser] = 7.0×10^{-2} mol dm^{-3} **Temp. = 35°C**
[Cunps] = 5.0×10^{-6} mol dm^{-3} **Titrant [Hypo] = 1.0×10^{-3} mol dm^{-3}**
[H^+] = 1.0×10^{-2} mol dm^{-3} **Aliquot = 5.0 ml**
I= 2.0×10^{-2} mol dm^{-3}

10^3 [PMS], mol dm^{-3}	**1.0***	**2.0**	**3.0**	**4.0**	**5.0**	**6.0**	**7.0**
Time in minutes	**Volume of Titrant (ml)**						
0	10.0	10.0	15.0	20.0	25.0	30.0	35.0
2	8.1	8.0	11.9	16.0	20.1	24.1	27.8
4	6.5	6.5	9.6	12.9	16.2	19.4	22.4
6	5.3	5.2	7.7	10.4	13.0	15.6	18.0
8	4.2	4.2	6.3	8.4	10.5	12.6	14.5
10	3.4	3.4	5.0	6.8	8.5	10.1	11.7
12	2.8	2.7	4.1	5.4	6.8	8.1	9.4
14	2.2	2.2	3.3	4.4	5.5	6.6	7.6
16	1.8	1.8	2.6	3.5	4.4	5.3	6.1
10^3 (k_{obs}), sec^{-1}	**1.79**	**1.80**	**1.79**	**1.80**	**1.80**	**1.81**	**1.81**

*Hypo = 5.0×10^{-4} mol dm^{-3}

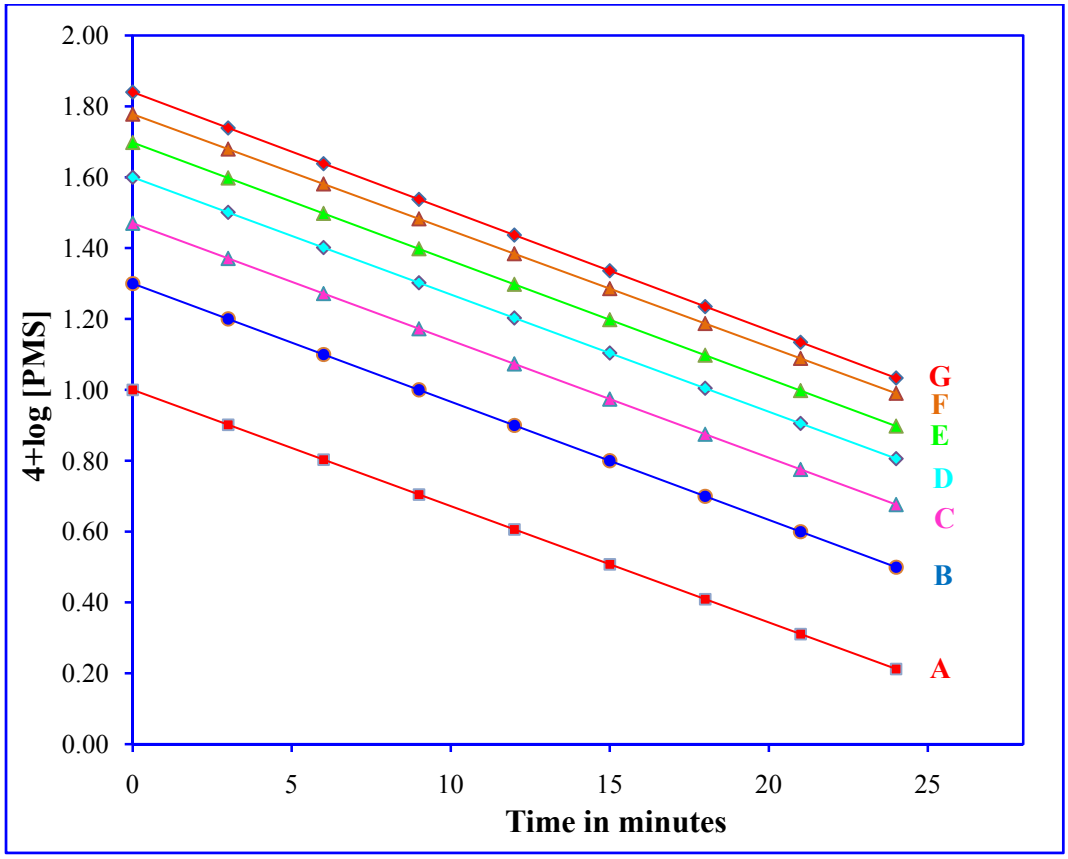

Figure 4.3: Variation of peroxomonosulphate

[Ser]= 5.0×10^{-2} moldm^{-3}; [Cunps] = 5.0×10^{-6} mol dm^{-3};

[H^+] = 1.0×10^{-2} mol dm^{-3}; I = 2.0×10^{-2} mol dm^{-3}, Temp. = 35^{o}C

[PMS] = (A) 1.0×10^{-3} mol dm^{-3} (B) 2.0×10^{-3} mol dm^{-3}

(C) 3.0×10^{-3} mol dm^{-3} (D) 4.0×10^{-3} mol dm^{-3}

(E) 5.0×10^{-3} mol dm^{-3} (F) 6.0×10^{-3} mol dm^{-3}

(G) 7.0×10^{-3} mol dm^{-3}

(Ref. Table: 4.2)

TABLE: 4.4

VARIATION OF SERINE

[PMS] = 3.0×10^{-3} mol dm^{-3} **Temp. = 35^{o}C**

[Cunps] = 5.0×10^{-6} mol dm^{-3} **Titrant [Hypo] = 1.0×10^{-3} mol dm^{-3}**

[H^{+}] = 1.0×10^{-2} mol dm^{-3} **Aliquot = 5.0 ml**

I = 2.0×10^{-2} mol dm^{-3}

10^2 [Ser], mol dm^{-3}	**1.0**	**2.0**	**3.0**	**4.0**	**5.0**	**6.0**	**7.0**
Time in minutes	**Volume of Titrant (ml)**						
0	(0)15.0	(0)15.0	(0)15.0	(0)15.0	15.0	15.0	15.0
3	(15)11.7	(8)11.6	(5)11.7	(4)11.6	11.7	11.2	10.7
6	(30)9.2	(16)9.1	(10)9.2	(8)9.1	9.3	8.5	7.7
9	(45)7.3	(24)7.2	(15)7.3	(12)7.1	7.4	6.5	5.6
12	(60)5.8	(32)5.7	(20)5.8	(16)5.6	5.9	4.9	4.1
15	(75)4.6	(40)4.4	(25)4.6	(20)4.4	4.7	3.7	2.9
18	(90)3.6	(48)3.5	(30)3.6	(24)3.4	3.7	2.8	2.1
21	(105)2.9	(56)2.8	(35)2.9	(28)2.7	3.0	2.1	1.5
24	(120)2.3	(64)2.2	(40)2.3	(32)2.1	2.4	1.6	1.1
10^3 (k_{obs}), sec^{-1}	**0.26**	**0.50**	**0.78**	**1.01**	**1.27**	**1.53**	**1.79**

Figures in parentheses denote time in minutes

TABLE: 4.5

VARIATION OF SERINE

[PMS] = 5.0×10^{-3} mol dm^{-3} **Temp. = 35^{o}C**

[Cunps] = 5.0×10^{-6} mol dm^{-3} **Titrant [Hypo] = 1.0×10^{-3} mol dm^{-3}**

[H^{+}] = 1.0×10^{-2} mol dm^{-3} **Aliquot = 5.0 ml**

I = 2.0×10^{-2} mol dm^{-3}

10^2 [Ser], mol dm^{-3}	**1.0**	**2.0**	**3.0**	**4.0**	**5.0**	**6.0**	**7.0**
Time in minutes	**Volume of Titrant (ml)**						
0	(0)25.0	(0)25.0	(0)25.0	(0)25.0	25.0	25.0	25.0
3	(15)19.7	(8)19.1	(5)19.7	(4)19.5	19.8	18.9	18.0
6	(30)15.6	(16)14.6	(10)15.5	(8)15.3	15.7	14.3	13.0
9	(45)12.4	(24)11.1	(15)12.3	(12)12.0	12.5	10.9	9.4
12	(60)9.8	(32)8.5	(20)9.7	(16)9.4	9.9	8.2	6.8
15	(75)7.7	(40)6.5	(25)7.6	(20)7.3	7.9	6.2	4.9
18	(90)6.1	(48)5.0	(30)6.0	(24)5.7	6.3	4.7	3.6
21	(105)4.8	(56)3.8	(35)4.7	(28)4.5	5.0	3.6	2.6
24	(120)3.8	(64)2.9	(40)3.7	(32)3.5	4.0	2.7	1.9
10^3 (k_{obs}), sec^{-1}	**0.26**	**0.56**	**0.79**	**1.02**	**1.28**	**1.54**	**1.80**

Figures in parentheses denote time in minutes

TABLE: 4.6

VARIATION OF SERINE

[PMS] = 7.0×10^{-3} mol dm^{-3} **Temp. = 35^{o}C**

[Cunps] = 5.0×10^{-6} mol dm^{-3} **Titrant [Hypo] = 1.0×10^{-3} mol dm^{-3}**

[H^{+}] = 1.0×10^{-2} mol dm^{-3} **Aliquot = 5.0 ml**

I = 2.0×10^{-2} mol dm^{-3}

10^2 [Ser], mol dm^{-3}	**1.0**	**2.0**	**3.0**	**4.0**	**5.0**	**6.0**	**7.0**
Time in minutes	**Volume of Titrant (ml)**						
0	(0)35.0	(0)35.0	(0)35.0	(0)35.0	35.0	35.0	35.0
3	(15)27.4	(8)27.2	(5)27.7	(5)25.6	27.4	26.4	25.2
6	(30)21.7	(16)21.4	(10)22.2	(10)19.0	21.7	20.2	18.4
9	(45)17.1	(24)16.8	(15)17.8	(15)14.1	17.2	15.4	13.4
12	(60)13.6	(32)13.2	(20)14.2	(20)10.4	13.7	11.7	9.7
15	(75)10.7	(40)10.4	(25)11.4	(25)7.7	10.8	9.0	7.1
18	(90)8.5	(48)8.2	(30)9.1	(30)5.7	8.6	6.8	5.2
21	(105)6.7	(56)6.4	(35)7.3	(35)4.2	6.8	5.2	3.8
24	(120)5.3	(64)5.1	(40)5.9	(40)3.1	5.4	4.0	2.7
10^3 (k_{obs}), sec^{-1}	**0.26**	**0.50**	**0.74**	**1.00**	**1.29**	**1.50**	**1.76**

Figures in parentheses denote time in minutes

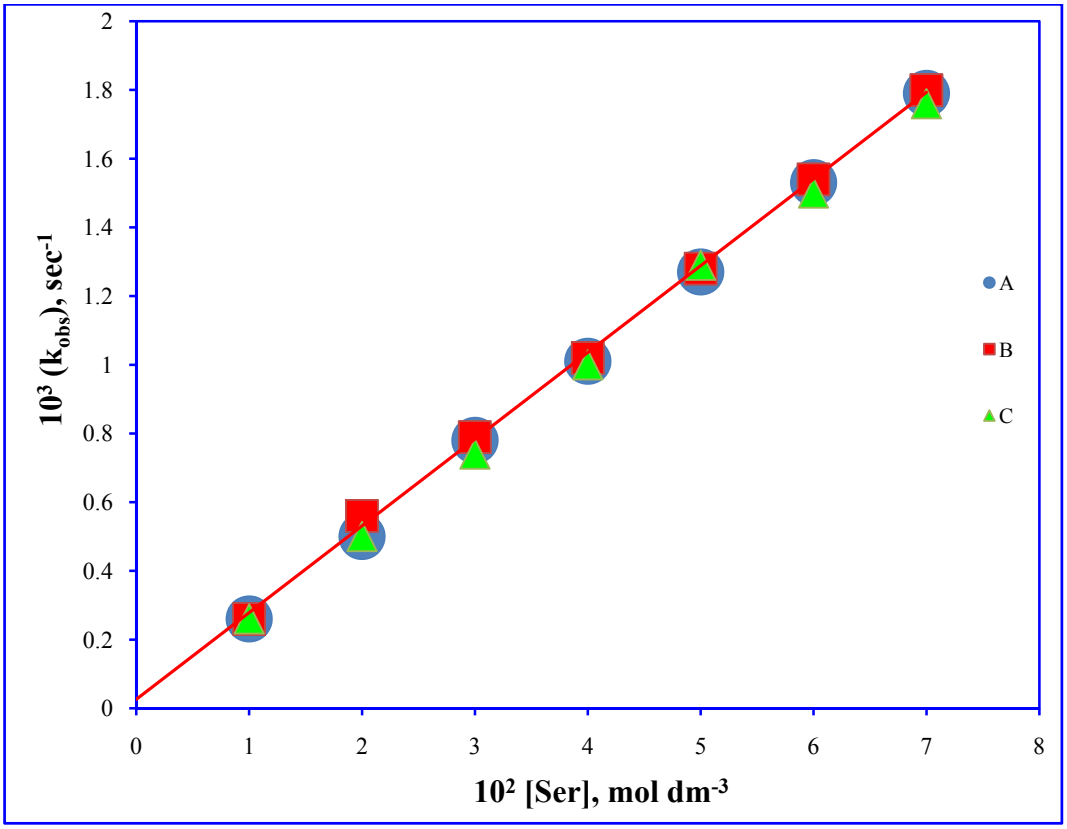

Figure 4.4: Variation of serine

[PMS] = (A) 3.0×10^{-3} mol dm^{-3} ; (B) 5.0×10^{-3} mol dm^{-3} ;
(C) 7.0×10^{-3} mol dm^{-3}

[Cunps] = 5.0×10^{-6} mol dm^{-3}; $[H^+] = 1.0\times10^{-2}$ mol dm^{-3};

I = 2.0×10^{-2} mol dm^{-3}; Temp. = 35^oC

(Ref. Table: 4.5, 4.6, 4.7)

4.4.3. Effect of Copper Nanoparticles

The effect of copper nanoparticles concentration on the oxidation of serine has been studied by varying its concentration from 1.0×10^{-6} – 1.0×10^{-5} mol dm^{-3} at three different size of nanoparticles (28, 16 and 12 nm), synthesized at three concentration (0.08, 0.09, 0.10 mol dm^{-3}) of ascorbic acid (as discussed in chapter 3), other reactant and reaction conditions were constant *viz.* [PMS] = 5.0×10^{-3} mol dm^{-3}, [Ser] = 5.0×10^{-2} mol dm^{-3}, [H^+] = 1.0×10^{-2} mol dm^{-3}, I = 2.0×10^{-2} mol dm^{-3} at 35°C. The rate of reaction increases with increasing concentration of copper nanoparticles. The catalytic activity of copper nanoparticles seems different when concentration of reducing agent is varied from 0.08 to 0.1 mol dm^{-3} during synthesis of copper nanoparticles. The difference in catalytic activity can be attributed to the size variation in the resulting copper nanoparticles. A plot of first order rate constants (k_{obs}, sec^{-1}) against concentration of copper nanoparticles [Cunps] (Cunps, has been used in place of Copper nanoparticles heretofore) were made, a straight line was obtained, confirming the first order dependence with respect to copper nanoparticles. The trend in the calculated rate constant being 12>16>28 nm size of copper nanoparticles **(Figure 4.5).** This effect can be attributed to the nanosize of the particles that as size decreases surface area increases and the active centre are also increases. Results are given in **Table-4.7, 4.8, 4.9.**

4.4.4. Effect of Hydrogen Ion Concentration

The effect of hydrogen ion was studied employing different concentration of perchloric acid in the range of 0.5×10^{-2} to 2.0×10^{-2} mol dm^{-3}, keeping all other reactant concentration and conditions constant *viz.* ionic strength (I) to be 2.0×10^{-2} mol dm^{-3} (Ionic strength was adjusted employing sodium perchlorate), [PMS] = 5.0×10^{-3} mol dm^{-3}, [Ser] = 5.0×10^{-2} mol dm^{-3}, [Cunps] = 5.0×10^{-6} mol dm^{-3} at temperature 35°C. The values of pseudo first order rate constants ($k_{obs,}$ sec^{-1}) were found to decreases with increasing concentration of hydrogen ion. The retardation of reaction rate by increase in high [H^+] may be attributed to the conversion of the more reactive neutral species of amino acid to the less reactive protonated form.

TABLE: 4.7

EFFECT OF COPPER NANOPARTICLES

(SIZE = 12 nm)

[PMS] = 5.0×10^{-3} mol dm^{-3} **Temp. = 35^{o}C**

[Ser] = 5.0×10^{-2} mol dm^{-3} **Titrant [Hypo] = 1.0×10^{-3} mol dm^{-3}**

[H^{+}] = 1.0×10^{-2} mol dm^{-3} **Aliquot = 5.0 ml**

I = 2.0×10^{-2} mol dm^{-3}

10^{6} [Cunps], mol dm^{-3}	**0.0**	**1.0**	**2.0**	**3.0**	**4.0**	**5.0**	**6.0**	**7.0**	**8.0**	**9.0**	**10.0**
Time in minutes	**Volume of Titrant (ml)**										
0	(0)25.0	(0)25.0	(0)25.0	(0)25.0	(0)25.0	25.0	25.0	25.0	25.0	25.0	25.0
3	(18)20.1	(10)19.6	(10)17.0	(5)19.4	(4)19.3	19.8	19.0	18.4	17.7	17.0	16.5
6	(36)16.2	(20)15.4	(20)11.6	(10)15.1	(8)15.0	15.7	14.4	13.5	12.6	11.5	10.9
9	(54)13.0	(30)12.1	(30)7.9	(15)11.7	(12)11.6	12.5	11.0	10.0	8.9	7.9	7.2
12	(72)10.5	(40)9.6	(40)5.4	(20)9.1	(16)9.0	9.9	8.4	7.3	6.4	5.3	4.8
15	(90)8.5	(50)7.5	(50)3.7	(25)7.1	(20)7.0	7.9	6.4	5.4	4.5	3.6	3.1
18	(108)6.8	(60)5.9	(60)2.5	(30)5.5	(24)5.4	6.3	4.8	4.0	3.2	2.5	2.1
21	(126)5.5	(70)4.7	(70)1.7	(35)4.3	(28)4.2	5.0	3.7	2.9	2.3	1.7	1.4
24	(144)4.4	(80)3.7	(80)1.2	(40)3.3	(32)3.3	4.0	2.8	2.2	1.6	1.1	-
10^{3} (k_{obs}), sec^{-1}	**0.20**	**0.40**	**0.64**	**0.84**	**1.06**	**1.28**	**1.52**	**1.70**	**1.90**	**2.14**	**2.30**

Figures in parentheses denote time in minutes

TABLE: 4.8

EFFECT OF COPPER NANOPARTICLES

(SIZE = 16 nm)

[PMS] = 5.0×10^{-3} mol dm^{-3} **Temp. = 35^{o}C**

[Ser] = 5.0×10^{-2} mol dm^{-3} **Titrant [Hypo] = 1.0×10^{-3} mol dm^{-3}**

[H^{+}] = 1.0×10^{-2} mol dm^{-3} **Aliquot = 5.0 ml**

I = 2.0×10^{-2} mol dm^{-3}

10^{6} [Cunps], mol dm^{-3}	**0.0**	**1.0**	**2.0**	**3.0**	**4.0**	**5.0**	**6.0**	**7.0**	**8.0**	**9.0**	**10.0**
Time in minutes	**Volume of Titrant (ml)**										
0	(0)25.0	(0)25.0	(0)25.0	(0)25.0	(0)25.0	25.0	25.0	25.0	25.0	25.0	25.0
4	(20)19.6	(10)20.1	(8)19.1	(6)19.4	(5)19.3	19.2	18.5	17.7	16.9	16.2	24.9
8	(40)15.4	(20)16.2	(16)14.6	(12)15.1	(10)14.9	14.9	13.8	12.6	11.5	10.5	15.4
12	(60)12.1	(30)13.0	(24)11.1	(18)11.7	(15)11.5	11.5	10.2	9.0	7.8	6.8	9.6
16	(80)9.6	(40)10.5	(32)8.5	(24)9.1	(20)8.9	8.8	7.6	6.4	5.3	4.4	5.9
20	(100)7.5	(50)8.5	(40)6.5	(30)7.1	(25)6.9	6.8	5.6	4.5	3.6	2.9	3.7
24	(120)5.9	(60)6.8	(48)5.0	(36)5.5	(30)5.3	5.3	4.2	3.2	2.4	1.9	2.3
28	(140)4.7	(70)5.5	(56)3.8	(42)4.3	(35)4.1	4.1	3.1	2.3	1.6	1.2	1.4
32	(160)3.7	(80)4.4	(64)2.9	(48)3.3	(40)3.2	3.1	2.3	1.6	1.1	-	-
10^{3} (k_{obs}), sec^{-1}	**0.20**	**0.36**	**0.56**	**0.70**	**0.86**	**1.08**	**1.24**	**1.42**	**1.62**	**1.80**	**2.00**

Figures in parentheses denote time in minutes

TABLE: 4.9

EFFECT OF COPPER NANOPARTICLES

(SIZE = 28 nm)

[PMS] = 5.0×10^{-3} mol dm^{-3} **Temp. = 35^{o}C**

[Ser] = 5.0×10^{-2} mol dm^{-3} **Titrant [Hypo] = 1.0×10^{-3} mol dm^{-3}**

[H^{+}] = 1.0×10^{-2} mol dm^{-3} **Aliquot = 5.0 ml**

I = 2.0×10^{-2} mol dm^{-3}

10^{6} [Cunps], mol dm^{-3}	**0.0**	**1.0**	**2.0**	**3.0**	**4.0**	**5.0**	**6.0**	**7.0**	**8.0**	**9.0**	**10.0**
Time in minutes	**Volume of Titrant (ml)**										
0	(0)25.0	(0)25.0	(0)25.0	(0)25.0	(0)25.0	25.0	25.0	25.0	25.0	25.0	25.0
4	(18)20.1	(10)19.9	(8)19.8	(6)20.1	(5)20.0	20.2	19.4	19.0	18.3	17.7	17.0
8	(36)16.2	(20)15.8	(16)15.7	(12)16.2	(10)16.0	16.4	15.1	14.4	13.4	12.6	11.6
12	(54)13.0	(30)12.6	(24)12.5	(18)13.0	(15)12.8	13.2	11.8	11.0	9.8	9.0	7.9
16	(72)10.5	(40)10.0	(32)9.9	(24)10.5	(20)10.3	10.7	9.2	8.4	7.2	6.4	5.4
20	(90)8.5	(50)8.0	(40)7.9	(30)8.5	(25)8.2	8.7	7.2	6.4	5.2	4.5	3.7
24	(108)6.8	(60)6.4	(48)6.3	(36)6.8	(30)6.6	7.0	5.6	4.8	3.8	3.2	2.5
28	(126)5.5	(70)5.1	(56)5.0	(42)5.5	(35)5.3	5.7	4.3	3.7	2.8	2.3	1.7
32	(144)4.4	(80)4.0	(64)4.0	(48)4.4	(40)4.2	4.6	3.4	2.8	2.1	1.6	1.2
10^{3} (k_{obs}), sec^{-1}	**0.20**	**0.38**	**0.48**	**0.60**	**0.74**	**0.88**	**1.04**	**1.14**	**1.30**	**1.42**	**1.60**

Figures in parentheses denote time in minutes

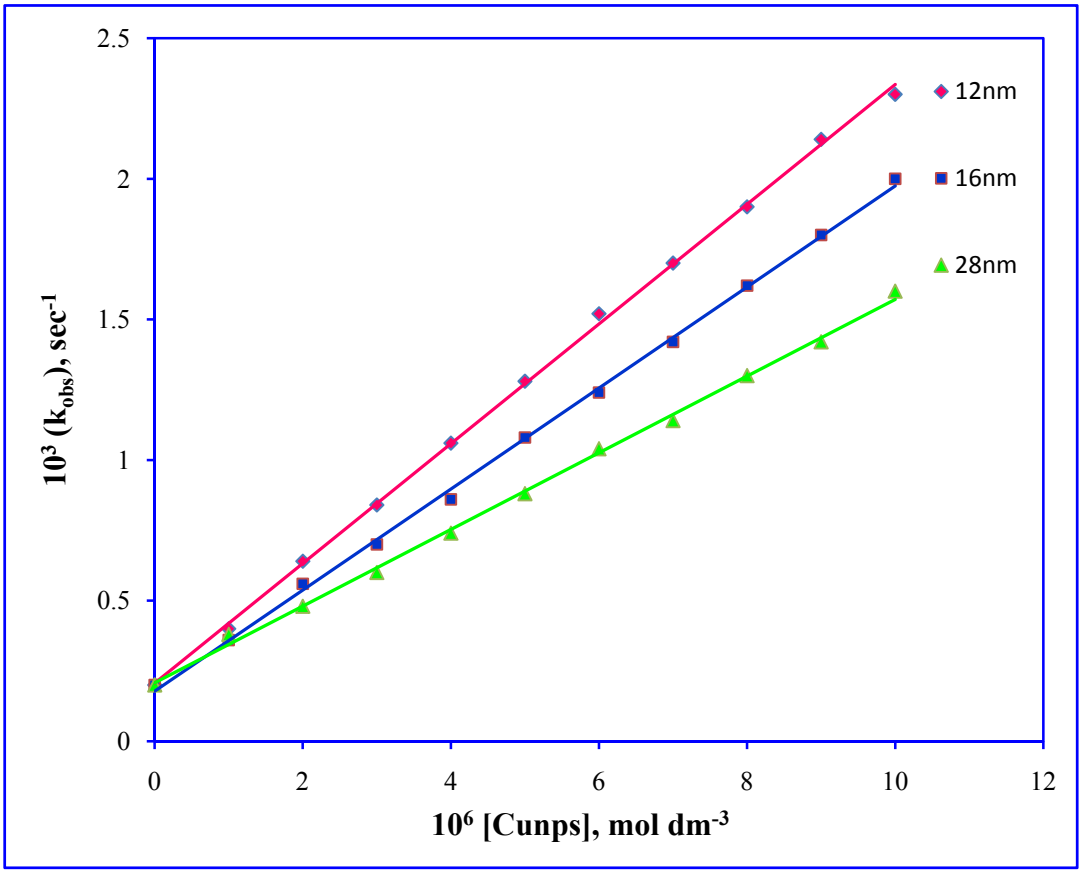

Figure 4.5: Effect of copper nanoparticles concentration at different size of copper nanoparticles (a) 12 nm, (b) 16 nm, (c) 28 nm

[PMS] = 5.0×10^{-3} mol dm^{-3}; [Ser] = 5.0×10^{-2} mol dm^{-3};
[H^+] = 1.0×10^{-2} mol dm^{-3} ; I = 2.0×10^{-2} mol dm^{-3};
Temp. = 35°C

(Ref. Table: 4.7, 4.8, 4.9)

Further, the plot of k_{obs} versus $[H^+]^{-1}$ were found to be linear with a positive slope and a non-zero intercept **(Figure 4.6).** This shows an inverse first-order dependence on $[H^+]$. Consequently the plots of k_{obs} $[H^+]$ versus $[H^+]$ were linear with intercept on the ordinate **(Figure 4.7).** This clearly proves that the reaction proceeds through two independent paths; one is H^+ ion dependent and the other is H^+ ion independent. Results are given in **Table- 4.10.**

4.4.5. Effect of Ionic Strength

Ionic strength variation 2.0×10^{-2} to 10.0×10^{-2} mol dm^{-3} was made employing sodium perchlorate at fixed concentration of all other reaction ingredients *viz.* [PMS] = 5.0×10^{-3} mol dm^{-3}, [Ser] = 5.0×10^{-2} mol dm^{-3}, [Cunps] = 5.0×10^{-6} mol dm^{-3}, $[H^+] = 1.0\times10^{-2}$ mol dm^{-3} at temperature 35°C. The rate of the reaction slightly increases with increasing ionic strength. However, increase in rate is not significant even for 5-fold increase in ionic strength. Results are given in **Table- 4.11** which indicates that in our experimental conditions HSO_5^- and serine (neutral) to be reactive form of peroxomonosulphate and serine respectively.

4.4.6. Effect of Temperature

The effect of temperature on the rate of reaction was studied at three temperature 30°C, 35°C, 40°C respectively at constant concentration of other reaction ingredients *viz.* [PMS] = 5.0×10^{-3} mol dm^{-3}, [Ser] = 5.0×10^{-2} mol dm^{-3}, [Cunps] = 5.0×10^{-6} mol dm^{-3}, $[H^+] = 1.0\times10^{-2}$ mol dm^{-3}, I = 2.0×10^{-2} mol dm^{-3}. The observed rate constants increased with increase in temperature, these results were tabulated in **Tables-4.12.** By applying Arrhenius **equation (4.2),** the logarithm of observed rate constant (k_{obs}, sec^{-1}) was plotted against 1/T in K^{-1} that yielded a straight line **(Figure 4.8).** From Arrhenius equation

$$\log k = \log A - E_a/2.303RT \qquad (4.2)$$

The slope of the graph is equal to $-E_a/2.303R$ the energy of activation (E_a) for oxidation of serine by peroxomonosulphate was calculated to be 21.02 ± 2 kJ mol^{-1} and the entropy of activation was calculated to be -240.67 ± 4 J K^{-1} mol^{-1}.

TABLE: 4.10

EFFECT OF HYDROGEN ION CONCENTRATION

[PMS] = 5.0×10^{-3} mol dm^{-3} **Temp. = 35°C**
[Ser] = 5.0×10^{-2} mol dm^{-3} **Titrant [Hypo] = 1.0×10^{-3} mol dm^{-3}**
[Cunps] = 5.0×10^{-6} mol dm^{-3} **Aliquot = 5.0 ml**
I = 2.0×10^{-2} mol dm^{-3}

10^2 [H^+], mol dm^{-3}	**0.50**	**0.75**	**1.00**	**1.20**	**1.40**	**1.60**	**1.80**	**2.00**
Time in minutes	**Volume of Titrant (ml)**							
0	(0)25.0	(0)25.0	(0)25.0	25.0	25.0	25.0	25.0	(0)25.0
4	(3)18.4	(3)19.2	(3)19.8	19.1	19.5	19.9	20.3	(5)19.6
8	(6)13.6	(6)14.9	(6)15.7	14.6	15.3	15.9	16.5	(10)15.4
12	(9)10.1	(9)11.5	(9)12.5	11.1	12.0	12.7	13.4	(15)12.1
16	(12)7.4	(12)8.8	(12)9.9	8.5	9.4	10.1	10.9	(20)9.6
20	(15)5.5	(15)6.8	(15)7.9	6.5	7.3	8.1	8.9	(25)7.5
24	(18)4.1	(18)5.3	(18)6.3	5.0	5.7	6.4	7.2	(30)5.9
28	(21)3.0	(21)4.1	(21)5.0	3.8	4.5	5.1	5.9	(35)4.7
32	(24)2.2	(24)3.1	(24)4.0	2.9	3.5	4.1	4.8	(40)3.7
10^3 (k_{obs}), sec^{-1}	**1.68**	**1.44**	**1.28**	**1.12**	**1.02**	**0.94**	**0.86**	**0.80**

Figures in parentheses denote time in minutes

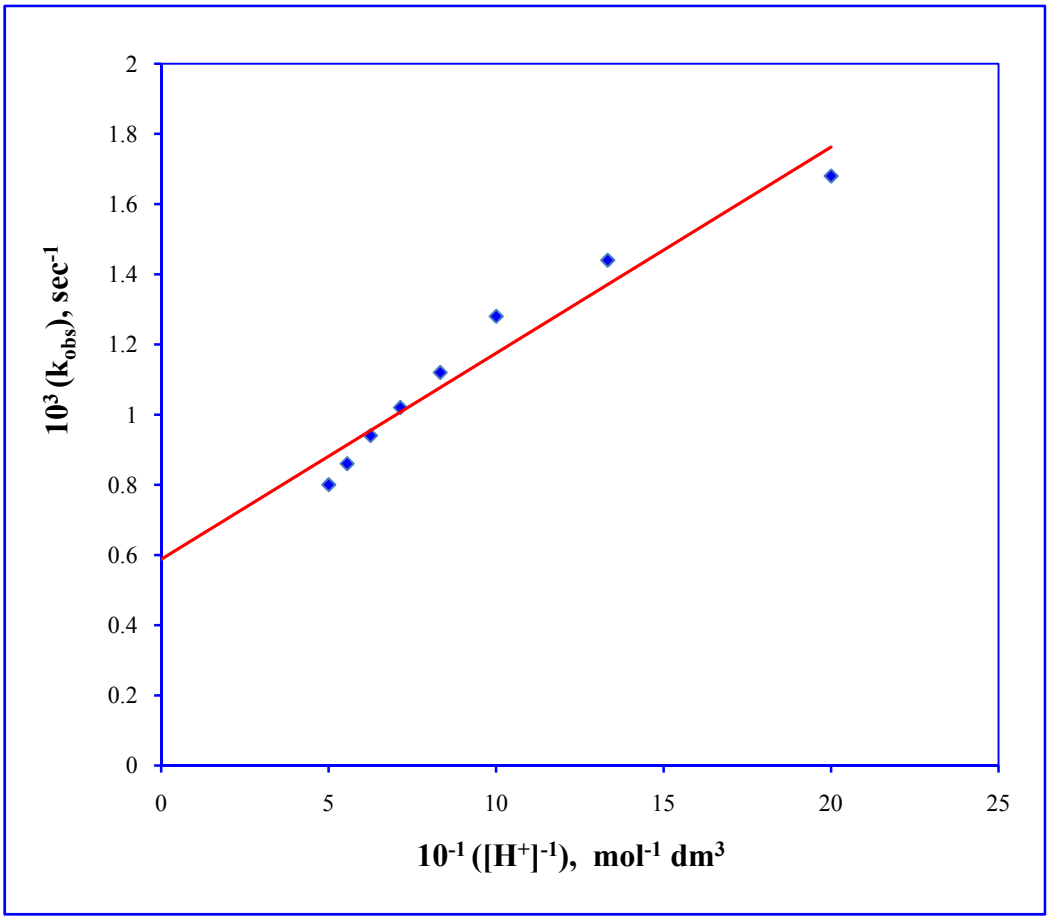

Figure 4.6: Plot of k_{obs} versus $[H^+]^{-1}$

[PMS] = 5.0×10^{-3} mol dm^{-3}; [Cunps] = 5.0×10^{-6} mol dm^{-3};

[Ser] = 5.0×10^{-2} mol dm^{-3}; I = 2.0×10^{-2} mol dm^{-3};

Temp. = 35°C

(Ref. Table: 4.10)

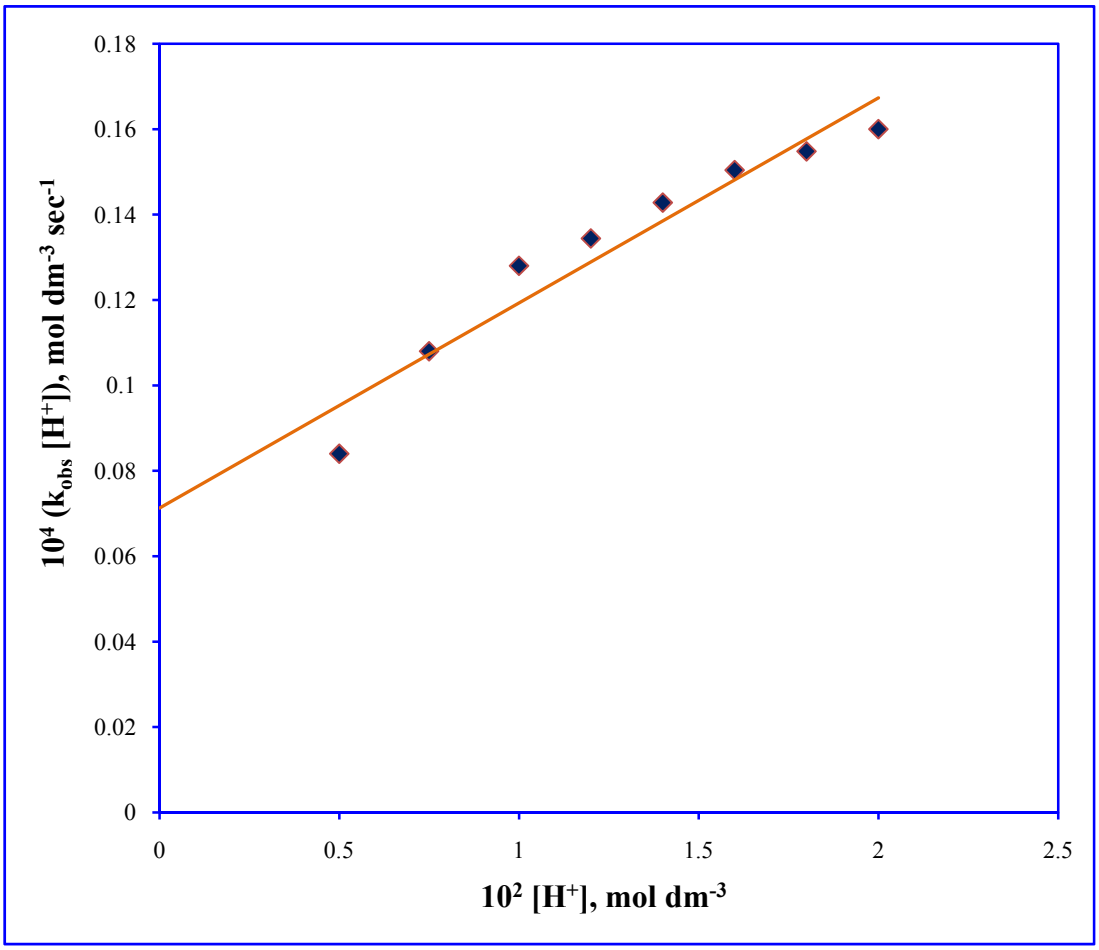

Figure 4.7: Plot of k_{obs} [H^+] versus [H^+]

[PMS] = 5.0×10^{-3} mol dm^{-3}; [Cunps] = 5.0×10^{-6} mol dm^{-3};

[Ser] = 5.0×10^{-2} mol dm^{-3}; I = 2.0×10^{-2} mol dm^{-3};

Temp. = 35°C

(Ref. Table: 4.10)

TABLE: 4.11

EFFECT OF IONIC STRENGTH

[PMS] = 5.0×10^{-3} mol dm^{-3} **Temp. = 35^{o}C**
[Ser] = 5.0×10^{-2} mol dm^{-3} **Titrant [Hypo] = 1.0×10^{-3} mol dm^{-3}**
[Cunps] = 5.0×10^{-6} mol dm^{-3} **Aliquot = 5.0 ml**
[H^{+}] = 1.0×10^{-2} mol dm^{-3}

10^2 I, mol dm^{-3}	**2.0**	**3.0**	**4.0**	**5.0**	**6.0**	**7.5**	**10.0**
Time in minutes	**Volume of Titrant (ml)**						
0	25.0	25.0	25.0	25.0	25.0	25.0	25.0
3	19.8	19.8	19.7	19.6	19.5	19.4	19.4
6	15.7	15.7	15.5	15.3	15.2	15.1	15.0
9	12.5	12.4	12.2	12.0	11.8	11.7	11.7
12	9.9	9.9	9.6	9.4	9.2	9.1	9.0
15	7.9	7.8	7.6	7.4	7.2	7.1	7.0
18	6.3	6.2	6.0	5.8	5.6	5.5	5.4
21	5.0	4.9	4.7	4.6	4.4	4.3	4.2
24	4.0	3.9	3.7	3.6	3.4	3.3	3.3
10^3 (k_{obs}), sec^{-1}	**1.28**	**1.29**	**1.32**	**1.35**	**1.38**	**1.40**	**1.41**

TABLE: 4.12

EFFECT OF TEMPERATURE

[PMS] = 5.0×10^{-3} mol dm^{-3}
[Ser] = 5.0×10^{-2} mol dm^{-3}
[Cunps] = 5.0×10^{-6} mol dm^{-3}
[H^+] = 1.0×10^{-2} mol dm^{-3}
I = 2.0×10^{-2} mol dm^{-3}

Titrant [Hypo] = 1.0×10^{-3} mol dm^{-3}
Aliquot = 5.0 ml

Temperature (^oC)	**30^oC**	**35^oC**	**40^oC**
Time in minutes	**Volume of Titrant (ml)**		
0	25.0	25.0	25.0
3	20.4	19.8	19.4
6	16.7	15.7	15.1
9	13.6	12.5	11.7
12	11.1	9.9	9.1
15	9.1	7.9	7.1
18	7.4	6.3	5.5
21	6.1	5.0	4.3
24	5.0	4.0	3.3
10^3 (k_{obs}), sec^{-1}	**1.12**	**1.28**	**1.4**

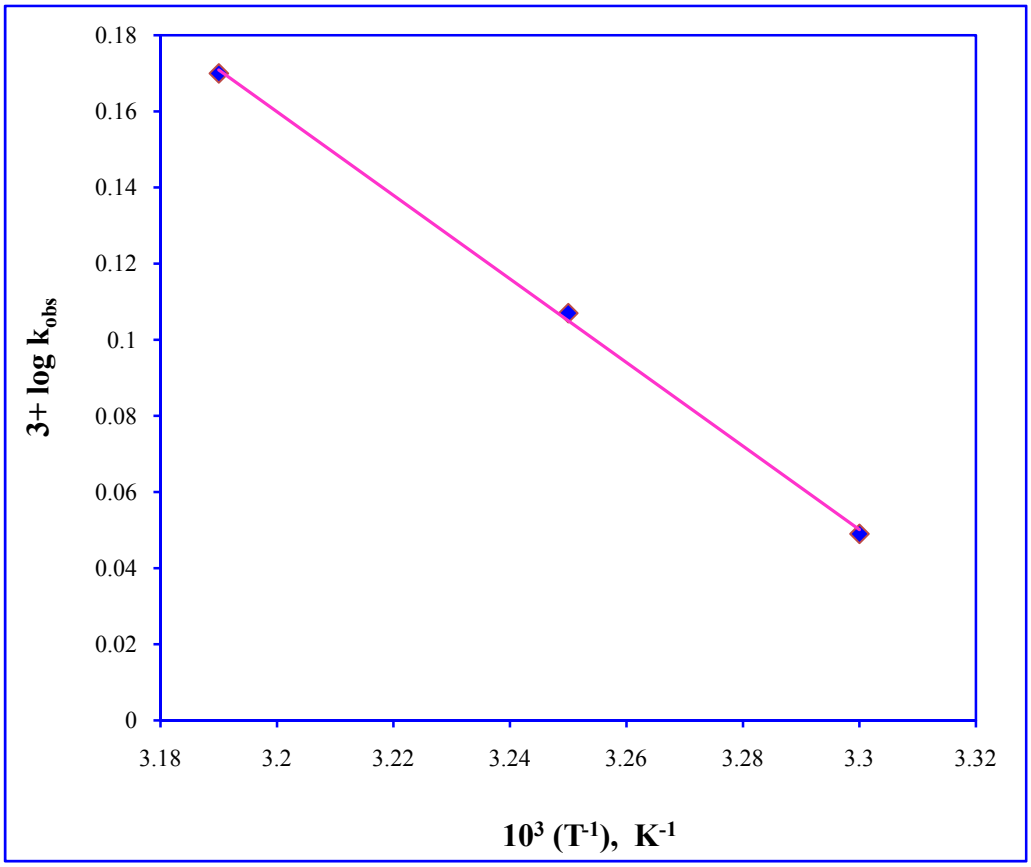

Figure 4.8: Plot of temperature dependence

[PMS] = 5.0×10^{-3} mol dm^{-3}; [Cunps] = 5.0×10^{-6} mol dm^{-3};

[Ser] = 5.0×10^{-2} mol dm^{-3}; I = 2.0×10^{-2} mol dm^{-3};

$[H^+] = 1.0\times10^{-2}$ mol dm^{-3}

(Ref. Table: 4.12)

The enthalpy of activation ($\Delta H^{\neq}$), free energy of activation ($\Delta G^{\neq}$) was also obtained 18.52 kJ mol^{-1} and 92.64 kJ mol^{-1} respectively. The moderate values of $\Delta H^{\neq}$ and $\Delta S^{\neq}$ were both favourable for electron transfer process. The high positive values of free energy of activation ($\Delta G^{\neq}$) and enthalpy of activation ($\Delta H^{\neq}$) indicated that the transition state was highly solvated while the negative values of entropy of activation (ΔS) was suggested the formation of more ordered transition state with reduction in the degree of freedom of the molecules.

4.4.7. Mechanism

Peroxomonosulphate ion being a monosubstituted hydrogen peroxide ($HOOSO_3^-$) is kinetically often more reactive despite the fact that former is slightly powerful oxidant ($E^{o}_{HSO_5^-/HSO_4^-}$ = 1.82 V) than hydrogen peroxide ($E^{o}_{H_2O_2/H_2O}$ = 1.776 V) [41, 42]. Moreover, HSO_5^- is more stable than H_2O_2 with respect to spontaneous decomposition in water **(equation 4.3)** when pKa_2 is equal to pH of the solution; HSO_5^- decomposes most rapidly with the reaction [43, 44].

$$HSO_5^- + SO_5^{2-} \longrightarrow 2SO_4^{2-} + O_2 + H^+ \qquad (4.3)$$

The hydrolysis of HSO_5^- as represented by **equation (4.4)** does not take place under experimental conditions.

$$HSO_5^- + H_2O \longrightarrow H_2O_2 + HSO_4^- \qquad (4.4)$$

Since the accepted structure [45] of the oxidant, oxone or peroxomonosulphuric acid used in the present study contains a sulphur atom surrounded tetrahedrally by a perhydroxyl groups and a hydroxyl group.

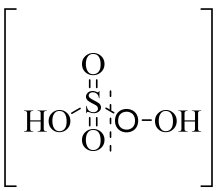

Peroxomonosulphuric acid has two ionisable protons viz. the proton of the hydroxyl group is equivalent to that of sulphuric acid proton and is highly ionized

[46] while that of polyhydroxyl group is weakly ionized. In aqueous solution, it exists as a mixture of HSO_5^- and SO_5^{2-} due the following equilibrium.

$$HSO_5^- \rightleftharpoons SO_5^{2-} + H^+$$

Under our experimental condition pH<9.8, oxone will exist as HSO_5^-. Furthermore, the species HSO_5^- is more reactive than SO_5^{2-} species. The higher reactivity of HSO_5^- is consistent both with the electrostatic effect and with weakening of the peroxide bond by the proton.

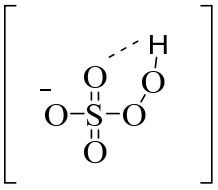

(HSO_5^-)

Serine is neutral amino acid, the probability of initial interaction in between serine and peroxomonosulphate is weak. Thus it is essential the reaction occurred in the presence of copper nanoparticles for the measurable rate of reaction. Metal nanoparticles possess large surface area as well as high surface energy of metal nanoparticles, other molecule easily adsorb upon their surface. Thus it is assumed here that serine anion gets adsorbed on copper nanoparticles through carbonyl oxygen. Copper nanoparticles react with HSO_5^- which gives peroxide oxygen which leads the oxidative decarboxylation of amino acid to form end product of aldehyde.

UV-visible spectrum of the mixture containing serine and peroxomonosulphate in presence of copper nanoparticles at temperature 35^oC showed an absorption maximum at 206 nm. Repeated spectral scans were recorded as a function of time versus absorbance (0-24 min.) shown in **figure 4.2.** The decrease peak in height with time indicates the deamination of serine. The kinetic results of oxidation of serine by peroxomonosulphate in acidic aqueous medium same as in the absence of copper nanoparticles as well as in the presence of copper nanoparticles but rate of reaction is ten times faster than uncatalyzed reaction.

The deamination of the amino group in serine to NH_3 occurs in the presence of copper nanoparticles by peroxomonosulphate, while peroxomonosulphate is change into hydrogen sulphate ion. The linear decrease in the rate with an increase in the $[H^+]$ suggest that the amino acid is being removed progressively as a kinetically inactive form. Although the definite mechanism of homogenous copper nanoparticles catalyzed oxidation of serine is not yet clear, based on previous report [47, 48] and a plausible route has been proposed to account for the experimental results which is shown in **scheme-1.**

$$HSO_5^- + Cu^o \longrightarrow Cu^{2+} + HSO_4^- + O^{2-}$$

$$Cu^{2+} + O^{2-} + R\text{-}\underset{\underset{NH_2}{|}}{\overset{\overset{H}{|}}{C}}\text{-}COOH \longrightarrow RCHO + NH_3 + CO_2 + Cu^o$$

$$HSO_5^- + R\text{-}\underset{\underset{NH_2}{|}}{\overset{\overset{H}{|}}{C}}\text{-}COOH \longrightarrow RCHO + NH_3 + HSO_4^- + CO_2$$

Scheme 1: The plausible route of copper nanoparticles catalyzed oxidation of serine

4.5. Conclusion

The oxidative decarboxylation of serine by peroxomonosulphate with highly efficient copper nanoparticles proceeds due the formation of peroxide oxygen atom and transfer to amino acid leads to the oxidation reaction. The synthesized mono-dispersed copper nanoparticles (ranging from 12-28 nm) by employing different concentration of L-ascorbic acid (ranging from 0.08 to 0.10 mol dm^{-3}) used as catalyst in the oxidation of serine in aqueous acid medium. The reaction is ten (10) times faster in the presence of a small amount (10^{-6} mol dm^{-3}) of copper nanoparticles in reaction mixture. The oxidation study revealed that the reaction was pseudo first order with respect to serine, peroxomonosulphate and copper nanoparticles. The study reveals that the size of copper nanoparticles decreases as the catalytic activity of copper nanoparticles increases. The role of hydrogen ions is crucial to the reaction. The study will be helpful in the biochemical and medical fields.

4.6. References

[1] G. C. Barrett, ***Amino acids, peptides and proteins, Royal society of Chem., UK, 1998***.

[2] Dr. Mrs. Ambika Shanmugam, ***Fundamental of biochemistry for medical students, Madras, 1996***.

[3] R. Pascual, M. A. Herraez, ***Can. J. Chem.,*** 63, (1985) 2349.

[4] S. Chandraju, K. S. Rangappa, N. M. Made Gowda, ***Int. J. Chem. Kinet.*** 31(1999) 525.

[5] S. Mathur, M. B. Yadav, V. Devra, ***J. Phys. Chem. Biophys.,*** 3 (2013) 128.

[6] R. S. Verma, M. J. Reddy, and V. R. Shastry, ***J. Chem. Soc., Perkin Trans.,*** 2 **(**1976) 469.

[7] V. Rao, S. B. Surender, and T. N. Rao, ***Int. J. Chem. Kiner.,*** 2 (1979) 165.

[8] G. Dryhurst, ***Periodate Oxidation of Diol and Other Functional Groups-Analytical and Structural Applications, Pergamon Press, London, 1970.***

[9] Kamaluddin, ***Indian J. Chem., Sect. A,*** 19 (1980) 431.

[10] G. Chandra and S. N. Srivastava, ***Rev. Roum. Chim.,*** 25 (1980) 1139.

[11] G. Ionita, Victor Em Sahini, G. Semenescu and P. Ionita, ***Acta Chim. Slov.,*** 47 (2000) 111.

[12] D. Laloo and M. M. Mahanti, ***J. Chem. Soc. Dalton Trans,*** 1 (1990) 311.

[13] I. Rao, S. Jain and P. D. Sharma, ***Int. J. Chem Kinetics,*** 24 (1992) 963.

[14] D. S. Munavalli, S. A. Chimatadar, S. T. Nandibewoor, ***Transition Metal Chemistry,*** 33 (2008) 535.

[15] M. S. Ramachandran and T. S. Vivekanandam, ***Bull. Chem. Soc. Jpn.,*** 60, (1987) 3397.

[16] M. S. Ramachandran, T. S. Vivekanandam, ***J. Chem. Soc. Perkin Trans. II,*** *00* (1984) 1341.

[17] M. S. Ramachandran, T. S. Vivekanandam, ***Tetrahedron,*** 40 (1984) 4929.

[18] R. Sayee Kannan, M. S. Ramachandran, ***Int. J. Chem. Kinetics,*** 35 (2003) 475.

[19] M. Sundar, D. Easwaramoorthy, S. K. Rani, I. M. Bilal, ***Catalysis Communication,*** 92 (2008) 340.

[20] S. Shailaja, M. S. Ramachandran, ***Inter. J. Chem. Kinet.,*** 43 (2011) 620.

[21] B. C. Gilbert, J. K. Stell, ***J. Chem. Soc. Perkin Trans.,*** 2 (1990)1281.

[22] R. SayeeKannan, D. Easwaramoorthy, K. Vijaya, S. Ramachandran, ***International Journal Chemical Kinetic***, 40 (2008) 44.

[23] V. Devra, M. B. Yadav, ***Rasayan J. Chem.,*** 5 (2012) 67.

[24] B. K. Singh, R. P. Singh, ***Asian J. of Chem.,*** 4 (1992) 508.

[25] D. Bilehal, R. Kulkarni, S. Nandibewoor, ***Journal of Molecular Catalysis A: Chemical,*** 232 (2005) 21.

[26] V. Seregar, T. M. Veeresh, S. T. Nandibewoor, ***Polyhedron***, 26 (2007) 1731.

[27] B. S. Berlett, P. B. Chock, M. B. Yim, E. R. Stadtman, ***Proc. Natl. Acad. Sci.,*** 87 (1990) 389.

[28] J. Sanathanlakshmi, P. Vankatesan, ***Chinese Journal of Catalysis,*** 33 (2012) 1306.

[29] X. Huang, I. H. El-Sayed, X. Yi, M. A. El-Sayed, ***J. Photochem. Photobiol. B,*** 81 (2005) 76.

[30] Z. J Jiang, C. Y Liu, L. W. Sun, ***J. of phys. chem. B,*** 109 (2005) 1730.

[31] D. Astruc, ***Nanoparticles and catalysis, Wiley-VCH: Weinheim, 2008.***

[32] V. G. Dan, M. Egon, ***New J. Chem.,*** 22 (1998) 1203.

[33] C. Y. Haung, S. R. Sheen, ***Materials Letters***, 30 (1997) 357.

[34] Song-ping Wu, Shu-yuan Meng, ***Materials Letters***, 60 (2006) 2438.

[35] S. H. Wu, D. H. Chen, ***Journal of Colloidal Interface Sciences***, 273 (2004) 165.

[36] L. Parimala, J. Santhanalakshmi, ***Nanoscience and Nanotechnology: An International Journal,*** 3 (2013) 4.

[37] C. J. Battaglia and J.O. Edwards, ***Inorg. Chem.,*** 4 (1965) 552.

[38] G. Raspi and M. Venturini. ***Chimia & Industria.,*** 50 (1968) 1.

[39] M. Venturini, A. Indelli and G. Raspi, ***J. Electroanalyt. Chem.,*** 38 (1971) 99.

[40] Y. Ramanandasarma, P. K. Saiprakash, ***Ind. J. Chem.,*** 19A (1980) 1175.

[41] J. Balez. ***Electro Chim. Acta,*** 29 (1984) 1239.

[42] M. Spiro, ***Electro. Chim. Acta***, 24 (1979) 313.

[43] J. O. Edwards, ***Ed., Peroxide Mechanism, Interscience, New York, 1962.***

[44] D. L. Ball, and J. O. Edwards, ***J. Am. Chem. Soc.,*** 78 (1956) 1125.

[45] F. A. Cotton, G. Wilkinson, C. A. Murillo, M. Bochmann, ***Advanced Inorganic Chemistry, 6th ed., John Wiley & Sons: Singapore, 2003.***

[46] L. B. Donald, J. O. Edwards, ***J. Chem. Soc.,*** 00 (1956) 1125.

[47] S. K. Upadhyay, M. C. Aggarwal, ***Indian J. Chem. A,*** 19 (1980) 5.

[48] V. K. Srivastava, K. K. Srivastava, M. N. Srivastava, B. L. Saxena, ***Indian J. Chem. A,*** 19 **(**1980) 1011.

Chapter-5

Kinetics of Copper Nanoparticles Catalyzed Oxidation of Threonine by Peroxomonosulphate in Aqueous Solution

Abstract

The undertaken kinetic study describes the oxidation of threonine (Thr) by peroxomonosulphate (PMS) in aqueous medium to evaluate catalytic activity of synthesized colloidal copper nanoparticles. Herein, the difference in catalytic activity can be attributed to the size variation in the resulting copper nanoparticles. The reaction is second order that is first order with respect to threonine and peroxomonosulphate. The main oxidation product of threonine has been identified as the aldehyde which is confirmed by the FTIR spectrum of a corresponding hydrazone. The effects of catalyst concentration, ionic strength and temperature on the reaction are also investigated. The energy and entropy of activation have been calculated to be 21.57±0.08 kJ mol^{-1} and -191.99±4 JK^{-1} mol^{-1} respectively. A plausible reaction mechanism for the oxidation of threonine accounting for all experimental observation has been suggested.

5.1. Introduction

The oxidations of amino acids particularly α-amino acids have been a subject of interest for the last three decades and the oxidants of varied thermodynamic potentialities have been employed both in acid and alkaline media. The oxidative decarboxylation of amino acid is of importance both from a photochemical view point and also from the view point of mechanism of amino acid metabolism. Their studies related to oxidative decarboxylation are important to understand more complicated enzyme catalyzed reaction and their mechanism. Threonine is an essential amino acid classified as nonpolar and forms active sites of enzyme and helps in maintaining proper confirmation by keeping them in proper ionic states.

Kinetics of oxidation of amino acids by a variety of oxidants like hexacyanoferrate(III) [1], peroxomonosulphate [2], peroxodisulphate [3], cerium(IV) [4], chromium(VI) [5] in the presence of transition metal catalyst as well as hexacyanoferrate(III) [6], Hydrogen peroxide [7], peroxomonosulphate [8] in the presence of transition metal nanoparticles in both acid and alkaline media have been studied. There are still controversies regarding the oxidation product of amino acids as keto acid is reported [9], both as intermediate and also the oxidation product. In most of the reaction, the end product is the aldehyde [10], the intermediate $RCH=N^{+}H_2$ undergoes to yield aldehyde whereas its interaction with the oxidant yields nitrile. However, various types of reaction modal have been suggested but the specific details are yet to be found out.

Peroxoacids are compounds of considerable potential. Peroxide act as oxygen donors to organic substrate [11]. In fact, it is the peroxide bond in these peracids is mainly responsible for its reactions. H_2O_2, being a parent analogue of the class of peracids, is a strong oxidizing and reducing agent both in acid and alkaline media [12, 13]. Peroxomonosulphate is one of them and is considered [14] to be a substituted hydrogen peroxide as one of the hydrogens of the latter is replaced by $–SO_3$ group, other hydrogen comes from acid group. The basicity of the acid is two. Its ionizable protons respectively resemble to that of sulphuric acid and hydrogen peroxide. Nevertheless the chemistry of peroxomonosulphate

is less understood as compared to that of peroxodisulphate but by and large should be similar as the cleavage of peroxide bond in both the cases occurs in their reactions. The reactions of peroxomonosulphate are, however, much faster than the reactions of peroxodisulphate despite structural resemblance. peroxo oxidants are environmentally libral because peroxo oxidants do not produce toxic compounds during the reaction thus study of kinetics of oxidation of amino acids by peroxo oxidants is an area of intensive research.

The applications of transition metal nanoparticles as catalyst for organic transformations include condensation [15], hydrosilation [16] and hydration reaction of unsaturated organic molecules [17] as well as redox [18] and other electron transfer process [19]. Research in nanoparticles has considerable attention since their use as unique properties and numerous applications in different area [20, 21]. Metallic nanoparticles are of great interest due to their excellent chemical, physical and catalytic properties [22]. In addition to their interesting physical properties exhibited due to quantum size effect, they also have applications in catalysis due to their large surface area and special morphologies. Copper nanoparticles were assumed cost effective as compare to noble metals like Ag, Au and Pt. Hence, they are potentially applied in the field of catalysis, cooling fluids [23] and conductive links [24].

Though studies on kinetics of oxidation of amino acid with peroxomonosulphate have been widely carried out, very few attempts have been made so far on the oxidative deamination of amino acid in presence of metal nanoparticles to assess their potential catalytic activity. In this series, an attempt has been made to construct a modal.

5. 2. Experimental Details

5.2.1. Material and Reagent

Peroxomonosulphate (PMS) was obtained from Sigma-Aldrich under the trade name “Oxone”. The purity of the triple salt $2KHSO_5 \cdot KHSO_4 \cdot K_2SO_4$ was estimated by iodometry [25] and found to be 98%. Doubly distilled water was used throughout the study; the second distillation was from alkaline permanganate

solution in an all glass assembly. All other reagents employed in this study were either of AnalaR grade or guaranteed reagent grade and were used as supplied without undertaking any further treatment.

5.2.2. Kinetic Measurements

Reaction mixture containing aqueous solution of all other reagents except peroxomonosulphate was adjusted to pH 7.0 employing potassium dihydrogen phosphate–sodium hydroxide buffer in a 250 ml glass stoppered Erlenmeyer flask and suspended in water bath thermostated at 35±0.1^{o}C unless stated otherwise. Peroxomonosulphate solution was taken in another flask and was immersed in the same water bath to attain the temperature of the reaction mixture. When these reaction solutions attained equilibrated temperature, an aliquot of requisite volume of concentration of peroxomonosulphate was taken out and immediately discharged into the reaction mixture, the time of initiation of the reaction was recorded when half of the contents from the pipette were released.

Kinetics was monitored by estimating peracid iodometrically at different time intervals. An aliquot (5 ml) was taken out of the reaction mixture periodically and then added to the solution of (10%) KI. The liberated iodine was titrated against thiosulphate solution using starch as an indicator without any interface from other components of the reaction mixture. The rate of reaction was studied under pseudo first order condition i.e. [Amino Acid]>> [PMS], the rate of reaction followed first order kinetics and rate constant (k_{obs}) was calculated from the linear plots of log [PMS] versus time. Kinetics was monitored by estimating [PMS] iodometrically [25] at different time intervals.

Initial rates were computed [26] employing plane mirror method. The pseudo first order plots were also made wherever, reaction conditions permitted. Results in triplicate were reproducible to within ±5%.

5.3. Stoichiometry and Product Analysis

The stoichiometry of the reaction was determined by identification of the oxidation product of the substrate under conditions of kinetics. The reaction

mixture with amino acid in excess over peroxomonosulphate was allowed to stand in thermostated water bath at 35±0.1^{o}C for 24 hour. After peroxomonosulphate completely utilized, the solution were concentrated and tested for the presence of nitrile and aldehyde, the products usually reported [22] in the oxidation of amino acids. Nitrile tests were negative and qualitative tests of aldehyde such as Tollen's reagent and Schiff's reagent were positive. Further, the reaction mixture was treated with acidified 2, 4-dinitrophenyl hydrazine solution, which yielded a hydrazone of corresponding aldehyde. The product appears to be aldehyde as is pointed out by IR spectra **(Figure 5.1)** and similarly the products was reported in presence of an excess of peroxomonosulphate in the oxidation of glycine and alanine in earlier study [27, 28]. The IR peaks at **3444 cm^{-1}, 2936.19 cm^{-1} and 1602.70 cm^{-1}** are attributed to –NH, –CH, –C=N stretching respectively. The functional group –C=N was produced from the condensation reaction of aldehyde and hydrazine. However, it was further confirmed by undertaking kinetics study of the reaction in stoichiometric concentration of the reactants. The results indicate the product to be aldehyde in one electron transfer oxidation. Therefore, the stoichiometry of the oxidation of threonine by an oxygen transfer from peroxomonosulphate in presence of copper nanoparticles with positive test of an aldehyde can be represented by **equation (5.1).**

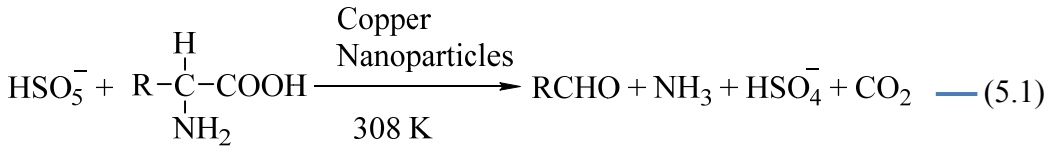

Where R represents –CH(CH$_3$)-OH

Further the reactions were undertaken with sufficient excess concentration of the oxidant over that of threonine, the excess was estimated iodometrically ensuring completion of the reaction. Results as mentioned in the **Table-5.1** support that a mole of oxidant consumes a mole of the substrate.

TABLE: 5.1

Stoichiometry of peroxomonosulphate and threonine in presence of copper nanoparticles in aqueous medium

S. No.	[PMS], mol dm^{-3}	[Thr], mol dm^{-3}	$\frac{\Delta[Thr]}{\Delta[PMS]}$
1.	0.005	0.002	1:1
2.	0.005	0.003	1:1
3.	0.005	0.004	1:0.98
4.	0.006	0.004	1:0.98

The reaction mixture containing peroxomonosulphate and threonine in presence of copper nanoparticles (size = 12 nm) at 35^{o}C was subjected to the UV-Visible absorption study which is presented in **figure 5.2.** The UV-visible spectrum shows a peak at 250 nm of threonine with maximum absorbance in the beginning of reaction. The decrease peak in height with time indicates the progression of catalyzed oxidation reaction of threonine. The spectrum shows the deamination of threonine. The liberated ammonia and carbon dioxide was confirmed by reaction with Nessler's test and lime water respectively.

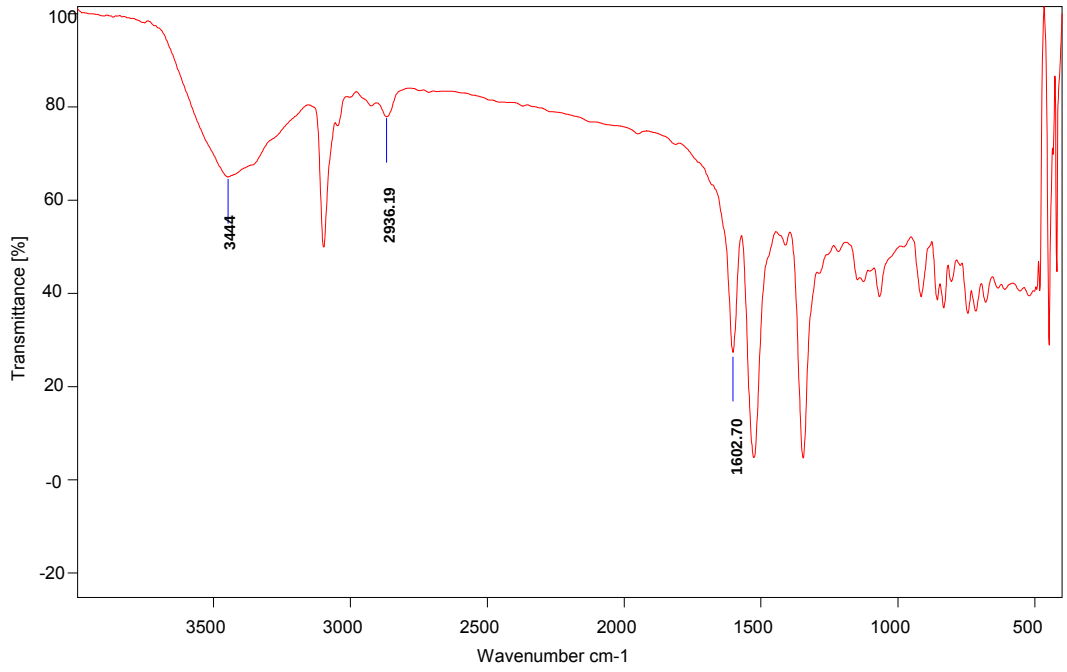

Figure 5.1: The FT-IR spectra of the hydrazone derivative from the reaction mixture of the threonine and peroxomonosulphate in the presence of copper nanoparticles

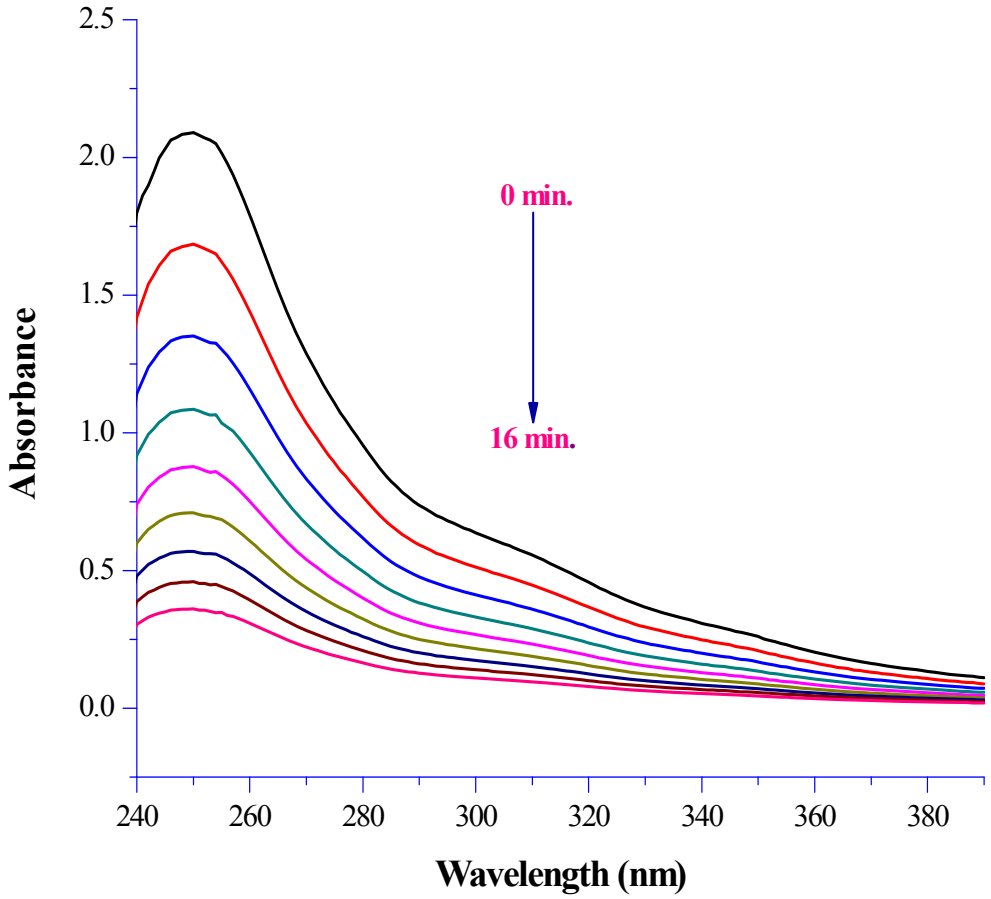

Figure 5.2: UV-Vis absorption spectra for the deamination of threonine (0-16 min.) in the presence of the copper nanoparticles (size = 12 nm)

[PMS] = 3.0×10^{-3} mol dm^{-3} ; [Thr] = 5.0×10^{-2} moldm^{-3} ;

[Cunps] = 5.0×10^{-6} mol dm^{-3}; pH = 7.0, Temp. = 35°C

5.4. Results and Discussion

5.4.1. Effect of Peroxomonosulphate Concentration

The concentration of peroxomonosulphate was varied in the range (1.0–5.0)×10^{-3} mol dm^{-3} at two but fixed concentrations of threonine to be 5.0×10^{-3} and 6.0×10^{-3} mol dm^{-3} respectively keeping fixed concentrations of other reaction ingredients viz.[Cunps] = 5.0×10^{-6} mol dm^{-3} and pH = 7.0 at 35^{o}C. Initial rates (k_i mol dm^{-3} sec^{-1}) were calculated employing plane mirror method and a plot of initial rate (k_i) versus [PMS] (PMS, has been used in place of peroxomonosulphate heretofore) was made that yielded a straight line passing through the origin **(Figure 5.3)** ascribing first order dependence with respect to peroxomonosulphate. Second order plots were also made by making plots of log ($[Thr]_t/[PMS]_t$) against time **(Figure 5.4).** Second order rate constants calculated from these plots were in excellent agreement with those calculated from initial rates. Results are given in **Table 5.2 and 5.3.**

5.4.2. Effect of Threonine Concentration

The concentration of threonine was varied from 5.0×10^{-3} to 1.0×10^{-2} mol dm^{-3}at three but fixed concentration of peracid viz. 1.0×10^{-3}, 2.0×10^{-3}, 3.0×10^{-3} mol dm^{-3}, [Cunps] = 5.0×10^{-6} mol dm^{-3} and pH = 7.0 at 35^{o}C. Initial rates were calculated and a plot of initial rate (k_i mol dm^{-3} sec^{-1}) against [Thr] was made, a straight line passing through the origin was obtained **(Figure 5.5)** confirming to first order dependence with respect to threonine. Certain reactions were also undertaken under pseudo first order conditions ([Thr]>> [PMS]) under identical experimental conditions, pseudo first order plots were made **(Figure 5.6)** and pseudo first order rate constants (k_{obs}, sec^{-1}) evaluated from these plots were found to increase proportionately with the increasing concentration of threonine.

Second order rate constants calculated from initial rate, pseudo first order rate constants and also obtained from second order plots are in good agreements. Results are given in **Table-5.4, 5.5, 5.6, 5.7 and 5.8.**

TABLE: 5.2

VARIATION OF PEROXOMONOSULPHATE

[Thr] = 5.0×10^{-3} mol dm^{-3} **Temp. = 35^{o}C**

[Cunps] = 5.0×10^{-6} mol dm^{-3} **Titrant [Hypo] = 1.0×10^{-3} mol dm^{-3}**

pH = 7.0 **Aliquot = 5.0 ml**

10^3 [PMS], mol dm^{-3}	**1.0***	**2.0**	**3.0**	**4.0**	**5.0**
Time in minutes	**Volume of Titrant (ml)**				
0	10.0	10.0	15.0	(0)20.0	(0)25.0
20	8.5	8.4	12.4	(30)15.0	(40)17.2
40	7.0	7.0	10.4	(60)11.3	(80)13.5
60	6.0	5.8	8.5	(90)9.0	(120)10.8
80	5.0	4.8	7.0	(120)7.3	(160)9.1
100	4.3	4.1	6.0	(150)5.0	(200)7.5
120	3.6	3.3	5.5	(180)3.9	-
140	3.0	2.8	5.2	-	-
160	2.1	2.5	4.3	-	-
10^7 (k_i), mol dm^{-3} sec^{-1}	**1.80**	**3.60**	**5.40**	**7.40**	**9.10**
10^2(k), mol^{-1} dm^3 sec^{-1}	**3.62**	**3.57**	**3.61**	**3.62**	**-**

*Hypo = 5.0×10^{-4} mol dm^{-3}

TABLE: 5.3

VARIATION OF PEROXOMONOSULPHATE

[Thr] = 6.0×10^{-3} mol dm^{-3} **Temp. = 35^{o}C**

[Cunps] = 5.0×10^{-6} mol dm^{-3} **Titrant [Hypo] = 1.0×10^{-3} mol dm^{-3}**

pH = 7.0 **Aliquot = 5.0 ml**

10^3 [PMS], mol dm^{-3}	**1.0***	**2.0**	**3.0**	**4.0**	**5.0**
Time in minutes			**Volume of Titrant (ml)**		
0	10.0	10.0	15.0	20.0	25.0
20	8.0	7.9	12.0	15.8	19.9
40	6.6	6.6	9.5	13.0	16.6
60	5.3	5.2	7.9	10.4	13.3
80	4.3	4.4	6.3	9.2	11.3
100	3.5	3.2	5.0	7.4	9.0
120	2.9	2.7	4.0	6.5	8.1
140	2.3	2.3	3.4	6.0	7.1
160	1.5	1.8	3.1	5.0	6.2
10^7 (k_i), mol dm^{-3} sec^{-1}	**2.16**	**4.33**	**6.50**	**8.66**	**10.80**
10^2 (k), mol^{-1} dm^3 sec^{-1}	**3.63**	**3.63**	**3.66**	**3.61**	**3.80**

*Hypo = 5.0×10^{-4} mol dm^{-3}

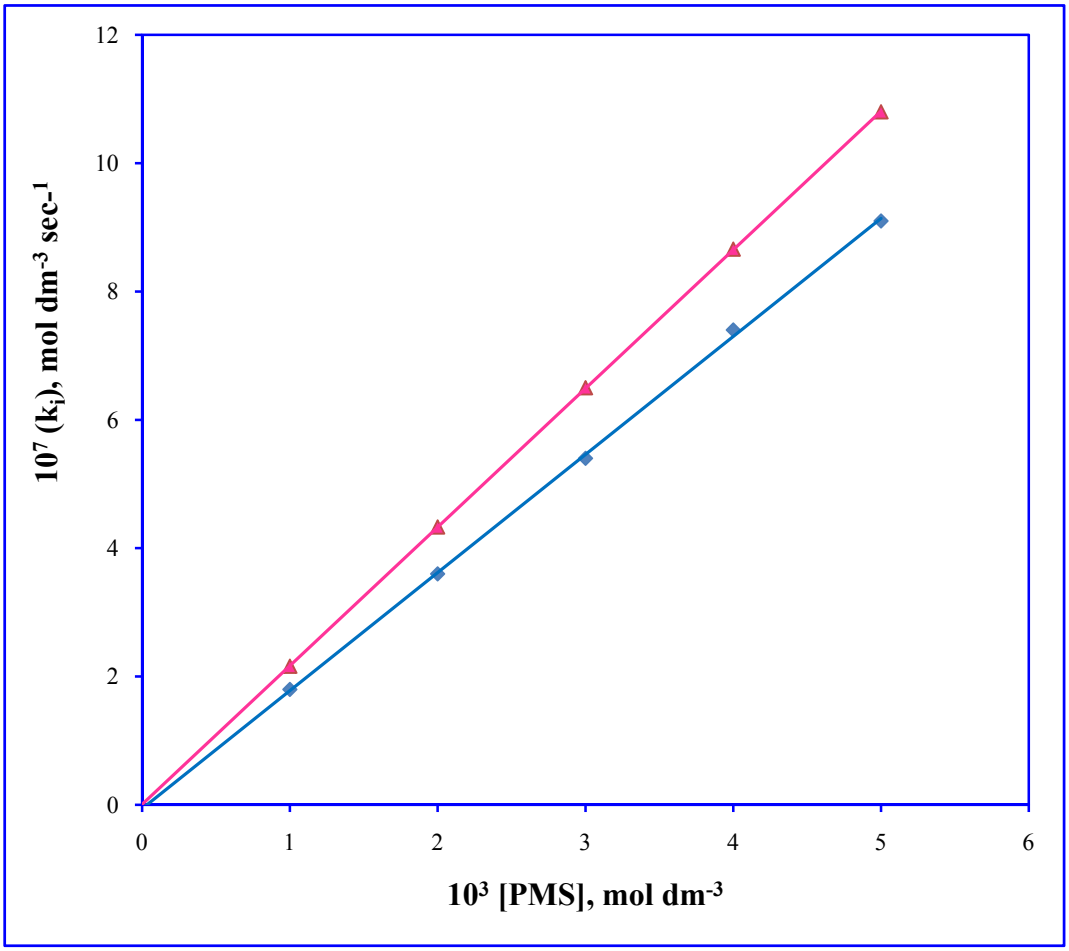

Figure 5.3: Variation of peroxomonosulphate

[Thr] = (♦), 5.0×10^{-3} mol dm^{-3}; (▲), 6.0×10^{-3} mol dm^{-3};
[Cunps] = 5.0×10^{-6} mol dm^{-3}; pH = 7.0, Temp. = 35°C

(Ref. Table: 5.2 and 5.3)

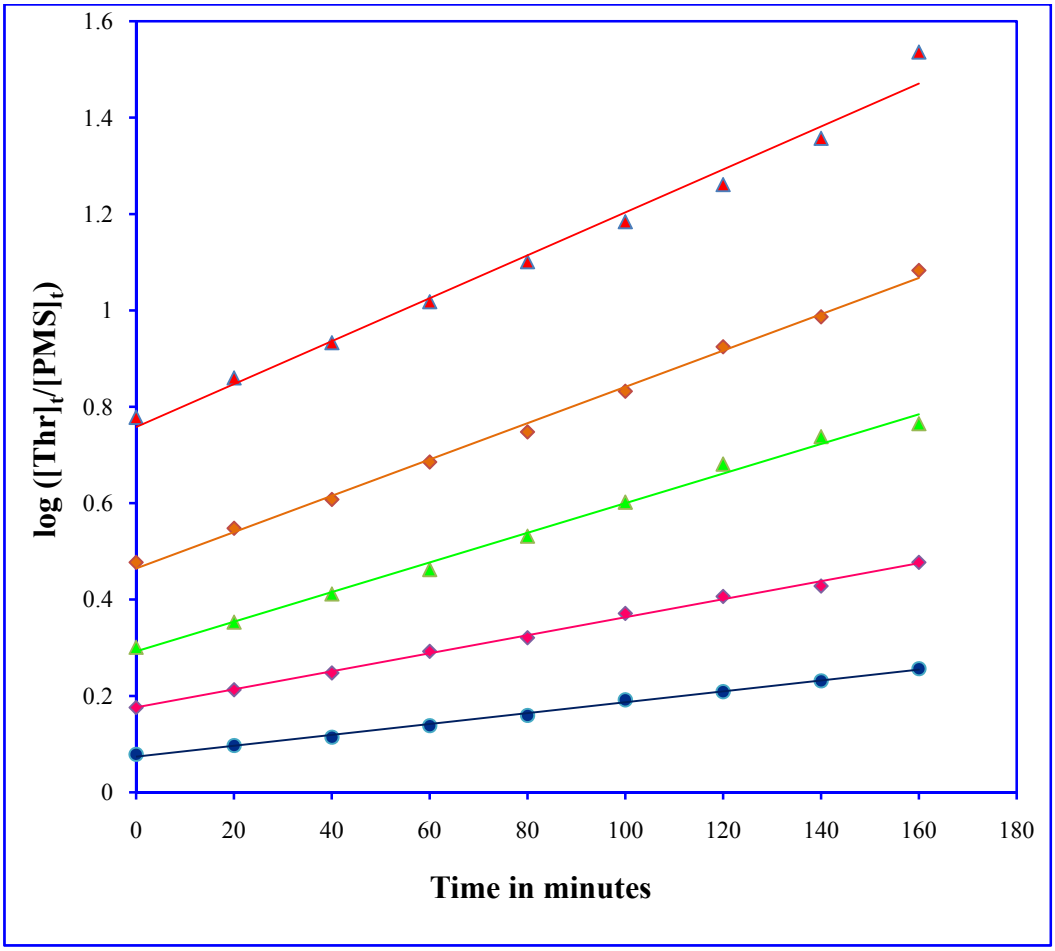

Figure 5.4: Second order plots

[Thr]= 6.0×10^{-3} mol dm^{-3}; [Cunps] = 5.0×10^{-6} mol dm^{-3};

pH = 7.0, Temp. = 35°C

[PMS] = (A) 1.0×10^{-3} mol dm^{-3} (B) 2.0×10^{-3} mol dm^{-3}

(C) 3.0×10^{-3} mol dm^{-3} (D) 4.0×10^{-3} mol dm^{-3}

(E) 5.0×10^{-3} mol dm^{-3}

(Ref. Table: 5.3)

TABLE: 5.4

VARIATION OF THREONINE

[PMS] = 1.0×10^{-3} mol dm^{-3} **Temp. = 35^{o}C**

[Cunps] = 5.0×10^{-6} mol dm^{-3} **Titrant [Hypo] = 5.0×10^{-4} mol dm^{-3}**

pH = 7.0 **Aliquot = 5.0 ml**

10^3 [Thr], mol dm^{-3}	**5.0**	**6.0**	**7.0**	**8.0**	**9.0**	**10.0**
Time in minutes	**Volume of Titrant (ml)**					
0	10.0	10.0	10.0	10.0	10.0	10.0
20	8.5	8.0	7.8	7.6	7.4	7.2
40	7.0	6.6	6.5	6.4	6.2	6.1
60	6.0	5.3	5.1	5.0	4.9	4.7
80	5.0	4.3	4.2	4.0	3.6	3.7
100	4.3	3.5	3.3	3.2	2.3	2.7
120	3.6	2.9	2.8	2.6	1.2	1.7
140	3.0	2.3	2.2	2.1	-	-
160	2.1	1.5	1.1	-	-	-
10^7 (k_i), mol dm^{-3} sec^{-1}	**1.80**	**2.16**	**2.58**	**2.95**	**3.28**	**3.65**
10^2 (k), mol^{-1} dm^3 sec^{-1}	**3.62**	**3.63**	**3.60**	**3.67**	**3.63**	**3.61**

TABLE: 5.5

VARIATION OF THREONINE

[PMS] = 2.0×10^{-3} mol dm^{-3} **Temp. = 35^{o}C**

[Cunps] = 5.0×10^{-6} mol dm^{-3} **Titrant [Hypo] = 1.0×10^{-3} mol dm^{-3}**

pH = 7.0 **Aliquot = 5.0 ml**

10^3 [Thr], mol dm^{-3}	**5.0**	**6.0**	**7.0**	**8.0**	**9.0**	**10.0**
Time in minutes	**Volume of Titrant (ml)**					
0	10.0	10.0	10.0	10.0	10.0	10.0
20	8.4	7.9	7.6	7.5	7.4	7.3
40	7.0	6.6	6.3	6.3	6.2	6.2
60	5.8	5.2	5.2	5.3	5.2	5.1
80	4.8	4.4	4.3	4.3	4.2	4.0
100	4.1	3.2	3.4	3.5	3.2	2.3
120	3.3	2.7	2.5	2.7	2.2	1.8
140	2.8	2.3	1.7	1.9	1.2	1.1
160	2.5	1.8	1.3	-	-	-
10^7 (k_i), mol dm^{-3} sec^{-1}	**3.60**	**4.33**	**5.10**	**5.80**	**6.60**	**7.30**
10^2 (k), mol^{-1} dm^3 sec^{-1}	**3.57**	**3.63**	**3.65**	**3.64**	**3.61**	**3.63**

TABLE: 5.6

VARIATION OF THREONINE

[PMS] = 3.0×10^{-3} mol dm^{-3} **Temp. = 35^{o}C**

[Cunps] = 5.0×10^{-6} mol dm^{-3} **Titrant [Hypo] = 1.0×10^{-3} mol dm^{-3}**

pH = 7.0 **Aliquot = 5.0 ml**

10^3 [Thr], mol dm^{-3}	**5.0**	**6.0**	**7.0**	**8.0**	**9.0**	**10.0**
Time in minutes	**Volume of Titrant (ml)**					
0	15.0	15.0	15.0	15.0	15.0	15.0
20	12.4	11.7	11.9	11.8	11.7	11.6
40	10.4	9.5	9.5	9.4	9.4	9.0
60	8.5	7.9	7.7	7.8	7.7	7.5
80	7.0	6.3	6.1	6.1	6.0	5.5
100	6.0	5.0	4.8	4.6	4.5	4.3
120	5.5	4.0	3.5	3.0	3.1	3.0
140	5.2	3.4	3.0	2.8	2.2	2.0
160	4.3	3.1	2.3	1.7	1.3	-
10^7 (k_i), mol dm^{-3} sec^{-1}	**5.40**	**6.50**	**7.50**	**8.66**	**9.67**	**10.80**
10^2 (k), mol^{-1} dm^3 sec^{-1}	**3.61**	**3.66**	**3.66**	**3.63**	**3.62**	**3.62**

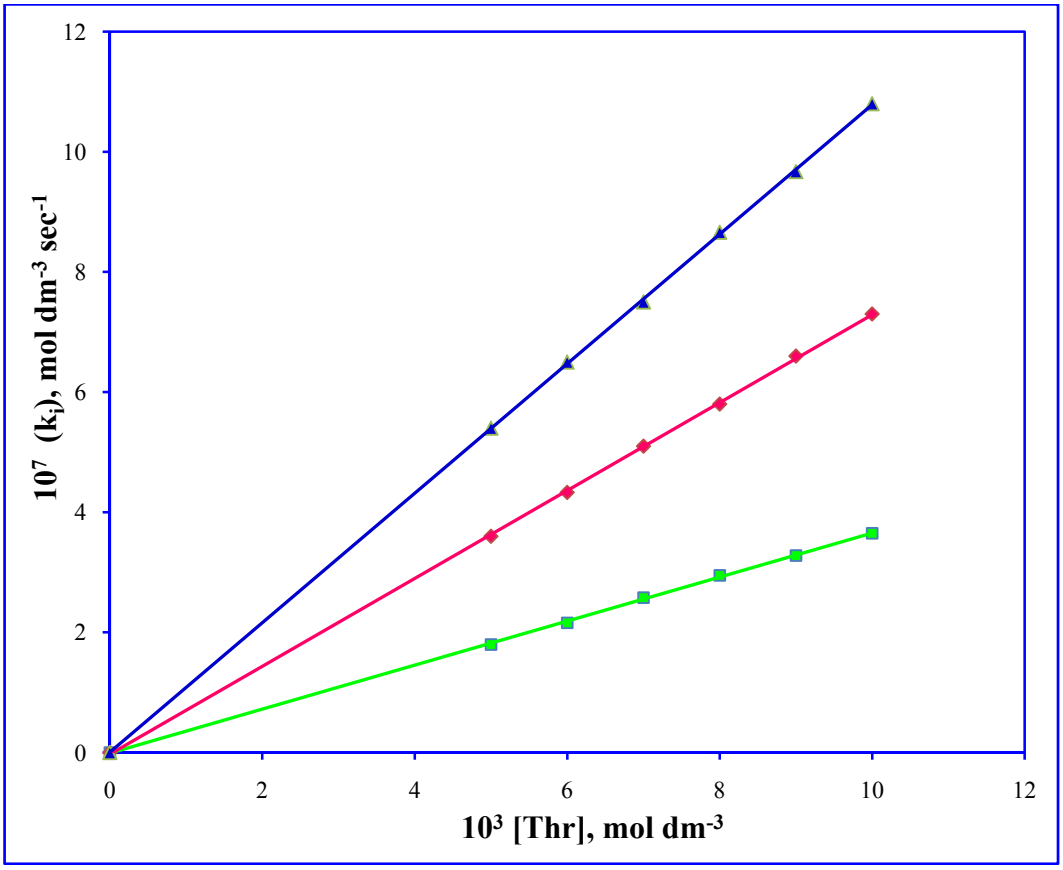

Figure 5.5: Variation of threonine

[PMS] = (■), 1.0×10^{-3} mol dm^{-3}; (♦), 2.0×10^{-3} mol dm^{-3};
(▲), 3.0×10^{-3} mol dm^{-3};
[Cunps]= 5.0×10^{-6} mol dm^{-3}; pH = 7.0, Temp. = 35°C

(Ref. Table: 5.4, 5.5, 5.6)

TABLE: 5.7

VARIATION OF THREONINE

[PMS] = 2.0×10^{-3} mol dm^{-3} **Temp. = 35^{o}C**

[Cunps] = 5.0×10^{-6} mol dm^{-3} **Titrant [Hypo] = 1.0×10^{-3} mol dm^{-3}**

pH = 7.0 **Aliquot = 5.0 ml**

10^2 [Thr], mol dm^{-3}	**3.0**	**3.5**	**4.0**	**4.5**	**5.0**	**5.5**	**6.0**
Time in minutes	**Volume of Titrant (ml)**						
0	(0)10.0	(0)10.0	(0)10.0	10.0	10.0	10.0	10.0
2	(3)8.2	(3)8.0	(3)7.8	8.2	8.0	7.9	7.7
4	(6)6.8	(6)6.3	(6)6.0	6.8	6.5	6.3	6.0
6	(9)5.6	(9)5.1	(9)4.7	5.6	5.2	5.0	4.7
8	(12)4.6	(12)4.0	(12)3.6	4.6	4.2	3.9	3.6
10	(15)3.8	(15)3.2	(15)2.8	3.8	3.4	3.1	2.8
12	(18)3.1	(18)2.6	(18)2.2	3.1	2.7	2.5	2.2
14	(21)2.6	(21)2.0	(21)1.7	2.6	2.2	2.0	1.7
16	(24)2.1	(24)1.6	(24)1.3	2.1	1.8	1.5	1.3
10^3 (k_{obs}), sec^{-1}	**1.07**	**1.26**	**1.40**	**1.62**	**1.80**	**1.94**	**2.12**

Figures in parentheses denote time in minutes

TABLE: 5.8

VARIATION OF THREONINE

[PMS] = 3.0×10^{-3} mol dm^{-3} **Temp. = 35^{o}C**

[Cunps] = 5.0×10^{-6} mol dm^{-3} **Titrant [Hypo] = 1.0×10^{-3} mol dm^{-3}**

pH = 7.0 **Aliquot = 5.0 ml**

10^2 [Thr], mol dm^{-3}	**3.0**	**3.5**	**4.0**	**4.5**	**5.0**	**5.5**	**6.0**
Time in minutes	**Volume of Titrant (ml)**						
0	(0)15.0	(0)15.0	(0)15.0	15.0	15.0	15.0	15.0
2	(3)12.3	(3)12.0	(3)11.6	12.3	12.1	11.9	11.6
4	(6)10.2	(6)9.6	(6)9.0	10.2	9.7	9.4	9.0
6	(9)8.4	(9)7.6	(9)7.0	8.4	7.8	7.4	6.9
8	(12)6.9	(12)6.1	(12)5.4	6.9	6.3	5.9	5.4
10	(15)5.7	(15)4.9	(15)4.2	5.7	5.1	4.7	4.2
12	(18)4.7	(18)3.9	(18)3.2	4.7	4.1	3.7	3.2
14	(21)3.8	(21)3.1	(21)2.5	3.8	3.3	2.9	2.5
16	(24)3.2	(24)2.5	(24)1.9	3.2	2.6	2.3	1.9
10^3 (k_{obs}), sec^{-1}	**1.08**	**1.25**	**1.42**	**1.62**	**1.81**	**1.95**	**2.14**

Figures in parentheses denote time in minutes

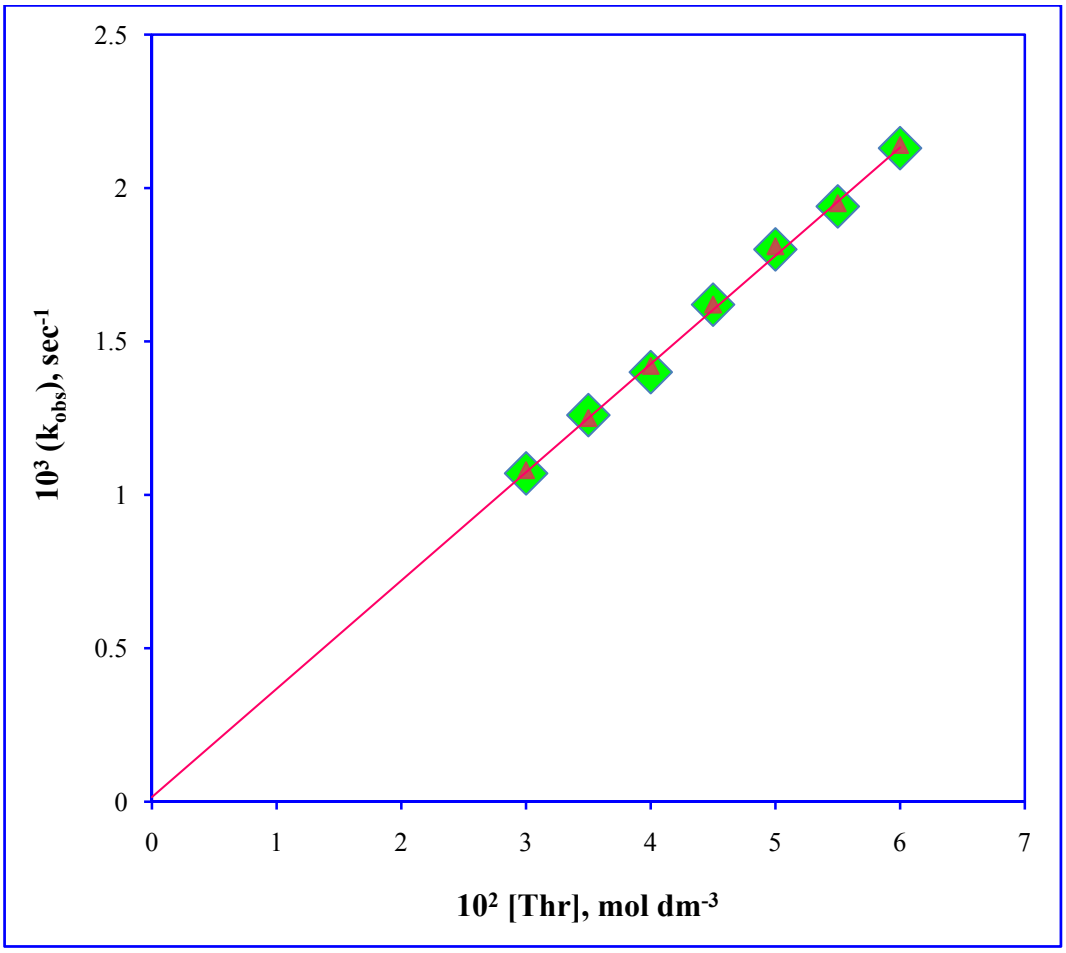

Figure 5.6: Variation of threonine

[PMS] = (♦), 2.0×10^{-3} mol dm^{-3}; (▲), 3.0×10^{-3} mol dm^{-3};
[Cunps] = 5.0×10^{-6} mol dm^{-3}; pH = 7.0, Temp. = 35°C

(Ref. Table: 5.7 and 5.8)

5.4.3. Effect of Copper Nanoparticles Concentration

The effect of copper nanoparticles on the rate of oxidation of threonine has been studied at varying concentration 1.0×10^{-6} – 8.0×10^{-6} mol dm^{-3} at three different nanoparticles, synthesized at three concentration (0.08, 0.09, 0.10 mol dm^{-3}) of ascorbic acid (as discussed in chapter 3) with average size 28, 16 and 12 nm respectively at constant concentration of [PMS] = 3.0×10^{-3} mol dm^{-3}, [Thr] = 5.0×10^{-2} mol dm^{-3} at pH = 7.0 and temperature 35°C. The rate of reaction increases with increasing concentration of copper nanoparticles. The pseudo first order rate constants as plotting against the concentration of copper nanoparticles yielded straight line with non-zero intercept **(Figure 5.7),** indicate simultaneously uncatalyzed reaction. The catalytic activity of copper nanoparticles seems different when concentration of reducing agent is varied from 0.08 to 0.1 mol dm^{-3}. The difference in catalytic activity can be attributed to the size variation in the resulting copper nanoparticles. The trend in the calculated rate constant being 12>16>28nm size of copper nanoparticles. Results are given in **Table-5.9, 5.10, 5.11.**

5.4.4. Effect of pH

The oxidation of threonine reaction is pH sensitive. The rate of oxidation of threonine was studied at different pH viz. 4.0, 7.0, 9.5 respectively while other reactant and reaction conditions were constant. pH was maintained employing sodium acetate-acetic acid buffer for pH 4.0, potassium dihydrogen phosphate-sodium hydroxide buffer for pH 7.0, sodium borate-sodium hydroxide buffer for pH 9.5 at constant concentration of [PMS] = 3.0×10^{-3} mol dm^{-3}, [Thr] = 5.0×10^{-2} mol dm^{-3}, [Cunps] = 5.0×10^{-6} mol dm^{-3} and temperature 35°C. The rate constant is obtained 1.65×10^{-3}, 1.81×10^{-3}, 1.30×10^{-3} sec^{-1} respectively. The optimum pH giving the maximum rate constant was found to be 7.0. Results are given in **Table-5.12.**

TABLE: 5.9

EFFECT OF COPPER NANOPARTICLES

(SIZE = 12 nm)

[PMS] = 3.0×10^{-3} mol dm^{-3} **Temp. = 35°C**

[Thr] = 5.0×10^{-2} mol dm^{-3} **Titrant [Hypo] = 1.0×10^{-3} mol dm^{-3}**

pH = 7.0 **Aliquot = 5.0 ml**

10^6 [Cunps], mol dm^{-3}	**0.0**	**1.0**	**2.0**	**3.0**	**4.0**	**5.0**	**6.0**	**7.0**	**8.0**
Time in minutes	**Volume of Titrant (ml)**								
0	(0)15.0	(0)15.0	(0)15.0	(0)15.0	(0)15.0	15.0	15.0	15.0	15.0
2	(12)12.5	(6)12.3	(4)12.1	(3)12.1	(3)11.5	12.1	11.7	11.3	10.8
4	(24)10.5	(12)10.0	(8)9.8	(6)9.7	(6)8.8	9.7	9.1	8.5	7.8
6	(36)8.7	(18)8.2	(12)8.0	(9)7.8	(9)6.7	7.8	7.1	6.4	5.7
8	(48)7.3	(24)6.7	(16)6.4	(12)6.3	(12)5.1	6.3	5.5	4.8	4.1
10	(60)6.1	(30)5.5	(20)5.2	(15)5.1	(15)3.9	5.1	4.3	3.6	3.0
12	(72)5.1	(36)4.5	(24)4.2	(18)4.1	(18)3.0	4.1	3.4	2.7	2.1
14	(84)4.3	(42)3.7	(28)3.4	(21)3.3	(21)2.3	3.3	2.6	2.0	1.6
16	(96)3.6	(48)3.0	(32)2.8	(24)2.7	(24)1.8	2.6	2.0	1.5	1.1
10^3 (k_{obs}), sec^{-1}	**0.25**	**0.56**	**0.88**	**1.20**	**1.49**	**1.81**	**2.08**	**2.38**	**2.70**

Figures in parentheses denote time in minutes

TABLE: 5.10

EFFECT OF COPPER NANOPARTICLES

(SIZE = 16 nm)

[PMS] = 3.0×10^{-3} mol dm^{-3} **Temp. = 35°C**

[Thr] = 5.0×10^{-2} mol dm^{-3} **Titrant [Hypo] = 1.0×10^{-3} mol dm^{-3}**

pH = 7.0 **Aliquot = 5.0 ml**

10^6 [Cunps], mol dm^{-3}	**0.0**	**1.0**	**2.0**	**3.0**	**4.0**	**5.0**	**6.0**	**7.0**	**8.0**
Time in minutes	**Volume of Titrant (ml)**								
0	(0)15.0	(0)15.0	(0)15.0	(0)15.0	(0)15.0	15.0	15.0	15.0	15.0
2	(12)12.5	(8)11.9	(4)12.4	(4)11.8	(3)11.9	12.5	12.1	11.8	11.4
4	(24)10.5	(16)9.5	(8)10.3	(8)9.3	(6)9.5	10.4	9.8	9.3	8.7
6	(36)8.7	(24)7.5	(12)8.6	(12)7.3	(9)7.5	8.7	8.0	7.3	6.6
8	(48)7.3	(32)6.0	(16)7.1	(16)5.7	(12)6.0	7.2	6.4	5.7	5.0
10	(60)6.1	(40)4.7	(20)5.9	(20)4.5	(15)4.7	6.0	5.2	4.5	3.8
12	(72)5.1	(48)3.8	(24)4.9	(24)3.6	(18)3.8	5.0	4.2	3.6	2.9
14	(84)4.3	(56)3.0	(28)4.0	(28)2.8	(21)3.0	4.2	3.4	2.8	2.2
16	(96)3.6	(64)2.4	(32)3.4	(32)2.2	(24)2.4	3.5	2.8	2.2	1.7
10^3 (k_{obs}), sec^{-1}	**0.25**	**0.48**	**0.78**	**1.00**	**1.28**	**1.52**	**1.76**	**2.00**	**2.28**

Figures in parentheses denote time in minutes

TABLE: 5.11

EFFECT OF COPPER NANOPARTICLES

(SIZE = 28 nm)

[PMS] = 3.0×10^{-3} mol dm^{-3} **Temp. = 35°C**

[Thr] = 5.0×10^{-2} mol dm^{-3} **Titrant [Hypo] = 1.0×10^{-3} mol dm^{-3}**

pH = 7.0 **Aliquot = 5.0 ml**

10^6 [Cunps], mol dm^{-3}	**0.0**	**1.0**	**2.0**	**3.0**	**4.0**	**5.0**	**6.0**	**7.0**	**8.0**
Time in minutes	**Volume of Titrant (ml)**								
0	(0)15.0	(0)15.0	(0)15.0	(0)15.0	(0)15.0	(0)15.0	15.0	15.0	15.0
2	(12)12.5	(7)12.5	(5)12.4	(4)12.3	(3)12.4	(3)12.0	12.6	12.3	12.0
4	(24)10.5	(14)10.4	(10)10.2	(8)10.0	(6)10.3	(6)9.6	10.6	10.0	9.6
6	(36)8.7	(21)8.6	(15)8.4	(12)8.2	(9)8.6	(9)7.7	8.9	8.2	7.6
8	(48)7.3	(28)7.2	(20)7.0	(16)6.7	(12)7.1	(12)6.1	7.5	6.7	6.1
10	(60)6.1	(35)6.0	(25)5.7	(20)5.5	(15)5.9	(15)4.9	6.3	5.5	4.9
12	(72)5.1	(42)4.9	(30)4.7	(24)4.5	(18)4.9	(18)3.9	5.3	4.5	3.9
14	(84)4.3	(49)4.1	(35)3.9	(28)3.7	(21)4.0	(21)3.1	4.5	3.7	3.1
16	(96)3.6	(56)3.4	(40)3.2	(32)3.0	(24)3.4	(24)2.5	3.8	3.0	2.5
10^3 (k_{obs}), sec^{-1}	**0.25**	**0.44**	**0.64**	**0.84**	**1.04**	**1.24**	**1.44**	**1.68**	**1.88**

Figures in parentheses denote time in minutes

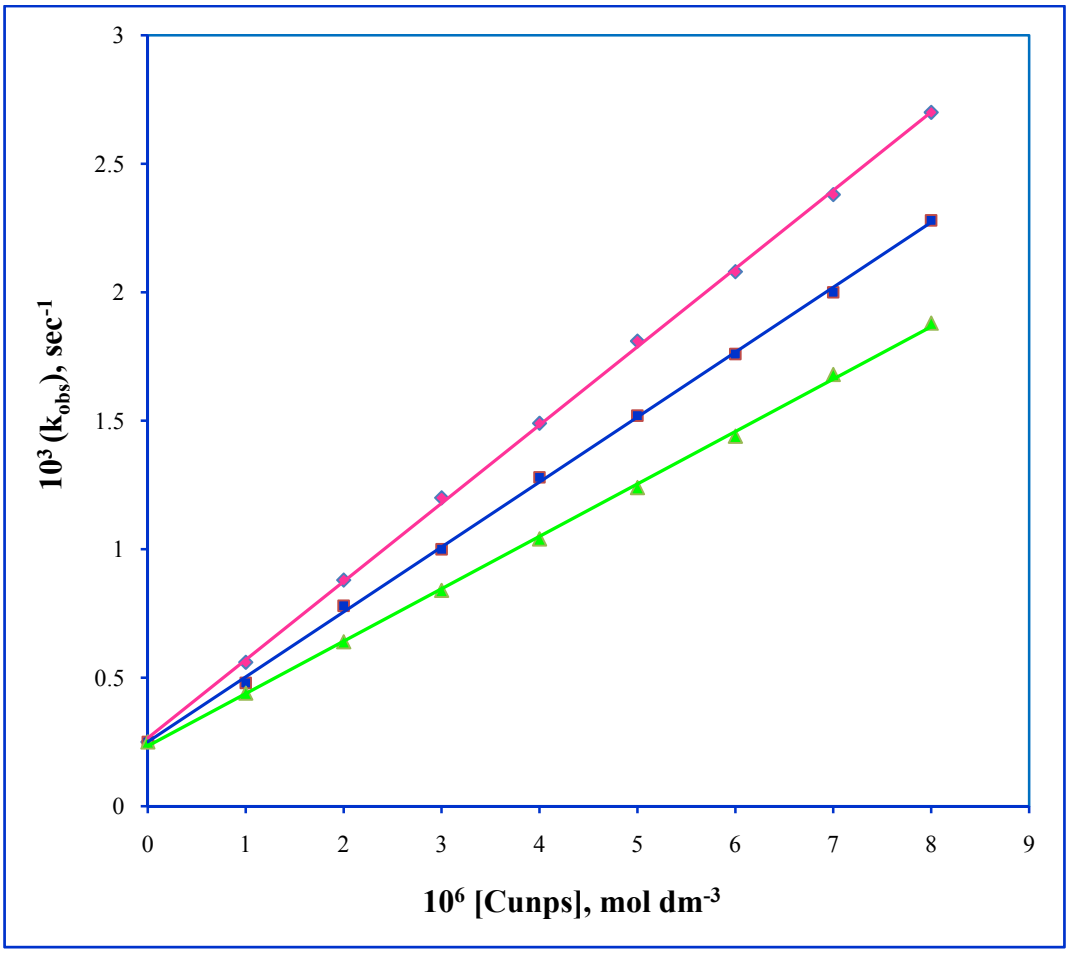

Figure 5.7: Effect of copper nanoparticles concentration at different size of copper nanoparticles (♦) 12 nm, (■) 16 nm, (▲) 28 nm

[PMS] = 3.0×10^{-3} mol dm^{-3}; [Thr] = 5.0×10^{-2} mol dm^{-3} ;
pH = 7.0, Temp. = 35°C

(Ref. Table: 5.9, 5.10 and 5.11)

TABLE: 5.12

EFFECT OF pH

[PMS] = 3.0×10^{-3} mol dm^{-3} **Temp. = 35^{o}C**

[Thr] = 5.0×10^{-2} mol dm^{-3} **Titrant [Hypo] = 1.0×10^{-3} mol dm^{-3}**

[Cunps] = 5.0×10^{-6} mol dm^{-3} **Aliquot = 5.0 ml**

pH	**4.0**	**7.0**	**9.5**
Time in minutes	**Volume of Titrant (ml)**		
0	15.0	15.0	(0)15.0
2	12.3	12.1	(3)11.9
4	10.1	9.7	(6)9.4
6	8.3	7.8	(9)7.4
8	6.8	6.3	(12)5.9
10	5.6	5.1	(15)4.7
12	4.6	4.1	(18)3.7
14	3.8	3.3	(21)2.9
16	3.1	2.6	(24)2.3
10^3 (k_{obs}), sec^{-1}	**1.65**	**1.81**	**1.30**

Figures in parentheses denote time in minutes

5.4.5. Effect of temperature

The reactions were studied at three different temperature (30°C, 35°C, 40°C) at constant concentration of [Thr] = 5.0×10^{-2} mol dm^{-3}, [PMS] = 3.0×10^{-3} mol dm^{-3}, [Cunps] = 5.0×10^{-6} mol dm^{-3} and pH = 7.0. The rate of reaction and observed rate constants increases with increasing temperature, these results were tabulated in **Table-5.13.** A plot of log k_{obs} was made against 1/T that yielded a straight line **(Figure 5.8).** The energy of activation (E_a) was calculated from the slope of the line to be 21.57±0.08 kJ mol^{-1}. The entropy of activation was calculated by employing the relationship [29],

$$k=\frac{k_B T}{h}\times e^{-\Delta H^{\neq}/RT}.e^{\Delta S^{\neq}/R}$$

Where $\Delta S^{\neq}$ is entropy of activation and other terms have their usual significance. Thus entropy of activation was calculated to be -191.99±4 JK^{-1} mol^{-1}.

A perusal of data shows that the reaction rates were characterized by large negative entropy of activation ($\Delta S^{\neq}$) and a low value of energy of activation (E_a). The latter is characteristic of a bimolecular reaction in solution while the former was mainly observed in polar solvents and also suggested the formation of a rigid transition state.

5.4.6. Mechanism

Peroxomonosulphate can be regarded as monosubstituted hydrogen peroxide ($HOOSO_3^-$) in which one of the hydrogens is replaced by a SO_3 group. Since peroxomonosulphate is dibasic acid in which the central sulfur atom is tetrahedrally surrounded by a perhydroxyl groups, a hydroxyl group and two oxo groups. As the final product of peroxomonosulphate oxidation is harmless sulphate.

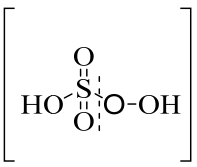

TABLE: 5.13

EFFECT OF TEMPERATURE

[PMS] = 3.0×10^{-3} mol dm^{-3}

[Thr] = 5.0×10^{-2} mol dm^{-3} **Titrant [Hypo] = 1.0×10^{-3} mol dm^{-3}**

[Cunps] = 5.0×10^{-6} mol dm^{-3} **Aliquot = 5.0 ml**

pH = 7.0

Temperature (^oC)	**30^oC**	**35^oC**	**40^oC**
Time in minutes	**Volume of Titrant (ml)**		
0	15.0	15.0	15.0
2	12.4	12.1	11.7
4	10.3	9.7	9.1
6	8.5	7.8	7.0
8	7.0	6.3	5.5
10	5.8	5.1	4.3
12	4.8	4.1	3.3
14	4.0	3.3	2.6
16	3.3	2.6	2.0
10^3 (k_{obs}), sec^{-1}	**1.58**	**1.81**	**2.10**

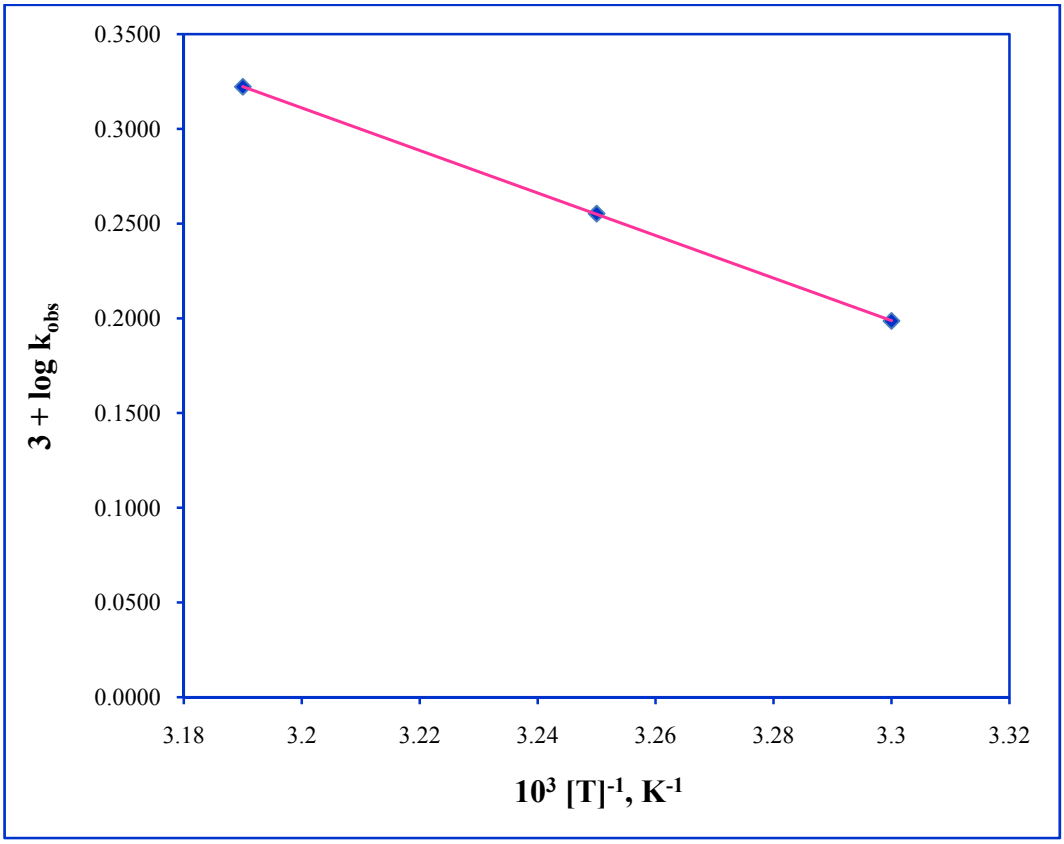

Figure 5.8: Plot of temperature dependence

[PMS] = 3.0×10^{-3} mol dm^{-3}; [Cunps] = 5.0×10^{-6} mol dm^{-3};
[Thr] = 5.0×10^{-2} mol dm^{-3}; pH = 7.0

(Ref. Table: 5.13)

If pKa_1 and pKa_2 of peroxomonosulphate are taken into account, two species of the peracid are expected in the solution.

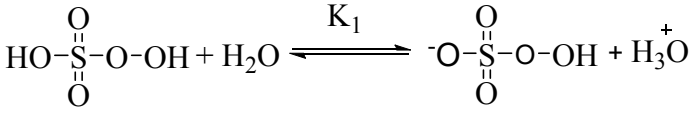

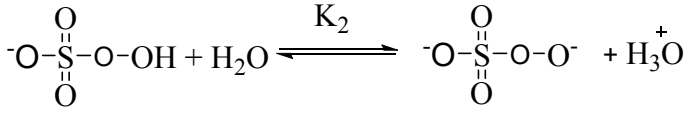

Thus the species of peracid are HSO_5^- and SO_5^{2-}, the latter is predominant in solution of which pH>9.88. In acidic pH proton is tightly held and HSO_5^- becomes predominant.

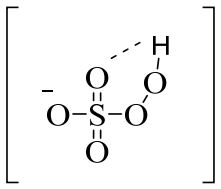

(HSO_5^-)

Threonine is a neutral amino acid. Then, the probability of initial interaction in between threonine and peroxomonosulphate is low. The deamination of the amino group in threonine to NH_3 occurs in the presence of copper nanoparticles by peroxomonosulphate, while peroxomonosulphate is change into hydrogen sulphate ion. Catalysis by metal nanoparticles can be considered as kind of semi-heterogeneous or quasi-homogeneous catalysis at the frontier between homogeneous and heterogeneous catalysis [8]. The catalysis mechanism must thus involve the reaction of peroxomonosulphate ions in solution with the adsorbed threonine. The copper nanoparticles catalyzed reaction between peroxomonosulphate and threonine occurs on the particle surface, as proposed for the HCF and $S_2O_3^{-2}$ via electron transfer from the Pt particle surface such that the Pt nanoparticles act as highly dispersed electrodes [30]. Metal nanoparticles possess large surface area as well as high surface energy of metal nanoparticles, other molecule easily adsorb upon their surface. Thus it is assumed here that threonine anion gets adsorbed on copper nanoparticles through carbonyl oxygen.

The U.V. Visible spectrophotometric examination of the reaction mixture was carried out to know the progress of the reaction in the present study. Further, in presence of peroxomonosulphate and copper nanoparticles the absorbance gradually decreases of the peak (250 nm) with the extension of time due to threonine decrease as a result of catalytic oxidation reaction. The kinetic results of oxidation of threonine by peroxomonosulphate in aqueous medium indicate that the rate of catalyzed reaction exhibit ten (10) order of magnitude faster than uncatalyzed reaction. Although definite mechanism of copper nanoparticle catalyzed oxidation of threonine is not clear, based on previous report [9] and a plausible mechanism of catalytic oxidation of threonine is depicted in scheme-1.

It is further interesting to mention that the stoichiometry of the reaction was further justified kinetically when reactions were carried out in stoichiometric concentrations. The plots of $[PMS]_t^{-1}$ versus time were made **(Figure 5.9 and Table-5.14)** and the rate constants evaluated from these plots agree with the second order rate constants calculated from initial rates, pseudo first order plots and second order plots **(Tables 5.15 and 5.16).**

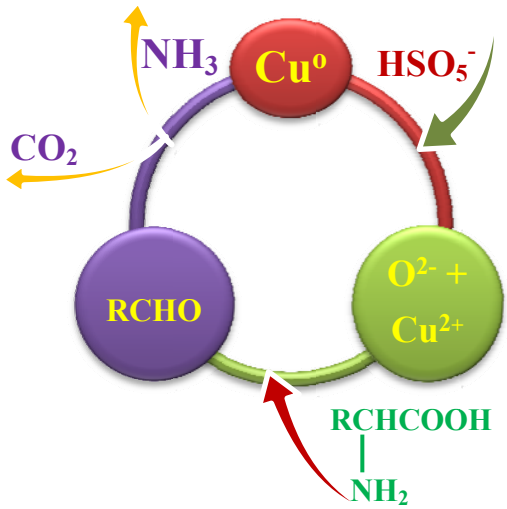

Scheme 1: The plausible route of copper nanoparticles catalyzed oxidation of threonine by peroxomonosulphate in aqueous medium

TABLE: 5.14

VARIATION OF [PMS] AND [THREONINE]

[Cunps] = 5.0×10^{-6} mol dm^{-3} **Temp. = 35^{o}C**

pH = 7.0 **Titrant [Hypo] = 1.0×10^{-3} mol dm^{-3}**

Aliquot = 5.0 ml

10^3 [PMS], mol dm^{-3}	**2.0**	**3.0**	**4.0**	**5.0**
10^3 [Thr], mol dm^{-3}	**2.0**	**3.0**	**4.0**	**5.0**
Time in minutes		**Volume of Titrant (ml)**		
0	(0)10.0	(0)15.0	20.0	25.0
20	(30)8.7	(30)12.5	17.2	20.8
40	(60)7.9	(60)10.8	15.1	17.2
60	(90)7.1	(90)9.6	13.5	15.0
80	(120)6.5	(120)8.6	11.9	13.5
100	(150)6.0	(150)7.7	10.8	11.9
120	(180)5.6	(180)6.9	10.0	10.8
140	-	-	9.3	10.0
160	-	-	8.5	9.1
10^2 (k), mol^{-1} dm^3 sec^{-1}	**3.61**	**3.60**	**3.60**	**3.64**

Figures in parentheses denote time in minutes

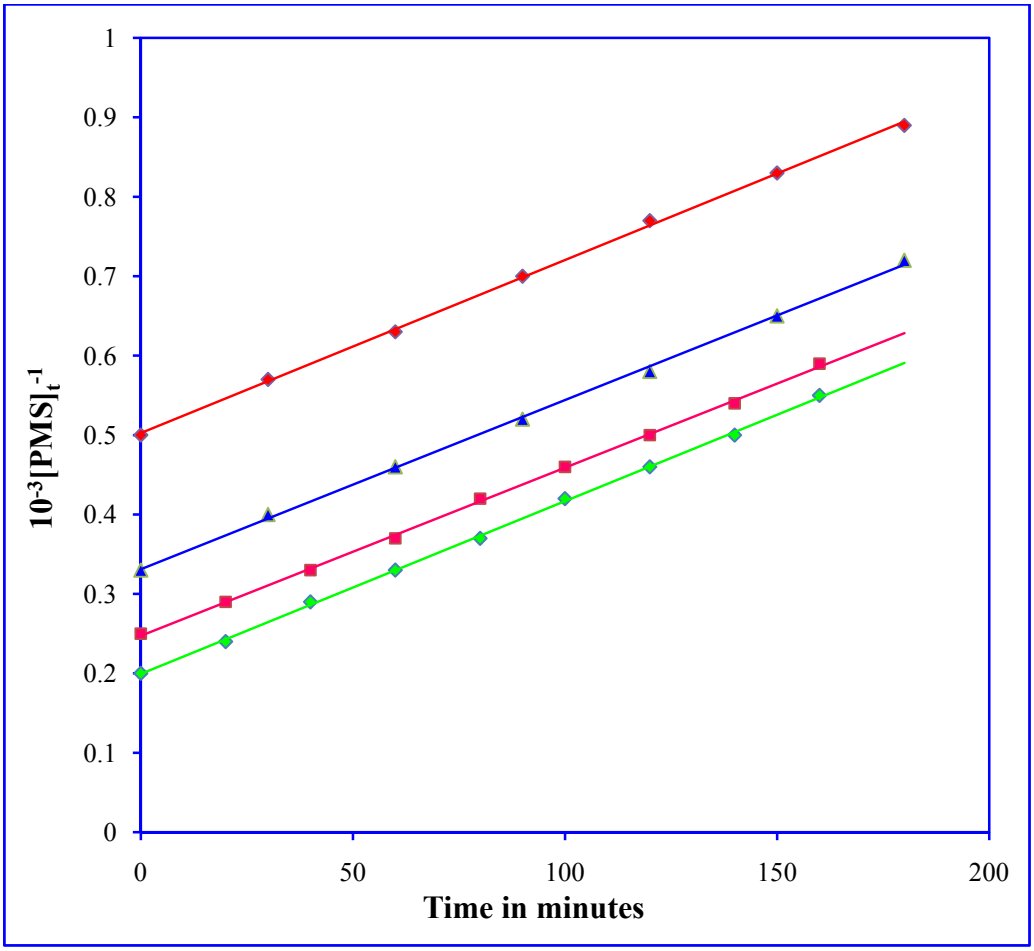

Figure 5.9: A plot of $[PMS]_t^{-1}$ versus time

[Cunps] = 5.0×10^{-6} mol dm^{-3} ; pH = 7.0, Temp. = 35°C;

[PMS] and [Thr] = (A) 2.0×10^{-3} mol dm^{-3} (B) 3.0×10^{-3} mol dm^{-3}

(C) 4.0×10^{-3} mol dm^{-3} (D) 5.0×10^{-3} mol dm^{-3}

(Ref. Table: 5.15)

TABLE: 5.15

Second order rate constants from stoichiometric plots in peroxomonosulphate and threonine reaction in presence of copper nanoparticles in aqueous medium

[Cunps] = 5.0×10^{-6} mol dm^{-3}; pH = 7.0; Temp. = $35^{o}C$

S. No.	10^3 [PMS], mol dm^{-3}	10^3 [Thr], mol dm^{-3}	10^2 (k), mol^{-1} dm^3 sec^{-1}
1.	2.0	2.0	3.61
2.	3.0	3.0	3.60
3.	4.0	4.0	3.60
4.	5.0	5.0	3.64

TABLE: 5.16

Initial rate (k_i), pseudo first order rate constants (k_{obs}) and second order rate constant (k) in the reaction of threonine with peroxomonosulphate in the presence of copper nanoparticles ([Cunps] =5.0×10^{-6} mol dm^{-3}) in aqueous medium at temp. 35°C and pH = 7.0.

S. No.	10^3 [PMS] (mol dm^{-3})	10^3 [Thr] (mol dm^{-3})	10^7 k_i (mol dm^{-3} sec^{-1})	10^3 k_{obs} (sec^{-1})	10^2 k (dm^3 mol^{-1} sec^{-1})
1.	1.0	5.0	1.80	-	3.62(3.60)
2.	1.0	6.0	2.16	-	3.63(3.60)
3.	1.0	7.0	2.58	-	3.60(3.69)
4.	1.0	8.0	2.95	-	3.67(3.69)
5.	1.0	9.0	3.28	-	3.63(3.64)
6.	1.0	10.0	3.65	-	3.61(3.65)
7.	2.0	5.0	3.60	-	3.57(3.60)
8.	2.0	6.0	4.33	-	3.63(3.61)
9.	2.0	7.0	5.10	-	3.65(3.64)
10.	2.0	8.0	5.80	-	3.64(3.62)
11.	2.0	9.0	6.60	-	3.61(3.66)
12.	2.0	10.0	7.30	-	3.63(3.65)
13.	3.0	5.0	5.40	-	3.61(3.60)
14.	3.0	6.0	6.50	-	3.66(3.61)
15.	3.0	7.0	7.50	-	3.66(3.57)
16.	3.0	8.0	8.66	-	3.63(3.61)
17.	3.0	9.0	9.67	-	3.62(3.58)
18.	3.0	10.0	10.80	-	3.62(3.60)
19.	4.0	5.0	7.47	-	3.62(3.7)
20.	5.0	5.0	9.1	-	- (3.64)
21.	4.0	6.0	8.66	-	3.61(3.61)
22.	5.0	6.0	10.80	-	3.80(3.60)
23.	2.0	30.0	-	1.07	3.56
24.	2.0	35.0	-	1.26	3.60

Table: 5.16 Contd…

Table: 5.16 Contd…

S. No.	10^3 [PMS] (mol dm^{-3})	10^3 [Thr] (mol dm^{-3})	10^7 k_i (mol dm^{-3} sec^{-1})	10^3 k_{obs} (sec^{-1})	10^2 k (dm^3 mol^{-1} sec^{-1})
25.	2.0	40.0	-	1.40	3.50
26.	2.0	45.0	-	1.62	3.60
27.	2.0	50.0	-	1.80	3.60
28.	2.0	55.0	-	1.94	3.52
29.	2.0	60.0	-	2.12	3.55
30.	3.0	30.0	-	1.08	3.60
31.	3.0	35.0	-	1.25	3.57
32.	3.0	40.0	-	1.42	3.55
33.	3.0	45.0	-	1.62	3.60
34.	3.0	50.0	-	1.81	3.62
35.	3.0	55.0	-	1.95	3.54
36.	3.0	60.0	-	2.14	3.56

Results in parenthesis were derived from initial rates.

5.5. Conclusions

The catalytic activity of synthesized copper nanoparticles was evaluated by the oxidation of threonine in aqueous medium. Monodispersed copper nanoparticles (ranging from 12 - 28 nm) were synthesized using different concentration of L-ascorbic acid as reducing agent and antioxidant. Increasing the size of copper nanoparticles decreases the catalytic activity of copper nanoparticles. The results of this study indicate that the reaction between threonine and peroxomonosulphate in the presence of copper nanoparticles is second-order that is first order with respect to threonine and peroxomonosulphate. pH has the remarkable effect on the rate of reaction. The copper nanoparticles are expected to be suitable alternative and play an important role in the field of catalysis and environmental remediation.

5.6. References

[1] M. Yadav, V. Devra, A. Rani, ***Journal of Indian Chemical Society***, 49 (2010) 442.

[2] M. Sundar, D. Easwaramoorthy, S. Kutti Rani, I. M. Bilal, ***Catalysis Communications***, 9 (2008) 2340.

[3] M. A. A. Khalid, Arabian ***Journal for Science and Engineering***, 33 (2007) 199.

[4] V. Devra, ***J. Indian Chem. Soc.,*** 82 (2005) 290.

[5] S. Mathur, M. B. Yadav, V. Devra, ***J. Phys. Chem. Biophys***. 3 (2013) 128.

[6] A. Goel, S. Sharma, ***Journal of Chemical, Biological and Physical Sciences***, 2 (2012) 628.

[7] J. Sanathanlakshmi, P. Vankatesan, ***Chinese Journal of Catalysis,*** 3 (2012) 1306.

[8] L. Parimala, J. Santhanalakshmi, ***Nanoscience and Nanotechnology: An International Journal***, 3 (2013) 4.

[9] D. Laloo, M. K. Mahanti, ***J. Chem. Soc. Dalton Trans.,*** 1(1990) 311.

[10] D. Gupta, M. Bhasin, V. Devra, I. Sharma, P. D. Sharma, ***Oxidation Communication,*** 19 (1996) 242.

[11] S. Debey, S. Hemkar, C. L. Khandelwal, P. D. Sharma, ***Inorg. Chem. Commun.,*** 5 (2002) 903.

[12] H. Remy, ***Treatise on Inorganic Chemistry, Elsevier, Amsterian, 1956.***

[13] F. A. Cotton and G. Wilkinson, ***Advanced Inorganic Chemistry, 2nd Edn, Wiley-Eastern, New Delhi, 1966.***

[14] P. Maruthamuthu and P. Neta, ***J. Phy. Chem.,*** 81 (1981) 937.

[15] A. Nasirian, ***Int. J. Nano Dim.,*** 2 (2012) 159.

[16] L. N. Lewis, N. Lewis, ***J. Am. Chem. Soc.*** 108 (1986) 7228; L. N. Lewis, R. Uriarte, **J. Organometallics**, 9 (1990) 621.

[17] H. Hirai, H. Komiyama, ***Bull. Chem. Soc. Jpn.,*** 59 (1986) 545.

[18] M. Spiro, ***Catal. Today,*** 17 (1993) 517.

[19] G. Maayan, R. Neumann, ***Catal. Lett.,*** 123 (2008) 41.

[20] A. Tiwari, S. K. Shukla, ***In Advanced Carbon Materials and Technology, WILEY-Scrivener Publishing LLC, USA, 2014;*** A. Tiwari, ***Adv. Mat. Lett.,*** 3 (2012) 1.

[21] P. Singh, A. Katyal, R. Kalra, R. Chandra, ***Tetrahedron Lett.***, 49 (2008) 727.

[22] T. M. D. Dang, T. T. T. Le, M. C. Fribourg-Blanc Dang, ***Adv. Nat. Sci. Nanosci. Nanotechnol.,*** 2 (2011) 015009.

[23] H. S. Kim, S. Dhage, D. E. Shim, H. T. Hahn, ***Appl. Phys. A***, 97 (2009) 791.

[24] J. C. Y. Lee, K. J. Lee, N. E. Stott, D. Kim, ***Nanotechnology,*** 19 (2008) 415604.

[25] J. Mendham, R. C. Denney, J. D. Barnes, M. J. K. Thomas, ***Vogel's Textbook of Quantitative Chemical Analysis, 6th edition., Pearson Education, Harlow, U.K, 2004.***

[26] M. Lat Show, ***J. Am. Chem. Soc.,*** 47 (1925) 789.

[27] R. M. Thombare, G. S. Gokavi, J***. Braz. Chem. Soc.,*** 0 (2014) 1.

[28] R. T. Malharrao, S. G. Gavisiddappa, ***J. Braz. Chem. Soc.,*** *00* (2014) 1.

[29] K. J. Laidler, ***Reaction kinetics, pergamon press, oxford, 1983***.

[30] Y. Li, J. Petroski, M. A. E1-Sayed, ***J. Phy. Chem. B,*** 104 (2000) 10956.

Chapter-6

Kinetics of Copper Nanoparticles Catalyzed Oxidation of Alanine by Peroxodisulphate in Acidic Aqueous Medium

Abstract

In this chapter, the catalysis by colloidal copper nanoparticles was observed kinetically on the rate of reaction of deamination and decarboxylation of alanine by peroxodisulphate in acidic medium by varying its concentration keeping constant concentration of other reaction ingredients at three temperatures (30^oC, 35^oC, 40^oC). The copper nanoparticles catalyst revealed very good catalytic activity and the kinetic data of the reaction presents the reaction was found to be first order with respect to peroxodisulphate and zero order with respect to alanine. The main product of the oxidation is the corresponding aldehyde which is corroborated by FTIR spectrum. Based on the experimental results, a plausible mechanism was proposed. The stoichiometry of the oxidation of alanine by peroxodisulphate in the presence of copper nanoparticles was presented by equation (1)

$$S_2O_8^{2-} + R-\underset{NH_2}{\overset{H}{C}}-COOH + H_2O \xrightarrow[H^+,\ 308\ K]{\text{Copper Nanoparticles}} RCHO + NH_3 + 2HSO_4^- + CO_2 \quad (1)$$

The thermodynamic parameters energy and entropy of activation have been calculated to be 23.846 kJ mol^{-1} and -238.17 JK^{-1} mol^{-1} respectively.

6.1. Introduction

Amino acids have been oxidized by a variety of reagent [1, 2] under different experimental condition. The kinetics and mechanism of oxidation of amino acids have been studied previously by some researchers [3]. However, the mechanism is different in the different reaction systems. The oxidation of amino acids is also of interest as the oxidation products differ from different oxidants [4, 5]. Alanine is a neutral amino acid, in which hydrogen of one of methyl group is replaced by amino group. The Kinetics of oxidation of alanine by a number of oxidants viz. Hexacyanoferrate [6], diperiodatoargentate [Ag(III)] [7], N-bromoacetamide [8] in alkaline medium and Chloramine–T [9], Cerium(IV) [10], $KMnO_4$ [11], Tetrabutyl ammonium tribromide (TBATB) [12], Dichloramine-T [13], Peroxomonosulphate [14], Peroxodisulphate [15] in acidic medium have been reported in literature. In addition, the mechanism of oxidative decarboxylation of amino acids by N- bromosuccinimide has been shown [16] to be significantly influenced by the presence of alkyl groups at the α-carbon. It will be tempting to see if this effect also extends to other oxidizing agents. In view of this, we have taken up systematic kinetic study of the oxidation of neutral amino acid namely alanine by peroxodisulphate in acidic medium.

Moreover, the kinetics of the oxidation of inorganic and organic substrates by peroxodisulphate under both catalyzed and uncatalyzed conditions have received considerable attention [17, 18]. The peroxodisulphate ion is one of the strongest oxidizing agents known in aqueous solution. The standard oxidation reduction potential for the reaction **(Equation 2)** is estimated to be -2.01V.

$$2\ SO_4^{2-} \longrightarrow S_2O_8^{2-} + 2e^- \qquad (2)$$

Its utility as an oxidizing agent for various substrates derived from its ability to oxidize in acidic, neutral and alkaline media [19]. The reaction involve this ion are generally very slow in the absence of suitable catalysts [20]. There are

also certain oxidations of amino acids where catalysts such as silver(I) [21], ruthenium(III) [22], osmium(VIII) [23] and palladium(II) [24] have been employed. In spite of that the metal nanoparticles possessing appreciable stability and high surface area per particle, their potential use as catalyst for organic biochemical relevant reactions [25, 26]. Metal nanoparticles with high specific catalytic activity are ubiquitous in modern synthetic organic chemistry during the recent decades [27]. The application of transition-metal nanoparticles as catalysts for organic transformations include decomposition of hydrogen peroxide [28], nitrobenzene reduction [29], CO oxidation [30], hydrogenation [31], hydrosilylation [32] and hydration reactions of unsaturated organic molecules [33]. Pt, Pd, Ru and Au nanoparticles have been used as a catalyst in electron transfer and oxidation reactions [34-37]. Amongst them copper nanoparticles are paid more attention due to their low cost and easy availability. The oxidation of amino acids is of the utmost importance, both from a chemical point and in view of its bearing on the mechanism of amino acid metabolism. It has been observed that there is not enough information in the literature on the kinetics of oxidation of amino acid by peroxodisulphate in presence of copper nanoparticles.

In view of the reported observations, we were prompted to undertake the title reaction to gain more about the reactivity pattern of alanine towards peroxodisulphate in the presence of copper nanoparticles in acid aqueous media and this will obviously be a fruitful avenue for additional study.

6.2. Experimental Details

6.2.1. Material and Reagents

The methods of preparation and standardization of the reagents including peroxodisulphate are given in chapter 2 (Instrumentation and Material section). The term peroxydisulphate is used by chemical abstract although the international union of pure and applied chemistry (IUPAC) has recommended the name peroxodisulphate [38], the trivial names; persulphate, peroxydisulphate and

peroxodisulphate were used in the literature. Peroxodisulphate oxidations are susceptible to impurities in the solution and the nature of the glass vessel. All the glass vessels and apparatus used in this investigation were of pyrex or coring makes. The solution of potassium persulphate was prepared by direct weighing. All other reagents employed in this study were either of AnalaR grade or guaranteed reagent grade and were used as supplied without undertaking any further treatment. A fresh solution of peroxodisulphate was prepared before starting the experiment. Doubly distilled water was used throughout the study the second distillation was from alkaline permanganate solution in an all glass assembly.

6.2.2. Kinetic Measurements

The reaction was allowed to occur in glass-stoppered Erlenmeyer flask which was immersed in a thermostat water bath at 35± 0.1^{o}C unless mentioned otherwise. Appropriate amount of the amino acid solution in acidic form, copper nanoparticles, potassium sulfate and water (to keep the total volume constant for all runs) were taken in the flask and thermostat at 35^{o}C for thermal equilibrium. A measured amount of peroxodisulphate was rapidly added to the mixture. When half of the contents from the pipette were released, the time of initiation of the reaction was recorded.

Aliquot portion (5cm^3) of the reaction mixture was withdrawn at different intervals of time and transferred into glass stoppered conical flasks, then added into an aqueous solution of KI (~10%) [39]. The liberated iodine was titrated against thiosulphate solution using starch as an indicator. The volume of thiosulphate obtained at any time interval was taken to represent the residual concentration of peroxodisulphate. The rate constants were computed from the linear plots of log [PDS] against time. The course of the reaction was followed for at least 75% of the reaction.

6.3. Stoichiometry and Product Analysis

The stoichiometry of the peroxodisulphate-alanine reactions was extensively studied [40-44] by several methods who found that the reaction followed a 1:1 stoichiometry. Attempts were made to determine the stoichiometry and the product, the reaction mixture containing an excess of peroxodisulphate (PDS) over alanine (Ala) in the presence of copper nanoparticles were allowed for 24 hours to react in a temperature controlled water bath. The excess of peroxodisulphate was determined iodometrically when the completion of the reaction was ensured. The main reaction products are aldehyde, ammonia and CO_2.

The qualitative oxidation product study was made under kinetic conditions i.e. with an excess of substrate over oxidant. The product of oxidation was corresponding aldehyde i.e. acetaldehyde was confirmed by FTIR spectrum of the corresponding hydrazone in **figure 6.1.** The reaction mixture was treated with solution of 2, 4- dinitrophenylhydrazine in 2.0 mol dm^{-3} HCl. The reaction mixture yield brown precipitate of hydrazone derivative of aldehyde. Furthermore the recorded infra-red spectra of this hydrazone were obtained and showed that the absorption of characteristic functional group –NH, –CH and –C=N of hydrazone derivative were observed at certain wave length **3343.9cm^{-1}, 2901.14 cm^{-1}, 1609.65 cm^{-1}** respectively. The functional group –C=N was produced from the condensation reaction of aldehyde and hydrazine.

Therefore, the stoichiometry of the reaction with positive test of an aldehyde can be represented by **equation (6.1).**

$$S_2O_8^{2-} + R-\underset{NH_2}{\overset{H}{C}}-COOH + H_2O \xrightarrow[H^+,\ 308\ K]{\text{Copper Nanoparticles}} RCHO + NH_3 + 2HSO_4^- + CO_2 \quad \text{(6.1)}$$

Where R represents -CH_3

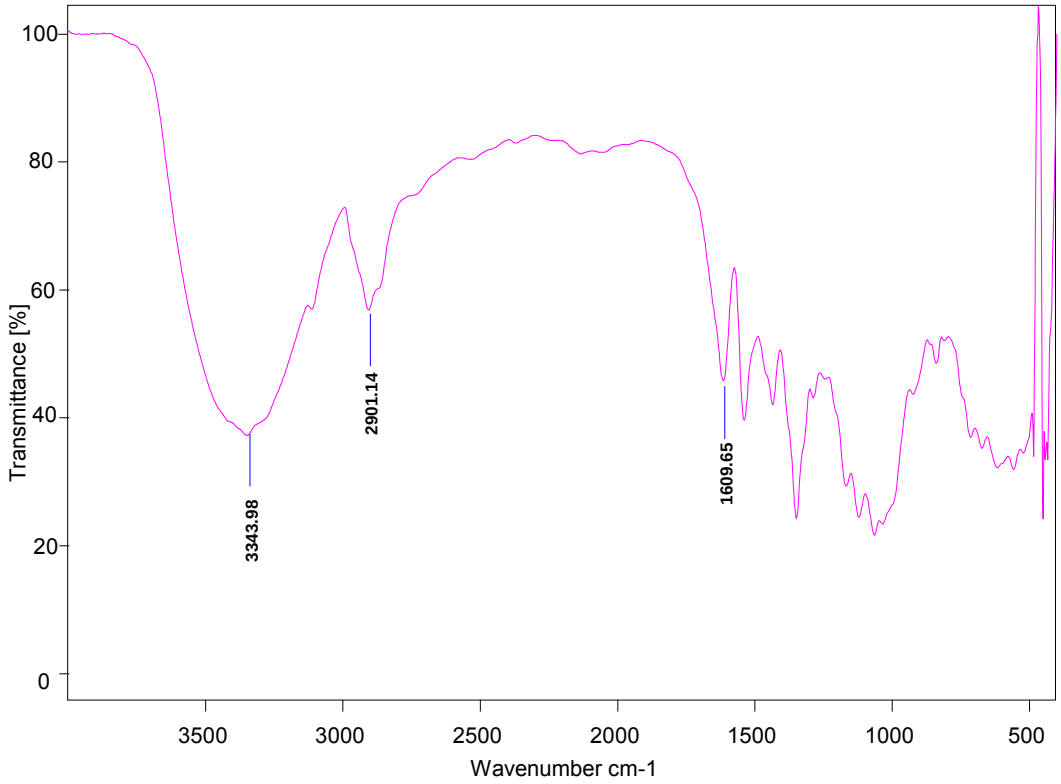

Figure 6.1: The FT-IR spectra of the hydrazone derivative from the reaction mixture of the alanine and peroxodisulphate in the presence of copper nanoparticles

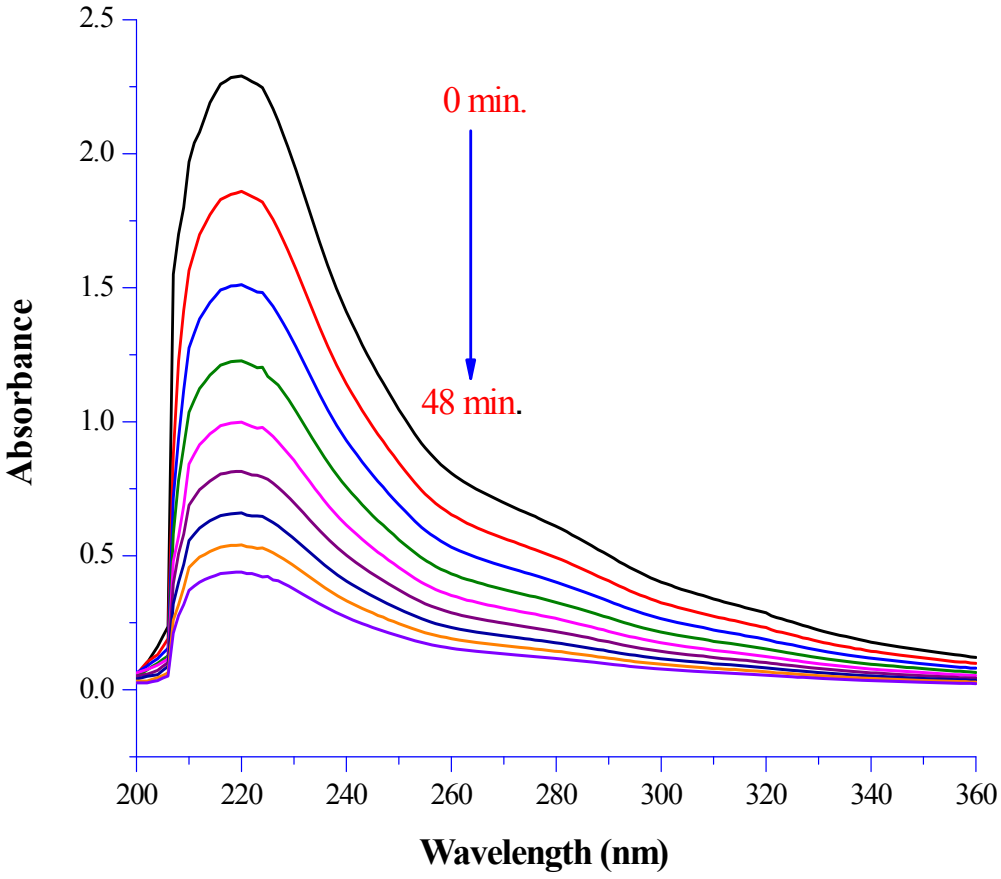

Figure 6.2: UV-Vis absorption spectra during the progression of L-alanine peroxodisulphate reaction (time 0-48 minutes) in the presence of the copper nanoparticles (size = 12 nm)

[PDS] = 5.0×10^{-3} mol dm^{-3}; [Alanine] = 5.0×10^{-2} mol dm^{-3};

[Cunps] = 1.0×10^{-5} mol dm^{-3}; $[H^+] = 1.0\times10^{-1}$ mol dm^{-3};

I = 2.0×10^{-1} mol dm^{-3}; Temp. =35°C

Deamination and decarboxylation of the L-alanine by persulphate in presence of copper nanoparticles was shown in UV- Visible absorption spectrum **(Figure 6.2).** The spectrum shows a peak at 220 nm with maximum absorbance in the beginning of the reaction. The decline in absorbance of peak is show the progress of reaction. Ammonia identified by nessler's reagent, brownish color was observed indicating deamination reaction, carbon dioxide was identified by freshly prepared lime water and the solution turned milky indicating decarboxylation reaction.

6.4. Results and Discussion

6.4.1. Peroxodisulphate Dependence

Kinetic runs were carried out by varying concentration of peroxodisulphate from 1.0×10^{-3} – 7.5×10^{-3} mol dm^{-3} at fixed concentration of [Ala] = 5.0×10^{-2} mol dm^{-3}, keeping constant concentrations of other reaction ingredients such as $[H^+] = 1.0\times10^{-1}$ mol dm^{-3}, I = 2.0×10^{-1} mol dm^{-3}, [Cunps] = 1.0×10^{-5} mol dm^{-3} at 35°C temperature. The plot of log [PDS] (PDS, has been used in place of peroxodisulphate heretofore) versus time was made that yielded linear plots **(Figure 6.3),** indicating that the reaction is first order dependence of the peroxodisulphate concentration and the value of pseudo first order rate constants (k_{obs}, sec^{-1}) were calculated from the slope of the above plots. The observed pseudo first order rate constant (k_{obs}) were independent of the concentration of peroxodisulphate. Results are given in **Table-6.1**.

6.4.2. Alanine Dependence

Reaction were carried out by varying initial concentration of alanine from 1.0×10^{-2} –7.0×10^{-2} mol dm^{-3} at constant concentration of other reaction ingredients *viz.* [PDS] = 5.0×10^{-3} mol dm^{-3}, [Cunps] = 1.0×10^{-5} mol dm^{-3}, $[H^+] = 1.0\times10^{-1}$ mol dm^{-3}, I = 2.0×10^{-1} mol dm^{-3} at 35°C temperature. The pseudo first order rate constants (k_{obs}) calculated in these reactions and the plot of log k_{obs} versus log [Ala] (Ala, has been used in place of Alanine heretofore) was made that yielded straight line parallel to log [Ala] axis **(Figure 6.4)** further confirming zero order dependence with respect to concentration of alanine**.** Results are given in **Table-6.2.**

TABLE: 6.1

VARIATION OF PEROXODISULPHATE

[Ala] = 5.0×10^{-2} mol dm^{-3} **Temp. = 35^{o}C**

[Cunps] = 1.0×10^{-5} mol dm^{-3} **Titrant [Hypo] = 1.0×10^{-3} mol dm^{-3}**

[H^{+}] = 1.0×10^{-1}mol dm^{-3} **Aliquot = 5.0 ml**

I = 2.0×10^{-1} mol dm^{-3}

10^3 [PDS], mol dm^{-3}	**1.0***	**2.0**	**3.0**	**4.0**	**5.0**	**6.0**	**7.5**
Time in minutes	**Volume of Titrant (ml)**						
0	10.0	10.0	15.0	20.0	25.0	30.0	37.5
6	8.1	8.1	12.2	16.3	20.3	24.4	30.2
12	6.6	6.6	9.9	13.2	16.5	19.8	24.5
18	5.4	5.4	8.1	10.8	13.4	16.1	20.0
24	4.4	4.4	6.6	8.8	10.9	13.1	16.2
30	3.6	3.6	5.4	7.1	8.9	10.7	13.2
36	2.9	2.9	4.4	5.8	7.2	8.7	10.8
42	2.4	2.4	3.5	4.7	5.9	7.0	8.7
48	1.9	1.9	2.9	3.8	4.8	5.7	7.1
10^4 (k_{obs}), sec^{-1}	**5.72**	**5.7**	**5.72**	**5.73**	**5.73**	**5.75**	**5.73**

*Hypo = 5×10^{-4} mol dm^{-3}

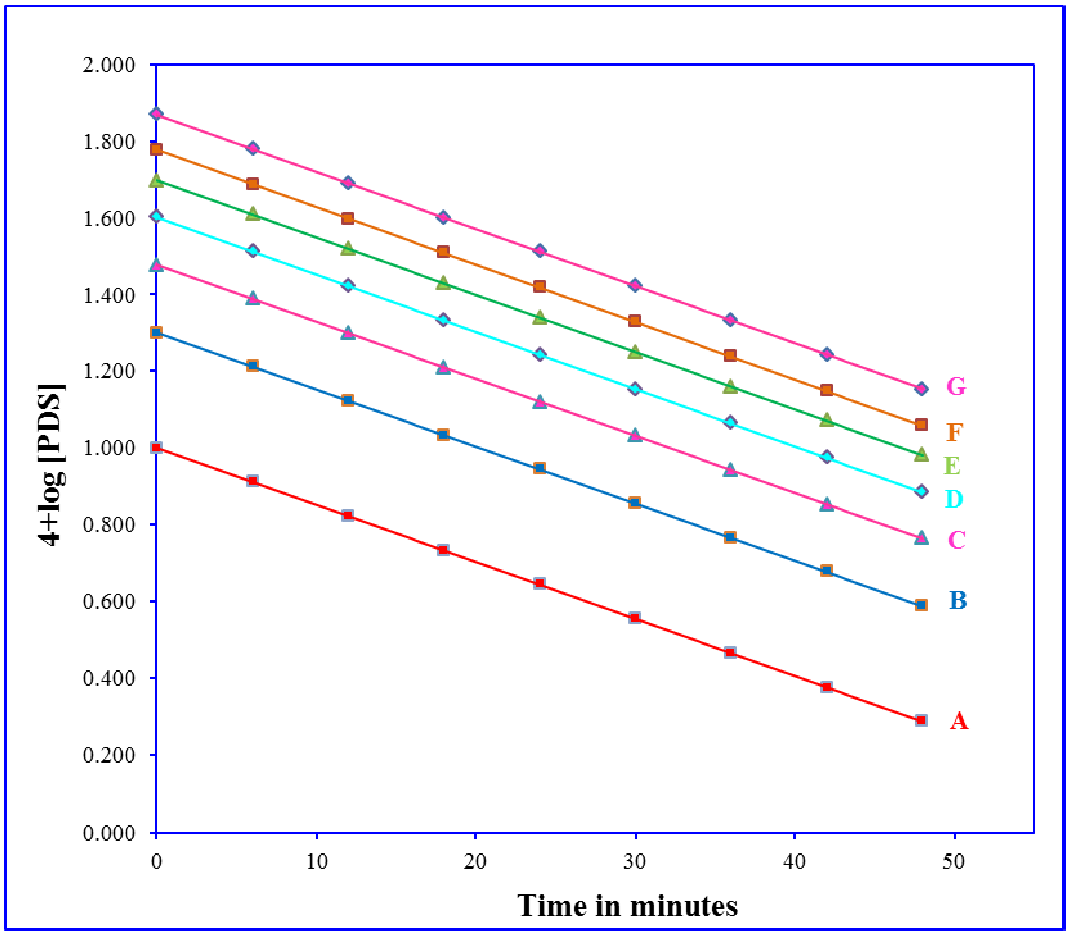

Figure 6.3: Variation of peroxodisulphate

[Ala]= 5.0×10^{-2} moldm^{-3}; [Cunps] = 1.0×10^{-5} mol dm^{-3};

[H^+] = 1.0×10^{-1} mol dm^{-3}; I =2.0×10^{-1} mol dm^{-3}, Temp. = 35^{o}C;

[PDS] = (A) 1.0×10^{-3} mol dm^{-3} (B) 2.0×10^{-3} mol dm^{-3}

(C) 3.0×10^{-3} mol dm^{-3} (D) 4.0×10^{-3} mol dm^{-3}

(E) 5.0×10^{-3} mol dm^{-3} (F) 6.0×10^{-3} mol dm^{-3}

(G) 7.5×10^{-3} mol dm^{-3}

(Ref. Table: 6.1)

TABLE: 6.2

VARIATION OF ALANINE

[PDS] = 5.0×10^{-3} mol dm^{-3} **Temp. = 35^{o}C**

[Cunps] = 1.0×10^{-5} mol dm^{-3} **Titrant [Hypo] = 1.0×10^{-3} mol dm^{-3}**

[H^{+}] = 1.0×10^{-1} mol dm^{-3} **Aliquot = 5.0 ml**

I = 2.0×10^{-1} mol dm^{-3}

10^2 [Ala], mol dm^{-3}	**1.0**	**2.0**	**3.0**	**4.0**	**5.0**	**6.0**	**7.0**
Time in minutes	**Volume of Titrant (ml)**						
0	25.0	25.0	25.0	25.0	25.0	25.0	25.0
6	20.3	20.3	20.3	20.3	20.3	20.3	20.3
12	16.5	16.5	16.5	16.5	16.5	16.5	16.5
18	13.4	13.5	13.4	13.5	13.4	13.4	13.5
24	10.9	10.9	10.9	10.9	10.9	10.9	10.9
30	8.8	8.9	8.9	8.9	8.9	8.9	8.9
36	7.2	7.3	7.2	7.3	7.2	7.2	7.3
42	5.8	5.9	5.9	5.9	5.9	5.9	5.9
48	4.7	4.8	4.8	4.8	4.8	4.8	4.8
10^4 (k_{obs}), sec^{-1}	**5.76**	**5.72**	**5.75**	**5.72**	**5.73**	**5.73**	**5.72**

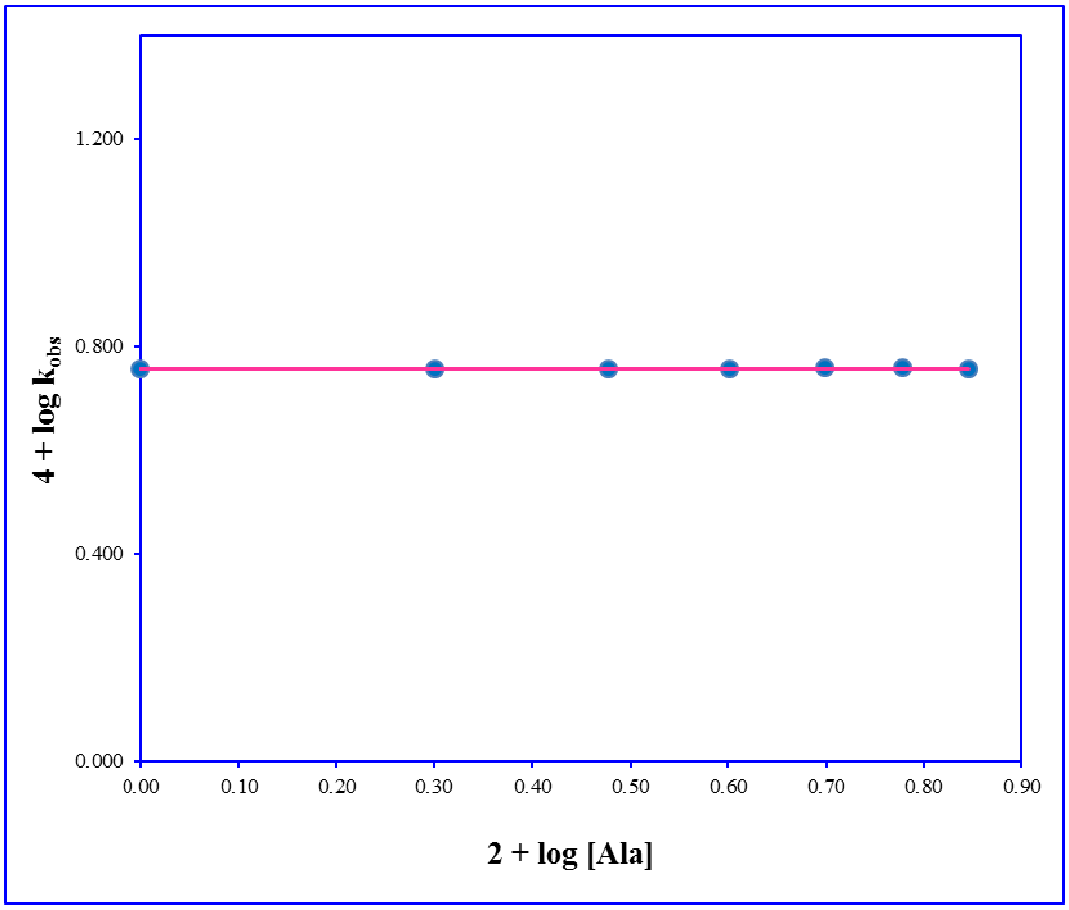

Figure 6.4: Variation of alanine

[PDS]= 5.0×10^{-3} mol dm^{-3}; [Cunps] = 1.0×10^{-5} mol dm^{-3};

$[H^+]$ =1.0×10^{-1} mol dm^{-3}; I =2.0×10^{-1} mol dm^{-3}, Temp. = 35°C

(Ref. Table: 6.2)

6.4.3. Copper Nanoparticles Dependence

The effect of concentration of the synthesized copper nanoparticles (as discussed in chapter 3) on the oxidation of alanine has been studied by varying its concentration from 1.0×10^{-6} – 1.0×10^{-5} mol dm^{-3}, keeping constant concentration of other reaction ingredients *viz.* [PDS] = 5.0×10^{-3} mol dm^{-3}, [Ala] = 5.0×10^{-2} mol dm^{-3}, $[H^+]$ =1.0×10^{-1} mol dm^{-3}, I = 2.0×10^{-1} mol dm^{-3} at three temperature (30^oC, 35^oC, 40^oC). The rate of reaction increases with increasing concentration of copper nanoparticles. In order to show the catalytic activity, a plot of first order rate constants (k_{obs}, sec^{-1}) at different temperature against concentration of copper nanoparticles [Cunps] (Cunps, has been used in place of Copper nanoparticles heretofore) were made, yielded straight line with non-zero intercept **(Figure 6.5).** Such a rate behavior confirms to first order dependence with respect to copper nanoparticles. However, a straight line with non-zero intercept also indicates a simultaneous uncatalyzed oxidation of alanine by peroxodisulphate is also possible. Results are given in **Table-6.3, 6.4, 6.5.**

6.4.4. Hydrogen Ion Dependence

Hydrogen ion variation was made by varying the concentration of sulfuric acid in the range of 1.0×10^{-1} to 2.0×10^{-1} mol dm^{-3}, at fixed concentration of [PDS] = 5.0×10^{-3} mol dm^{-3}, [Ala] = 5.0×10^{-2} mol dm^{-3}, [Cunps] = 1.0×10^{-5} mol dm^{-3}, I = 2.0×10^{-1} mol dm^{-3} at temperature 35^oC. The rate of the reaction were found to decreases with increasing concentration of hydrogen ion and then tends towards a limiting value at higher concentration of hydrogen ion **(Table-6.6).** A plot of k_{obs} versus $[H^+]$ was found to be polynomial with a positive slope **(Figure 6.6).** This shows an inverse dependence on $[H^+]$ and tends towards a limiting value at higher concentration of hydrogen ion. Since rate does not depend upon the concentration of alanine, hydrogen ion dependence cannot be related to the amino acid. However, decrease in rate with increasing hydrogen ion concentration accounts for the higher reactivity of the molecular form of the acid.

TABLE: 6.3

VARIATION OF COPPER NANOPARTICLES

(SIZE=12 nm)

[PDS] = 5.0×10^{-3} mol dm^{-3} **Temp. = 30^{o}C**

[Ala] = 5.0×10^{-2} mol dm^{-3} **Titrant [Hypo] = 1.0×10^{-3} mol dm^{-3}**

[H^{+}] = 1.0×10^{-1} mol dm^{-3} **Aliquot = 5.0 ml**

I = 2.0×10^{-1} mol dm^{-3}

10^{6} [Cunps], mol dm^{-3}	**0.0**	**1.0**	**2.0**	**3.0**	**4.0**	**5.0**	**6.0**	**7.0**	**8.0**	**9.0**	**10.0**
Time in minutes	**Volume of Titrant (ml)**										
0	(0)25.0	(0)25.0	(0)25.0	(0)25.0	(0)25.0	(0)25.0	(0)25.0	(0)25.0	25.0	25.0	25.0
10	(35)20.2	(25)20.2	(20)20.1	(18)19.7	(15)19.8	(12)20.2	(12)19.6	(12)19.1	19.5	19.0	18.6
20	(70)16.4	(50)16.4	(40)16.2	(36)15.5	(30)15.8	(24)16.3	(24)15.4	(24)14.6	15.3	14.5	13.9
30	(105)13.3	(75)13.3	(60)13.0	(54)12.2	(45)12.5	(36)13.2	(36)12.1	(36)11.2	11.9	11.1	10.4
40	(140)10.8	(100)10.8	(80)10.5	(72)9.6	(60)10.0	(48)10.7	(48)9.5	(48)8.6	9.3	8.5	7.8
50	(175)8.7	(125)8.7	(100)8.5	(90)7.6	(75)7.9	(60)8.6	(60)7.5	(60)6.6	7.3	6.5	5.8
60	-	(150)7.1	(120)6.8	(108)6.0	(90)6.3	(72)7.0	(72)5.9	(72)5.0	5.7	4.9	4.4
70	-	(175)5.7	(140)5.5	(126)4.7	(105)5.0	(84)5.6	(84)4.6	(84)3.9	4.5	3.8	3.3
80	-	-	(160)4.4	(144)3.7	(120)4.0	(96)4.6	(96)3.6	(96)3.0	3.5	2.9	2.4
10^{4} (k_{obs}), sec^{-1}	**1.00**	**1.40**	**1.80**	**2.20**	**2.55**	**2.95**	**3.35**	**3.70**	**4.10**	**4.50**	**4.85**

Figures in parentheses denote time in minutes

TABLE: 6.4

VARIATION OF COPPER NANOPARTICLES

(SIZE=12 nm)

[PDS] = 5.0×10^{-3} mol dm^{-3} **Temp. = 35^{o}C**

[Ala] = 5.0×10^{-2} mol dm^{-3} **Titrant [Hypo] = 1.0×10^{-3} mol dm^{-3}**

[H^{+}] = 1.0×10^{-1} mol dm^{-3} **Aliquot = 5.0 ml**

I = 2.0×10^{-1} mol dm^{-3}

10^{6} [Cunps], mol dm^{-3}	**0.0**	**1.0**	**2.0**	**3.0**	**4.0**	**5.0**	**6.0**	**7.0**	**8.0**	**9.0**	**10.0**
Time in minutes	**Volume of Titrant (ml)**										
0	(0)25.0	(0)25.0	(0)25.0	(0)25.0	(0)25.0	(0)25.0	(0)25.0	25.0	25.0	25.0	25.0
8	(25)19.9	(18)20.2	(15)20.2	(15)19.4	(12)19.8	(12)19.2	(10)19.4	20.1	19.7	19.3	18.9
16	(50)15.9	(36)16.4	(30)16.3	(30)15.1	(24)15.7	(24)14.7	(20)15.2	16.2	15.6	15.0	14.4
24	(75)12.7	(54)13.3	(45)13.2	(45)11.7	(36)12.5	(36)11.3	(30)11.8	13.0	12.3	11.6	10.9
32	(100)10.1	(72)10.7	(60)10.7	(60)9.1	(48)9.9	(48)8.7	(40)9.2	10.5	9.7	9.0	8.3
40	(125)8.1	(90)8.7	(75)8.7	(75)7.1	(60)7.9	(60)6.7	(50)7.2	8.5	7.7	7.0	6.3
48	(150)6.5	(108)7.1	(90)7.0	(90)5.5	(72)6.3	(72)5.2	(60)5.6	6.8	6.1	5.4	4.8
56	(175)5.2	(126)5.7	(105)5.7	(105)4.3	(84)5.0	(84)4.0	(70)4.4	5.5	4.8	4.2	3.6
64	-	(144)4.6	(120)4.6	(120)3.3	(96)4.0	(96)3.0	(80)3.4	4.4	3.8	3.3	2.8
10^{4} (k_{obs}), sec^{-1}	**1.50**	**1.95**	**2.35**	**2.80**	**3.20**	**3.65**	**4.15**	**4.50**	**4.90**	**5.30**	**5.73**

Figures in parentheses denote time in minutes

TABLE: 6.5

VARIATION OF COPPER NANOPARTICLES

(SIZE=12 nm)

[PDS] = 5.0×10^{-3} mol dm^{-3} **Temp. = 40^{o}C**

[Ala] = 5.0×10^{-2} mol dm^{-3} **Titrant [Hypo] = 1.0×10^{-3} mol dm^{-3}**

[H^{+}] = 1.0×10^{-1} mol dm^{-3}, **Aliquot = 5.0 ml**

I =2.0×10^{-1} mol dm^{-3}

10^{6} [Cunps], mol dm^{-3}	**0.0**	**1.0**	**2.0**	**3.0**	**4.0**	**5.0**	**6.0**	**7.0**	**8.0**	**9.0**	**10.0**
Time in minutes	**Volume of Titrant (ml)**										
0	(0)25.0	(0)25.0	(0)25.0	(0)25.0	(0)25.0	25.0	25.0	25.0	25.0	25.0	25.0
8	(20)20.1	(15)20.3	(15)19.5	(12)19.7	(10)19.9	20.3	19.9	19.4	19.0	18.6	18.1
16	(40)16.2	(30)16.5	(30)15.2	(24)15.6	(20)15.9	16.6	15.9	15.1	14.5	13.8	13.2
24	(60)13.0	(45)13.4	(45)11.9	(36)12.4	(30)12.7	13.5	12.7	11.8	11.1	10.3	9.6
32	(80)10.5	(60)10.9	(60)9.3	(48)9.8	(40)10.1	11.0	10.1	9.2	8.4	7.7	7.0
40	(100)8.5	(75)8.9	(75)7.2	(60)7.7	(50)8.1	9.0	8.1	7.2	6.4	5.7	5.1
48	(120)6.8	(90)7.2	(90)5.7	(72)6.1	(60)6.5	7.3	6.4	5.6	4.9	4.2	3.7
56	(140)5.5	(105)5.9	(105)4.4	(84)4.8	(70)5.2	6.0	5.1	4.3	3.7	3.2	2.7
64	(160)4.4	(120)4.8	(120)3.4	(96)3.8	(80)4.1	4.9	4.1	3.4	2.9	2.4	1.9
10^{4} (k_{obs}), sec^{-1}	**1.80**	**2.30**	**2.75**	**3.25**	**3.75**	**4.25**	**4.70**	**5.20**	**5.65**	**6.50**	**6.65**

Figures in parentheses denote time in minutes

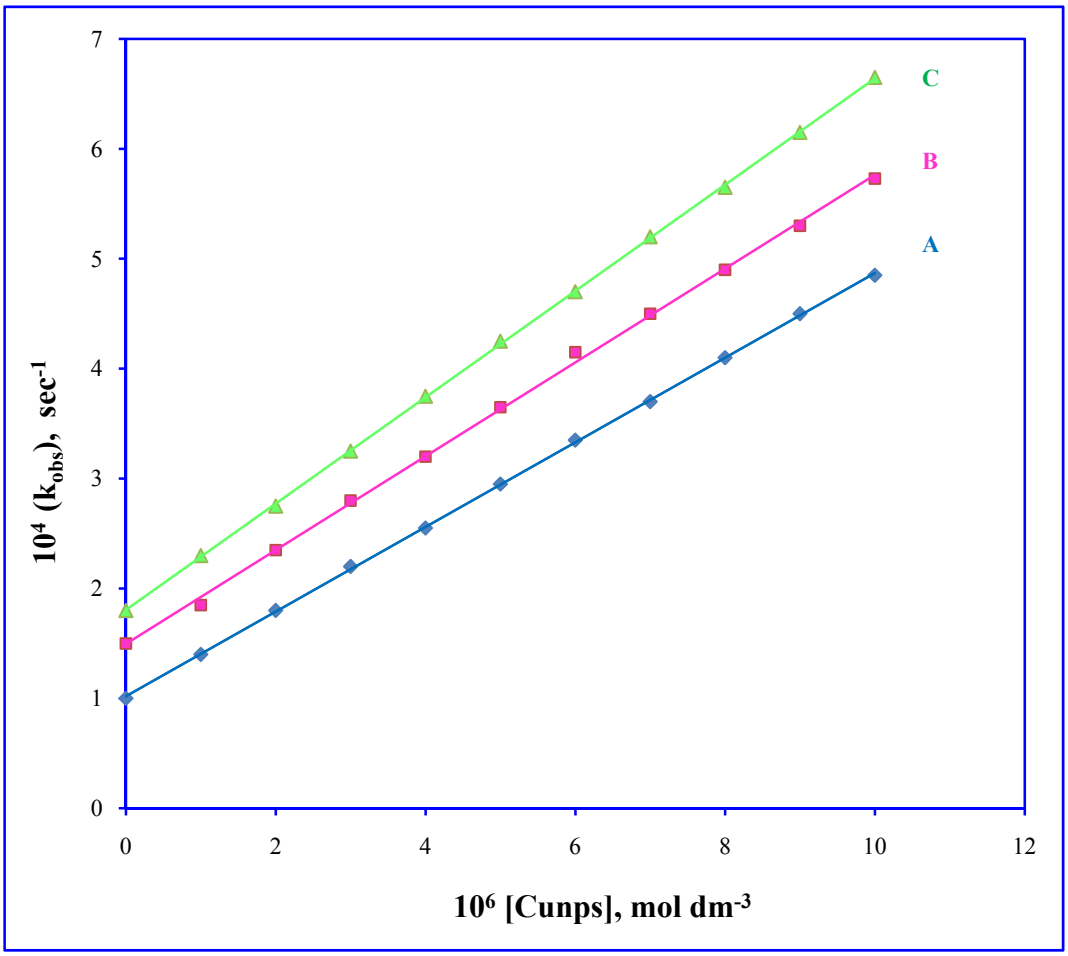

Figure 6.5: Variation of copper nanoparticles at different temperature (A) 30°C, (B) 35°C, (C) 40°C

[PDS] = 5.0×10^{-3} mol dm^{-3}; [Ala] = 5.0×10^{-2} mol dm^{-3};

[H^+] = 1.0×10^{-1} mol dm^{-3}; I = 2.0×10^{-1} mol dm^{-3}

(Ref. Table: 6.3, 6.4, 6.5)

TABLE: 6.6

VARIATION OF HYDROGEN ION

[PDS] = 5.0×10^{-3} mol dm^{-3} **Temp. = 35^{o}C**

[Ala] = 5.0×10^{-2} mol dm^{-3} **Titrant [Hypo] = 1.0×10^{-3} mol dm^{-3}**

[Cunps] =1.0×10^{-5} mol dm^{-3} **Aliquot = 5.0 ml**

I =2.0×10^{-1} mol dm^{-3}

10^{1} $[H^{+}]$, mol dm^{-3}	**1.0**	**1.1**	**1.2**	**1.3**	**1.4**	**1.5**	**1.6**	**1.7**	**1.8**	**1.9**	**2.0**
Time in minutes	**Volume of Titrant (ml)**										
0	25.0	25.0	25.0	25.0	(0)25.0	(0)25.0	(0)25.0	(0)25.0	(0)25.0	(0)25.0	(0)25.0
10	17.7	18.6	19.3	20.0	(12)19.8	(15)19.4	(15)19.9	(18)19.7	(18)20.1	(20)20.1	(22)20.2
20	12.5	13.9	14.9	16.0	(24)15.7	(30)15.1	(30)15.9	(36)15.5	(36)16.2	(40)16.2	(44)16.4
30	8.9	10.3	11.5	12.8	(36)12.5	(45)11.7	(45)12.7	(54)12.2	(54)13.0	(60)13.0	(66)13.2
40	6.3	7.7	8.9	10.3	(48)9.9	(60)9.1	(60)10.1	(72)9.6	(72)10.5	(80)10.5	(88)10.7
50	4.5	5.7	6.9	8.2	(60)7.9	(75)7.1	(75)8.1	(90)7.6	(90)8.5	(100)8.5	(110)8.7
60	3.2	4.3	5.3	6.6	(72)6.3	(90)5.5	(90)6.5	(108)6.0	(108)6.8	(120)6.8	(132)7.0
70	2.2	3.2	4.1	5.3	(84)5.0	(105)4.3	(105)5.2	(126)4.7	(126)5.5	(140)5.5	(154)5.7
80	1.6	2.4	3.2	4.2	(96)4.0	(120)3.3	(120)4.1	(144)3.7	(144)4.4	(160)4.4	(176)4.6
10^{4} (k_{obs}), sec^{-1}	**5.73**	**4.90**	**4.30**	**3.70**	**3.20**	**2.80**	**2.50**	**2.20**	**2.00**	**1.70**	**1.60**

Figures in parentheses denote time in minutes

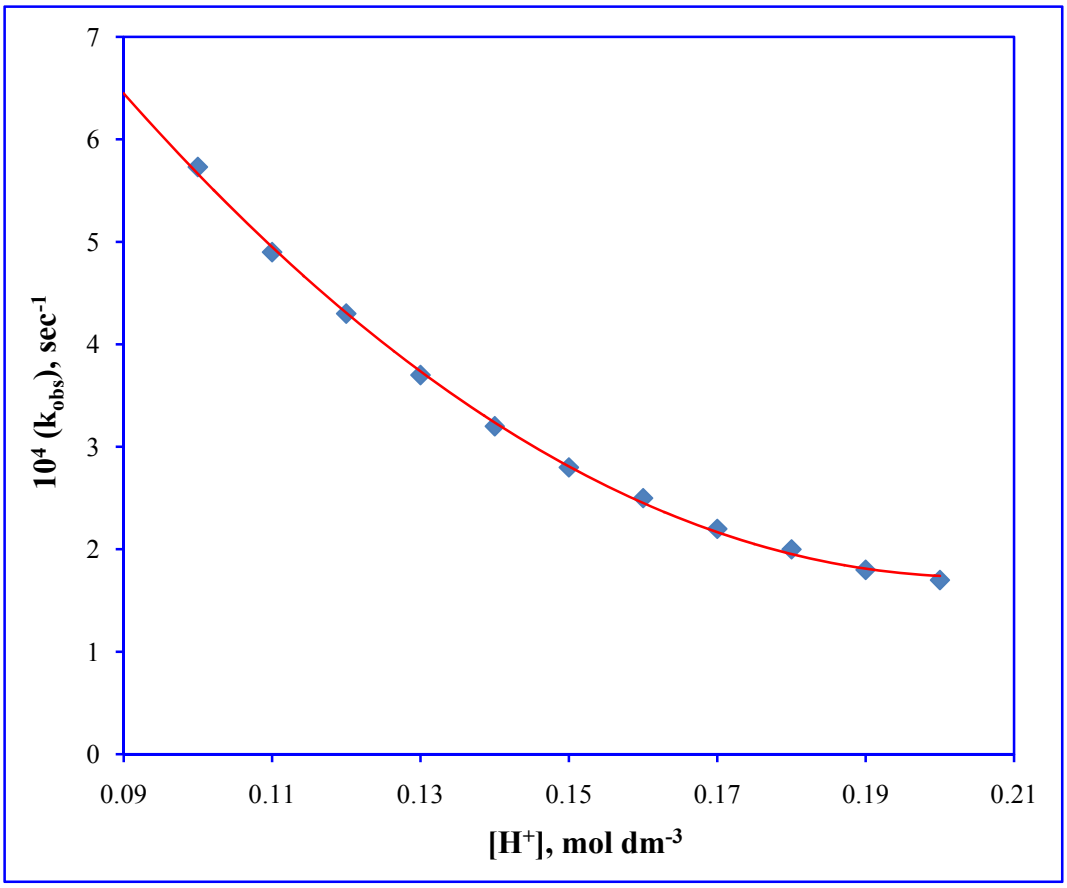

Figure 6.6: Plot of k_{obs} Versus $[H^+]$

[PDS] = 5.0×10^{-3} mol dm^{-3}; [Cunps] = 1.0×10^{-5} mol dm^{-3};
[Ala] = 5.0×10^{-2} mol dm^{-3}; I = 2.0×10^{-1} mol dm^{-3};
Temp. = 35^{o}C

(Ref. Table: 6.6)

6.4.5. Ionic Strength Dependence

The effect of ionic strength on the rate of reaction was studied by varying the concentration of potassium sulphate (0.1 to 0.4 mol dm^{-3}) at constant concentration of reactants and conditions [PDS] = 5.0×10^{-3} mol dm^{-3}, [Ala] = 5.0×10^{-2} mol dm^{-3}, [Cunps] = 1.0×10^{-5} mol dm^{-3}, $[H^+]$ = 1.0×10^{-1} mol dm^{-3} at temperature 35°C. The change in the rate constant (k_{obs}, sec^{-1}) with increase in the ionic strength is found to be very small, indicating the rate of the reaction slightly affected with increasing ionic strength. Results are given in **Table- 6.7** which indicates that in our experimental conditions, the reaction may be between an ion and a neutral molecule or between neutral molecules. Herein, $S_2O_8^{2-}$ and alanine (neutral) was reactive form of peroxodisulphate and alanine respectively.

6.4.6. Effect of Temperature

The effect of temperature on the rate of reaction was studied at three temperature 30°C, 35°C, 40°C respectively at constant concentration of other reaction ingredients *viz.* [PDS] = 5.0×10^{-3} mol dm^{-3}, [Ala] = 5.0×10^{-2} mol dm^{-3}, [Cunps] = 1.0×10^{-5} mol dm^{-3}, $[H^+]$ =1.0×10^{-1} mol dm^{-3}, I =2.0×10^{-1} mol dm^{-3}. The observed rate constants increased with increase in temperature, these results were tabulated in **Tables-6.3, 6.4, 6.5**. By applying Arrhenius **equation (6.2),** the logarithm of observed rate constant ($k_{obs,}$ sec^{-1}) was plotted against 1/T (K^{-1}) that yielded a straight line **(Figure 6.7).** From Arrhenius equation

$$\log k = \log A - E_a/2.303RT \qquad (6.2)$$

The slope of the graph is equal to $-E_a/2.303R$; the energy of activation (E_a) for oxidation of alanine by peroxodisulphate was calculated to be 23.846±2 kJ mol^{-1} and the entropy of activation (ΔS), enthalpy of activation ($\Delta H^{\neq}$), free energy of activation($\Delta G^{\neq}$) were obtained 238.17 J K^{-1} mol^{-1}, 21.29 kJ mol^{-1}, 94.651 kJ mol^{-1} respectively. The negative value of entropy of activation (ΔS) has been ascribed to the loss of the degree of freedom formerly available to the reactants upon the formation of rigid transition state and high positive values of free energy of activation ($\Delta G^{\neq}$) and enthalpy of activation ($\Delta H^{\neq}$) indicated that the transition state was highly solvated.

TABLE: 6.7

VARIATION OF K_2SO_4

[PDS] = 5.0×10^{-3} mol dm^{-3} **Temp. = 35^oC**

[Ala] = 5.0×10^{-2} mol dm^{-3} **Titrant [Hypo] = 1.0×10^{-3} mol dm^{-3}**

[Cunps] = 1.0×10^{-5} mol dm^{-3} **Aliquot = 5.0 ml**

[H^+] = 1.0×10^{-1} mol dm^{-3}

10^1 [K_2SO_4], mol dm^{-3}	**1.0**	**1.5**	**2.0**	**2.5**	**3.0**	**3.5**	**4.0**
Time in minutes	**Volume of Titrant (ml)**						
0	25.0	25.0	25.0	25.0	25.0	25.0	25.0
6	20.3	20.3	20.3	20.3	20.3	20.2	20.2
12	16.5	16.5	16.5	16.5	16.5	16.4	16.4
18	13.5	13.5	13.4	13.4	13.4	13.3	13.3
24	11.0	10.9	10.9	10.9	10.9	10.8	10.8
30	8.9	8.9	8.9	8.8	8.8	8.8	8.8
36	7.3	7.3	7.2	7.2	7.2	7.1	7.1
42	5.9	5.9	5.9	5.8	5.8	5.8	5.8
48	4.8	4.8	4.8	4.7	4.7	4.7	4.7
10^4 (k_{obs}), sec^{-1}	**5.71**	**5.72**	**5.73**	**5.76**	**5.77**	**5.8**	**5.82**

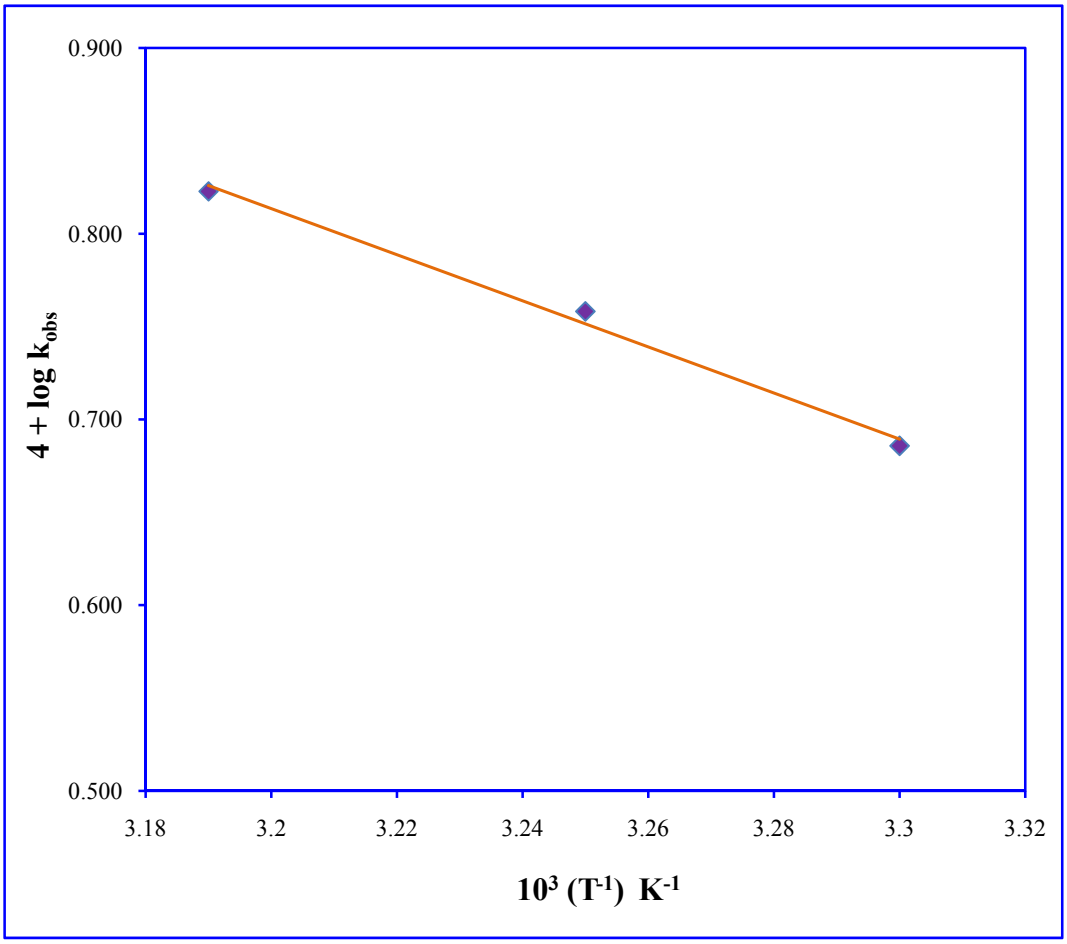

Figure 6.7: Plot of temperature dependence

[PDS] = 5.0×10^{-3} mol dm^{-3}; [Cunps] = 1.0×10^{-5} mol dm^{-3};

[Ala] = 5.0×10^{-2} mol dm^{-3}; I = 2.0×10^{-1} mol dm^{-3};

$[H^+] = 1.0\times10^{-1}$ mol dm^{-3}

(Ref. Table: 6.3, 6.4, 6.5)

6.4.7. Mechanism

The progress of the reaction was followed by estimating the concentration of peroxodisulphate in the reaction mixture at different time intervals iodometrically. Persulfate salts are dissociated in water to the persulfate anion ($S_2O_8^{2-}$) which, despite having a strong oxidation potential (E_o = 2.01 V), is kinetically slow to react with the amino acid. The rate of reaction does not depend upon the concentration of alanine while the reaction was found to be first order with respect to peroxodisulphate and copper nanoparticles. Oxidative deamination of alanine occurs in presence of peroxodisulphate by addition of copper nanoparticles although peroxodisulphate converted to hydrogen sulfate ion. The reaction is highly catalyzed by copper nanoparticles in low concentration than other reactants were used in the oxidation of alanine. Metal nanoparticles possess large surface energy; hence have the ability to adsorb small molecules. The mechanism of catalysis thus involves the reaction of persulfate anion ($S_2O_8^{2-}$) with the adsorbed alanine on the copper nanoparticles.

In the onset, the reaction mixture which accommodates peroxodisulphate and alanine in the presence of copper nanoparticles shows an absorbance peak at 220 nm. The change in the concentration of alanine can be followed using U.V. Visible spectrophotometer to monitor the change in the absorbance. Further, with the exposure of time, the absorbance peak is diminishing in presence of peroxodisulphate and copper nanoparticles corresponding to alanine concentration decreases. Repeated spectral scans were as function of time versus absorbance (0-48 min.) shown in **figure 6.2**. The foregoing observations indicate the copper nanoparticles catalyzed reaction rate of the oxidation reaction is faster than the uncatalyzed reaction with the same kinetic results, in like manner observation have been acquired in earlier study [45]. The definite mechanism of the colloidal metal nanoparticles catalyzed oxidation is not yet clear. Although identify the formation of transition species through certain physical measurements but it is very difficult to isolate and characterize from homogeneous mixture. The proposed plausible mechanism in support of the observed kinetics is given in **scheme-1.**

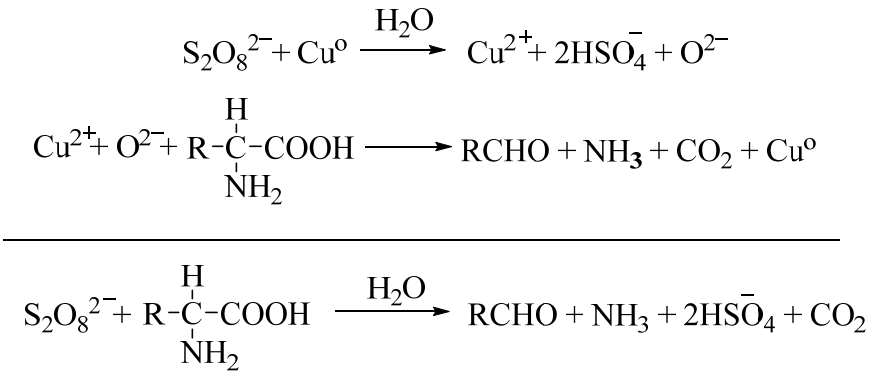

Scheme 1: The plausible route of copper nanoparticles catalyzed oxidation of alanine

6.5. Conclusion

In the present work, the catalytic activity of copper nanoparticles was investigated through the oxidation of alanine in aqueous acid medium. The reaction is four times faster in the presence of very small copper nanoparticles concentration (10×10^{-6} mol dm^{-3}) due to large surface area to volume ratio. The kinetics of oxidation of alanine and its affecting factors including temperature, oxidant nanocatalyst concentration and $[H^+]$ concentration were particularly examined. The results of the study indicate the reaction was first order with the respect of peroxodisulphate, catalyst concentration and zero order with the respect of alanine concentration. Temperature has peculiarly effect on the rate of reaction. The experiment observations indicate that the reactive species are $S_2O_8^{2-}$ and alanine molecule.

6.6. References

[1] V. N. Puttaswamy, ***Proc. Indian Acad. Sci. Chem. Sci.,*** 113 (2001) 325.

[2] D. S. Mahadevappa, K. S. Rangappa, N. N. M. Gouda, B. Thimmegouda, ***Int. J. Chem. Kinet.,*** 14 (1982) 1183.

[3] C. Song, L. Chen and J. Shan, ***Research Letters in Inorg. Chem.,* 2008**; D. S. Munavalli, S. A. Chimatadar, S. T. Nandibewoor, ***Transition Metal Chemistry,*** 33 (2008) 535; M. S. Ramachandran and T. S. Vivekanandam, ***Bull. Chem. Soc. Jpn.,*** 60 (1987) 3397.

[4] D. Laloo and M. M. Mahanti, ***J. Chem. Soc. Dalton Trans.,*** 1 (1990) 311.

[5] K. B. Reddy, B. Sethuram and T. N. Rao, ***Ind. J. Chem.,*** 20 (1981) 395.

[6] P. K. Chourasia, N. C. Bhattacharjee and T. K. Singh, ***J. Ind. Chem. Soc.,*** 86 (2009) 364; R.C. Acharya, N. K. Saran, S. R. Rao, M. N. Das, ***International J. Chem. Kinet.,*** 14 (1981) 143.

[7] C. Song, L. Chen and J. Shan, ***Research Letters in Inorg. Chem.,* 2008**.

[8] M. Komal Reddy, C. S. Reddy and E. V. Sundaram, ***Tetrahedron,*** 41, (1985) 3071.

[9] N. Grover, N. Kambo, S. K. Upadhyay, ***Ind. J. Chem. Sect. A,*** 41 (2002) 2482.

[10] V. Devra, ***J. Ind. Chem. Soc.,*** 82 (2005) 290.

[11] R. M. Hassan***. Can. J. Chem.*** 69 (1991) 2018.

[12] R. Shukla, P. K. Sharma and K. K Banerji, ***J. Chem. Sci.,*** 116 (2004) 101.

[13] T. Gowda and J. M. Rao, ***Bull. Chem. Soc. Jpn.,*** 62 (1989) 3303.

[14] S. M. Rayappan, D. Easwaramurthy, M. Palanichamy, V. Murugesan, ***Inorgani. Chemistry Communications*****,** 13 **(**2010**)** 131.

[15] G. Chandra, S. N. Srivastava, ***Bull. Chem. Soc.*****,** 44 (1971) 3000.

[16] R. C. Hiremath, S. N. Mayanna and N. Venkatasubramaniam, ***J. Chem. Soc. Perkin Trans*****.,** 2 (1987) 1569.

[17] M. A. A. Khalid, ***Kinetics and Mechanism of Peroxodisulphate oxidation of certain Amino Acids in Acidic Aqueous Solution, Ph.D. Thesis, University of Khartoum, 2006.***

[18] D. A. House, ***Chem. Rev.,*** 62 (1962) 185.

[19] W. K. Wilmarth, A. Haim, ***edited by J. O. Edwards (Interscience, London), 1962.***

[20] G. Chandra, and S. N. Srivastava, ***Bull. Chem. Soc.,*** 44 (1971) 3000.

[21] A. Prakash, P. Dwvedi, M. N. Srivastava and B. B. L. Saxena, ***Nat. Acad. Sci. Letters,*** 2 (1988) 4.

[22] D. C. Hiremath, K. T. Sirsalmath, S. T. Nandibewoor, ***Catalysis Lett.,*** 122 (2008) 144.

[23] N. P. Shetti, R. R. Hosamani and S. T. Nandibewoor, ***Research Letters in Inorg. Chem.,*** 2008.

[24] N. Grover, N. Kambo, S. K. Upadhyay, ***Ind. J. Chem.,*** 12 (2002) 2482.

[25] J. Sanathanlakshmi, P. Vankatesan, ***Chinese Journal of Catalysis*****,** 33 (2012) 1306.

[26] X. Huang, I. H. El-Sayed, X. Yi, M. A. El-Sayed, ***J. Photochem. Photobiol. B*****,** 81 (2005) 76.

[27] S. Jansat, M. Gomez, K. Philippot, G. Muller, E. Guiu, C. Claver, S. Castillon, B. Chaudret, ***J. Am. Chem. Soc.,*** 126 (2004) 1592.

[28] D. Astruc, F. Lu, J. R. Aranzaes, ***Angew. Chem. Int. Ed.,*** *44* (2005) 7852.

[29] K. E. Kavanagh, F. F. Nord, ***J. Am. Chem. Soc.***, *65*, (1943**)** 2121.

[30] M. Haruta, T. Kobayashi, H. Sano, N. Yamada, ***Chem. Lett.,*** *16* (1987) 405.

[31] A. Nasirian, ***Int. J. Nano. Dim.*****,** 2 (2012) 159.

[32] L. N. Lewis, N. Lewis, ***J. Am. Chem. Soc****.,* 108 (1986) 7228, L. N. Lewis, R. Uriarte, ***J. Organometallics,*** 9 (1990) 621.

[33] H. Hirai, H. Komiyama, ***Bull. Chem. Soc. Jpn.****,* 59 (1986) 545.

[34] G. Maayan, R. Neumann, ***Catal. Lett.*****,** 123 (2008) 41.

[35] C. W. Yen, M. L. Lin, A. Wang, S. A. Chen, ***J. Phys. Chem. C,***113 (2009) 17831.

[36] V. Kiran, T. Ravikumar, A. K. Shukala, ***J. Electrochem. Soc.,*** 157 (2010**)** 1201.

[37] B. P. Fabio, R. O. Elaine, V. M. Oliveira, B. N. Fabio, ***Catal. Lett.*****,** 110 (2006**)** 261.

[38] J. Amer, ***J. Chem. Soc.,*** 82 (1960) 5535.

[39] M. A. Khalid, A. M. Kheir, ***Sudan Journal of Basic Sciences*****,** 15 (2008) 69.

[40] M. G. Ram reddy, B. Sethuram, T. Z. Navaneeth Rao, ***Phys. Chem.,*** 256 (1975) 880.

[41] F. Feigl, ***Spot Test in Inorganic Analysis (Elsevier London), 1958.***

[42] A. I. Vogel, ***A textbook of macro and semimicro qualitative inorganic analysis (Orient Longman, New Delhi), 1967.***

[43] F. Feigl, ***Spot Test in Inorganic Analysis (Elsevier London), 1966.***

[44] P. D. Bragg, L. Hough, ***J. Chem. Soc.,*** 00 (1958) 4050.

[45] A. Goel, S. Sharma, ***J. Chem. Bio. Phy. Sci. Sec. A,*** 2 (2012) 628.

Chapter-7

Kinetics of Copper Nanoparticles Catalyzed Oxidation of Glycine by Peroxodisulphate In Aqueous Solution

Abstract

In the present chapter, the kinetics of copper nanoparticles catalyzed oxidation of glycine (Gly) by peroxodisulphate (PDS) in aqueous medium at 35^{o}C has been investigated. The effect of copper nanoparticles on the rate of oxidation of glycine has been studied at different concentration of copper nanoparticles at four different sizes of synthesized nanoparticles (55, 28, 16 and 12 nm). Interestingly, it was found that, the catalytic activity depends on the size of nanoparticles and the kinetics of the reaction was found to be first order with respect to peroxodisulphate and independent of glycine concentration. The main oxidation product of glycine is the corresponding aldehyde i.e. formaldehyde. Addition of neutral salts shows a retarding effect. The progress of the reaction is reported by UV-Visible spectrophotometer. The activation and thermodynamic parameters have also been calculated.

7.1. Introduction

Amino acids represent organism forerunners of essential bio-molecules such as proteins, hormones, enzymes, etc. Amino acids derived largely from protein in the diet or degradation of intracellular proteins one the final class of biomolecules which oxidation makes a significant contribution to the generation of metabolic energy. They may also serve as energy source losing their amino functional groups by two pathways: transamination or oxidative deamination [1, 2]. The kinetic investigation on the oxidation of amino acids is of the utmost importance, both from a chemical point and in view of its bearing on the mechanism of amino acid metabolism [3]. Amino acids can undergo many kinds of reactions, depending upon whether a particular amino acid contains non-polar substituent. Glycine is an essential amino acid classified as non-polar and forms active sites of enzymes and helps in maintaining proper conformation by keeping them in proper ionic states. The study of oxidation of glycine may help in the understanding of some aspects of enzyme catalysis. The oxidation of glycine has received much attention because of an inhibitory neurotransmitter in the central nervous system, especially in the spinal cord, brain stem, and retina [4].

The study of oxidation of amino acids is interesting as the oxidation products are different from different oxidants [5, 6]. Many kinetic studies have been carried out on the oxidation of glycine, using different oxidants such as Mn(VII) [7, 8], ferricyanide [9], peroxodisulphate ($K_2S_2O_8$) [10], $KMnO_4$ [11], potassium bromate [12] and aquomanganese(III) [13]. Peroxodisulphate in several cases fulfills most requirements [14]. The standard oxidation reduction potential is estimated to be -2.01V. The reactions involving this ion are generally sluggish in the absence of suitable catalyst [15]. The most thoroughly investigated catalyst is Ag(I) ion although reaction involving Cu(II) and Fe(III) ions also have been studied [16]. Kinetics and mechanism of decarboxylation of amino acids by peroxo oxidants is an area of intensive research because peroxo oxidants are

environmentally benign oxidants and do not produce toxic compounds during their reduction.

In recent years, the use of transition metals such as Os, Ru, Ir, Ag etc. either alone or as binary mixtures, as catalysts in various redox processes has attracted considerable interest [17]. Moreover, the applications of transition metal nanoparticles as catalyst for organic transformations include hydrogenation [18], hydrosilation [19] and hydration reaction of unsaturated organic molecules [20] as well as redox [21] and other electron transfer process. Among the metal nanoparticles, Copper nanoparticles (Cunps) are very attractive due to their heat transfer properties such as high thermal conductivity. Copper nanoparticles also have high surface area to volume ratio, low production cost, antibacterial potency and catalytic activity, optical and magnetic properties as compared to precision metals such as gold, silver or palladium.

Though studies on kinetics of oxidation of amino acid with peroxodisulphate have been widely carried out [22, 23], but in literature the use of copper nanoparticles in the oxidation reaction by peroxodisulphate is scanty. In an attempt to obtain further insight on the universal nature of copper nanoparticles as catalysts was highlighted by employing highly efficient copper nanoparticles for the oxidation of glycine by peroxodisulphate in aqueous medium.

7.2. Experimental Details

7.2.1. Material and Reagents

The methods of preparation and standardization of the reagents including peroxodisulphate are given in chapter 2 (Instrumentation and Methods section). Peroxodisulphate oxidations are susceptible to impurities in the solution and the nature of the glass vessel. The solution of potassium persulphate was prepared by direct weighing. A fresh solution of peroxodisulphate was prepared before starting the experiments. All other reagents employed in this study were either of AnalaR

grade or guaranteed reagent grade and were used as supplied without undertaking any further treatment. Doubly distilled water was used throughout the study.

7.2.2. Kinetic Measurements

All reactions were carried out in Erlenmeyer flasks painted black from the outside to check photochemical decomposition which was immersed in a thermostated water bath at 35±0.1^{o}C unless mentioned otherwise. Calculated amount of copper nanoparticles and glycine were taken in a reaction vessel and thermostated at 35^{o}C for thermal equilibrium. A measured amount of peroxodisulphate was rapidly added to the mixture. When half of the contents from the pipette were released, the time of initiation of the reaction was recorded. The progress of the reaction was studied by estimating the remaining peroxodisulphate iodometrically at different interval of time. A known aliquot (5cm^{3}) of the reaction mixture was withdrawn at different intervals of time and then added into an aqueous solution of KI (~10%) [23]. The liberated iodine was titrated against thiosulphate solution using starch as an indicator, the titer values at any time were taken to represent the residual peroxodisulphate concentrations at that time and will referred to as [$S_2O_8^{2-}$]. Since the concentration of amino acid is ten times more than that of the peroxodisulphate, the rate constants (k_{obs}, sec^{-1}) were evaluated from plots of logarithm of peroxydisulfate concentration against time, the data were collected and analyzed using excel program. The course of the reaction was followed for at least 75% of the reaction.

7.3. Stoichiometry and Product analysis

Under the kinetic conditions to determine the stoichiometry, the reaction was carried out with excess of peroxodisulphate over glycine in presence of copper nanoparticles in a thermostat water bath at 35^{o}C for 24 hours. The excess of peroxodisulphate was determined iodometrically when the completion of the reaction was ensured. The main reaction products are aldehyde, ammonia and CO_2.

The products analysis was carried out under the kinetic conditions. The FTIR spectrum of the corresponding hydrazone of the product **(Figure 7.1)** is corroborated the product of oxidation was corresponding aldehyde i.e. formaldehyde. The reaction mixture was treated with solution of 2, 4-dinitrophenyl hydrazine in 2.0 mol dm^{-3} HCl. The reaction mixture yield brown precipitate of hydrazone derivative of aldehyde. Furthermore this hydrazone were subjected to the recorded infra-red spectra and showed that the absorption of characteristic functional group –NH, –CH and –C=N of hydrazone derivative were observed at certain wave length **3330.13 cm^{-1}, 2906.77 cm^{-1}, 1607.25 cm^{-1}** respectively. Further, aldehyde group was confirmed by qualitative test such as tollen's reagent [24] and schiff's reagent.

The identification of product by IR (Infra-red spectrum) and formation of 2, 4-dinitrophenyl hydrazone derivative indicate the stoichiometry as represented by **equation (7.1).**

$$S_2O_8^{2-} + H-\underset{NH_2}{\overset{H}{\underset{|}{\overset{|}{C}}}}-COOH + H_2O \xrightarrow[308\ K]{\text{Copper Nanoparticles}} HCHO + NH_3 + 2HSO_4^- + CO_2 \quad (7.1)$$

Deamination of the glycine by persulphate in presence of copper nanoparticles was shown in UV- Visible absorption spectrum **(Figure 7.2).** The spectrum is shown a peak of glycine at 210 nm with maximum absorbance in the initial of the reaction. The decrease peak in height with time indicates progress of reaction. Ammonia was identified by Nessler's reagent; in all cases a brownish color was observed indicating a deamination reaction.

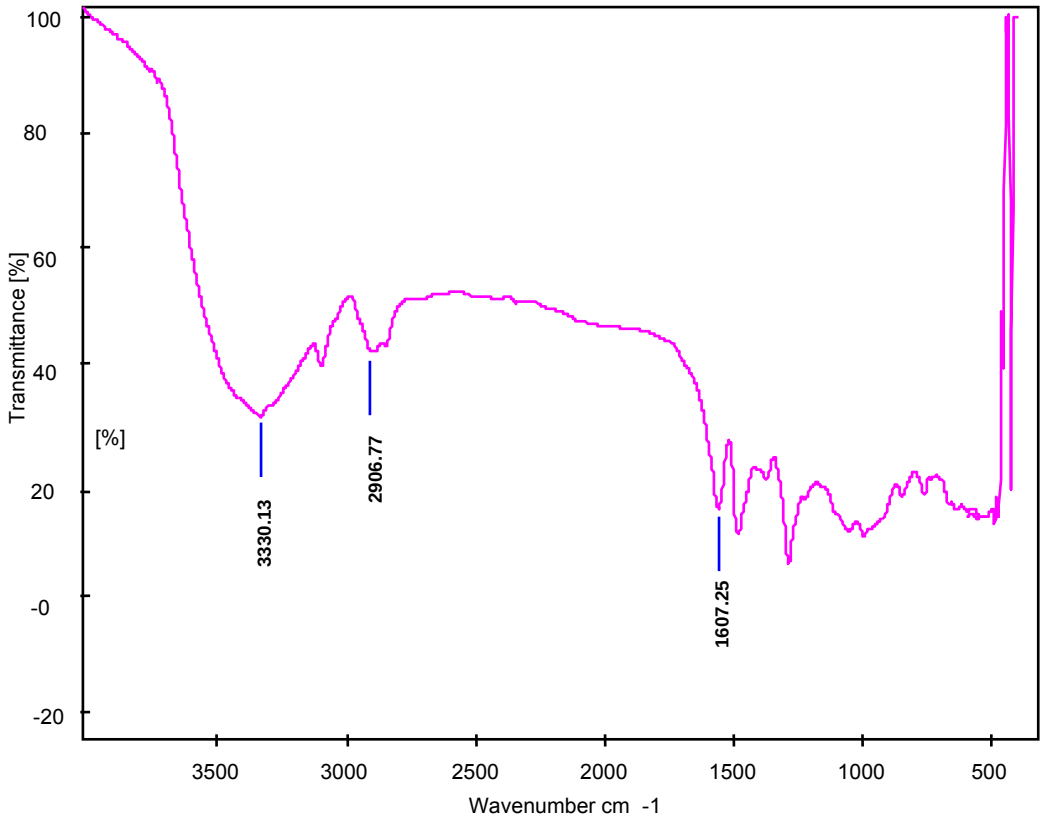

Figure 7.1: The FTIR spectra of the hydrazone derivative from the reaction mixture of the glycine and peroxodisulphate in the presence of copper nanoparticles

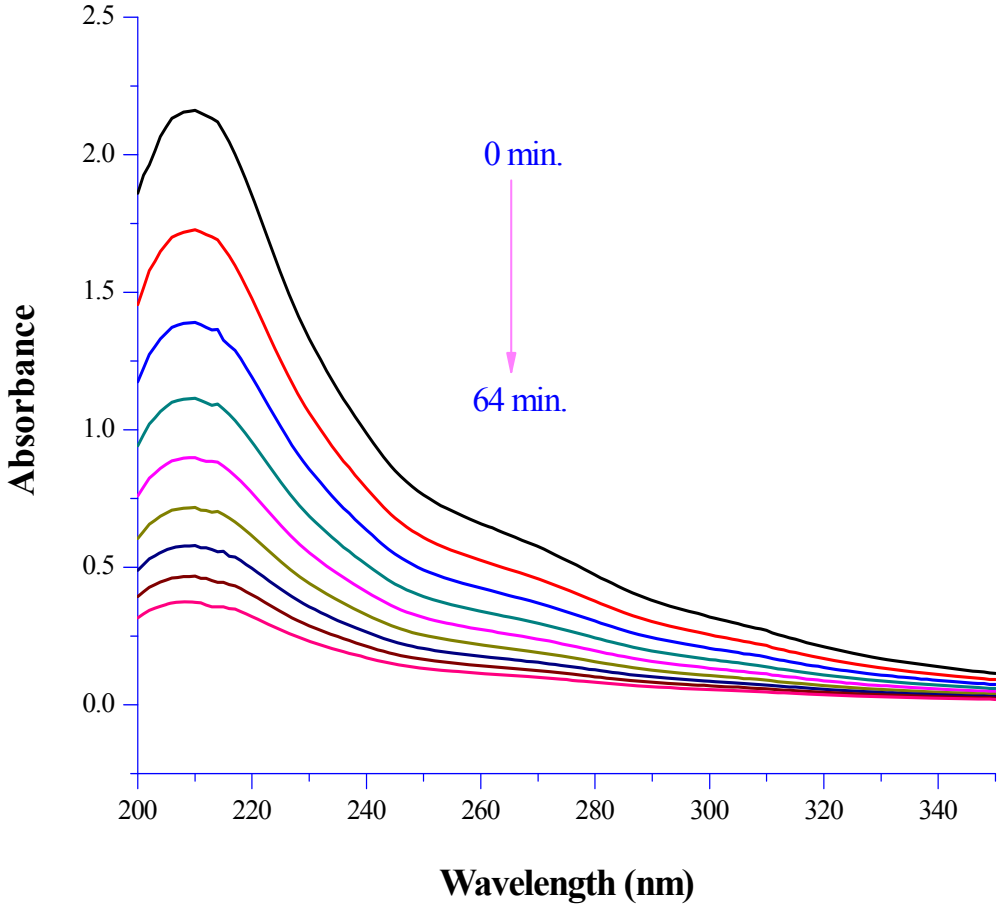

Figure 7.2: UV-Vis absorption spectra for the deamination of glycine (time 0-64 minutes) in the presence of the copper nanoparticles (size = 12 nm)

[PDS] = 5.0×10^{-3} mol dm^{-3}; [Glycine] = 5.0×10^{-2} mol dm^{-3};
[Cunps] = 1.0×10^{-5} mol dm^{-3}; Temp. = $35^{o}C$

7.4. Results and Discussion

7.4.1. Peroxodisulphate Dependence

The copper nanoparticles catalyzed oxidation of glycine was studied at different concentration of peroxodisulphate varying from 1.0×10^{-3}– 7.5×10^{-3} mol dm^{-3}, keeping constant concentration of other reaction ingredients *viz.*[Gly] = 5.0×10^{-2} mol dm^{-3}, [Cunps] = 1.0×10^{-5} mol dm^{-3} at 35°C. The plot of log [PDS] (PDS, has been used in place of peroxodisulphate heretofore) versus time was made that yielded linear plots for each initial concentration of peroxodisulphate which was shown in **figure 7.3,** indicating that rate of the reaction increases with increasing the concentration of peroxodisulphate and the reaction is first order with respect to peroxodisulphate concentration. The rate constants (k_{obs}, sec^{-1}) were calculated from the slope of the above plots. The observed pseudo first order rate constant (k_{obs}, sec^{-1}) were independent of the concentration of peroxodisulphate. Results are given in **Table-7.1.**

7.4.2. Glycine Dependence

Kinetic runs were carried out by varying initial concentration of glycine ranging from 1.0×10^{-2} – 7.0×10^{-2} mol dm^{-3}at constant concentration of other reaction ingredients *viz.*[PDS] = 5.0×10^{-3}mol dm^{-3}, [Cunps] = 1.0×10^{-5}mol dm^{-3} at 35°C temperature. The plot of log k_{obs} versus log [Gly] (Gly, has been used in place of glycine heretofore) was made that yielded straight line parallel to log [Gly] axis **(Figure 7.4),** indicating zero order dependence with respect to glycine**.** Results are given in **Table-7.2.**

7.4.3. Copper Nanoparticles Dependence

The effect of copper nanoparticles on the rate of oxidation of glycine has been studied at different concentration of copper nanoparticles varying from 1.0×10^{-6}– 1.0×10^{-5} mol dm^{-3} at four different size of copper nanoparticles (55, 28, 16 and 12 nm), synthesized at four concentration (0.07, 0.08, 0.09, 0.10 mol dm^{-3}) of ascorbic acid respectively (as discussed in chapter 3), other reactant and reaction conditions were constant *viz.* [PDS] = 5.0×10^{-3} mol dm^{-3}, [Gly] = 5.0×10^{-2} mol dm^{-3} at 35°C.

TABLE: 7.1

VARIATION OF PEROXODISULPHATE

[Gly] = 5.0×10^{-2} mol dm^{-3} **Temp. = 35^{o}C**

[Cunps] = 1.0×10^{-5} mol dm^{-3} **Titrant [Hypo] = 1.0×10^{-3} mol dm^{-3}**

Aliquot = 5.0 ml

10^3 [PDS], mol dm^{-3}	**1.0***	**2.0**	**3.0**	**4.0**	**5.0**	**6.0**	**7.5**
Time in minutes	**Volume of Titrant (ml)**						
0	10.0	10.0	15.0	20.0	25.0	30.0	37.5
8	8.0	8.0	12.0	16.1	20.0	24.1	29.8
16	6.5	6.5	9.7	12.9	16.1	19.4	23.9
24	5.2	5.2	7.8	10.4	12.9	15.6	19.2
32	4.2	4.2	6.2	8.3	10.4	12.5	15.4
40	3.4	3.4	5.0	6.7	8.3	10.1	12.4
48	2.7	2.7	4.0	5.4	6.7	8.1	9.9
56	2.2	2.2	3.2	4.3	5.4	6.5	8.0
64	1.8	1.7	2.6	3.5	4.3	5.2	6.4
10^4 (k_{obs}), sec^{-1}	**4.53**	**4.55**	**4.57**	**4.56**	**4.57**	**4.55**	**4.57**

*Hypo = 5×10^{-4} mol dm^{-3}

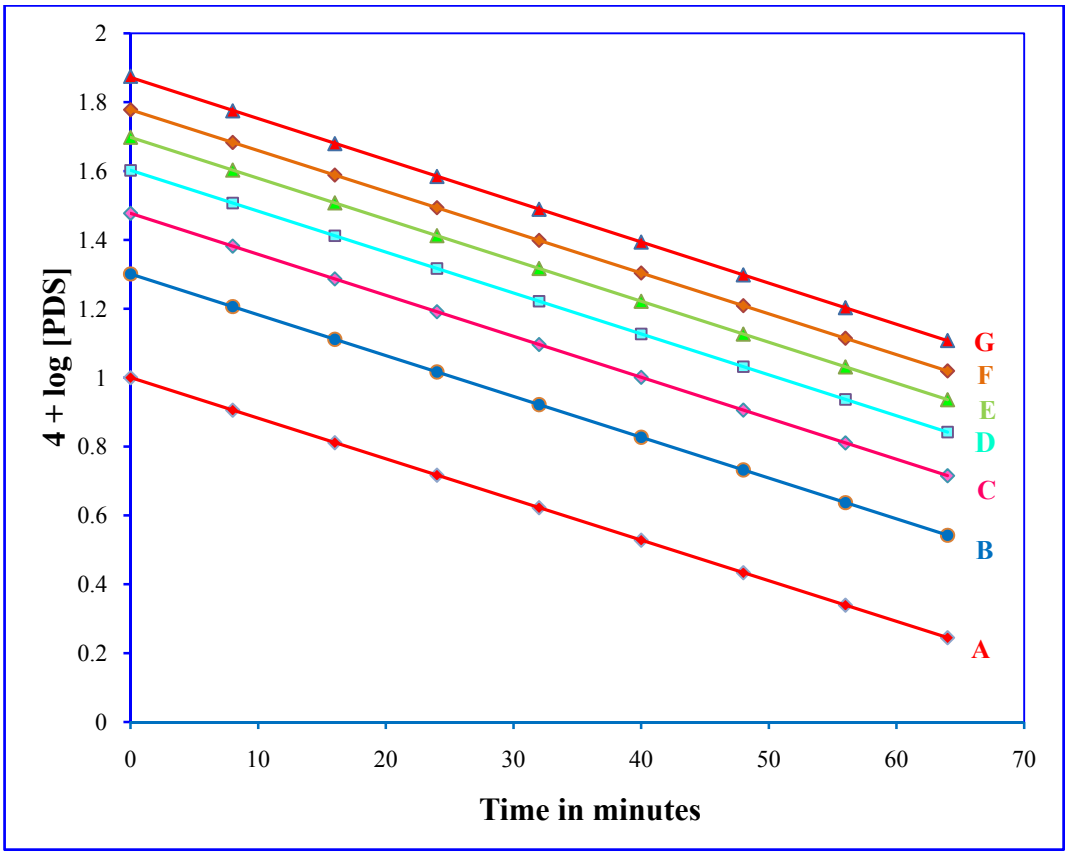

Figure 7.3: Variation of peroxodisulphate

[Ala]= 5.0×10^{-2} mol dm^{-3}; [Cunps] = 1.0×10^{-5} mol dm^{-3};

Temp. =35°C

[PDS]= (A) 1.0×10^{-3} mol dm^{-3} (B) 2.0×10^{-3} mol dm^{-3}

(C) 3.0×10^{-3} mol dm^{-3} (D) 4.0×10^{-3} mol dm^{-3}

(E) 5.0×10^{-3} mol dm^{-3} (F) 6.0×10^{-3} mol dm^{-3}

(G) 7.5×10^{-3} mol dm^{-3}

(Ref. Table: 7.1)

TABLE: 7.2

VARIATION OF GLYCINE

[PDS] = 5.0×10^{-3} mol dm^{-3} **Temp. = 35^{o}C**

[Cunps] = 1.0×10^{-5} mol dm^{-3} **Titrant [Hypo] = 1.0×10^{-3} mol dm^{-3}**

Aliquot = 5.0 ml

10^2 [Gly], mol dm^{-3}	**1.0**	**2.0**	**3.0**	**4.0**	**5.0**	**6.0**	**7.0**
Time in minutes	**Volume of Titrant (ml)**						
0	25.0	25.0	25.0	25.0	25.0	25.0	25.0
8	20.1	20.1	20.1	20.0	20.0	20.0	20.0
16	16.1	16.1	16.1	16.1	16.1	16.1	16.1
24	13.0	13.0	13.0	12.9	12.9	12.9	12.9
32	10.4	10.5	10.4	10.4	10.4	10.4	10.4
40	8.4	8.4	8.4	8.3	8.3	8.3	8.3
48	6.7	6.8	6.7	6.7	6.7	6.7	6.7
56	5.4	5.4	5.4	5.4	5.4	5.4	5.4
64	4.3	4.4	4.3	4.3	4.3	4.3	4.3
10^4 (k_{obs}), sec^{-1}	**4.55**	**4.53**	**4.55**	**4.57**	**4.57**	**4.58**	**4.57**

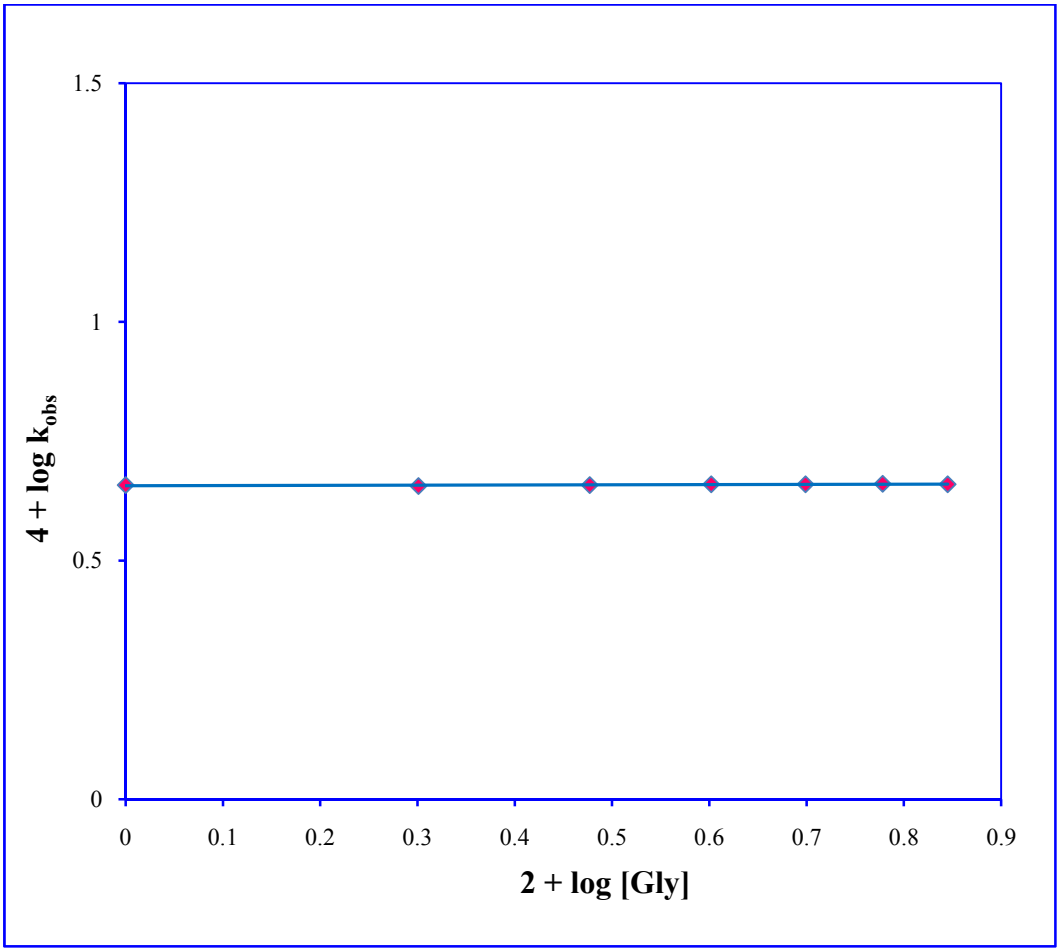

Figure 7.4: Variation of Glycine

[PDS]= 5.0×10^{-3} mol dm^{-3}; [Cunps] = 1.0×10^{-5} mol dm^{-3};

Temp. = $35^{o}C$

(Ref. Table: 7.2)

The rate of reaction increases with increasing concentration of copper nanoparticles. The catalytic activity of copper nanoparticles seems different when concentration of reducing agent is varied from 0.07 to 0.1 mol dm^{-3}. The difference in catalytic activity can be attributed to the size variation in the resulting copper nanoparticles. The observed rate constant (k_{obs}, sec^{-1}) was plotted against concentration of copper nanoparticles [Cunps] (Cunps, has been used in place of copper nanoparticles hitherto) were made, a straight line was obtained with non-zero intercept, confirming the first order dependence with respect to copper nanoparticles. Non-zero intercept indicates the reaction occurring in the absence of copper nanoparticles. The trend in the calculated rate constant being 12>16>28>55nm **(Figure 7.5).** This effect can be attributed to the nanosize of the particles that as size decreases surface area increases and the active center are also increases. The observed pseudo first order rate constant (k_{obs}) increases with increasing concentration of copper nanoparticles. Results are given in **Table-7.3, 7.4, 7.5, 7.6.**

7.4.4. Neutral Salts dependence

The effect of added neutral salt on the rate of oxidation of glycine has been studied at different concentration of neutral salts (KCl, NH_4Cl and K_2SO_4) varying from 1.0×10^{-3}- 4.0×10^{-3} mol dm^{-3} at fixed concentration of other reactant and constant conditions *viz.* [PDS] = 5.0×10^{-3} mol dm^{-3}, [Gly] = 5.0×10^{-2} mol dm^{-3}, [Cunps] = 1.0×10^{-5} mol dm^{-3} at 35°C. The change in the rate constant (k_{obs}, sec^{-1}) with increase in the concentration of neutral salts (KCl, NH_4Cl and K_2SO_4) is found to be very small.

The observed rate constant (k_{obs}) was plotted against the concentration of neutral salts (KCl, NH_4Cl and K_2SO_4) **(Figure 7.6)** that yielded a straight line, indicating the rate of the reaction slightly decreases with increasing the concentration of neutral salt. The results show **(Table 7.7, 7.8, 7.9)** the retarding effect of some ions on the rate of reaction of copper nanoparticles catalyzed oxidation of glycine by peroxodisulphate. The decrease in the rate constant is not strictly related to the increase in ionic strength and evidently there is a considerable specific effect of the ions. Similar observations have been obtained in earlier study [25, 26] in the oxidation of glycine in the presence of Ag (I) as a catalyst [27].

TABLE: 7.3

EFFECT OF COPPER NANOPARTICLES

(SIZE = 12nm)

[PDS] = 5.0×10^{-3} mol dm^{-3} **Temp. = 35^{o}C**

[Gly] = 5.0×10^{-2} mol dm^{-3} **Titrant [Hypo] = 1.0×10^{-3} mol dm^{-3}**

Aliquot = 5.0 ml

10^6 [Cunps], mol dm^{-3}	**0.0**	**1.0**	**2.0**	**3.0**	**4.0**	**5.0**	**6.0**	**7.0**	**8.0**	**9.0**	**10.0**
Time in minutes	**Volume of Titrant (ml)**										
0	(0)25.0	(0)25.0	(0)25.0	(0)25.0	(0)25.0	(0)25.0	25.0	25.0	25.0	25.0	25.0
10	(25)20.2	(20)20.2	(18)19.9	(15)20.1	(15)19.6	(12)20.1	20.4	20.0	19.7	19.3	19.0
20	(50)16.3	(40)16.4	(36)15.8	(30)16.2	(30)15.3	(24)16.2	16.7	16.1	15.5	15.0	14.4
30	(75)13.2	(60)13.3	(54)12.6	(45)13.0	(45)12.0	(36)13.0	13.7	12.9	12.3	11.6	11.0
40	(100)10.6	(80)10.8	(72)10.1	(60)10.5	(60)9.4	(48)10.5	11.2	10.4	9.7	9.0	8.3
50	(125)8.6	(100)8.7	(90)8.0	(75)8.5	(75)7.4	(60)8.5	9.1	8.3	7.6	7.0	6.3
60	(150)7.0	(120)7.1	(108)6.4	(90)6.8	(90)5.8	(72)6.8	7.5	6.7	6.0	5.4	4.8
70	(175)5.6	(140)5.7	(126)5.1	(105)5.5	(105)4.6	(84)5.5	6.1	5.4	4.7	4.2	3.7
80	-	(160)4.7	(144)4.1	(120)4.4	(120)3.6	(96)4.4	5.0	4.3	3.7	3.2	2.8
10^4 (k_{obs}), sec^{-1}	**1.42**	**1.75**	**2.10**	**2.40**	**2.70**	**3.00**	**3.35**	**3.65**	**3.95**	**4.25**	**4.57**

Figures in parentheses denote time in minutes

TABLE: 7.4

EFFECT OF COPPER NANOPARTICLES

(SIZE = 16nm)

[PDS] = 5.0×10^{-3} mol dm^{-3} **Temp. = 35^{o}C**

[Gly] = 5.0×10^{-2} mol dm^{-3} **Titrant [Hypo] = 1.0×10^{-3} mol dm^{-3}**

Aliquot = 5.0 ml

10^6 [Cunps], mol dm^{-3}	**0.0**	**1.0**	**2.0**	**3.0**	**4.0**	**5.0**	**6.0**	**7.0**	**8.0**	**9.0**	**10.0**
Time in minutes	**Volume of Titrant (ml)**										
0	(0)25.0	(0)25.0	(0)25.0	(0)25.0	(0)25.0	(0)25.0	25.0	25.0	25.0	25.0	25.0
12	(25)20.2	(20)20.3	(20)19.7	(20)19.2	(15)19.9	(15)19.5	20.1	19.7	19.4	19.0	18.6
24	(50)16.3	(40)16.6	(40)15.5	(40)14.7	(30)15.9	(30)15.3	16.2	15.6	15.1	14.5	13.9
36	(75)13.2	(60)13.5	(60)12.2	(60)11.3	(45)12.7	(45)12.0	13.1	12.4	11.8	11.1	10.4
48	(100)10.6	(80)11.0	(80)9.6	(80)8.7	(60)10.1	(60)9.4	10.6	9.8	9.2	8.5	7.8
60	(125)8.6	(100)9.0	(100)7.6	(100)6.7	(75)8.1	(75)7.3	8.5	7.7	7.2	6.5	5.8
72	(150)7.0	(120)7.3	(120)6.0	(120)5.1	(90)6.5	(90)5.7	6.9	6.1	5.6	4.9	4.3
84	(175)5.6	(140)6.0	(140)4.7	(140)3.9	(105)5.2	(105)4.5	5.6	4.8	4.3	3.8	3.2
96	-	(160)4.9	(160)3.7	(160)3.0	(120)4.1	(120)3.5	4.5	3.8	3.4	2.9	2.4
$10^4(k_{obs})$, sec^{-1}	**1.42**	**1.70**	**1.98**	**2.20**	**2.50**	**2.72**	**2.98**	**3.25**	**3.47**	**3.75**	**4.05**

Figures in parentheses denote time in minutes

TABLE: 7.5

EFFECT OF COPPER NANOPARTICLES

(SIZE = 28nm)

[PDS] = 5.0×10^{-3} mol dm^{-3} **Temp. = 35^{o}C**

[Gly] = 5.0×10^{-2} mol dm^{-3} **Titrant [Hypo] = 1.0×10^{-3} mol dm^{-3}**

Aliquot = 5.0 ml

10^6 [Cunps], mol dm^{-3}	**0.0**	**1.0**	**2.0**	**3.0**	**4.0**	**5.0**	**6.0**	**7.0**	**8.0**	**9.0**	**10.0**
Time in minutes	**Volume of Titrant (ml)**										
0	(0)25.0	(0)25.0	(0)25.0	(0)25.0	(0)25.0	25.0	25.0	25.0	25.0	25.0	25.0
15	(25)20.2	(25)19.6	(20)20.1	(20)19.7	(20)19.1	20.1	19.8	19.5	19.2	18.9	18.6
30	(50)16.3	(50)15.4	(40)16.2	(40)15.5	(40)14.6	16.2	15.7	15.2	14.8	14.3	13.8
45	(75)13.2	(75)12.1	(60)13.0	(60)12.2	(60)11.2	13.1	12.4	11.9	11.4	10.8	10.3
60	(100)10.6	(100)9.6	(80)10.5	(80)9.6	(80)8.6	10.6	9.8	9.3	8.8	8.2	7.7
75	(125)8.6	(125)7.5	(100)8.5	(100)7.6	(100)6.6	8.5	7.8	7.3	6.8	6.2	5.7
90	(150)7.0	(150)5.9	(120)6.8	(120)6.0	(120)5.0	6.9	6.2	5.7	5.2	4.7	4.2
105	(175)5.6	(175)4.7	(140)5.5	(140)4.7	(140)3.9	5.5	4.9	4.4	4.0	3.5	3.2
120	-	-	(160)4.4	(160)3.7	(160)3.0	4.5	3.9	3.5	3.1	2.7	2.4
$10^4(k_{obs})$, sec^{-1}	**1.42**	**1.60**	**1.80**	**1.98**	**2.22**	**2.39**	**2.59**	**2.74**	**2.90**	**3.10**	**3.28**

Figures in parentheses denote time in minutes

TABLE: 7.6

EFFECT OF COPPER NANOPARTICLES

(SIZE = 55nm)

[PDS] = 5.0×10^{-3} mol dm^{-3} **Temp. = 35°C**

[Gly] = 5.0×10^{-2} mol dm^{-3} **Titrant [Hypo] = 1.0×10^{-3} mol dm^{-3}**

Aliquot = 5.0 ml

10^6 [Cunps], mol dm^{-3}	**0.0**	**1.0**	**2.0**	**3.0**	**4.0**	**5.0**	**6.0**	**7.0**	**8.0**	**9.0**	**10.0**
Time in minutes	**Volume of Titrant (ml)**										
0	(0)25.0	(0)25.0	(0)25.0	25.0	25.0	25.0	25.0	25.0	25.0	25.0	25.0
20	(25)20.2	(25)19.9	(25)19.7	20.3	20.1	19.9	19.6	19.4	19.0	18.8	18.6
40	(50)16.3	(50)15.8	(50)15.6	16.6	16.2	15.8	15.4	15.1	14.5	14.2	13.9
60	(75)13.2	(75)12.6	(75)12.3	13.5	13.0	12.6	12.1	11.7	11.1	10.7	10.3
80	(100)10.6	(100)10.0	(100)9.7	11.0	10.5	10.0	9.6	9.1	8.5	8.1	7.7
100	(125)8.6	(125)8.0	(125)7.7	9.0	8.5	8.0	7.5	7.1	6.5	6.1	5.7
120	(150)7.0	(150)6.4	(150)6.1	7.3	6.8	6.4	5.9	5.5	4.9	4.6	4.3
140	(175)5.6	(175)5.1	(175)4.8	6.0	5.5	5.1	4.7	4.3	3.8	3.5	3.2
160	-	-	-	4.9	4.4	4.0	3.7	3.3	2.9	2.6	2.4
$10^4(k_{obs})$, sec^{-1}	**1.42**	**1.52**	**1.57**	**1.70**	**1.80**	**1.90**	**2.00**	**2.10**	**2.25**	**2.35**	**2.45**

Figures in parentheses denote time in minutes

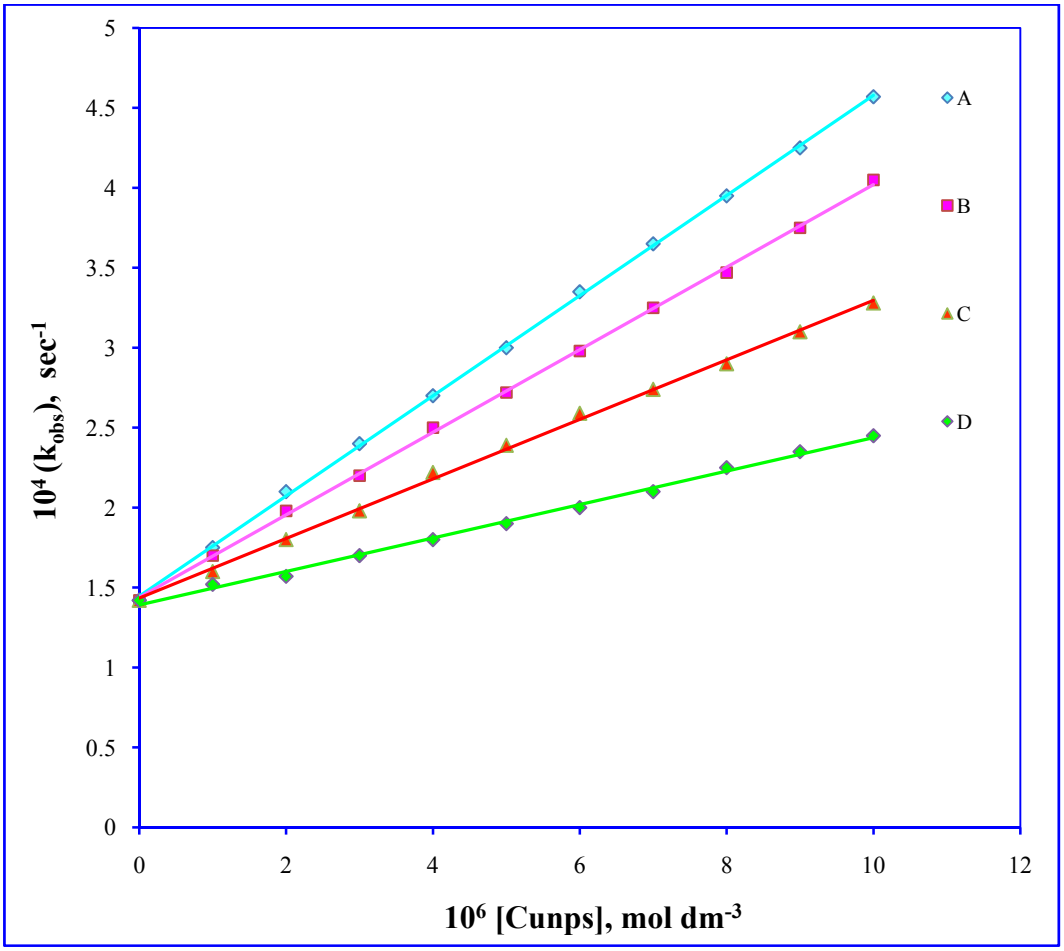

Figure 7.5: Variation of copper nanoparticles at different size of copper nanoparticles (A) 12 nm, (B) 16 nm, (C) 28 nm, (D) 55 nm

[PDS] = 5.0×10^{-3} mol dm^{-3}; [Gly] = 5.0×10^{-2} mol dm^{-3};
Temp. = 35^{o}C

(Ref. Table: 7.3, 7.4, 7.5, 7.6)

TABLE: 7.7

EFFECT OF NEUTRAL SALT

(KCl)

[PDS] = 5.0×10^{-3} mol dm^{-3} **Temp. = 35°C**

[Gly] = 5.0×10^{-2} mol dm^{-3} **Titrant [Hypo] = 1.0×10^{-3} mol dm^{-3}**

[Cunps] = 1.0×10^{-5} mol dm^{-3} **Aliquot = 5.0 ml**

10^3 [KCl], mol dm^{-3}	**0.0**	**1.0**	**2.0**	**3.0**	**4.0**
10^3 I, mol dm^{-3}	**0.0**	**1.0**	**2.0**	**3.0**	**4.0**
Time in minutes	**Volume of Titrant (ml)**				
0	25.0	25.0	25.0	25.0	25.0
8	20.0	20.1	20.2	20.4	20.5
16	16.1	16.2	16.4	16.7	16.9
24	12.9	13.1	13.3	13.7	13.9
32	10.4	10.6	10.8	11.2	11.4
40	8.3	8.5	8.7	9.1	9.4
48	6.7	6.9	7.1	7.5	7.7
56	5.4	5.6	5.7	6.1	6.3
64	4.3	4.5	4.6	5.0	5.2
10^4 (k_{obs}), sec^{-1}	**4.57**	**4.47**	**4.38**	**4.18**	**4.08**

TABLE: 7.8

EFFECT OF NEUTRAL SALT

(NH_4Cl)

[PDS] = 5.0×10^{-3} mol dm^{-3} **Temp. = 35°C**

[Gly] = 5.0×10^{-2} mol dm^{-3} **Titrant [Hypo] = 1.0×10^{-3} mol dm^{-3}**

[Cunps] = 1.0×10^{-5} mol dm^{-3} **Aliquot = 5.0 ml**

10^3 [NH_4Cl], mol dm^{-3}	**0.0**	**1.0**	**2.0**	**3.0**	**4.0**
10^3 I, mol dm^{-3}	**0.0**	**1.0**	**2.0**	**3.0**	**4.0**
Time in minutes			**Volume of Titrant (ml)**		
0	25.0	25.0	25.0	25.0	25.0
8	20.0	20.2	20.3	20.5	20.7
16	16.1	16.3	16.5	16.9	17.2
24	12.9	13.2	13.5	13.9	14.2
32	10.4	10.7	11.0	11.5	11.8
40	8.3	8.7	8.9	9.4	9.8
48	6.7	7.0	7.3	7.8	8.1
56	5.4	5.7	5.9	6.4	6.8
64	4.3	4.6	4.8	5.3	5.6
10^4 (k_{obs}), sec^{-1}	**4.57**	**4.41**	**4.28**	**4.05**	**3.89**

TABLE: 7.9

EFFECT OF NEUTRAL SALT

(K_2SO_4)

[PDS] = 5.0×10^{-3} mol dm^{-3} **Temp. = 35°C**

[Gly] = 5.0×10^{-2} mol dm^{-3} **Titrant [Hypo] = 1.0×10^{-3} mol dm^{-3}**

[Cunps] = 1.0×10^{-5} mol dm^{-3} **Aliquot = 5.0 ml**

10^3 [K_2SO_4], mol dm^{-3}	**0.0**	**1.0**	**2.0**	**3.0**	**4.0**
10^3 I, mol dm^{-3}	**0.0**	**3.0**	**6.0**	**9.0**	**12.0**
Time in minutes	**Volume of Titrant (ml)**				
0	25.0	25.0	25.0	25.0	25.0
10	19.0	19.5	19.7	19.9	20.2
20	14.4	15.2	15.6	15.8	16.4
30	11.0	11.9	12.3	12.6	13.3
40	8.3	9.3	9.7	10.0	10.7
50	6.3	7.3	7.7	8.0	8.7
60	4.8	5.7	6.1	6.4	7.1
70	3.7	4.4	4.8	5.1	5.7
80	2.8	3.5	3.8	4.0	4.6
10^4 (k_{obs}), sec^{-1}	**4.57**	**4.11**	**3.93**	**3.79**	**3.51**

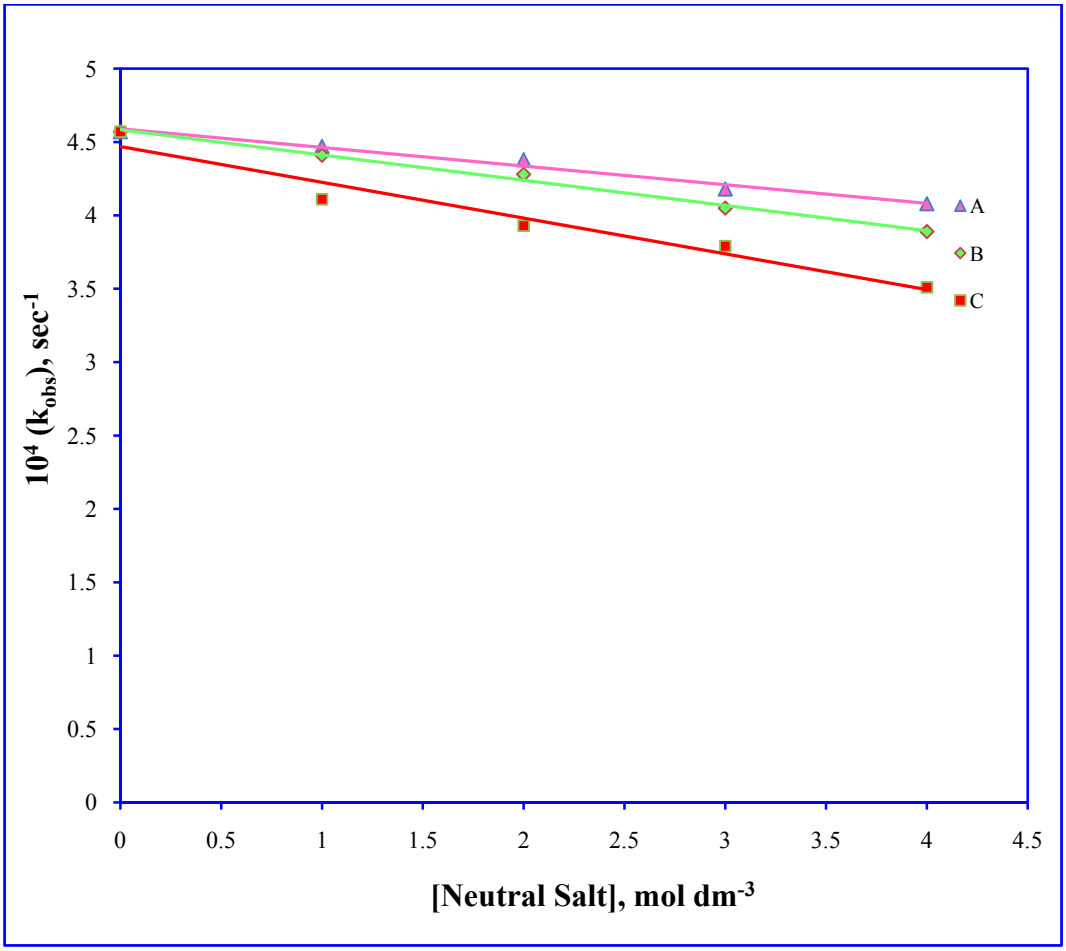

Figure 7.6: Plot of neutral salt dependence (A) KCl, (B) NH_4Cl, (C) K_2SO_4

[PDS] = 5.0×10^{-3} mol dm^{-3}; [Cunps] = 1.0×10^{-5} mol dm^{-3};
[Gly] = 5.0×10^{-2} mol dm^{-3}; Temp. = 35^oC

(Ref. Table: 7.7, 7.8, 7.9)

7.4.5. Temperature Dependence

The effect of temperature on the rate of reaction was studied at three temperature 30°C, 35°C, 40°C respectively at constant concentration of other reaction ingredients *viz.* [PDS] = 5.0×10^{-3} mol dm^{-3}, [Gly] = 5.0×10^{-2} mol dm^{-3}, [Cunps] = 1.0×10^{-5} mol dm^{-3}. The observed rate constants increased with increase in temperature, these results were tabulated in **Tables-7.10.** By applying Arrhenius equation, the logarithm of observed rate constant ($k_{obs,}$ sec^{-1}) was plotted against 1/T in K^{-1} that yielded a straight line **(Figure 7.7).**

The slope of the graph is equal to $-E_a/R$ the energy of activation (E_a) for oxidation of glycine by peroxodisulphate was calculated to be 24.69 kJ mol^{-1} and entropy of activation was calculated to be -237.32 J K^{-1} mol^{-1}. The enthalpy of activation ($\Delta H^{\neq}$), free energy of activation ($\Delta G^{\neq}$) was also obtained 22.13 kJ mol^{-1} and 95.226 kJ mol^{-1} respectively. Fairly high positive values of free energy of activation ($\Delta G^{\neq}$) and enthalpy of activation ($\Delta H^{\neq}$) in the present study indicated that the transition state was highly solvated while the negative values of entropy of activation (ΔS) was suggested the formation of more ordered transition state with reduction in the degree of freedom of the molecules involved.

7.4.6. Mechanism

Many peroxodisulphate oxidations have been studied kinetically [28]. Its utility as an oxidizing agent for various substrates is derived from its ability to oxidize in acidic, neutral, and alkaline media [28]. The decomposition of persulphate in aqueous solution involves the reactions **(Equation 7.2)** [29].

Neutral solution,

$$S_2O_8^{2-} + H_2O \longrightarrow 2HSO_4^- + \tfrac{1}{2}\, O_2 \qquad (7.2)$$

Reactions involving this ion are however, generally slow at ordinary temperatures, but are catalysed by adding transition metal ions [30-35]. Catalytic activity of copper nanoparticles on oxidation of glycine was demonstrated by using the peroxodisulphate as oxidant in aqueous solution.

TABLE: 7.10

EFFECT OF TEMPERATURE

[PDS] = 5.0×10^{-3} mol dm^{-3}

[Gly] = 5.0×10^{-2} mol dm^{-3} **Titrant [Hypo] = 1.0×10^{-3} mol dm^{-3}**

[Cunps] = 1.0×10^{-5} mol dm^{-3} **Aliquot = 5.0 ml**

Temperature, (^{o}C)	**30^{o}C**	**35^{o}C**	**40^{o}C**
Time in minutes	**Volume of Titrant (ml.)**		
0	25.0	25.0	25.0
10	19.8	19.0	18.0
20	15.6	14.4	13.0
30	12.4	11.0	9.4
40	9.8	8.3	6.8
50	7.8	6.3	4.9
60	6.2	4.8	3.6
70	4.9	3.7	2.6
80	3.9	2.8	1.9
10^{4} (k_{obs}), sec^{-1}	**3.89**	**4.57**	**5.4**

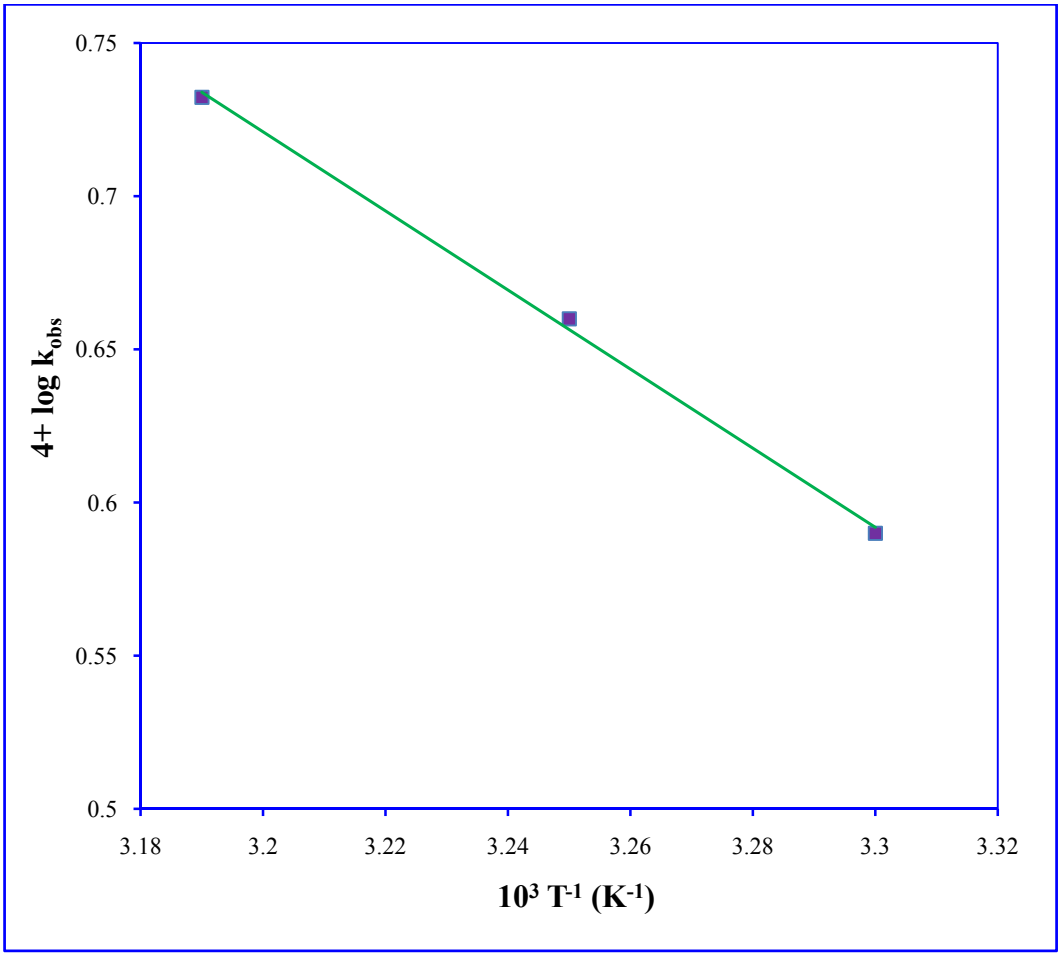

Figure 7.7: Plot of temperature dependence

[PDS] = 5.0×10^{-3} mol dm^{-3}; [Cunps] = 1.0×10^{-5} mol dm^{-3};
[Gly] = 5.0×10^{-2} mol dm^{-3}

(Ref. Table: 7.10)

The rate of reaction does not depend upon the concentration of glycine while peroxodisulphate converted to hydrogen sulfate ion during the reaction.

Therefore the kinetics of the reaction was found to be first order with respect to peroxodisulphate, copper nanoparticles and independent of glycine concentration. Hence it is requisite for measurable rate of oxidation of glycine reaction go over in the presence of copper nanoparticles. Smaller metal nanoparticles (12 nm) offer larger surface area and large surface energy as a result, most of the substrate loaded onto them will be exposed to the particle surface leading to reaction faster than uncatalyzed reaction. The mechanism of catalysis thus involves the reaction of persulfate anion ($S_2O_8^{2-}$) with the adsorbed glycine on the copper nanoparticles. The oxidation of glycine was carried out in the presence of copper nanocatalyst at different time intervals. The absorption spectrum demonstrates the decrease peaks for glycine with the time intervals. Initially, the absorption peak is obtained at 210 nm for the glycine in the reaction mixture. The absorption peak was decreased gradually with the increase exposure time and that indicates the catalytic oxidation reaction procession. The completion of the oxidation of glycine is known from gradual decrease of the absorbance value approaching the baseline. The kinetic results of oxidation of glycine by peroxodisulphate in aqueous medium catalyzed by Cu-nano are same as uncatalyzed reaction, similarly observations have been obtained in earlier study [36] in the oxidation of glycine by HCF(III) in the presence of iridium nanoparticles as a catalyst.

The definite mechanism of the colloidal metal nanoparticles catalyzed oxidation is not yet clear, based on previous report [37, 38]. Although identify the formation of transition species through certain physical measurements but it is very difficult to isolate and characterize from homogeneous mixture. The proposed plausible mechanism in support of the observed kinetics is depicted in **scheme-1.**

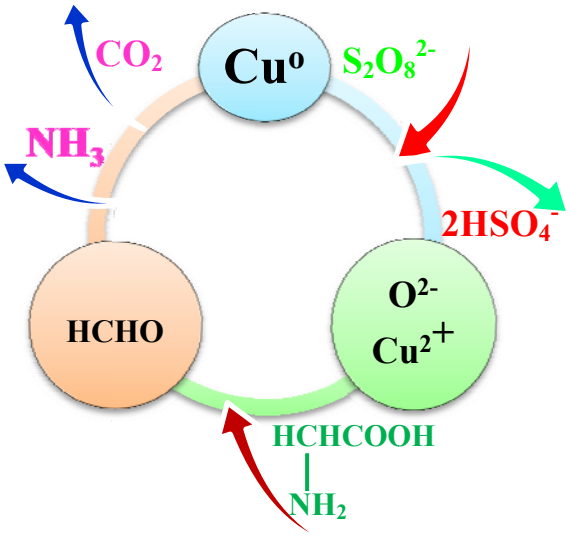

Scheme 1: The plausible route of copper nanoparticles catalyzed oxidation of glycine

7.5. Conclusion

The present study shows that the reaction between peroxodisulphate and glycine is sluggish in aqueous medium. The reaction occurs with measurable velocity in the presence of a small amount of copper nanoparticles. Copper nanoparticles acts as effective catalyst in the oxidation of glycine by peroxodisulphate. By the green method, synthesis of monodispersed copper nanoparticles (ranging from 12 – 55 nm) employing by different concentration of L- ascorbic acid act as reducing agent and antioxidant. Moreover, it was clearly shown that concentration of reducing agents has a remarkable effect on particle size of the synthesized copper nanoparticles. The decreases in the size of copper nanoparticles increase the catalytic activity of copper nanoparticles in the reaction of peroxodisulphate and glycine. Apart from the effect of the temperature and neutral salts on the kinetics of the reaction is also investigated. Neutral salts show the retarding effect on the rate of reaction.

7.6. References

[1] D. Laloo, M. K. Mahanti, ***J. Chem. Soc. Dalton Trans.,*** 1 (1990) 311.

[2] M. P. Alvarez-Macho, ***Rev. Roum. Chim.,*** 38 (1993) 999.

[3] V. Devra, ***J. Ind. Chem. Soc.,*** 82 (2005) 290.

[4] T. Sumathi, P. Shanmugasundararam, G. Chandramohan, D. Deepa, R. Renganathan, ***International Journal of Chemical Science and Technology,*** 2 (2012) 44.

[5] D. Laloo, M. M. Mahanti, ***J. Chem. Soc. Dalton Trans.,*** 1 (1990) 311**.**

[6] K. B. Reddy, B. Sethuram and T. N. Rao, ***Ind. J. Chem.,*** 20 (1981) 395.

[7] M. Yousuf Hussain and F. Ahmad, ***Transition Metal Chemistry,*** **15** (1990) 185**.**

[8] V. R. Chourey, S. Pande, L.V. Shastry and V.R. Shastry, ***Asian J. Chem.,*** 9 (1997) 435**.**

[9] S. K. Upadhyay and M. C. Agarwal, ***Indian J. Chem.,*** A15 (1977) 416.

[10] G. Chandra and S. N. Srivastava***, Indian J. Chem.,*** 11 (1973) 773.

[11] I. M. Bharadwaj, and P. C. Nigam, ***Indian J. Chem.,*** A20 (1981) 308.

[12] S. Anandan, P.S. Subramanian and R. Gopalan, ***Indian J. Chem.,*** A25, (1985) 308.

[13] R. G. Varadarajan and M. Joseph, ***Indian J. Chem.,*** A19 (1980) 977.

[14] F. Minisci, A. Citterio, C. Giordano, ***Acc. Chem. Res.,*** 16 (1983) 27.

[15] H. Marshell, ***J. Chem. Soc.,*** 59 (1891**)** 771.

[16] R. Woods, I. M. Kolthoff, E. J. Meehan**, *Inorg. Chem.,*** 4 (1965) 697.

[17] A. K. Das, ***Coordination Chemistry Reviews,*** 213 (2001) 307**.**

[18] A. Nasirian, ***Int. J. Nano. Dim.,*** 2 (2012) 159.

[19] L. N. Lewis, N. Lewis, ***J. Am. Chem. Soc****.,* 108 (1986) 7228; L. N. Lewis, R. Uriarte, ***J. Organometallics,*** 9 (1990) 621.

[20] H. Hirai, H. Komiyama, ***Bull. Chem. Soc. Jpn.,*** 59 (1986) 545.

[21] M. Spiro, ***Catal. Today***, 17 (1993) 517.

[22] M. A. A. Khalid, ***Arabian Journal for Science and Engineering***, 33 (2008) 199.

[23] M. A. Khalid, A. M. Kheir, ***Sudan Journal of Basic Sciences***, 15 (2008) 69.

[24] Y. Ramanandasarma, P. K. Saiprakash, ***Ind. J. Chem.,*** 19A (1980) 1175.

[25] P. D. Barlett and J. D. Cottman, ***J. Amer. Chem. Soc.***, 71 (1949) 419.

[26] L.S. Levitt, and E.R. Malinowki, ***J. Amer. Chem. Soc.***, 72 (1955) 4517.

[27] G. Chandra, S. N. Srivastava, ***Bull. Chem. Soc.,*** 44 (1971) 3000.

[28] W. K. Wilmarth, A. Haim, ***Peroxide reaction mechanisms. Edited by J. 0. Edwards. Wiley Inter-Science, New York, 1962.***

[29] M. A. A. Khalid, ***Ph.D. Thesis, Kinetics and Mechanism of Peroxodisulphate Oxidation of Certain Amino Acids in Acidic Aqueous Solution, University of Khartoum, 2006.***

[30] J. M. Anderson, J. K. Kochi, ***J. Am. Chem. Soc.,*** 92 (1970) 1651.

[31] C. Walling, D. M. Camaioni, ***J. Org. Chem.,*** 43 (1978) 3266.

[32] C. Arnoldi, A. Citterio, F. Minisci, ***J. Chem. Soc., Perkin Trans.,*** 2 (1983) 531.

[33] A. Citterio, C. Arnoldi***, J. Chem. Soc. Perkin Trans.,*** 1 (1983) 891.

[34] C. Giordano, A. Belli, A. Citterio, F. Minisci, ***J. Org. Chem.,*** 44 (1979) 2314.

[35] C. Giordano, A. Belli, A. Citterio, F. Minisci, ***J. Chem. Soc., Perkin Trans****.,* 1 (1981) 1574.

[36] A. Goel, S. Sharma, ***J. Chem. Bio. Phy. Sci. Sec. A,*** 2 (2012) 628.

[37] S. K. Upadhyay, M. C. Aggarwal, ***Indian J. Chem. A,*** 19 (1980) 5.

[38] V. K. Srivastava, K. K. Srivastava, M. N. Srivastava, B. L. Saxena, ***Indian J. Chem. A,*** 19 **(**1980) 1011.

Annexures

ANNEXURE-I

LIST OFPAPER PUBLISHED: 10

1. "Synthesis and Characterization of Silver Nanoparticles via Green Route", Niharika Nagar, **Shikha Jain,** Vijay Devra, **Korean J chem Eng,** Accepted in May 2016.

2. "Copper Nanoparticles Catalyzed Oxidation of Threonine by Peroxomonosulphate",**Shikha Jain,** Ankita Jain, Vijay Devra, **Journal of Saudi Chemical Society (Elsevier),** 20 (2016).

3. "Synthesis and Size Control of Copper Nanoparticles and their Catalytic Application", **Shikha Jain,** Ankita Jain, Pranav Kachhawaha, Vijay Devra, **Trans. Nonferrous Met. Soc. China (Elsevier),** 25 (2015) 3995−4000.

4. "Synthesis and Characterization of Highly Efficient Copper Nanoparticles and their Catalytic Application in Oxidative Kinetic Study", **Shikha Jain,** Niharika Nagar and Vijay Devra, **Adv. Appl. Sci. Res.,** 6 (2015) 171-180.

5. "Synthesis, Characterization and Catalytic Application of Copper Nanoparticles on Oxidation of Alanine in Acid Aqueous Medium", **Shikha Jain**, Niharika Nagar and Vijay Devra, **International Journal of Current Engineering and Technology**, 5 (2015) 966-973.

6. "A Kinetic Study on Copper Nanocatalysis in the Oxidation of Serine by Peroxomonosulphate", **Shikha Jain**, Ankita Jain, Vijay Devra, **International Journal of Advanced Research in Engineering and Applied Sciences**, 4 (2015) 1-16.

7. "Kinetics and Mechanism of Permanganate Oxidation of Ciprofloxacin in Aqueous Sulphuric Acid Medium",Ankita Jain, **Shikha Jain,** Vijay Devra,

International Journal of Pharmaceutical Sciences and Drug Research, 7 (2015) 205-210.

8. "Experimental Investigation on the Synthesis of Copper Nanoparticles By Chemical Reduction Method", **Shikha Jain**, Ankita Jain, Vijay Devra, **International Journal of Scientific and Engineering Research,** 5 (2014) 973-978.

9. "Kinetic Analysis of oxidation of Ofloxacin by Permanganate in Sulphuric Acid Medium: A Mechanistic Approach", Vijay Devra, Ankita Jain, **Shikha Jain**,**World Journal of Pharmaceutical Research**, 4 (2014) 963-977.

10. "Correlation Analysis of Physico-Chemical Parameters and Water Quality of Chambal River: A case study of Kota city", Ankita Jain, **Shikha Jain,** Vijay Devra, **A International Journal of Engineering, Research and Technology,** 00 (2014).

ANNEXURE-II

Paper Presented and participated in International and National Conferences/ Seminars

1. "Synthesis of Copper Nanoparticles and their Catalytic Application in Oxidation Reaction", **Shikha Jain,** GajalaTazwar, Vijay Devra. Oral presentation of research work in **5th International Conference on Advance Trends in Engineering, Technology and research (ICATETR-2015),** held atBal Krishna Institute of Technology, Ranpur, Kota, Rajasthan, during 23th-24th, December 2015.

2. "Synthesis of Copper Nanoparticles and their Catalytic Application in Oxidation of Amino Acids", **Shikha Jain,** Vijay Devra.Oral presentation of research work of thesis in **Annual Research Seminar organized by center for excellence (Model College)** at J.D.B. Govt. Girls College, Kota, Rajasthan, held on 30th, January 2015.

3. "Synthesis of Dispersed Copper Nanoparticles by Chemical Reduction Method"**Shikha Jain,**Niharika Nagar, Vijay Devra.Oral presentation of research work in**3rd International Conference on "Advance Trends in Engineering, Technology and research (ICATETR-2014)"** held at Bal Krishna Institute of Technology, Ranpur, Kota, Rajasthan, during 22nd-24th, December 2014.

4. "Correlation analysis of Physico-chemical parameters and water quality of Chambal River: A case study of Kota city" participated in **National Conference on Emerging Trends in Water Quantity and Quality Management**, Poornima University, Jaipur, during 19th-20th, December 2014.

5. Participated in **National Seminar & Science Model Exhibition on "Innovation in Science & Technology for Inclusive Development**"

Organized by Dr. B. Lal Institute of Biotechnology and Indian Science Congress Association, Jaipur, held on 16th-17th, January 2014.

6. "Synthesis of Copper Nanoparticles and their Catalytic Application in Oxidative Kinetic Study" **Shikha Jain,** Vijay Devra. Paper presentation of research work in **National Seminar on Pure & Applied Chemical Sciences (Current Trends and Future Prospects)** in Assosiation with Indian Chemical Society, Kolkata NSPACS-2014. Organized by Department of Chemistry, Faculty of Science, Jai NarainVyas University, Jodhpur (Rajasthan) held on 10th-11th,January 2014.

7. "Synthesis of Metal Nanoparticles and their Catalytic Application in Oxidative Kinetic Study" **Shikha Jain,** Ankita Jain, Vijay Devra, presented a posterin **National Conference on Global Environmental Changes and Disaster Management for Sustainable Life on Earth-A burning Issue,** Maharishi Arvind College of Engineering & Technology, Ranpur, Kota, on 21st October, 2013.

8. "Photocatalytic Degradation of Crystal Voilet by use of Copper Oxide as Semiconductor" **Shikha Jain,** Naveen Mittal, Vijay Devra, oral presentation of research work in **1st Rajasthan Science Congress** held at Tagore International School, Jaipur, during 11th-13th, May 2013.

9. "Metal Nanoparticles Catalyzed Oxidation Of Amino Acids in Aqueous Medium: A Kinetic Study" **Shikha Jain,** Vijay Devra oral presentation of research work in **Annual Research Seminar organized by centre for excellence (Model College)** at J.D.B. Govt. Girls College, Kota, Rajasthan, held on 2nd, March 2013.

Journal of Saudi Chemical Society (2016) **xxx**, xxx–xxx

King Saud University

Journal of Saudi Chemical Society

www.ksu.edu.sa
www.sciencedirect.com

ORIGINAL ARTICLE

Copper nanoparticles catalyzed oxidation of threonine by peroxomonosulfate

Shikha Jain, Ankita Jain, Vijay Devra *

Department of Chemistry, J.D.B. Govt. P.G. Girls College, Kota, Rajasthan 324001, India

Received 15 September 2015; revised 17 December 2015; accepted 23 December 2015

KEYWORDS

Copper nanoparticle;
L-Ascorbic acid;
Threonine;
Peroxomonosulfate;
Oxidation;
Kinetics

Abstract The undertaken study describes the synthesis of copper nanoparticles (Cunps) in an aqueous medium using ascorbic acid as a reducing agent via the chemical reduction method. The synthesized copper nanoparticles have resistance to oxidation by atmospheric oxygen for two months. The copper nanoparticles were characterized by UV–Visible spectrophotometry, FTIR spectroscopy, scanning electron microscopy (SEM) and transmission electron microscopy (TEM). The average sizes of copper nanoparticles were found to be 28, 16, 12 nm at increasing concentrations of L-ascorbic acid respectively. Interestingly, it was found that, the catalytic activity depends on the size of nanoparticles. The catalysis by colloidal copper nanoparticles was studied kinetically with the oxidation of L-threonine (Thr) by peroxomonosulfate (PMS) in aqueous medium. The oxidation rate was found to follow first order kinetics with respect to threonine and peroxomonosulfate. The copper nanoparticles are expected to be a suitable alternative and play an important role in the field of catalysis and environmental remediation.

1. Introduction

Research on nanoparticles has received considerable attention since they have unique properties and numerous applications in different areas [1,2]. Metallic nanoparticles are of great interest due to their excellent chemical, physical and catalytic properties [3]. Among colloidal transition metal nanoparticles, copper nanoparticles receive considerable attention since they are used as an advanced material with electronic, optical and thermal properties [4]. In addition to their interesting physical properties exhibited due to quantum size effect, they also have applications in catalysis due to their large surface area and special morphologies. Copper nanoparticles were assumed to be cost effective as compared to noble metals like Ag, Au and Pt. Hence, they are potentially applied in the field of catalysis, cooling fluids and conductive links [5]. Among various methods, the chemical reduction method is widely selected for the synthesis of copper nanoparticles because it is of low cost, efficient in yield and requires limited equipment. It is simple and control of size and shape of particles obtained under controlled parameters is seen [6]. Although the synthesis of copper nanoparticles has been carried via numerous routes [7], very less is known about the size dependent performance of copper nanoparticles as a suitable catalyst. The main question arises

* Corresponding author. Tel.: +91 7597747381.
E-mail address: v_devra1@rediffmail.com (V. Devra).
Peer review under responsibility of King Saud University.

Production and hosting by Elsevier

http://dx.doi.org/10.1016/j.jscs.2015.12.004

from the stability of copper nanoparticles including the extreme sensitivity to oxygen and colloidal agglomeration. Therefore there are several approaches related to the dispersion and oxidation resistance that needs to be solved before application. Some studies reveal that to protect copper nanoparticles against oxidation, ascorbic acid is utilized as a reductant and antioxidant [8–10]. The L-ascorbic acid (hydrogen potential of +0.08 V) can easily reduce metal ions with standard reduction potential higher than 0 V, such as Cu^{2+}, Ag^{+}, Au^{3+} and Pt^{4+} but cannot reduce these ions with potential less than 0 V such as Fe^{2+}, Co^{2+}, Ni^{2+}. Hydrogen free radicals released from ascorbic acid react rapidly with hydroxyl free radicals and oxygen, whose existence is usually related to the oxidation of the nanoparticles. So our experiment was performed without inert gas protection.

The oxidative decarboxylation of amino acid is of importance both from a photochemical view point and also from the view point of the mechanism of amino acid metabolism. Metallic ions play a significant role in the oxidative decarboxylation of amino acids. Kinetics of oxidation of amino acids by a variety of oxidants like hexacyanoferrate(III) [11], peroxomonosulfate [12], peroxodisulfate [13], cerium(IV) [14], chromium(VI) [15] in the presence of transition metal catalysts as well as hexacyanoferrate(III) [16], hydrogen peroxide [17], peroxomonosulfate [18] in the presence of transition metal nanoparticles in both acid and alkaline media have been studied. There are still controversies reported regarding the oxidation product of amino acids as keto acids [19], both as intermediate and also as the oxidation product. In most of the reaction, the end product is the aldehyde [20], the intermediate R–CH = $N^{+}H_2$ undergoes hydrolysis to yield aldehyde whereas its interaction with the oxidant yields nitrile as an end product. However, various types of reaction mechanisms have been suggested but the specific details are yet to be found out. Peroxomonosulfate can be considered as a monosubstituted hydrogen peroxide in which one hydrogen is replaced by the SO_3 group, the other hydrogen comes from the acid group. Peroxide act as an oxygen donor to the organic substrate [21]. In fact, it is the peroxide bond in these peracids that is mainly responsible for its reactions. Study of kinetics of oxidation of amino acids by peroxo oxidants is an area of intensive research because peroxo oxidants are environmentally benign and do not produce toxic compounds during the reaction. The applications of transition metal nanoparticles as catalyst for organic transformations include condensation [22], hydrosilation [23] and hydration reaction of unsaturated organic molecules [24] as well as redox [25] and other electron transfer process [26]. Though studies on kinetics of oxidation of amino acid with peroxomonosulfate have been widely carried out, very few attempts have been made so far on the oxidative deamination of amino acids in the presence of metal nanoparticles. In this work, an attempt has been made to construct a model.

2. Experimental

2.1. Materials

Peroxomonosulfate (PMS) was obtained from Sigma–Aldrich under the trade name "Oxone". The purity of the triple salt $2KHSO_5{\cdot}KHSO_4{\cdot}K_2SO_4$ was estimated by iodometry and found to be 98%. However, the presence of H_2O_2 in the oxone sample was tested. Tests with permanganate showed the absence of free hydrogen peroxide and hence this reagent was used without further purification. A fresh solution of oxone was prepared before starting the experiments. Copper chloride dihydrate ($CuCl_2{\cdot}2H_2O$-97%), L-ascorbic acid (vitamin C-98%), and threonine were obtained from E. Merck. All other chemicals used in this study were of Analar grade and used as such without any further treatment. Double distilled water was employed throughout the study.

2.2. Synthesis of copper nanoparticles

In a synthetic procedure, the wet chemical reduction route was used for synthesis of the copper nanoparticles. $CuCl_2{\cdot}2H_2O$ aqueous solution was prepared by dissolving $CuCl_2{\cdot}2H_2O$ (0.02 mol L^{-1}) in 50 ml deionized water. The flask containing aqueous solution of $CuCl_2{\cdot}2H_2O$ was heated to 353 K in an oil bath with magnetic stirring. 50 ml of L-ascorbic acid (0.1 mol L^{-1}) aqueous solution was added drop wise into the flask while stirring. With the passage of time, the color of the solution gradually changed from white to dark brown with a number of intermediate stages. The reduction process and copper nanoparticle growth process was completed after 24 h and the resulting dispersion was centrifuged for 15 min at 6000 rpm. The supernatant was placed under ambient conditions for 2 months. The redox equation of L-ascorbic acid and copper ion can be expressed by Eq. (1).

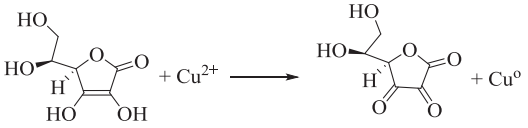

(1)

L-ascorbic acid dehydroascorbic acid

2.3. Characterization

UV–Visible spectrophotometer from a double beam spectrophotometer (U.V. 3000^{+} LABINDIA) was used for the preliminary estimation of copper nanoparticles synthesis. FTIR (ALPHA-T – Bruker) provided information about oxidation product of the reaction. Morphological study of the copper nanoparticles was carried out with scanning electron microscopy (SEM) (EVO 18 carlzeiss) image analysis, for which dispersed nanoparticles were centrifuged (Laboratory Centrifuges Remi, model R-8C) and ultrasonicated (Ultrasonic processor model EI-250UP) for 40 min. 30 µl aliquots were extracted and deposited on stub for SEM analysis. Transmission electron microscope (TEM) (FEI Techni G2S2 Twin) images were recorded to confirm size distribution and shape homogeneity of newly synthesized copper nanoparticles. Samples were prepared by taking small quantities of copper nanoparticles separated by centrifugation then ultrasonicated dispersed suspensions were mounted on carbon coated copper grids.

2.4. Kinetic measurements

Reaction mixture containing aqueous solution of all other reagents except peroxomonosulfate was adjusted to pH 7.0 employing potassium dihydrogen phosphate–sodium

Please cite this article in press as: S. Jain et al., Copper nanoparticles catalyzed oxidation of threonine by peroxomonosulfate, Journal of Saudi Chemical Society (2016), http://dx.doi.org/10.1016/j.jscs.2015.12.004

hydroxide buffer in a 250 ml blackened iodine flask and suspended in a water bath thermostat at 308 K. An aliquot of the requisite volume of peroxomonosulfate solution, thermostat at the same temperature separately, was pipette out into the reaction mixture. The time of initiation of the reaction was recorded when half of the contents from the pipette were released. Kinetics was monitored by estimating [PMS] iodometrically [27] at different time intervals. Initial rates were estimated employing a plane mirror method. The pseudo first order plots were also made wherever, reaction conditions permitted. Results in triplicate were reproducible to within ± 5%.

3. Results and discussion

3.1. Metal nanoparticle characterization results

The solution became colorless when L-ascorbic acid was added, then gradually turned to yellow, orange, brown and finally dark in 24 h (Fig. 1). The appearance of a yellow color followed by orange color indicated the formation of fine nano scale copper particles from L-ascorbic acid assisted reduction.

UV–Visible absorbance spectroscopy has proved to be a very useful technique for studying metal nanoparticles because the peak position and shapes are sensitive to particle size. The first absorption peak of different curves is at 335 nm corresponding to the oxidation product of L-ascorbic acid [28]. The second absorption peak of copper nanoparticles has been reported at around 560 nm of UV–Visible wavelength which proves the formation of copper nanoparticles [29,30]. In this work, the resulting copper nanoparticles did not show a peak at 560 nm but displayed a broadened peak at shorter wavelength i.e. 550 nm, indicating the presence of small separated copper nanoparticles. We investigated the effect of L-ascorbic acid concentration (0.08, 0.09 and 0.10 mol L^{-1}) on the synthesis of copper nanoparticles by UV–Visible spectrophotometer (Fig. S1). The absorption peak is increasingly broadening with an increasing concentration of L-ascorbic acid.

These results indicate that a higher L-ascorbic acid concentration leads to a more effective capping capacity of L-ascorbic acid and then formed smaller copper nanoparticles. The shapes of copper nanoparticles are spherical which can be proved by the SEM images of copper nanoparticles (Fig. 2). TEM images show that the size of particles decreases with the increase of L-ascorbic acid concentration (Fig. 3). The size of copper nanoparticles with various concentrations (0.08, 0.09, 0.10 mol L^{-1}) of L-ascorbic acid are 28, 16, and 12 nm respectively. The reason is that L-ascorbic acid molecules encapsulate Cu^{2+} and reduce Cu^{2+} into Cu (0), then the oxidation products adsorb on the resulting copper nanoparticle surfaces, preventing the particles from growing further. As a result, smaller copper nanoparticles can be obtained.

3.2. The stability of copper nanoparticles

The stability of nanoparticles dispersion is a key factor in their application. In this study L-ascorbic acid was used as a reducing agent and antioxidant of copper nanoparticles. During the synthesis process, excessive L-ascorbic acid is essential to avoid the oxidation of copper nanoparticles. The antioxidant properties of L-ascorbic acid come from its ability to scavenge free radicals and reactive oxygen molecules [31], accompanying the donation of electrons to give semi-dehydroascorbate radical and dehydroascorbic acid.

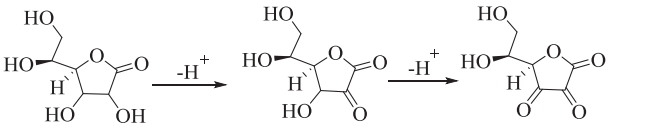

L-Ascorbic acid semi-dehydroascorbate radical dehydroascorbic acid

(2)

The dehydroascorbic acid has three carbonyls in its structure. The 1, 2, 3 tricarbonyl is too electrophilic to survive more than a few seconds in aqueous solution. Hydration of 2-carbonyl is also reported [32]; finally the polyhydroxyl structure is obtained through hydrolysis [28].

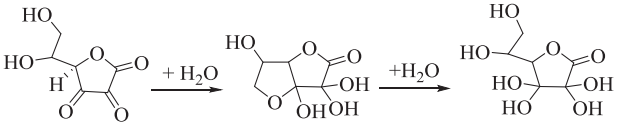

Hydrolysis of dehydroascorbic acid

(3)

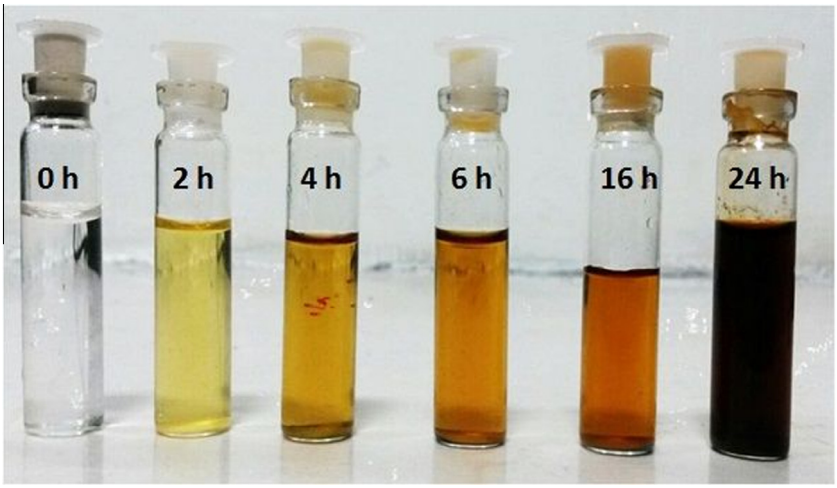

Figure 1 The time evolution photograph of copper nanoparticles formation.

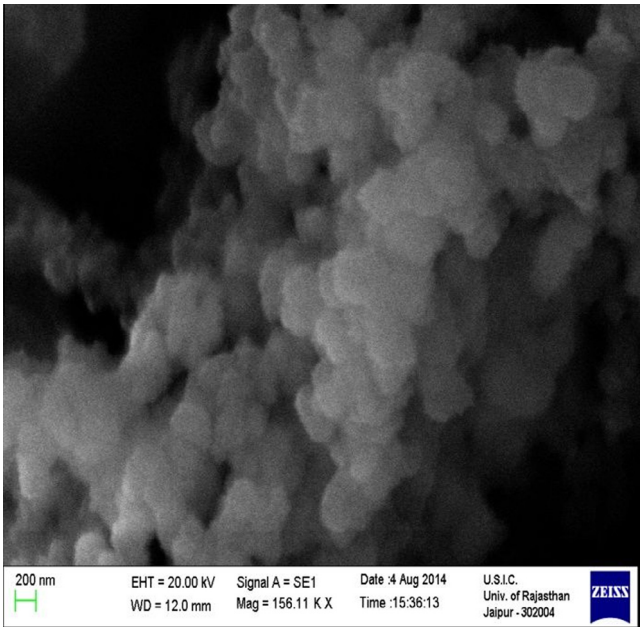

Figure 2 SEM images of copper nanoparticles.

The excessive number of hydroxyl groups can be facilitated by the complexation of copper nanoparticles to the number of matrices by inter–intramolecular hydrogen bond and thus prevent the agglomeration of copper nanoparticles. The result is confirmed with FT-IR Spectroscopy (Fig. S2). FTIR spectrum shows the peaks at 3481 cm^{-1}, 1710 cm^{-1} and 1680 cm^{-1}. These peaks correspond to the hydroxyl, oxidated carbonyl ester and conjugated carbonyl group respectively. These results indicate the presence of a polyhydroxyl structure on the surface of copper nanoparticles. Therefore, L-ascorbic acid plays a dual role as a reducing agent and antioxidant of copper nanoparticles. Thus, the reaction can be performed without any protective inert gas.

3.3. Stoichiometry

The stoichiometry of the reaction was determined by identification of the oxidation product of the substrate under conditions of kinetics. The product appears to be aldehyde as is pointed out by IR spectra and similarly with the products for glycine and alanine oxidation [33]. An addition of 2, 4-dinitrophenyl hydrazine in the reaction mixture yields a brown precipitate of hydrazone derivative of aldehyde. The product aldehyde was confirmed by its FTIR spectrum (Fig. S3). IR peaks at 3097.88 cm^{-1}, 1602.07 cm^{-1} are attributed to –NH, –C=N stretching respectively. However, it was further confirmed by undertaking a kinetic study of the reaction in stoichiometric concentration of the reactants. Results indicate the product to be aldehyde in two electron transfer oxidation. The qualitative tests of aldehyde were positive. Therefore the stoichiometry of the reaction based on the formation of an aldehyde can be represented by Eq. (4):

$$HSO_5^- + \underset{\displaystyle NH_2}{\overset{\displaystyle |}{RCH.COOH}} \xrightarrow[308\ K]{\text{Copper Nanoparticles}} RCHO + NH_3 + HSO_4^- + CO_2 \quad (4)$$

where R represents

$$-\underset{\displaystyle CH_3}{\overset{\displaystyle |}{CH\text{-}OH}}$$

Further the reactions were undertaken with sufficient excess concentration of the oxidant over that of threonine, the excess was estimated iodometrically ensuring completion of the reaction. Results as mentioned in the Table 1 support that a mole of oxidant consumes a mole of the substrate.

3.4. Effect of peroxomonosulfate (PMS) concentration

The concentration of peroxomonosulfate was varied in the range (1.0×10^{-3} mol L^{-1} to 5.0×10^{-3} mol L^{-1} at a fixed concentration of [Thr] = 6.0×10^{-3} mol L^{-1}, [Cunps] = 5.0×10^{-6} mol L^{-1} and pH = 7.0 at 308 K. Initial rates (rate, mol L^{-1} s^{-1}) were calculated employing a plane mirror method and a plot of rate versus [PMS] was made that yielded a straight line passing through the origin, describing first order dependence with respect to peroxomonosulfate. Second order plots were also made by plots of log ([Thr]/[PMS]) against time (Fig. 4). Second order rate constants calculated from these plots were in excellent agreement with those calculated from initial rates (Table 2).

3.5. Effect of threonine (Thr) concentration

The concentration of threonine was varied from 5.0×10^{-3} to 10.0×10^{-3} mol L^{-1}, at a fixed concentration of [PMS] = 3.0×10^{-3} mol L^{-1}, [Cunps] = 5.0×10^{-6} mol L^{-1} and pH = 7.0 at 308 K. Initial rates were calculated and a plot of initial rate (rate, mol L^{-1} s^{-1}) against [Thr] was made, a straight line passing through the origin confirming to first order dependence with respect to threonine. Certain reactions were also undertaken under pseudo first order conditions [Thr] $\gg$ [PMS], under these conditions, pseudo first order plots were made and pseudo first order rate constants (k_1, s^{-1}) evaluated from these plots were found to increase proportionately with the increasing concentration of threonine. Second order rate constants calculated from initial rate, pseudo first order rate constants are in good agreement (Table 2).

3.6. Effect of copper nanoparticles (Cunps) concentration

The effect of copper nanoparticles on the rate of oxidation of threonine has been studied at varying concentration 1.0×10^{-6}– 8.0×10^{-6} mol L^{-1} at three different nanoparticles, synthesized at three concentrations (0.08, 0.09, 0.10 mol L^{-1}) of ascorbic acid with an average size of 28, 16 and 12 nm respectively at a constant concentration of [PMS] = 3.0×10^{-3} mol L^{-1}, [Thr] = 5.0×10^{-2} mol L^{-1} at pH = 7.0 and temperature of 308 K. The rate of reaction increases with increasing concentration of copper nanoparticles. The pseudo first order rate constants as plotting against the concentration of copper nanoparticles yielded a straight line with non-zero intercept (Fig. 5), indicates simultaneously the uncatalyzed reaction. The catalytic activity of copper nanoparticles seems different when the concentration of the reducing agent is varied in the range of 0.08–0.1 mol L^{-1}. The difference in catalytic activity can be attributed to the size

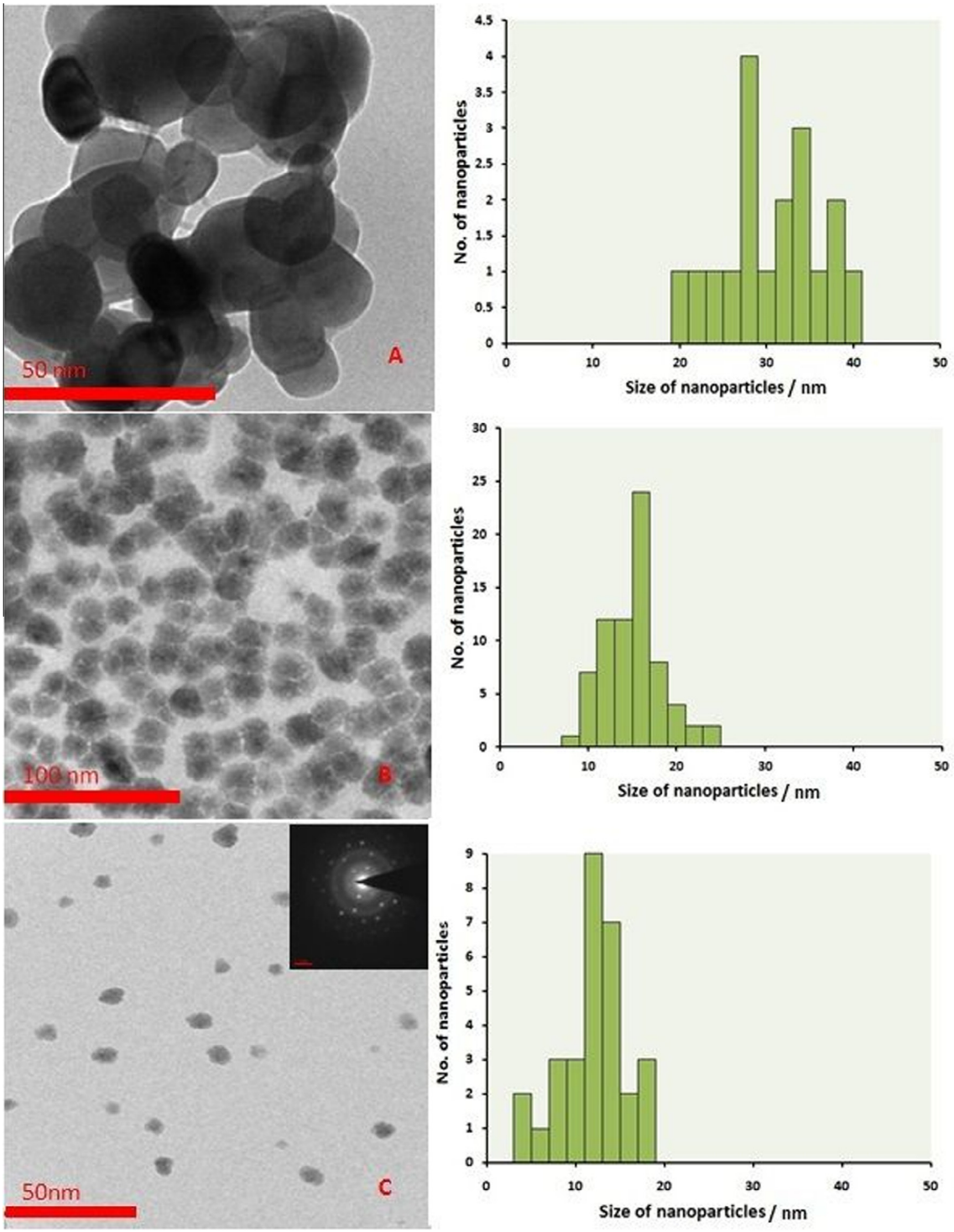

Figure 3 TEM images with a histogram of the synthesized copper nanoparticles with various concentrations of L-ascorbic acid: the average particle size is: (a) 0.08 mol L^{-1}, $d = 28$ nm (b) 0.09 mol L^{-1}, $d = 16$ nm (c) 0.10 mol L^{-1}, $d = 12$ nm.

variation in the resulting copper nanoparticles. The trend in the calculated rate constant being 12 > 16 > 28 nm. This effect can be attributed to the nanosize particles and as size decreases, surface area increases and the active center also increases.

3.7. Effect of pH

The oxidation of threonine reaction is pH sensitive. The rate of oxidation of threonine was studied at different pH viz. 4.0, 7.0, 9.5 respectively while other reactant and reaction conditions

Table 1 Stoichiometry of PMS and threonine in the presence of copper nanoparticles in aqueous medium.

S. No.	[PMS], mol L^{-1}	[Thr], mol L^{-1}	[Thr]/[PMS]
1	0.005	0.002	1:1
2	0.005	0.003	1:1
3	0.005	0.004	1:0.98
4	0.006	0.004	1:0.98

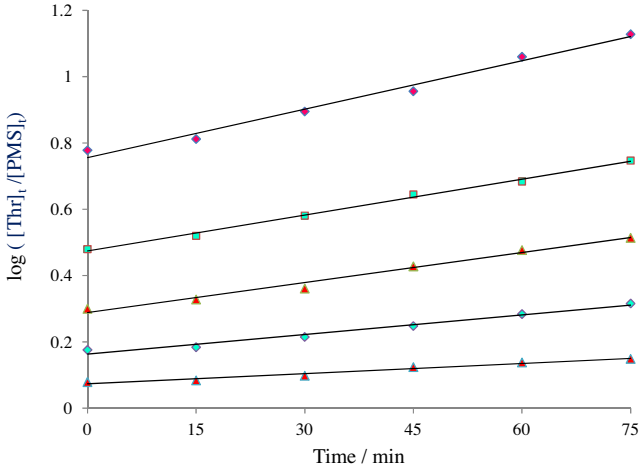

Figure 4 Second order plots. [Thr] = 6.0×10^{-3} mol L^{-1}, [Cunps] = 5.0×10^{-6} mol L^{-1}, pH = 7.0, Temp. = 308 K, [PMS] $\times 10^{-3}$ mol L^{-1} = (A) 1.0, (B) 2.0, (C) 3.0, (D) 4.0, (E) 5.0.

were constant. The rate constants obtained are 1.65×10^{-3}, 1.8×10^{-3}, 1.3×10^{-3} s^{-1} respectively. The optimum pH giving the maximum rate constant was found to be 7.0.

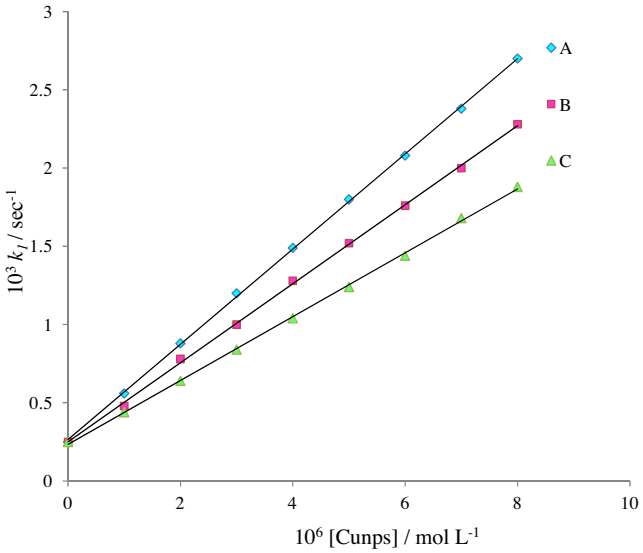

Figure 5 The effect of [Cunps] at different size of Cunps (A) 12 nm, (B) 16 nm, (C) 28 nm at fixed [PMS] = 3.0×10^{-3} mol L^{-1}, [Thr] = 5.0×10^{-2} mol L^{-1}, pH = 7.0 at 308 K temperature.

3.8. Effect of ionic strength

The rate of reaction was unaffected by the variation of concentration of KNO_3. In this study, threonine is neutral and therefore no change in rate constants is expected in the presence of electrolyte. From these results we conclude that HSO_5^- and threonine (neutral) are the reactive forms of peroxomonosulfate and threonine respectively.

Table 2 Initial rate (rate), pseudo first order rate constants (k_1) and second order rate constant (k_2) in the reaction of threonine with peroxomonosulfate in the presence of copper nanoparticles ([Cunps] = 5.0×10^{-6} mol L^{-1}) in aqueous medium at temp. 308 K and pH = 7.0.

S. No.	10^3 [PMS] (mol L^{-1})	10^3 [Thr] (mol L^{-1})	10^7 rate (mol L^{-1} s^{-1})	10^3 k_1 (s^{-1})	10^2 k_2 (L mol^{-1} s^{-1})
1	1.0	6.0	1.80	–	3.61 (3.58)
2	2.0	6.0	3.58	–	3.61 (3.41)
3	3.0	6.0	5.32	–	3.59 (3.63)
4	4.0	6.0	7.20	–	3.62 (3.58)
5	5.0	6.0	8.90	–	3.60 (3.58)
6	3.0	5.0	5.40	–	3.60
7	3.0	6.0	6.42	–	3.58
8	3.0	7.0	7.45	–	3.55
9	3.0	8.0	8.40	–	3.60
10	3.0	9.0	9.54	–	3.56
11	3.0	10.0	10.07	–	3.58
12	3.0	30.0	–	1.08	3.60
13	3.0	35.0	–	1.25	3.57
14	3.0	40.0	–	1.42	3.55
15	3.0	45.0	–	1.62	3.60
16	3.0	50.0	–	1.81	3.62
17	3.0	55.0	–	1.95	3.54
18	3.0	60.0	–	2.14	3.56

Results in parenthesis were derived from initial rates.

Please cite this article in press as: S. Jain et al., Copper nanoparticles catalyzed oxidation of threonine by peroxomonosulfate, Journal of Saudi Chemical Society (2016), http://dx.doi.org/10.1016/j.jscs.2015.12.004

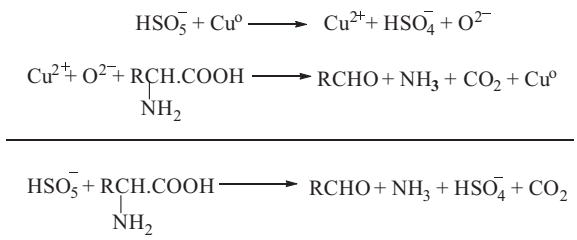

Scheme 1 The plausible route of copper nanoparticles catalyzed oxidation of threonine.

3.9. Effect of temperature

The reactions were studied at three different temperatures (303, 308, 313 K) at a constant concentration of [Thr] = 5.0×10^{-2} mol L^{-1}, [PMS] = 3.0×10^{-3} mol L^{-1}, [Cunps] = 5.0×10^{-6} mol L^{-1} and pH = 7.0. The rate of reaction increases with increasing temperature. A plot of log k_2 (mol^{-1} L s^{-1}) was made against $1/T$ that yielded a straight line. The energy of activation (E_a) was calculated from the slope of the line to be 21.57 ± 0.08 kJ mol^{-1}. The entropy of activation was calculated by employing the relationship [34],

$$k = \frac{k_B T}{h} \times e^{-\Delta H^{1}/RT} \cdot e^{\Delta S^{1}/R}$$

where $\Delta S^{\neq}$ is entropy of activation and other terms have their usual significance. Thus entropy of activation was calculated to be −191.99 ± 4 J K^{-1} mol^{-1}.

3.10. Mechanism

Threonine is a neutral amino acid. Then, the probability of initial interaction between threonine and peroxomonosulfate is low. The deamination of the amino group in threonine to NH_3 occurs in the presence of copper nanoparticles by peroxomonosulfate, while peroxomonosulfate is changed into the hydrogen sulfate ion. A definite mechanism of copper nanoparticle catalyzed oxidation of threonine is not clear, based on previous reports [14] and present observations on the catalytic cycle are shown in Scheme 1.

4. Conclusions

In the present study, highly stable dispersed copper nanoparticles were synthesized in aqueous medium without employing any protecting inert gas. By this green method, synthesis of monodispersed copper nanoparticles (ranging from 12 to 28 nm) was obtained using different concentrations of reducing agent. L-ascorbic acid is used as a reducing agent and antioxidant. The catalytic activity of synthesized copper nanoparticles was investigated by the oxidation of threonine in aqueous medium. Increasing the size of copper nanoparticles decreases the catalytic activity of copper nanoparticles. The results of this study indicate that the reaction between threonine and peroxomonosulfate in the presence of Cunps is second-order.

Acknowledgements

The authors gratefully acknowledge the support of Department of Science and Technology sponsored FIST Laboratory of our institution for experimental work and the University of Rajasthan, Jaipur for characterization of nanoparticles samples i.e. SEM and TEM.
This work was supported in this part by University Grant Commission, New Delhi through a Junior Research Fellowship.

Appendix A. Supplementary data

Supplementary data associated with this article can be found, in the online version, at http://dx.doi.org/10.1016/j.jscs.2015.12.004.

References

[1] A. Tiwari, S.K. Shukla, in: Advanced Carbon Materials and Technology, WILEY-Scrivener Publishing LLC, USA, 2014; A. Tiwari, Intelligent nanomaterials for prospective nanotechnology, Adv. Mater. Lett. 3 (2012) (1-1).
[2] P. Singh, A. Katyal, R. Kalra, R. Chandra, Copper nanoparticles in an ionic liquid: an efficient catalyst for the synthesis of bis-(4-hydroxy-2-oxothiazolyl) methanes, Tetrahedron Lett. 49 (2008) 727–730.
[3] T.M.D. Dang, T.T.T. Le, M.C. Fribourg-Blanc Dang, Synthesis and optical properties of copper nanoparticles prepared by a chemical reduction method, Adv. Nat. Sci. Nanosci. Nanotechnol. 2 (2011) 015009–015015.
[4] V.L. Colvin, M.C. Schlamp, A.P. Alivisatos, Light-emitting diodes made from cadmium selenide nanocrystals and a semiconducting polymer, Nature 370 (1994) 354–357.
[5] J.C.Y. Lee, K.J. Lee, N.E. Stott, D. Kim, Large-scale synthesis of copper nanoparticles by chemically controlled reduction for applications of inkjet-printed electronics, Nanotechnology 19 (2008) 415604–415609.
[6] Q. Liu, R.L. Yu, G.Z. Qiu, Z. Fang, A.L. Chen, Z.W. Zhao, Optimization of separation processing of copper and iron of dump bioleaching solution by Lix 984N in dexing copper mine, Trans. Nonferrous Met. Soc. China 18 (2008) 1258–1261.
[7] A. Umer, S. Naveed, N. Ramzan, M.S. Rafique, Selection of a suitable method for the synthesis of copper nanoparticles, Nano 7 (2012) 1230005–1230023.
[8] W. Yu, H. Xie, L. Chen, Y. Li, C. Zhang, Synthesis and characterization of monodispersed copper colloids in polar solvents, Nanoscale Res. Lett. 4 (2009) 465–470.
[9] A. Umer, S. Naveed, N. Ramzan, M.S. Rafique Imran, A green method for the synthesis of copper nanoparticles using L-ascorbic acid, Materia-Rio De Janeiro 19 (2014) 197–203.
[10] B.L. Preston, H.M. Alexander, T.R. Carlos, J.G. Jose, R. Lal, Facile, green synthesis of large single crystal copper micro and nanoparticles with ascorbic acid and gum, Arabic Open J. Appl. Sci. 3 (2013) 332–336.
[11] M. Yadav, V. Devra, A. Rani, Kinetics and mechanism of silver (I) catalysed oxidation of valine by cerium (IV) in acid perchlorate medium, J. Indian Chem. Soc. 49 (2010) 442–447.
[12] M. Sundar, D. Easwaramoorthy, S. Kutti Rani, I.M. Bilal, Mn (II) catalysed decomposition of peroxomonosulphate – kinetic and mechanistic study, Catal. Commun. 9 (2008) 2340–2344.

[13] M.A.A. Khalid, Oxidative kinetics of amino acids by peroxydisulphate: effect of dielectric constant, Arabian J. Sci. Eng. 33 (2007) 199–210.
[14] V. Devra, Kinetics and mechanism of electron transfer reactions in aqueous solutions: silver (I) catalyzed oxidation of alanine by cerium (IV) in acid perchlorate medium, J. Indian Chem. Soc. 82 (2005) 290–294.
[15] S. Mathur, M.B. Yadav, V. Devra, Kinetics and mechanism of uncatalyzed and Ag (I) catalyzed oxidation of hydroxylysine by cerium (IV) in acid medium, J. Phys. Chem. Biophys. 3 (2013) 128–133.
[16] A. Goel, S. Sharma, A kinetic study on the oxidation of glycine by hexacyanoferrate (III) ions in presence of iridium nanoparticles, J. Chem. Biol. Phys. Sci. 2 (2012) 628–636.
[17] J. Sanathanlakshmi, P. Vankatesan, Kinetic of oxidation of L-leucine by mono- and bimetallic gold and silver nanoparticles in hydrogen peroxide solution, Chin. J. Catal. 3 (2012) 1306–1311.
[18] L. Parimala, J. Santhanalakshmi, Studies on the oxidation of α-amino acids by peroxomonosulphate catalysed by biopolymers stabilized copper nanoparticles – effect of stabilizers, Nanosci. Nanotechnol. 3 (2013) 4–11.
[19] D. Laloo, M.K. Mahanti, Kinetics of oxidation of amino acids by alkaline hexacyanoferrate (III), J. Chem. Soc., Dalton Trans, 1 (1990) 311–313.
[20] D. Gupta, M. Bhasin, V. Devra, I. Sharma, P.D. Sharma, Kinetics and mechanism of electron transfer reactions in aqueous solutions: silver (I) catalyzed oxidation of glutamic acid by cerium (IV) in acid perchlorate medium, Oxid. Commun. 19 (1996) 242–250.
[21] S. Debey, S. Hemkar, C.L. Khandelwal, P.D. Sharma, Kinetics and mechanism of oxidation of hypophosphorous acid by peroxomonosulphate in acid aqueous medium, Inorg. Chem. Commun. 5 (2002) 903–908.
[22] A. Nasirian, Synthesis and characterization of Cu nanoparticles and studying of their catalytic properties, Int. J. Nano Dimension 2 (2012) 159–164.
[23] L.N. Lewis, N. Lewis, Platinum-catalyzed hydrosilylation – colloid formation as the essential step, J. Am. Chem. Soc. 108 (1986) 7228–7231;
L.N. Lewis, R. Uriarte, Hydrosilylation catalyzed by metal colloids: a relative activity study, J. Organomet. 9 (1990) 621–625.
[24] H. Hirai, H. Komiyama, Catalytic hydration of unsaturated nitriles to unsaturated amides using colloidal copper dispersion, Bull. Chem. Soc. Jpn. 59 (1986) 545–550.
[25] M. Spiro, Catalysis by noble metals of redox reaction in solution, Catal. Today 17 (1993) 517–525.
[26] G. Maayan, R. Neumann, Direct aerobic oxidation of secondary alcohols catalysed by Pt(0) nanoparticles stabilized by $PV_2Mo_{10}O_{40}^{5-}$ polyoxmetalate, Catal. Lett. 123 (2008) 41–45.
[27] J. Mendham, R.C. Denney, J.D. Barnes, M.J.K. Thomas, Vogel's Textbook of Quantitative Chemical Analysis, sixth ed., Pearson Education, Harlow, U.K., 2004.
[28] J. Xiong, Y. Wang, Q. Xue, X. Wu, Synthesis of highly stable dispersion of nanosized copper particles using L-ascorbic acid, Green Chem. 13 (2011) 900–904.
[29] S. Kapoor, R. Joshi, T. Mukherjee, Influence of I-anions on the formation and stabilization of copper nanoparticles, Chem. Phys. Lett. 354 (2002) 443–452.
[30] H.X. Zhang, U. Siegert, R. Liu, W.B. Cai, Facile fabrication of ultrafine copper nanoparticles in organic solvent, Nanoscale Res. Lett. 4 (2009) 705–708.
[31] C.W. Wu, B.P. Mosher, T.F. Zeng, Z.L. Yin, One step green route to narrowly dispersed copper nanocrystals, J. Nanopart. Res. 8 (2006) 965–969.
[32] R.C. Kerber, As simple as possible, but not simpler – the case of dehydroascorbic acid, J. Chem. Educ. 85 (2008) 1237–1242.
[33] R.M. Thombare, G.S. Gokavi, Kinetics and mechanism of oxidation of glycine and alanine by oxone® catalyzed by bromide ion, J. Braz. Chem. Soc. (2014) 1–7.
[34] K.J. Laidler, Reaction Kinetics, Pergamon Press, Oxford, 1983.

Please cite this article in press as: S. Jain et al., Copper nanoparticles catalyzed oxidation of threonine by peroxomonosulfate, Journal of Saudi Chemical Society (2016), http://dx.doi.org/10.1016/j.jscs.2015.12.004

Available online at www.sciencedirect.com
ScienceDirect
Trans. Nonferrous Met. Soc. China 25(2015) 3995−4000
Transactions of Nonferrous Metals Society of China
www.tnmsc.cn

Synthesis and size control of copper nanoparticles and their catalytic application

Shikha JAIN[1], Ankita JAIN[1], Pranav KACHHAWAH[2], Vijay DEVRA[1]

1. Department of Chemistry, J.D.B. Govt. Girls P.G. College, Kota, Rajasthan 324001, India;
2. Institution of Chemical Technology, Matunga, Mumbai, Maharashtra 400019, India

Received 24 January 2015; accepted 18 June 2015

Abstract: The synthesis and catalytic properties of copper nanoparticles (Cunps) were reported using L-ascorbic acid as reducing and capping agent in aqueous medium. The effect of different concentrations of L-ascorbic acid on the particle size of Cunps was investigated. The synthesized Cunps were characterized by UV-Visible spectrophotometer, scanning electron microscopy (SEM), transmission electron microscopy (TEM) and Fourier transform infrared (FTIR) spectrophotometer. The result indicates that the size of copper nanoparticles decreases with the increase in concentration of L-ascorbic acid. L-Ascorbic acid plays an important role to protect the copper nanoparticles from oxidation and agglomeration which helps nanoparticles to get better stability for the application. The synthesized Cunps show excellent catalytic activity in the oxidation of serine (Ser) by peroxomonosulphate (PMS). The catalytic activity of Cunps increases with the decrease in size of Cunps. The Cunps are expected to be suitable alternative and play an imperative role in the fields of catalysis and environmental remediation.

Key words: copper nanoparticle; ascorbic acid; serine; peroxomonosulphate (PMS); oxidation; kinetics

1 Introduction

Major scientific interest targeting fabrication of metal nanoparticals of distinct shape and diminutive size has been developed in recent years because of their exclusive properties as compared to their bulk materials [1−3]. Metal nanoparticals with variety of shape and size allow exploring their fascination applications in fields like catalysis, electronics, sensor, and optical device [4−6]. Most of the unique properties of metal nanoparticals are a consequence of their nano-size scale regime. However, recently, MURPHY [7] has observed that properties of nano-materials are also influenced by their shape and size. Thus, special shaped nano-materials are the focus of the present scientific research. From the present literature perspective, development of suitable method for such nano-materials and their uses in various practical applications is an important task. Among all methods such as micro emulsions method [8], thermal decomposition method [9], laser ablation method [10] and aqueous chemical reduction method [11,12], aqueous reduction route is the most preferred for its simplicity, economical and ease of control over particle size and distribution with various experimental parameters [13−16]. The parameters such as temperature, reaction time, reducing agent, precursor type, concentration and even mixing, affect the nucleation, growth and agglomeration phenomena, consequently particle size distribution of nano-materials. Although UMER et al [17] reported that synthesis of copper nanoparticles has been carried via numerous routes, very less is known about the size dependent performance of copper nanoparticles as a suitable catalyst. The main question arises from stability of copper nanoparticles including the extreme sensitivity to oxygen and colloidal agglomeration. Therefore, there are several approaches related to the dispersion and oxidation resistance that needs to be solved before application. Some study reveals that to protect copper nanoparticles against oxidation, natural antioxidant ascorbic acid is utilized as reductant and antioxidant [18−20]. In the present investigation, the raw materials are same but synthesis routes have been changed, which result in the size variation of copper nanoparticles.

In this work, ascorbic acid (hydrogen potential of +0.08 V) can easily reduce metal ions with standard reduction potential higher than 0 V, such as Cu^{2+}, Ag^{+}, Au^{3+} and Pt^{4+} but cannot reduce these ions with potential less than 0 V such as Fe^{2+}, Co^{2+} and Ni^{2+}. Hydrogen free radicals released from ascorbic acid react rapidly with

Corresponding author: Vijay DEVRA; Tel: +91-7597747381; E-mail: v_devra1@rediffmail.com
DOI: 10.1016/S1003-6326(15)64048-1

hydroxyl free radicals and oxygen, whose existence is usually related to the oxidation of the nanoparticles, so our experiment was performed without inert gas protection, and pure copper nanoparticles were obtained.

The catalytic activity of synthesized copper nanoparticles was evaluated in the oxidation of serine by peroxomonosulphate in aqueous medium. The applications of transition metal nanoparticles as catalyst for many organic transformations [21−24]. Though studies on kinetics of oxidation of amino acid with peroxomonosulphate have been widely carried out [25,26], very few attempts have been made so far on the oxidative deamination of amino acid in the presence of metal nanoparticles [23]. So, we have attempted the synthesis of size controlled copper nanoparticles through a simple one phase aqueous route using ascorbic acid as reducing and capping agent and catalytic activities of these particles with different sizes have been tested on the oxidation of serine.

2 Experimental

2.1 Materials

Analytical grade chemicals such as copper chloride dihydrate ($CuCl_2·2H_2O$, purity of 97%) and L-ascorbic acid (vitamin C, purity of 98%) and serine obtained from E. Merck were used. Peroxomonosulphate (PMS) was obtained from Sigma-Aldrich under the trade name "Oxone". A fresh solution of Oxone was prepared before starting the experiments. Remaining chemicals used were of analytical grade without any further treatment. Double distilled water was employed throughout the study.

2.2 Synthesis of copper nanoparticles

The one step synthesis scheme of copper nanoparticles initiates with dissolving copper chloride dihydrate (0.02 mol/L) in deionized water to obtain a blue solution. L-ascorbic acid (0.1 mol/L) was dropwise added to the aqueous solution of copper salt with vigorous stirring at 353 K in oil bath. With the passage of time, the color of dispersion gradually changed from white, yellow, orange, brown finally to dark brown with a number of intermediate stages. The appearance of yellow color followed by orange color indicated the formation of fine nanoscale copper particles from L-ascorbic acid assisted reduction. The resulting dispersion was centrifuged for 15 min. The supernatant was placed under ambient conditions for two months. The studies were performed at different concentrations of ascorbic acid to investigate the size and shapes of copper nanoparticles.

2.3 Characterization

UV-Visible spectroscopy from a double beam spectrophotometer (UV 3000$^+$ LABINDIA, path length 1.0 cm, spectral range from 200 nm to 800 nm) was used for preliminary estimation of copper nanoparticles synthesis. FTIR (ALPHA-T, Bruker) provided information about the binding interactions of L-ascorbic acid with zero valent copper particles. Morphological study of the copper nanoparticles was carried out with SEM (EVO 18, Carl Zeiss) image analysis. These dispersed nanoparticles were centrifuged and ultrasonicated for 40 min. 30 μL aliquots were then extracted and deposited on stub for SEM analysis. Ultrasonicated dispersed suspension was mounted on carbon coated copper grid and TEM (FEI Techni G2S2 Twin) images were recorded to confirm size distribution and shape homogeneity of synthesized copper nanoparticles.

3 Results and discussion

3.1 Metal nanoparticles characterization results

UV-Visible absorbance spectroscopy has proved to be a very useful technique for studying metal nanoparticles because the peak position and shapes are sensitive to particle size. During the synthesis of copper nanoparticles in aqueous solution, the UV-Visible spectra of samples were recorded at different time intervals for every color change presented in Fig. 1.

The solution becomes colorless when L-ascorbic acid was added and turned to yellow, orange, brown and finally dark brown. Initially, there was no absorption peak, the absorption peak can be observed after two hours of reaction. There was an intensity increase with the reaction progressing, this was due to the growth

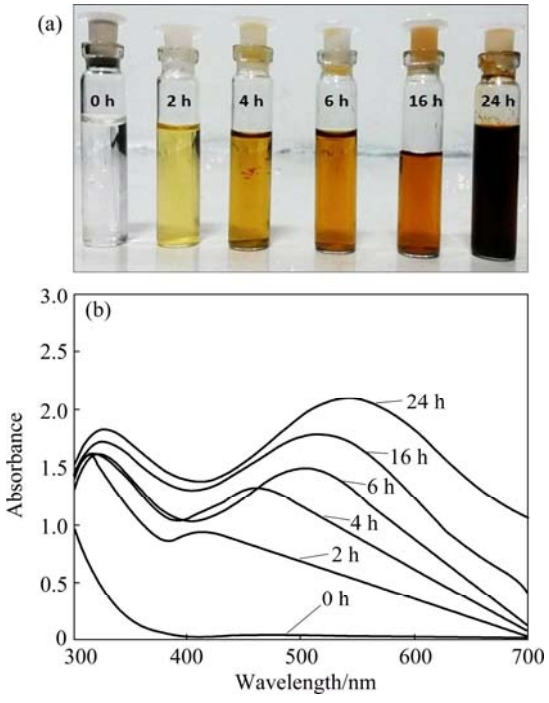

Fig. 1 Dispersion photographs (a) and UV-Visible spectra (b) of samples at different time intervals

of copper nanoparticles. The synthesis process was completed after 24 h.

The effect of L-ascorbic acid concentrations (0.08, 0.09 and 0.10 mol/L) on the UV-Visible absorbance spectroscopy of the synthesized copper nanoparticles is shown in Fig. 2. XIONG et al [27] observed that the first absorption peak of different curves was at 335 nm corresponding to oxidation product of L-ascorbic acid. The red shift of second absorption peak increases with an increasing concentration of L-ascorbic acid. The absorption peak of copper nanoparticles has been reported at around 560 nm which proves the formation of copper nanoparticles [28,29]. In this work, the resulting copper nanoparticles show a broadened peak at this wavelength indicating the presence of small separated copper nanoparticles.

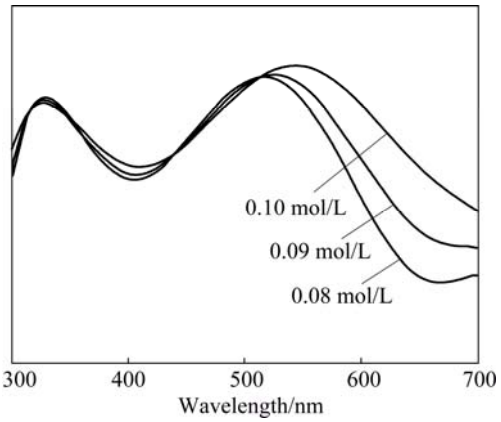

Fig. 2 UV-Visible absorption spectra of copper nanoparticles stabilized in L-ascorbic acid with various concentrations

The above result indicates that a higher L-ascorbic acid concentration leads to more effective capping capacity of L-ascorbic acid and then forms smaller Cu nanoparticles, which can also be proved by the TEM images with histograms of particle size distribution of synthesized copper nanoparticles presented in Fig. 3. The

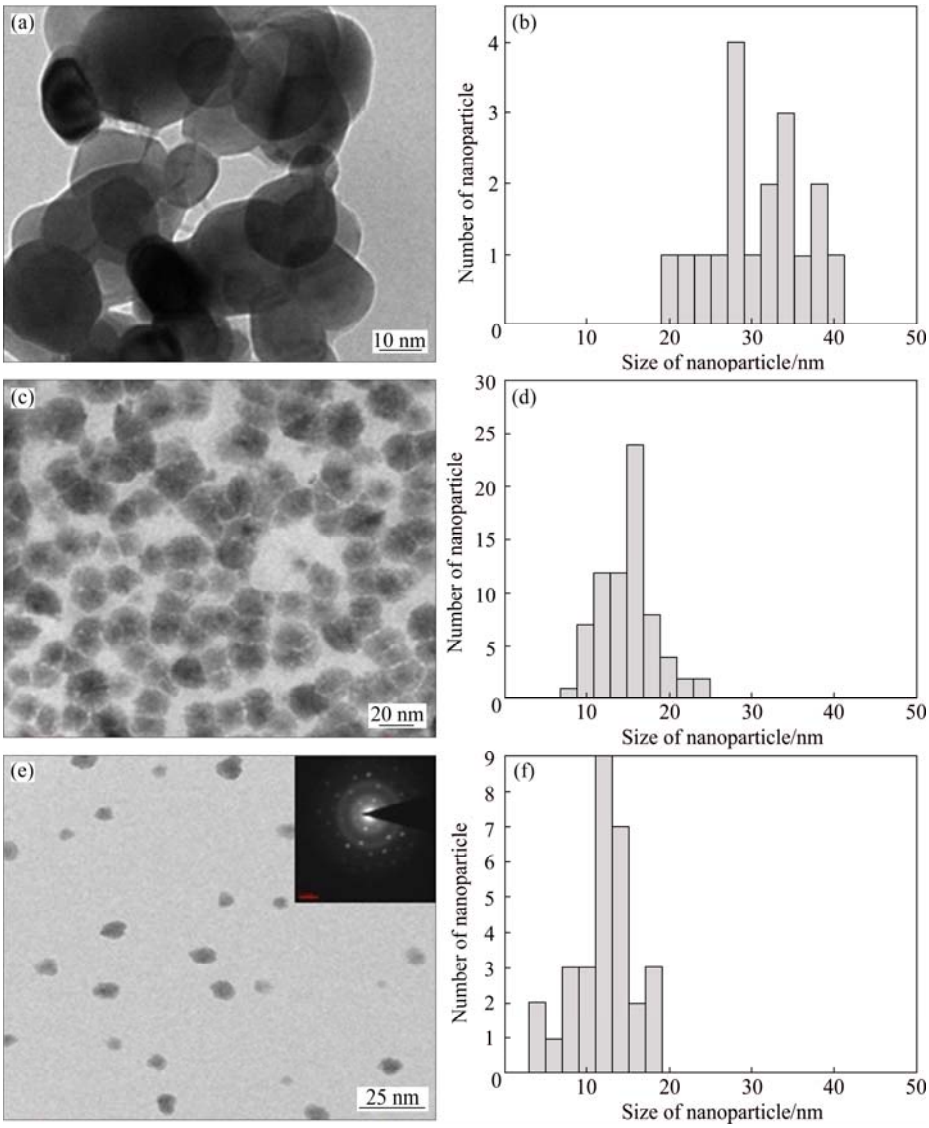

Fig. 3 TEM images with histogram of synthesized copper nanoparticles with various concentrations of L-ascorbic acid and average particle sizes: (a,b) 0.08 mol/L, *d*=28 nm; (c,d) 0.09 mol/L, *d*=16 nm; (e,f) 0.10 mol/L, *d*=12 nm

TEM images exhibit that the particles are spherical in shape. The histogram reveals that the size of copper nanoparticles decreases with increase in concentration of L-Ascorbic acid. The size of the copper nanoparticles at various concentrations (0.08, 0.09, 0.10 mol/L) of L-ascorbic acid are 28, 16, 12 nm respectively. The reason is that the number of Cu^{2+} encapsulated in ascorbic acid molecules decreases with increasing concentration of L-ascorbic acid, leading to the formation of smaller copper nanoparticles which is also confirmed by the SEM image of copper nanoparticles shown in Fig. 4. SEM image confirms that the nanoparticles are grown with well defined morphology and are almost spherical in shape. So, the optimal conditions for the synthesis are 0.02 mol/L concentration of $CuCl_2{\cdot}2H_2O$ and 0.10 mol/L concentration of L-ascorbic acid at 353 K.

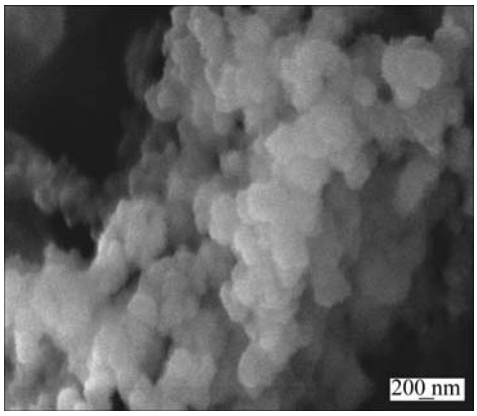

Fig. 4 SEM image of copper nanoparticles at optimal experimental conditions of $c(CuCl_2{\cdot}2H_2O)$=0.02 mol/L, c(L-ascorbic acid)=0.10 mol/L and 353 K

3.2 Stability of copper nanoparticles

The stability of nanoparticles dispersion is the key factor in their application. In this study, L-ascorbic acid was used as both reducing and capping agent without any other special capping agent. The photographs of dispersion before and after the storage (two months) are shown in Fig. 5.

During the synthesis process, excessive L-ascorbic acid is essential to avoid the oxidation of copper nanoparticles. WU et al [15] reported that the antioxidant property of L-ascorbic acid comes from its ability to scavenge free radicals and reactive oxygen molecules, accompanying the donation of electrons to give semi-dehydroascorbate radical and dehydroascorbic acid (Eq. (1)).

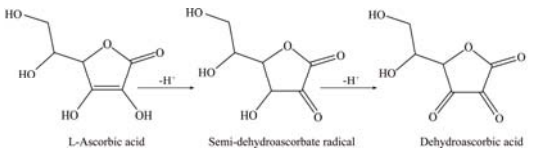

(1)

Fig. 5 Photos of dispersion of synthesized copper nanoparticles before (a) and after (b) two months of storage

The dehydroascorbic acid has three carbonyl groups in its structure. The 1, 2, 3 tricarbonyl is too electrophilic to survive for few seconds in aqueous solution. Finally, the polyhydroxyl structure is obtained through hydrolysis (Eq. (2)) [27].

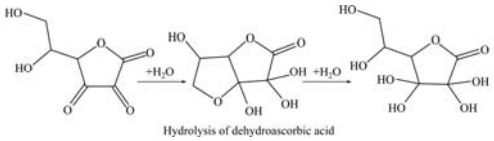

(2)

The extensive number of hydroxyl group can facilitate the complexation of copper nanoparticles to the molecular matrix by inter- and intra-molecular hydrogen bonding, and thus prevent the aggregation of copper nanoparticles. This result is consistent with that of FTIR analysis presented in Fig. 6.

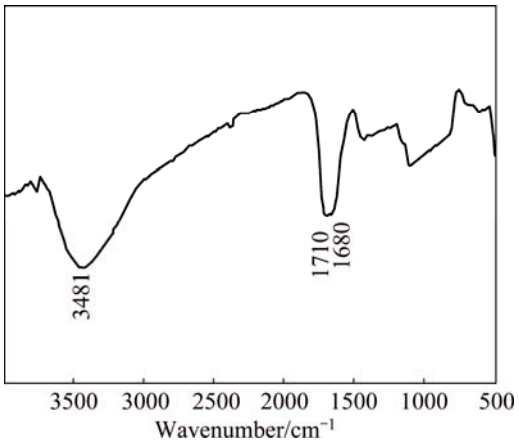

Fig. 6 FTIR spectrum of L-ascorbic acid stabilized copper nanoparticles

FTIR spectrum shows the peaks at 3481, 1710 and 1680 cm^{-1}. These peaks correspond to the hydroxyl, oxidated ester carbonyl groups and conjugated carbonyl groups, respectively. These results indicate the presence

of polyhydroxyl structure on the surface of copper nanoparticles. The polyhydroxyl structure has an excellent dispersion effect on copper nanoparticles. Therefore, L-ascorbic acid plays dual role as reducing agent and antioxidant of copper nanoparticles. Thus, reaction can be completed without any protective inert gas.

3.3 Catalytic activity of copper nanoparticles

The catalytic activity of synthesized copper nanoparticles was evaluated in the oxidation of serine by peroxomonosulphate (PMS). The deamination of L-serine studied by the decrease in absorbance of serine at 206 nm at different intervals of time is shown in Fig. 7. The effect of copper nanoparticles on the rate of oxidation of serine has been studied at varying concentrations (1×10^{-6}–10×10^{-6} mol/L) at three different nanoparticles, synthesized at three concentrations (0.08, 0.09 and 0.10 mol/L) of ascorbic acid with average sizes 28, 16 and 12 nm, respectively, at fixed c(PMS)=5×10^{-3} mol/L, c(Ser)=5×10^{-2} mol/L, $c(H^+)$=0.01 mol/L and 308 K. The rate of reaction increases with the increase in concentration of copper nanoparticles. The catalytic activity of copper nanoparticles seems different when concentration of reducing agent is varied from 0.08 to 0.10 mol/L. The difference in catalytic activity can be dependent on the size variation (28, 16, 12 nm) in the resulting copper nanoparticles, while keeping other reactant concentration and conditions constant, the catalytic activity depends on the size of copper nanoparticles. The trend of the rate constant (k_{obs}) with the size of nanoparticles is shown in Fig. 8. This effect can be attributed to the nanosize of the particles that surface area and the active center increase as particle size decreases.

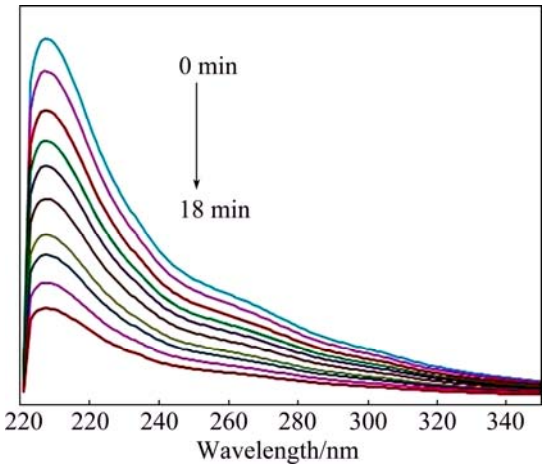

Fig. 7 UV spectra for deamination of L-serine at 206 nm in the presence of copper nanoparticles at fixed c(PMS)=5×10^{-3} mol/L, c(Cunps)=5×10^{-6} mol/L, $c(H^+)$=0.01 mol/L at 308 K

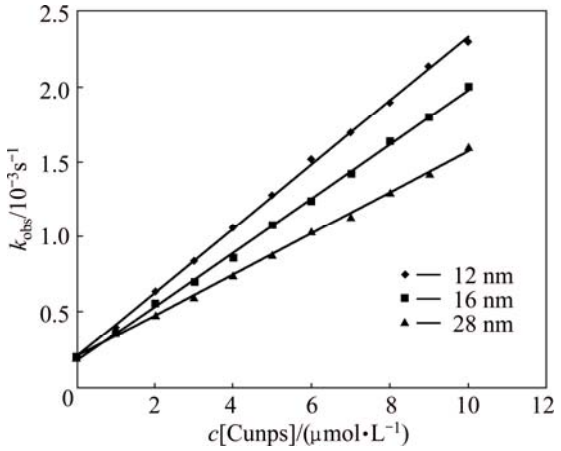

Fig. 8 Effect of c(Cunps) on oxidation of serine with different sizes of 12 nm (a), 16 nm (b), 28 nm (c) at fixed c(PMS)=5.0×10^{-3} mol/L, c(Ser)=5.0×10^{-2} mol/L, $c(H^+)$=0.01 mol/L and 308 K

4 Conclusions

1) Monodispersed copper nanoparticles (range 12−28 nm) employing different concentrations of L-ascorbic acid were synthesized by green method.

2) The characterization results indicate that a higher L-ascorbic acid concentration leads to more effective capping capacity and then forms smaller copper nanoparticles. FTIR spectra show the presence of polyhydroxyl structure on the surface of the copper nanoparticle that gives an excellent dispersion effect on copper nanoparticles.

3) The experimental investigation indicates that the optimal conditions for the synthesis are 0.02 mol/L concentration of $CuCl_2{\cdot}2H_2O$ and 0.10 mol/L concentration of L-ascorbic acid at 353 K.

4) The catalytic activity of synthesized copper nanoparticles was investigated in the oxidation of serine in aqueous acidic medium. The study reveals that the size of copper nanoparticles decreases as the catalytic activity of copper nanoparticles increases.

References

[1] MALLICK K, WITCOMB M J, SCURRELL M S. Preparation and characterization of a conjugated polymer and copper nanoparticle composite material: A chemical synthesis route [J]. Materials Science and Engineering B, 2005, 123: 181−186.

[2] DAS R, NATH S S, BHATTACHARJEE R. Luminescence of copper nanoparticles [J]. Journal of Luminescence, 2011, 131: 2703−2706.

[3] ABDULLA-AL-MAMUN M, KUSUMOTO Y, MURUGANANDHAM M. Simple new synthesis of copper nanoparticles in water/acetonitrile mixed solvent and their characterization [J]. Materials Letters, 2009, 63: 2007−2009.

[4] CUENYA B R. Synthesis and catalytic properties of metal nanoparticles: Size, shape, support, composition, and oxidation state effect [J]. Thin Solid Films, 2010, 518: 3127−3150.

[5] LI Y, QIAN F, XIANG J, CHARLES M L. Nanowire electronics and opteoelectronics devices [J]. Material Today, 2006, 9: 18−27.
[6] FELDHEIM D L, FOSS C A. Metal nanoparticles: Synthesis, characterization and applications [M]. New York, USA: Marcel Dekker Incorporated, 2002.
[7] MURPHY N R J C J. Controlling the aspect ratio of inorganic nanorods and nanowires [J]. Advanced Materials, 2002, 14: 80−82.
[8] SOLANKI J N, SENGUPTA R, MURTHY Z V P. Synthesis of copper sulphide and copper nanoparticles with microemulsion method [J]. Solid State Sciences, 2010, 12: 1560−1566.
[9] KIM Y H, KANG Y S, LEE W J. Synthesis of cu nanoparticles prepared by using thermal decomposition of cuoleate complex [J]. Molecular Crystals and Liquid Crystals, 2006, 445: 231−238.
[10] YAN R B Z, DINU C Z, HUANG Y, CARUSO A N, CHRISEY D B. Laser ablation induced agglomeration of Cu nanoparticles in sodium dodecyl sulfate aqueous solution [J]. Journal of Optoelectronics and Advanced Materials, 2010, 12: 437−439.
[11] LIU Q M, YASUNAMI T, KURUDA K, OKIDO M. Preparation of Cu nanoparticles with ascorbic acid by aqueous solution reduction method [J]. Transactions of Nonferrous Metal Society of China, 2012, 22(9): 2198−2203.
[12] ZHANG Qiu-li, YANG Zhi-mao, DING Bing-jun, LAN Xin-zhe, GUO Ying-juan. Preparation of copper nanoparticles by chemical reduction method using potassium borohydride [J]. Transactions of Nonferrous Metal Society of China, 2010, 20(S1): s240−s244.
[13] LIU Qing-ming, YU Run-lan, QIU Guan-zhou, FANG Zheng, CHEN Ai-liang, ZHAO Zhong-wei. Optimization of separation processing of copper and iron of dump bioleaching solution by Lix 984N in Dexing Copper Mine [J]. Transactions of Nonferrous Metal Society of China, 2008, 18(5): 1258−1261.
[14] YU W, XIE H, CHEN L, LI Y, ZHANG C. Synthesis and characterization of monodispersed copper colloids in polar solvents [J]. Nanoscale Research Letters, 2009, 4: 465−470.
[15] WU C, MOSHER B P, ZENG T. One-step green route to narrowly dispersed copper nanocrystals [J]. Journal of Nanoparticle Research, 2006, 8: 965−969.
[16] SHERAZI S T H, SOOMRO R A, UDDIN S, MEMON N. Synthesis and characterizations of highly efficient copper nanoparticles and their use in ultra fast catalytic degradation of organic dyes [J]. Advanced Materials Research, 2014, 829: 93−99.
[17] UMER A, NAVEED S, RAMZAN N, RAFIQUE M S. Selection of a suitable method for the synthesis of copper nanoparticles [J]. Nano, 2012, 7: 1230005−1230023.
[18] YU W, XIE H, CHEN L, LI Y, ZHANG C. Synthesis and characterization of monodispersed copper colloids in polar solvents [J]. Nanoscale Research Letters, 2009, 4: 465−470.
[19] UMER A, NAVEED S, RAMZAN N, RAFIQUE M S, IMRAN M. A green method for the synthesis of copper nanoparticles using L-ascorbic acid [J]. Materia-Rio De Janeiro, 2014, 19: 197−203.
[20] ZHOU J C, HE W, TANG Y, HU Y S. Synthesis of well-dispersed copper nanoparticles by L-ascorbic acid in diethyleneglycol [J]. Advanced Materials Research, 2012, 549: 378−381.
[21] MAAYAN G, NEUMANN R. Direct aerobic oxidation of secondary alcohols catalysed by Pt (0) nanoparticles stabilized by $PV_2Mo_{10}O_{40}^{5-}$ polyoxmetalate [J]. Catalysis Letters, 2008, 123: 41−45.
[22] GOEL A, SHARMA S. A kinetic study on the oxidation of glycine by hexacyanoferrate (III) ions in presence of iridium nanoparticles [J]. Journal of Chemical, Biological and Physical Sciences, 2012, 2: 628−636.
[23] SANATHANLAKSHMI J, VANKATESAN P. Kinetic of oxidation of L-leucine by mono- and bimetallic gold and silver nanoparticles in hydrogen peroxide solution [J]. Chinese Journal of Catalysis, 2012, 33: 1306−1311.
[24] SOOMRO R A, SHERAZI S T H, SIRAJUDDIN1, MEMON N, SHAH M R, KALWAR N H, HALLAM K R, SHAH A. Synthesis of air stable copper nanoparticles and their use in catalysis [J]. Advanced Material Letters, 2014, 5: 191−198.
[25] THOMBARE M R, GOKAVI G S. Kinetics and mechanism of oxidation of glycine and alanine by oxone catalyzed by bromide ion [J]. Journal of Brazilian Chemical Society, 2014, 0: 1−7.
[26] SUNDAR M, EASWARAMOORTHY D, KUTTI RANI S, PALANICHAMY M. Mechanistic investigation of the oxidation of lysine by oxone [J]. Journal of Solution Chemistry, 2007, 36: 1129−1137.
[27] XIONG J, WANG Y, XUE Q, WU X. Synthesis of highly stable dispersion of nanosized copper particles using L-ascorbic acid [J]. Green Chemistry, 2011, 13: 900−904.
[28] KAPOOR S, JOSHI R, MUKHERJEE T. Influence of I-anions on the formation and stabilization of copper nanoparticles [J]. Chemical Physics Letters, 2002, 354: 443−452.
[29] ZHANG H X, SIEGERT U, LIU R, CAI W B. Facile fabrication of ultrafine copper nanoparticles in organic solvent [J]. Nanoscale Research Letter, 2009, 4: 705−708.

铜纳米颗粒的制备、尺寸控制及催化应用

Shikha JAIN[1], Ankita JAIN[1], Pranav KACHHAWAH[2], Vijay DEVRA[1]

1. Department Of Chemistry, J.D.B. Govt. Girls P.G. College, Kota, Rajasthan, 324001, India;
2. Institution of Chemical, Matunga, Mumbai, Maharashtra, 400019, India

摘　要：以维生素 C 为还原剂和覆盖剂，在水溶液中制备铜纳米颗粒，并研究其催化性能。研究不同维生素 C 浓度对铜纳米颗粒尺寸的影响。采用紫外−可见光分光光度计、扫描电子显微镜(SEM)、透射电子显微镜及傅里叶变换红外光谱计(FTIR)对所制备的铜纳米颗粒进行表征。结果表明，随着维生素 C 浓度的增加，铜纳米颗粒的尺寸减小。维生素 C 在防止纳米颗粒氧化和团聚过程中起重要作用，可帮助纳米颗粒在应用过程中保持较高的稳定性。所制备的铜纳米颗粒在 PMS 氧化丝氨酸过程中表现出优良的催化活性。铜纳米颗粒的催化活性随颗粒尺寸的减小而提高。铜纳米颗粒有望用于催化和环境修复领域并发挥重要作用。

关键词：铜纳米颗粒；维生素 C；丝氨酸；PMS；氧化；动力学

(Edited by Yun-bin HE)

Available online at www.pelagiaresearchlibrary.com

Pelagia Research Library

Advances in Applied Science Research, 2015, 6(6): 171-180

ISSN: 0976-8610
CODEN (USA): AASRFC

Synthesis and characterization of highly efficient copper nanoparticles and their catalytic application in oxidative kinetic study

Shikha Jain, Niharika Nagar and Vijay Devra

Department of Chemistry, J. D. B. Govt. P.G. Girls College, Kota, Rajasthan, India

---

ABSTRACT

In the present work, we described the synthesis of copper nanoparticles (Cunps) through a single route of chemical reduction method.The effect of different concentration of reducing agent andtemperature on the morphology of Cunps was investigated. The synthesized copper nanoparticles were characterized by UV-Visible spectrophotometer, Fourier Transform Infrared (FTIR) Spectroscopy, Scanning Electron Microscopy (SEM), Transmission Electron Microscopy (TEM) analysis. The average sizes of copper nanoparticles were found to be 12, 16, 28, 55 nm at different concentration of L-ascorbic acid.The kinetics of copper nanoparticles catalyzed oxidation of glycine (Gly) by peroxodisulphate(PDS) in aqueous medium at 308 K has been studied. The copper nanoparticles catalyst exhibited very good catalytic activity.Interestingly, it was found that, the catalytic activity depends on the size of nanoparticlesand the kinetics of the reaction was found to be first order with respect to peroxodisulphate and independent of glycine concentration. Addition of neutral salts shows a retarding effect.

Keywords: Copper nanoparticles, glycine, L-ascorbic acid, peroxodisulphate, oxidation, kinetics.

INTRODUCTION

Amino acids are the precursors of essential bio-molecules such as proteins, hormones, enzymes, etc. Amino acids derived largely from protein in the diet or degradation of intracellular proteins one the final class of biomolecules which oxidation makes a significant contribution to the generation of metabolic energy. They are liable to lose their amino functional groups by two pathways: transamination or oxidative deamination [1, 2]. The kinetic investigation on the oxidation of amino acids is of great importance both from chemical point of view and its bearing on the mechanism of amino acids metabolism [3].Amino acids can undergo many kinds of reactions, depending upon whether a particular amino acid contains non-polar substituent. The specific metabolic role of amino acid includes the biosynthesis of polypeptides, proteins and synthesis of nucleotides [4].Glycine is an essential amino acid classified as non-polar and forms active sites of enzymes and helps in maintaining proper conformation by keeping them in proper ionic states.Several kinetic studies on the oxidation of amino acids both in acid and alkaline medium and also in presence of metal and non-metal ions catalysts have been reported [5-8]. Aqueous solutions of amino acids have been oxidized by Mn(II) [9],($[Fe(CN)_6]^{3-}$) [10], Chloramines T [11], Peroxomonosulphate [12],Peroxodisulphate[13] etc. in both acid and alkaline media. The peroxodisulphate ion is one of the strongest oxidizing agents known in aqueous solution. The standard oxidation reduction potential is estimated to be -2.01V.

$$2\ SO_4^{2-} \longrightarrow S_2O_8^{2-} + 2e^-$$

The reactions involving this ion are generally very slow in the absence of suitable catalyst [14]. The most thoroughly investigated catalyst is Ag(I) ion although reaction involving Cu(II) and Fe(III) ions also have been studied [15]. Kinetics and mechanism of decarboxylation of amino acids by peroxo oxidants is an area of intensive research because peroxo oxidants are environmentally benign oxidants and do not produce toxic compounds during their reduction.

The applications of transition metal nanoparticles as catalyst for organic transformations include hydrogenation [16], hydrosilation[17] and hydration reaction of unsaturated organic molecules [18] as well as redox [19] and other electron transfer process. Among the metal nanoparticles, Copper nanoparticles (Cunps) are very attractive due to their heat transfer properties such as high thermal conductivity. Copper nanoparticles also have high surface area to volume ratio, low production cost, antibacterial potency and catalytic activity, optical and magnetic properties as compared to precision metals such as gold, silver or palladium. The main difficulty lies in their preparation and preservation as they oxidized immediately when exposed in air. Scientists are using different inert media such as Argon, Nitrogen[20-22] to overcome this oxidation problem also using reducing, capping or protecting agents for the reduction of copper salt used. Some reducing and capping agents are very expensive and also have toxic effects. Physical and chemical methods are two basic techniques for the synthesis of Copper nanoparticle. Vacuum vapor deposition [23], pulsed laser ablation [24], pulsed wire discharge [25] and mechanical milling [26] are physical techniques while Chemical reduction [27], Micro emulsion techniques[28], sonochemical reduction [29], Electrochemical [30], Microwave assisted [31], and hydrothermal [32] are chemical approaches for the synthesis of nanoparticles. Biological or biosynthesis [33] techniques are also considered as chemical methods. Copper nanoparticles have high thermal conductivity [34] and also the production cost is very low as compare to noble metals. Copper nanoparticles production using chemical reduction method gives good results and it has simple control on the size and shape of particles under controlled parameters like concentration of reducing agent, temperature etc. but use of hazardous reducing and costly and protecting agent [35-41] makes the process toxic in some cases. To avoid the toxicity and to prepare Copper nanoparticles in green environment, we have used ascorbic acid in our chemical reduction process. Ascorbic acid works both as reducing and protecting agent, which makes the process economical, nontoxic and environment friendly [34]. Though studies on kinetics of oxidation of amino acid with peroxodisulphate have been widely carried out [42, 43], but in the present study, the universal nature of copper nanoparticles as catalysts was highlighted by employing highly efficient copper nanoparticles for the oxidation of glycine by peroxodisulphate in aqueous medium.

MATERIALS AND METHODS

Material

For the present work, we used analytical grade chemicals such as copper chloride dihydrate ($CuCl_2.2H_2O$-97%), L-ascorbic acid (vitamin C-98%), glycine and peroxodisulphate were obtained from E. Merck. A fresh solution of peroxodisulphate was prepared before starting the experiments. All chemicals were used as received without further purification. Double distilled water was employed throughout the study.

Synthesis of Copper Nanoparticles

The one step synthesis scheme for copper nanoparticles initiates with dissolving require amount of copper chloride dihydrate in 50 ml deionized water to obtain a blue solution. L-ascorbic acid (0.01 mol L^{-1}) drop wise added to the aqueous solution of copper salt while vigorously stirring at 353 K in oil bath. With the passage of time, the colour of dispersion gradually changed from white, yellow, orange, brown finally dark brown with a number of intermediate stages. The appearance of yellow colour followed by orange colour indicated the formation of fine nanoscale copper particles from L-ascorbic acid assisted reduction, finally changed into brown color the resulting dispersion was centrifuged for 15 minutes. The supernatant was placed under ambient conditions for 2 months. The studies were performed at different concentration of ascorbic acid to investigate the size and shapes of copper nanoparticles.

Characterization

UV-Visible spectroscopy from a double beam spectrophotometer (U.V. 3000^+ LABINDIA) was used for preliminary estimation of copper nanoparticles synthesis. FTIR (ALPHA-T –Bruker) provided information about oxidation product of the reaction. Morphological study of the copper nanoparticles was carried out with scanning electron microscope (SEM) (EVO 18 carlzeiss) and Transmission electron microscope (TEM) (FEI Techni G2S2 Twin). TEM and SEM images were recorded to confirm size distribution and shape homogeneity of synthesized copper nanoparticles.

Kinetic Measurements

All reactions were carried out in Erlenmeyer flasks painted black from the outside to check photochemical decomposition. Calculated volumes of copper nanoparticles and glycine were taken in a reaction vessel and were put in a thermostat maintained at 308K. To start the reaction the calculated quantities of potassium peroxodisulphate solution were added to the reaction flasks. The progress of the reaction was studied by estimating the remaining peroxodisulphate iodometrically at different interval of time. Since the concentration of amino acid is ten times more than that of the peroxodisulphate, a pseudo first order plots is drawn from which the values of k_{obs} is determined.

RESULTS AND DISCUSSION

Copper Nanoparticles Characterization Results

In recent years, several studies have shown that optical properties of metal nanoparticles depend upon the geometry and size, thus the optical response of metal nanoparticles can be control shape and size of metal nanoparticles [44].Since surface Plasmon modes of metal nanoparticles like Au, Ag, Cu reside within the optical region of electromagnetic spectrum [45, 46], optical spectroscopy can be used as primary tool for investigation of such nanoparticles. UV-visible spectral profile for copper nanoparticles was recorded with time. During the synthesis of copper nanoparticles in aqueous solution, the dispersion became colourless when L-ascorbic acid was added, and gradually turned to yellow, orange, brown and finally change into dark brown solution. The UV-Visible spectra of samples were recorded at different time intervals for every colour (Figure 1).

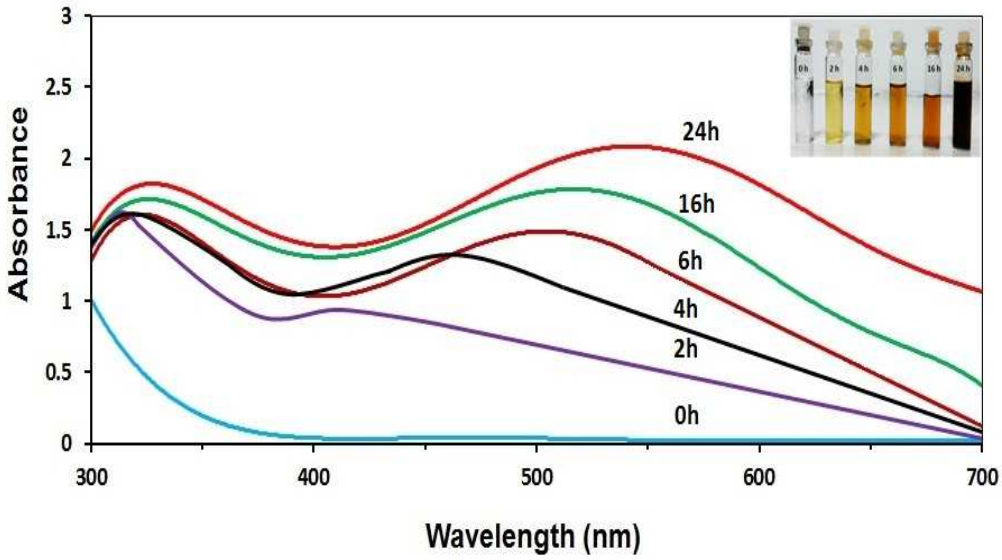

Figure 1:The time evolution of the dispersion photographs and the UV-Visible spectra

The spectacular colour change correlates with large shift of UV-Visible spectra. The first absorption peak of different curves is at 335 nm corresponding to oxidation product of L-ascorbic acid [47]. The second absorption peak is increasingly broadening with an increasing concentration of L-ascorbic acid. The absorption peak of copper nanoparticles has been reported at around 560 nm of UV-Visible wavelength which proves the formation of copper nanoparticles [48, 49].In this work, the resulting copper nanoparticles displayed a broadened peak at 550 nm wavelength, indicating the presence of small separated copper nanoparticles, it is well established fact that peak position and width are highly influenced by particle shape and size [50].

Effect of reducing agent concentration

To evaluate the effect of L-ascorbic acid concentration (0.07, 0.08, 0.09, and 0.10 mol L^{-1}) on the synthesis of copper nanoparticles were recorded on UV-Visible spectroscopy. The results indicate that a higher L-ascorbic acid concentration leads to a more effective capping capacity of L-ascorbic acid and then formed smaller Cu nanoparticles which can also be proved by the TEM images of copper nanoparticles (Figure 2).The TEM images show that the particles are spherical in shape and decrease in particle size with an increase in L-ascorbic acid concentration. The size of the copper nanoparticles with various concentration (0.07, 0.08, 0.09, 0.10 mol L^{-1}) of L-ascorbic acid are 55, 28, 16, 12 nm respectively. The reason is that L-ascorbic acid molecules encapsulateCu^{+2} and reduce Cu^{+2}into Cu(0), then oxidation products absorbs on the resulting copper nanoparticles surface preventing the particles from growing further as a result smaller copper nanoparticles obtained. Thus, the number of Cu^{+2}encapsulated in ascorbic acid molecules decreases with increasing concentration of L-ascorbic acid, leading to the formation of smaller copper nanoparticles.

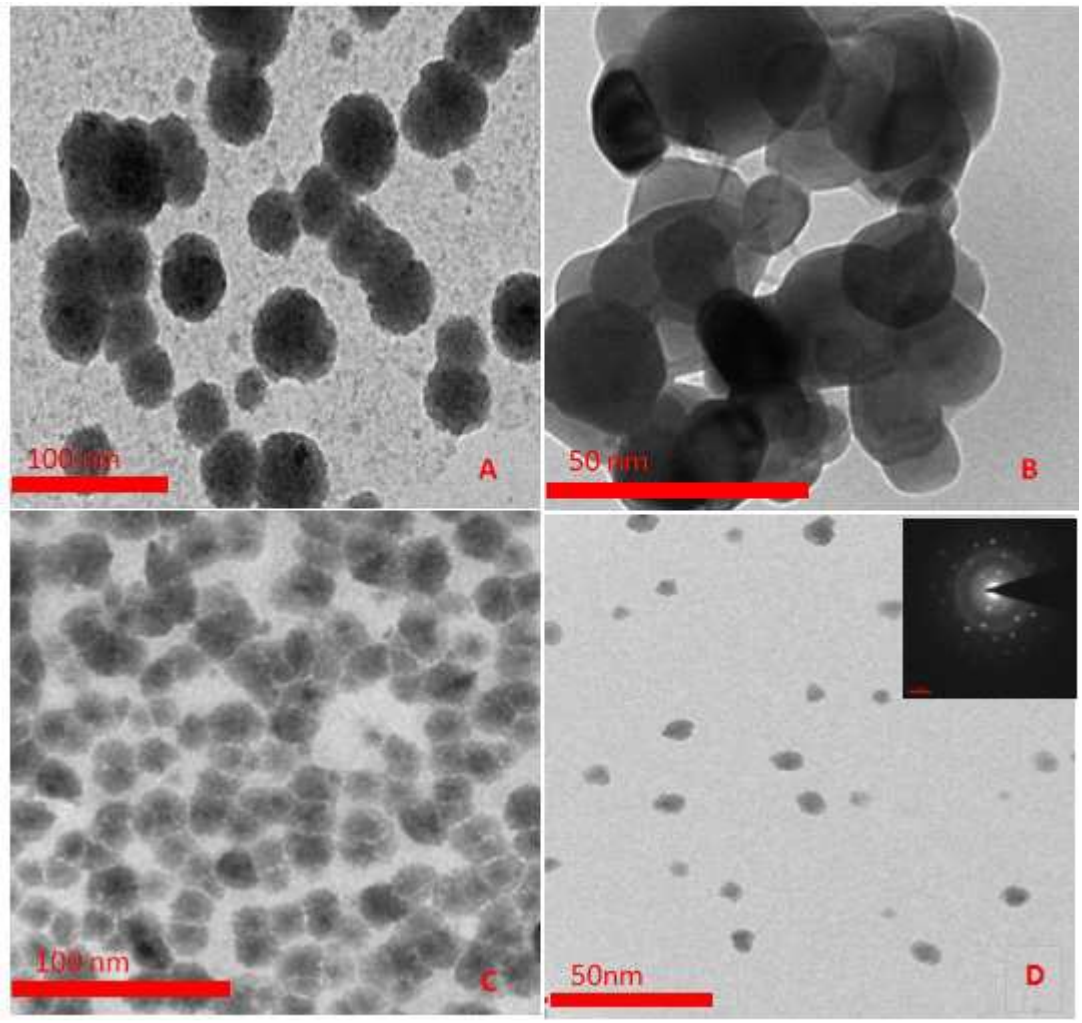

Figure 2:TEM images of copper nanoparticles with variable concentration of L-ascorbic acid: (A) 0.07, (B) 0.08, (C) 0.09, (D) 0.1 mol L^{-1}

Effect of reaction temperature

The present investigation reveals that nanoparticles did not synthesize below the temperature 333K in any conditions. This shows that reaction constant at this temperature is too low to progress the reaction. Therefore reaction temperature higher than 333K with appropriate concentration of the reactants should be inserted to the progress of the reaction for synthesis of copper nanoparticles. In Figure 3, SEM images A, B, C of copper nanoparticles synthesized at 343 K, 353 K, 363 K respectively, comparison of the images shows that the copper nanoparticles synthesized at 363 K have a wider range of size distribution. In addition, the nanoparticles were agglomerated in these conditions while copper nanoparticles synthesized at 353 K are well dispersed with an average size about 12 nm.

Basically, the reduction rate of Cu^{+2}ions was increases by increasing the reaction temperature. Therefore the synthesis rate is too high to control particle size at high temperature. When reducing agent adds to precursor solution at 363 K, rate of growth and agglomeration as well as nucleation of copper nanoparticles accelerated almost coincidently. These phenomena result in the formation of copper nanoparticles with high averaged size of the copper nanoparticles were precipitated. Thus moderate temperature (353 K) should be selected for synthesis of the copper nanoparticles with appropriate controlling on size.

Stability of nanoparticles

The stability of nanoparticles dispersion is key factor in their application. In this study L-ascorbic acid was used as both reducing and capping agent without any other special capping agent. The antioxidant properties of L-ascorbic acid came from its ability to scavenge free radicals and reactive oxygen molecules[51], accompanying the donation of electrons to give semi-dehydroascorbate radical and dehydroascorbic acid hydration of 2-carbonyl is also reported[52]and finally converted into polyhydroxyl structure through hydrolysis[47]. Therefore L-ascorbic acid

plays dual role as reducing agent and antioxidant of copper nanoparticles. As a result, the reaction can be done without any protective inert gas and the dispersion of copper nanoparticles is stable for 2 months after storage.

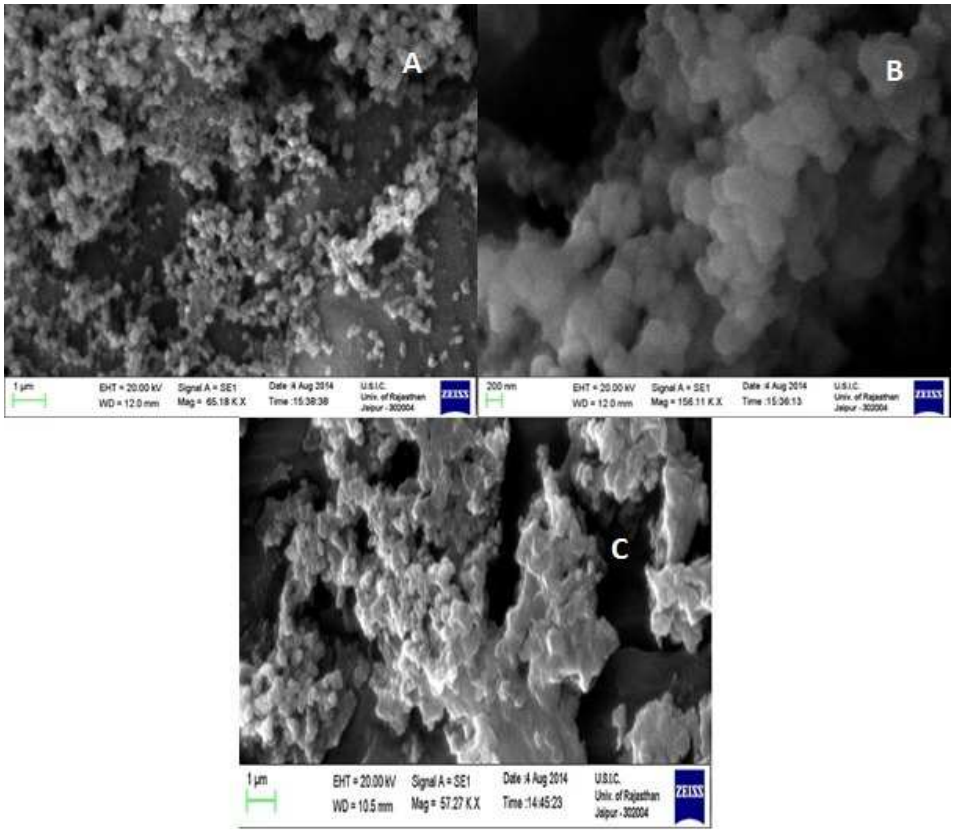

Figure 3: SEM images of synthesized copper nanoparticles with variation of temperature (A) 343 K, (B) 353 K, (C) 363 K

Stoichiometry and Product analysis

Under the kinetic conditions, the reaction was carried out with excess of peroxodisulphate over glycine in presence of nanoparticles in a thermostat water bath at 308K for 24 hours. The excess of peroxodisulphate was determined iodometrically. An addition of 2, 4-dinitrophenyl hydrazine in the reaction mixture yield brown precipitate of hydrazone derivative of aldehyde[13]. The product aldehyde was confirmed by its FTIR spectrum (Figure 4). The IR peaks at 3330 cm^{-1}, 2907 cm^{-1}, 1607 $cm^{-1}$are attributed to –NH, –CH, –C=N stretching respectively. From observations of different sets, the Stoichiometry of the reaction can therefore be presented by equation (1).

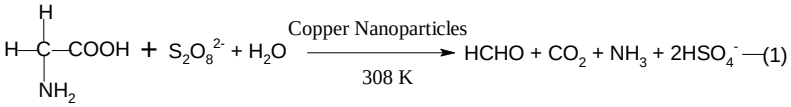

Ammonia identified by nessler′s reagent, brownish color was observed indicating deamination reaction, carbon dioxide was identified by freshly prepared lime water and the solution turned milky indicating decarboxylation reaction. The deamination of the glycine in presence of copper nanoparticles was shown in UV- Visible absorption spectrum (Figure 5).

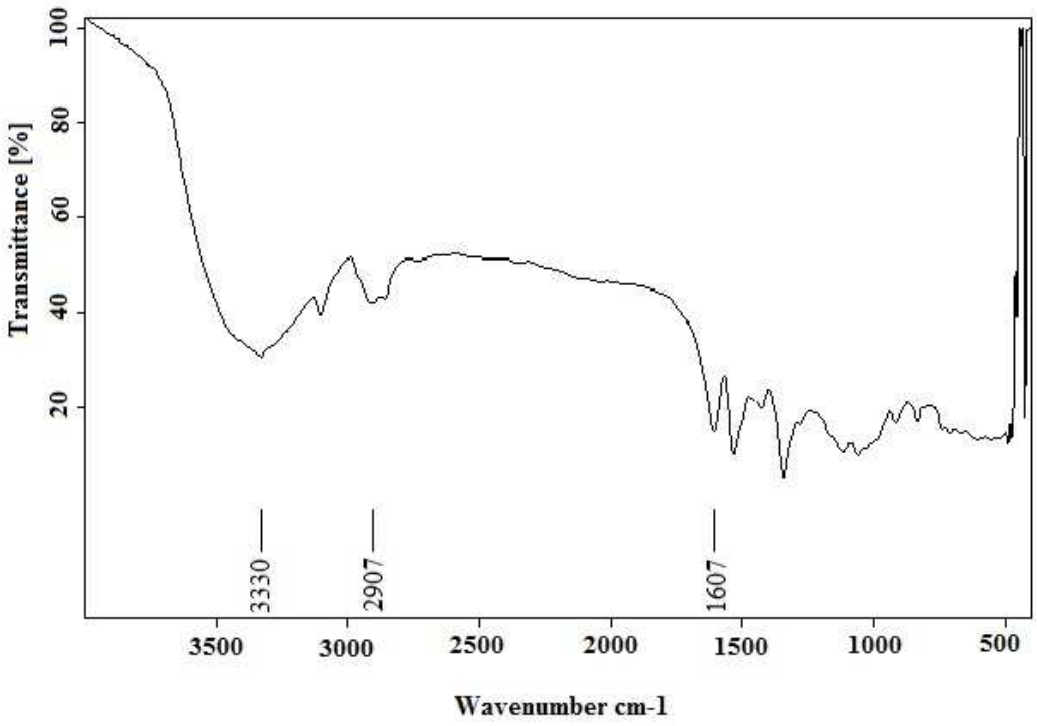

Figure 4: The FTIR Spectra of the oxidation product of glycine oxidation

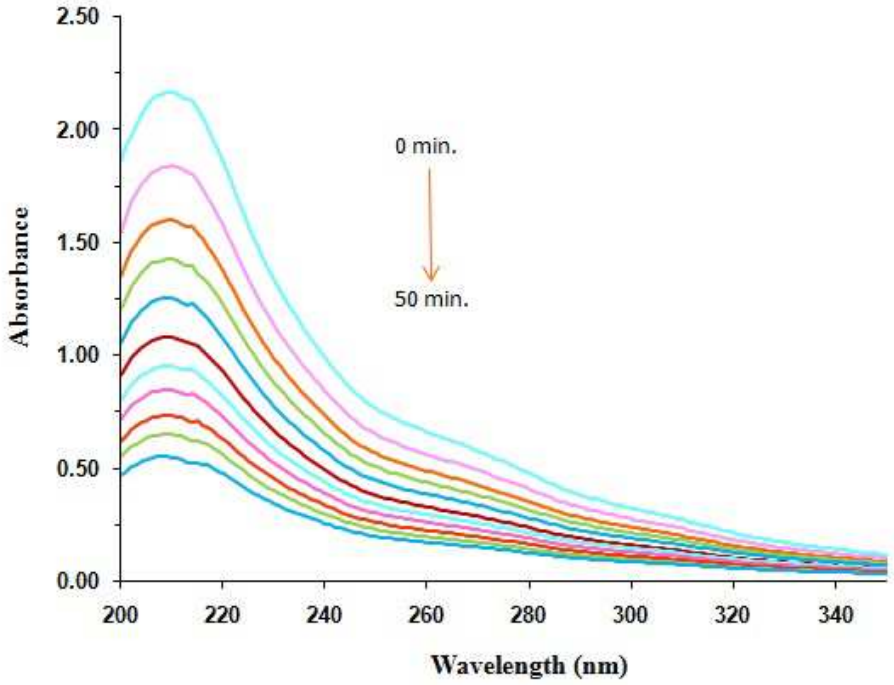

Figure5: UV spectra for the deamination of glycine (time 0-50 min.) in the presence of the copper nanoparticles at fixed [PDS] = 5×10^{-3} mol L^{-1}, [Cunps] = 1×10^{-5} mol L^{-1} at 308 K

Peroxodisulphate dependence

Kinetic runs were carried out by varying concentration of peroxodisulphate from 1×10^{-3}– 7.5×10^{-3} mol L^{-1}at fixed concentration of [Gly] = 5×10^{-2}mol L^{-1},[Cunps] = 1×10^{-5} mol L^{-1}at 308 K temperature. The plot of log [PDS] versus time was linear for each initial concentration of PDS (Figure 6), indicating that the reaction is first order with respect to [PDS].

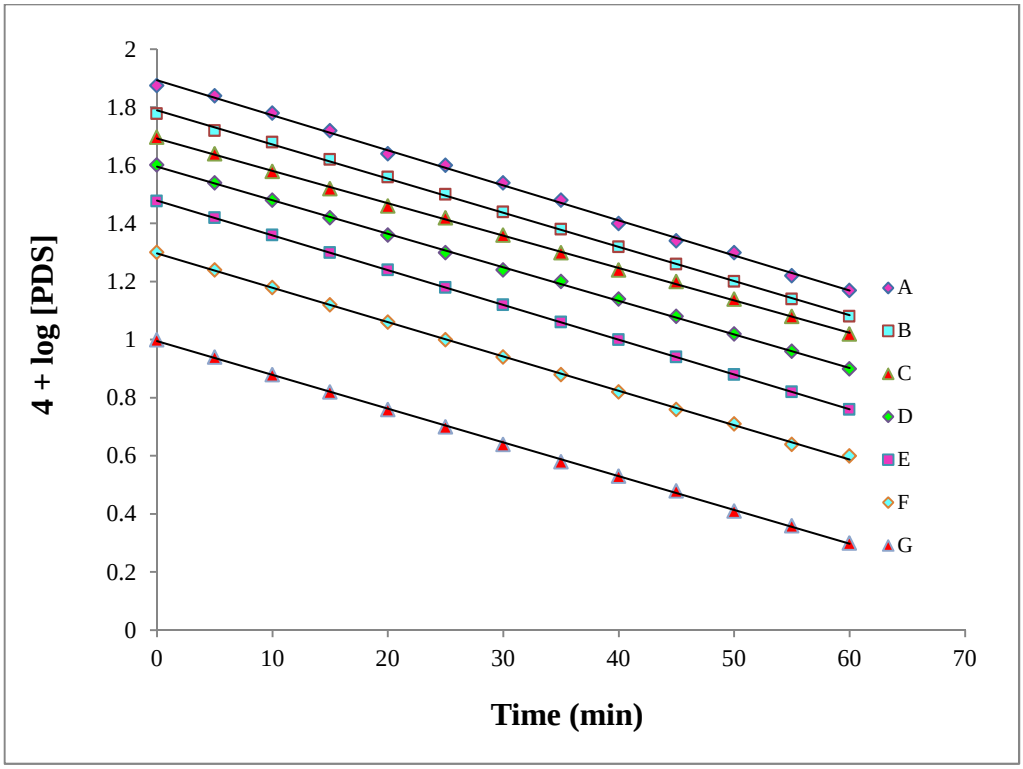

Figure 6: First order plots of the variation of peroxodisulphate concentration at 308 K
[Gly]= 5.0×10^{-2}mol L^{-1}, [Cunps] = 1.0×10^{-5} mol L^{-1}, [PDS]×10^{-3} mol L^{-1} = (A) 1.0, (B) 2.0, (C) 3.0, (D) 4.0, (E) 5.0, (F) 6.0, (G) 7.5

Glycine dependence

Reaction were carried out at constant concentration of all reactants [PDS] = 5×10^{-3} mol L^{-1}, [Cunps] = 1×10^{-5} mol L^{-1}and by varying initial concentration of glycine from1×10^{-2} – 7×10^{-2} mol L^{-1} at 308 K temperature. Plot of log k_{obs} versus log [Gly] give straight line parallel to log [Gly] axis indicating zero order dependence with respect to glycine(Figure 7).

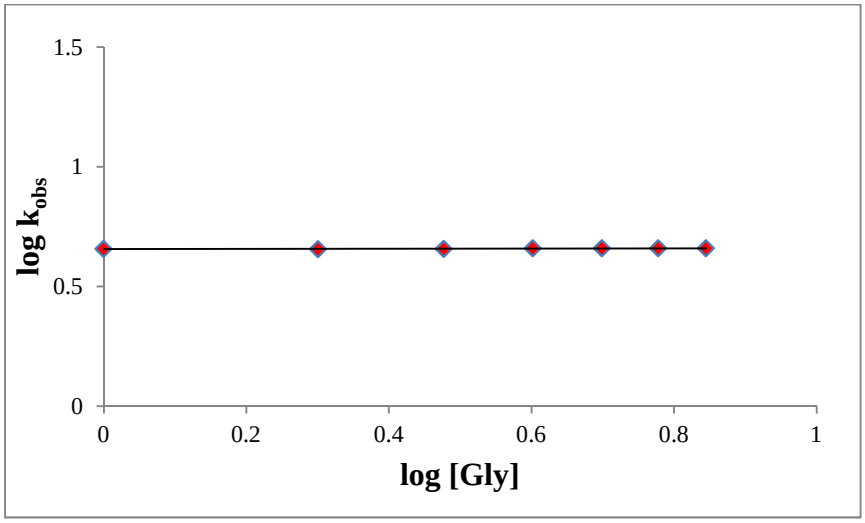

Figure 7: First order plots of the variation of glycine concentration at 308 K
[PDS]= 5.0×10^{-3}mol L^{-1}, [Cunps] = 1.0×10^{-5}mol L^{-1}, [Gly]×10^{-2}mol L^{-1} = (A) 1.0, (B) 2.0, (C) 3.0, (D) 4.0, (E) 5.0, (F) 6.0, (G) 7.0

Copper nanoparticles dependence

The effect of copper nanoparticles on the rate of oxidation of glycine has been studied at varying concentration of copper nanoparticles 1×10^{-6} - 1×10^{-5} mol L^{-1} at four different size of nanoparticles (55, 28, 16 and 12 nm), synthesized at four concentration (0.07, 0.08, 0.09, 0.10 mol L^{-1}) of ascorbic acid respectively, other reactant and reaction conditions were constant. The rate of reaction increases with increasing concentration of copper nanoparticles. The catalytic activity of copper nanoparticles seems different when concentration of reducing agent is

varied from 0.07 to 0.1mol L^{-1}.The difference in catalytic activity can be attributed to the size variation in the resulting copper nanoparticles. The trend in the calculated rate constant being 12>16>28>55nm (Figure 8). This effect can be attributed to the nanosize of the particles that as size decreases surface area increases and the active centre are also increases.

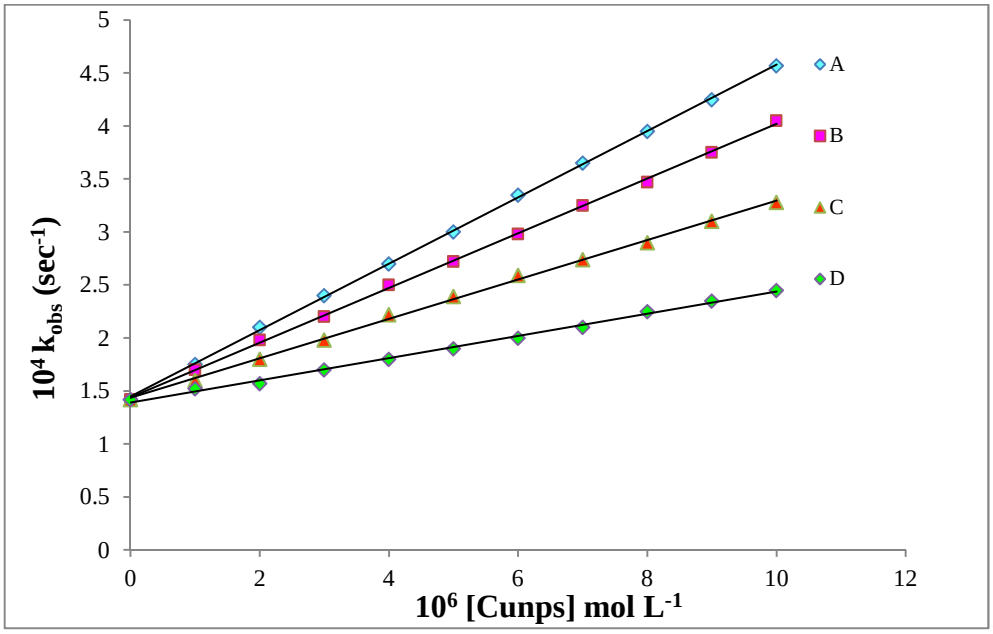

Figure 8: The effect of [Cunps] at different size of Cunps in nm (A) 12, (B)16, (C) 28, (D) 55 at fixed [PDS] = 5.0×10^{-3} mol L^{-1}, [Gly] = 5.0×10^{-2}mol L^{-1} at 308K

Temperature dependence

The effect of temperature on the rate of reaction was studied at three temperature 303 K, 308 K, 313 K respectively at constant concentration of other reaction ingredients. A plot of log k_{obs} was made against 1/T, yielded a straight line. The energy of activation (E_a),entropy of activation ($\Delta S^{\neq}$), enthalpy of activation ($\Delta H^{\neq}$), free energy of activation (ΔG) were obtained 24.69 KJ mol^{-1}, -237.32JK^{-1} mol^{-1}, 22.13 KJ mol^{-1}, 95.226 KJ mol^{-1} respectively.The high positive values of free energy of activation (ΔG) and enthalpy of activation (ΔH) indicated that the transition state was highly solvated while the negative values of entropy of activation (ΔS) was suggested the formation of rigid transition state with reduction in the degree of freedom of molecules.

Neutral Salts dependence

The effect of added neutral salt on the rate of reaction has been studied at varying concentration $1x10^{-3}$- $4x10^{-3}$of KCl, NH_4Cl and K_2SO_4 at fixed concentration of other reactant and constant conditions. The results shows (Table-1)the retarding effect of some ions on the rate of reaction of copper nanoparticles catalyzed oxidation of glycine by peroxodisulphate. The decrease in the rate constant is not strictly related to the increase in ionic strength and evidently there is a considerable specific effect of the ions. Similar observations have been obtained in earlier study [13].

Table 1: [PDS] = 5×10^{-3}mol L^{-1}, [Cunps] = 1×10^{-5}mol L^{-1}, [Gly] = 5×10^{-2}mol L^{-1}, Temp. = 308 K

Neutral Salts	10^3 Concentration mol L^{-1}	Ionic Strength Contributed $10^3\times\mu$	Rate Constant 10^4 k_{obs} sec^{-1}
KCl	1.0	1.0	4.47
	2.0	2.0	4.38
	3.0	3.0	4.18
	4.0	4.0	4.08
NH_4Cl	1.0	1.0	4.41
	2.0	2.0	4.28
	3.0	3.0	4.05
	4.0	4.0	3.89
K_2SO_4	1.0	3.0	4.11
	2.0	6.0	3.93
	3.0	9.0	3.79
	4.0	12.0	3.51

Mechanism

The definite mechanism of the homogeneous metal nanoparticles catalyzed oxidation is not clear. Although identify the formation of transition species through certain physical measurements but it is very difficult to isolate and

characterize from homogeneous mixture. Since in the present study, the rate of reaction does not depend upon the concentration of glycine, oxidative deamination of glycine occurs in presence of peroxodisulphate only upon addition of copper nanoparticles while peroxodisulphate converted to hydrogen sulphate ion. The plausible mechanism in support of the observed kinetics is given in scheme-1.

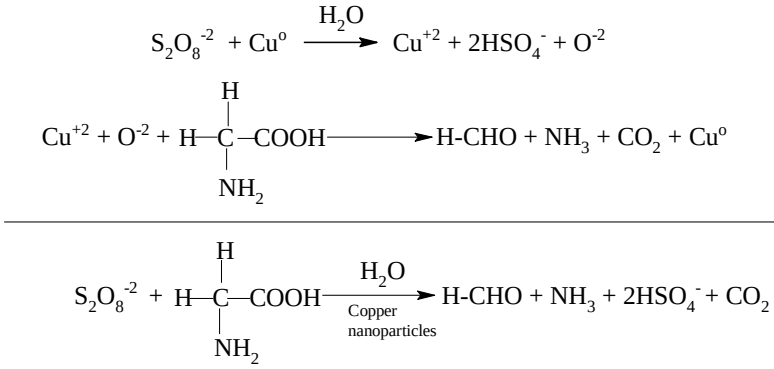

Scheme 1: The plausible route of copper nanoparticles catalyzed oxidation of glycine

CONCLUSION

In the present work, highly stable dispersed copper nanoparticles were synthesized in aqueous medium without employing any protecting gas. By this green method, synthesis of monodispersed copper nanoparticles (ranging from 12 – 55 nm) employing by different concentration of reducing agent. L-ascorbic acid is used as both reducing and capping agent. The synthesized nanoparticles are highly stable and do not show sedimentation even after storage for 2 months. Moreover, it was clearly shown that reaction temperature has a remarkable effect on particle size and agglomeration of the synthesized copper nanoparticles. The catalytic activity of synthesized copper nanoparticles was investigated by the oxidation of glycine in aqueous medium. The size of copper nanoparticles decreases the catalytic activity of copper nanoparticles increases. The results of this study indicate that the reaction between glycine and peroxodisulphate in the presence of Cunps was first order.

Acknowledgement
This work was supported in part by University Grant Commission, New Delhi through Junior Research Fellowship and Department of Science and Technology sponsored FIST Laboratory of our institution for experimental work.

REFERENCES

[1] Laloo D,Mahanti MK,*JChem SocDalton Trans*, **1990**,1, 311.
[2] Alvarez-Macho MP, *Rev RoumChim*,**1993**, 38, 999.
[3] Devra V,*JIndChemSoc*, **2005**,82, 290.
[4] Barrett GC, Amino acids, peptides and proteins, Royal society of Chem., UK, **2006,** pp 219.
[5] Hiraemath RC, Mayanna SM, Venkatasubramanian N, *JChem Soc Perkin Trans II*,**1987,**2, 1569.
[6] Gupta D, Bhasin M, Devra V, Sharma I, Sharma PD, *Oxidation Communications*,**1996,**19, 242.
[7] Yadav MB, Devra V and Rani A,*Indian Journal of chemistry*,**2010,** 49A, 442.
[8] Chandraju S, Rangappa KS, Made Gowda NM,*Int J ChemKinet*,**1999,**31,525.
[9] Iloukhani H, Bahrami H,*IntJ ChemKinet*,**1999,**31,95.
[10] Jose TP, Nandibewoor ST, Tuwar SM, *J Solution Chem*,**2006,**35,51.
[11] Grover N, Kambo N, Upadhyay SK, *Indian JChem***,2002**, 41A**,**2482.
[12] Rayappan SM, Easwaramurthy D, Palanichamy M, Murugesan V, *Inorgani Chemistry Communications*, **2010,**13,131.
[13] Chandra G and Srivastava SN, *Bull Chem Soc*, **1971**, 44, 3000.
[14] Marshell H, *JChem Soc*,**1891,**59, 771.
[15] Woods R, Kolthoff IM and Meehan EJ, *InorgChem*,**1965,**4, 697.
[16] Nasirian A, *Int J Nano Dim*, **2012**, 2, 159.
[17] Lewis LN, Lewis N, *J Am Chem Soc*,**1986**, 108, 7228,Lewis LN, Uriarte R, *JOrganometallics*,**1990**, 9, 621.
[18] Hirai H, Komiyama H, *Bull Chem Soc Jpn*, **1986**, 59, 545.
[19] Spiro M, *Catal Today*, **1993**, 17, 517.
[20] Feldheim DL, Foss JR, *Metal Nanoparticles; Synthesis, Characterization, and Applications*, New York, USA, Marcel Dekker Incorporated, **2002,** pp 17.

[21] Siegel RW, Hu E, Roco MC, *Nanostructure Science and Technology: R & D Status and Trends in Nanoparticles, Nanostructured Materials, and Nano-devices*, 1 ed., In: WTEC Panel Report, Kluwer Academic Press, Dordrecht, Netherland, **1999**pp 1.
[22] Jana NR, Wang ZL, Sau TK, *Current Science*, **2000**, 79,1367.
[23] Yeh MS, Yang YS, Lee YP, *Journal of Physical Chemistry-B*, **1999**, 103, 6851.
[24] Liu Z, Bando Y,*Advanced Materials*,**2003**, 15, 303.
[25] Yatsui K, Grigoriu C, Kubo H, *Applied Physics Letters*, **1995**, 67, 1214.
[26] Oleszak D, Shingu PH, *Journal of Applied Physics*, **1996**, 79, 2975.
[27] Wang Y, Chen P, Liu M, *Nanotechnology*, **2006,**17, 6000.
[28] Pileni MP, *Journal of Physical Chemistry*, **1993**, 97, 6961.
[29] Kumar RV, Mastai Y, Diamant Y, *Journal of Materials Chemistry*, **2001**, 11, 1209.
[30] Molares M, Buschmann V, Dobrev D, *Advanced Materials*, **2001,** 13, 62.
[31] Takayama S, Link G, Sato M, *Microwave and Radio Frequency Applications, In: Proceedings of the Fourth World Congress on Microwave and Radio Frequency Applications*,, Austin, Texas, USA, **2004,**pp 311.
[32] Chu LY, Zhou Y, Dong L, *Advanced Functional Materials*, **2007**, 17, 933.
[33] Bali R, Razak N, Lumb A, *International Conferenceon Nanoscience and Nanotechnology*, **2006,** 0, 224.
[34] Umer A, Naveed S, Ramzan N, *NANO: Brief Reports and Reviews*, **2012**, 7, 1230005.
[35] Bonet F, Delmas V, Grugeon S, *Nano Structured Materials*, **1999**, 11, 1277.
[36] Murphy CJ, San TK, Gole AM, *Journal of Physical Chemistry B*, **2005**, 109, 13857.
[37] Pastoriza-Santos I,Liz-Marzan LM, *Langmuir*, **1999**, 15, 948.
[38] Tan YW, Dai XH, Li YF, *Journal of Materials Chemistry*, **2003**, 13, 1069.
[39] Chou KS, Ren CY, *Materials Chemistry and Physics*, **2000**, 64, 241.
[40] Lee Y, Choi JR, Lee KJ, *Nanotechnology*, **2008**, 19.
[41] Leopold N,Lendl B, *Journal of Physical Chemistry B*,**2003**, 107, 5723.
[42] Khalid MAA, *Arabian Journal for Science and Engineering*, **2008**, 33, 199.
[43] Khalid MA, Kheir AM, *Sudan Journal of Basic Sciences*, **2008**, 15, 69.
[44] Noguez C, *J Phys Chem C*,**2007**, 111, 3806.
[45] Chen F, Alemu N and Johnston RL, *AIP Advances*, **2011**, 1, 032134.
[46] Ghosh SK, Pal T,*Chem Rev*, **2007**, 107, 4797.
[47] Xiong J,Wang Y, Xue Q and Wu X, *Green Chemistry*, **2011**, 13, 900.
[48] Kapoor S, Joshi R, Mukherjee T, *Chemical Physics Letters*, **2002**, 354, 443.
[49] Zhang HX, Siegert U, Liu R and Cai WB, *Nanoscale Research Letter*, **2009**, 4, 705.
[50] Sharma V, Park K, Srinivasarao M, *Materials Science and Engineering R*,**2009,**65, 1.
[51] Wu CW, Mosher BP, Zeng TF, Yin ZL, *J Nanopart Res*, **2006**, 8, 965.
[52] Kerber RC, *J Chem Educ*, **2008**, 85, 1237.

International Journal of Current Engineering and Technology
E-ISSN 2277 – 4106, P-ISSN 2347 – 5161

Available at http://inpressco.com/category/ijcet

Research Article

Synthesis, Characterization and Catalytic Application of Copper Nanoparticles on Oxidation of Alanine in Acid Aqueous Medium

Shikha Jain†, Niharika Nagar† and Vijay Devra†*

†Department Of Chemistry, J.D.B. Govt. P.G. Girls College, Kota, Rajasthan, India

Accepted 31 March 2015, Available online 05 April 2015, **Vol.5, No.2 (April 2015)**

Abstract

In this paper, we report on the synthesis of copper nanoparticles (Cunps) through a single route of chemical reduction method. The effect of different concentration of precursor salt and temperature on the morphology of Copper nanoparticals was investigated. The synthesized copper nanoparticles were characterized by UV-Visible spectrophotometer, Fourier Transform Infrared (FTIR) Spectrophotometer, Scanning Electron Microscopy (SEM), Transmission Electron Microscopy (TEM) analysis. The average size of copper nanoparticles was found to be 12 nm and spherical in shape at the optimal experimental conditions. The catalysis by colloidal copper nanoparticles was studied kinetically in the oxidation of L-Alanine (Ala) by peroxodisulphate (PDS) in acid aqueous medium. The copper nanoparticles catalyst exhibited very good catalytic activity and the kinetics of the reaction was found to be first order with respect to peroxodisulphate and independent of alanine concentration. The effects of catalyst concentration, ionic strength and temperature on the reaction were also investigated.

Keywords: *Copper nanoparticles, L-alanine, Peroxodisulphate, Oxidation, Kinetics.*

1. Introduction

The field of nanocatalysis has undergone an explosive growth during the past decades, both in homogeneous and heterogeneous catalysis (Bradley and Scmided, 1994), (Thomas, *et al*, 2003). Since nanoparticles have a large surface to volume ratio compared to bulk materials, they are attractive to use as catalyst (Bruss, *et al*, 2006), (Firooz, *et al*, 2011). Metal nanoparticles with high specific catalytic activity are ubiquitous in modern synthetic organic chemistry during the recent decades (Jansat, *et al*, 2004). However how to reduce their dosage is one of the most exciting challenges due to the limiting reserves of noble metals. Some selective oxidation reactions are reported involving transition metal ions of Ag, Rh, Cr, Ru, Mn etc. are reported to act as catalyst for amino acids oxidations (Devra and Yadav, 2012), (Singh and Singh, 1992), (Bilehal, *et al*, 2005), (Seregar, *et al*, 2007), (Berlett, *et al*, 1990) with the emergence of metal nanoparticles possessing appreciable stability and high surface area per particle, their potential use as catalyst for organic biochemical relevant reactions (Sanathanlakshmi and Vankatesan, 2012), (Huang, *et al*, 2005). Amongst them Copper nanoparticles are paid more attention due to their low cost and easy availability. Copper nanoparticles have also been considered (Hoover, *et al*, 2006), (Niu and Crooks, 2003) as an alternative for noble metals in many applications such as heat transfer and microelectronics (Eastman, *et al*, 2001). In this study, highly stable colloidal dispersion of copper nanoparticles has been synthesized by chemical reduction method, using ascorbic acid as a reducing agent as well as capping agent. The particle size has been effectively controlled by the variation of precursor salt and temperature during the synthesis. The synthesized Cunps were characterized by UV-Visible Spectrum, FTIR, SEM, TEM etc. techniques.

The kinetics of the oxidation of inorganic and organic substrates by peroxodisulphate under both catalyzed and uncatalyzed conditions have received considerable attention (Wilmarth and Haim, 1961), (House, 1962). The peroxodisulphate ion is one of the strongest oxidizing agents known in aqueous solution. The standard oxidation reduction potential for the reaction is estimated to be -2.01V.

$$2\ SO_4^{2-} \longrightarrow S_2O_8^{2-} + 2e^-$$

The reaction involve this ion are generally very slow in the absence of suitable catalysts (Chandra and Srivastava, 1971).The transition metal ion catalysis oxidation of amino acid by peroxodisulphate was reported in aqueous acidic medium (Chandra and Srivastava, 1973), (Zelechonok and Silverman, 1992), (Khalid, 2008). The oxidation of amino acids is of the

*Corresponding author: **Vijay Devra**

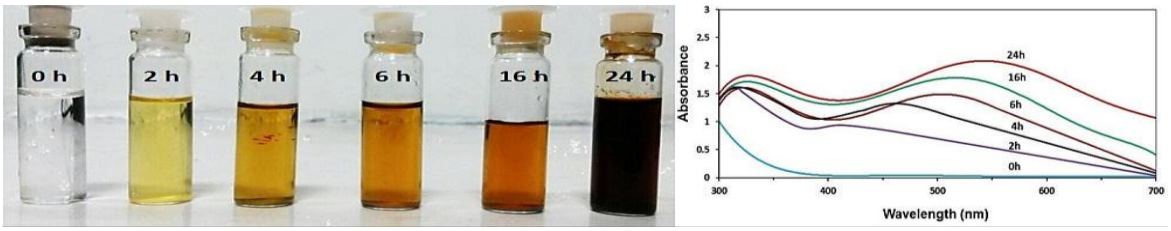

Figure 1 The time evolution of the dispersion photographs and the UV-Visible spectra

utmost importance, both from a chemical point and in view of its bearing on the mechanism of amino acid metabolism. It has been observed that there is not enough information in the literature on the kinetics of oxidation of amino acid by peroxodisulphate in presence of copper nanoparticles. The present investigation is a part of a broad programme of study of the catalytic effect of copper nanoparticles on the oxidation of alanine by peroxodisulphate in acid aqueous media.

2. Experimental

2.1 Material

For the present work, we used analytical grade chemicals such as copper chloride dihydrate ($CuCl_2.2H_2O$-97%), L-ascorbic acid (vitamin C-98%), L-Alanine and Peroxodisulphate were obtained from E. Merck. A fresh solution of peroxodisulphate was prepared before starting the experiments. All chemicals were used as received without further purification. Double distilled water was employed throughout the study.

2.2 Synthesis of Copper Nanoparticles

The one step synthesis scheme for copper nanoparticles initiates with dissolving copper chloride dihydrate (0.02 mol L^{-1}) in deionized water to obtain a blue solution. L-ascorbic acid (0.01 mol L^{-1}) drop wise added to the aqueous solution of copper salt while vigorously stirring at 353 K in oil bath. With the passage of time, the colour of dispersion gradually changed from white, yellow, orange, brown finally dark brown with a number of intermediate stages. The appearance of yellow colour followed by orange colour indicated the formation of fine nanoscale copper particles from L-ascorbic acid assisted reduction. The resulting dispersion was centrifuged for 15 minutes. The supernatant was placed under ambient conditions for 2 months. The studies were performed at different concentration of $CuCl_2.2H_2O$ and temperature to investigate the morphology of copper nanoparticles.

2.3 Characterization

UV-Visible spectroscopy from a double beam spectrophotometer (U.V. 3000+ LABINDIA) was used for preliminary estimation of copper nanoparticles synthesis. FTIR (ALPHA-T –Bruker) provided information about oxidation product of the reaction. Morphological study of the copper nanoparticles was carried out with scanning electron microscope (SEM) (EVO 18 carlzeiss) and Transmission electron microscope (TEM) (FEI Techni G2S2 Twin). TEM and SEM images were recorded to confirm size distribution and shape homogeneity of synthesized copper nanoparticles.

2.4 Kinetic Measurements

The reaction was carried out in glass-stoppered Pyrex round bottom flask. Appropriate amount of the amino acid solution in acidic form, potassium sulphate, and water (to keep the total volume constant for all runs) were taken in the round bottom flask and thermostatted at 308 K for thermal equilibrium. A measured amount of peroxodisulphate was rapidly added to the mixture. The progress of the reaction was monitored by iodometric determination of unreacted peroxodisulphate in a measured aliquot of the reaction mixture at different intervals of time (Khalid and Kheir, 2008). The rate constants were computed from the linear plots of log [PDS] against time. The course of the reaction was followed for at least 80% of the reaction.

3. Results and Discussion

3.1(a) Metal Nanoparticles Characterization Results

UV-Visible absorbance spectroscopy has proved to be a very useful technique for studying metal nanoparticles because the peak position and shapes are sensitive to particle size. During the synthesis of copper nanoparticles in aqueous solution, the UV-Visible spectra of samples were recorded at different time intervals for every colour change presented in (Figure 1).

The spectacular colour change correlates with large shift of UV-Visible spectra. The first absorption peak of different curves is at 335 nm corresponding to oxidation product of L-ascorbic acid (Xiong, *et al*, 2011). The second absorption peak is increasingly broadening with an increasing concentration of L-ascorbic acid. The absorption peak of copper nanoparticles has been reported at around 560 nm of

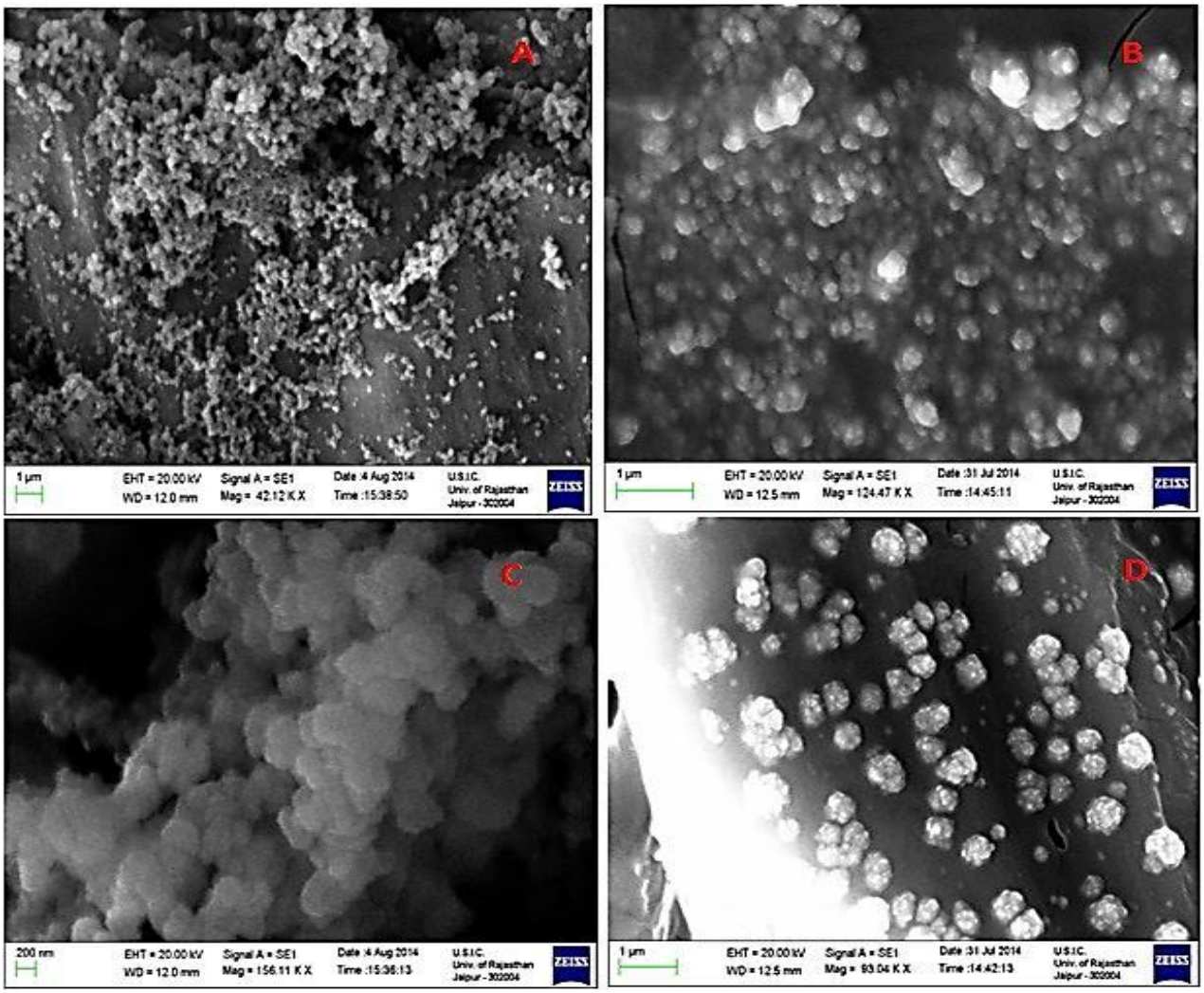

Figure 2 SEM images of the synthesized copper nanoparticles with various concentration of the precursor salt ($CuCl_2.2H_20$) (A) 0.01 mol L^{-1}, (B) 0.015 mol L^{-1}, (C) 0.02 mol L^{-1}, (D) 0.03 mol L^{-1}

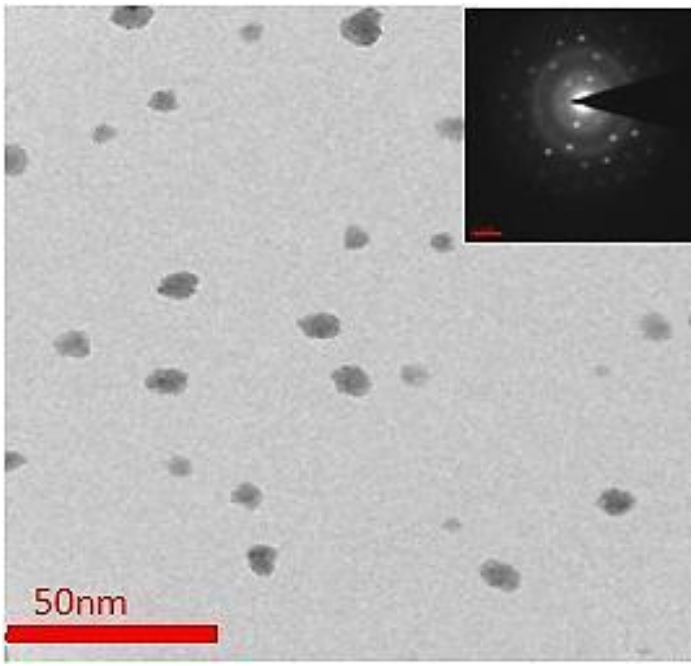

Figure 3 TEM image of synthesized copper nanoparticles at the optimal experimental conditions

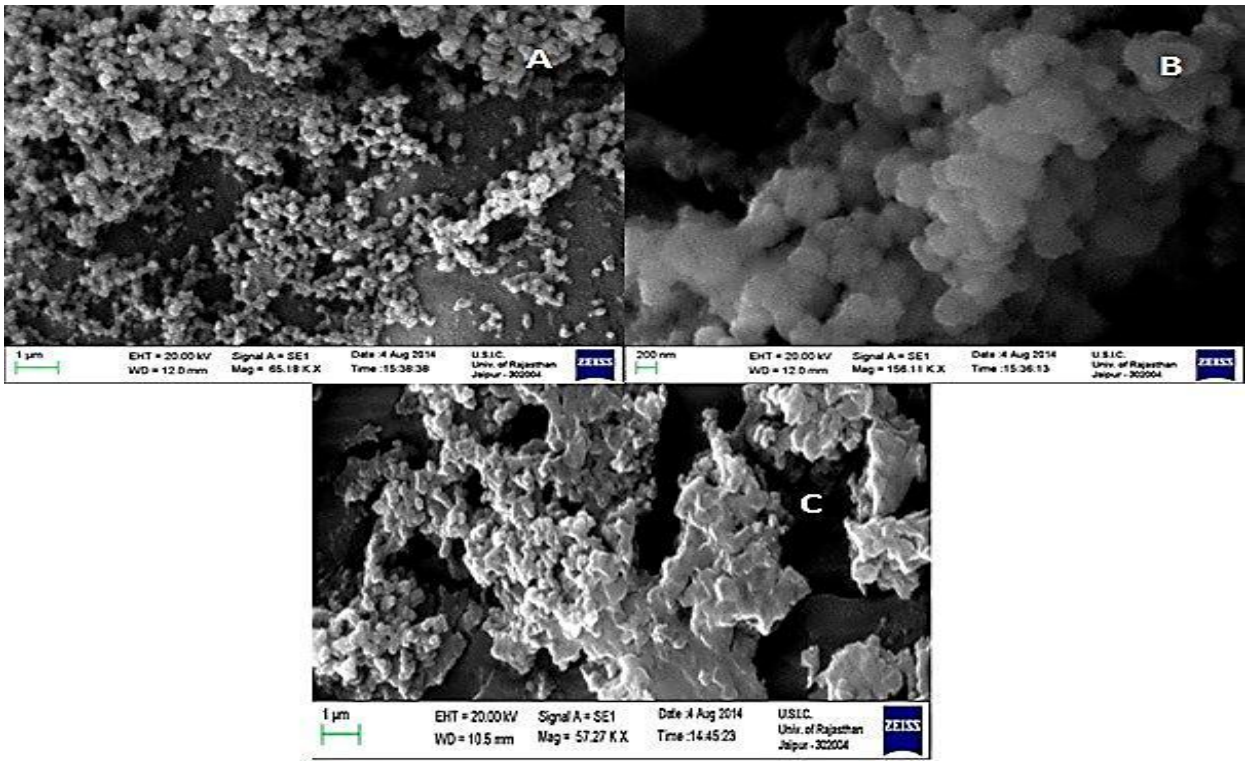

Figure 4 SEM images of synthesized copper nanoparticles with variation of temperature (A) 343 K, (B) 353 K, (C) 363 K

UV-Visible wavelength which proves the formation of copper nanoparticles (Kapoor, *et al*, 2002), (Zhang, *et al*, 2009).

3.1(b) Effect of initial concentration of precursor salt

The effect of initial concentration of precursor salt on synthesis of copper nanoparticles was studied at four different concentrations $CuCl_2.2H_20$ viz. 0.01, 0.015, 0.02, 0.03 mol L^{-1}. There are two stages in the synthesis of copper nanoparticles, the first stage is to generate copper nuclei and second stage is the growth of copper (Liu, *et al* 2010). So it is important to control preparation process that copper nuclei must generate faster and grow up slower which requires better control of the initial concentration of Cu^{+2}. It can be seen that reaction rate increases with increases the concentration of Cu^{+2}. With the increasing reaction rate, the amount of copper nuclei rises and smaller particle size are obtained correspondingly which is shown in SEM images A, B, C of (Figure 2) further increases the concentration of Cu^{+2}, the result is the agglomeration of the nuclei and growing the particle size as shown in SEM image D of (Figure 2). This may be due to collision between small particles, which leads to particle growth (Dang, *et al*, 2011). So the optimal concentration of precursor salt is 0.02 mol L^{-1} and 0.1 mol L^{-1} of L-ascorbic acid at 353 K. In this experimental condition, the TEM image of the synthesized copper nanoparticles is shown in (Figure 3). It can be seen that the nanoparticles are spherical in shape and monodispersed with size 12 nm ± 0.5 nm.

3.1(c) Effect of reaction temperature

The present investigation reveals that nanoparticles did not form below the temperature 333 K in any conditions. Therefore reaction temperature higher than 333 K with appropriate concentration of the reactants should be inserted to the synthesis of copper nanoparticles. In (Figure 4), SEM images A, B, C of copper nanoparticles synthesized at 343 K, 353 K, 363 K respectively, shown that at higher temperature (363 K), the nanoparticles were agglomerated, while at 353 K are well dispersed with an average size at about 12 nm.

Basically, the reduction of Cu^{+2} were increase by increasing the reaction temperature. Therefore the synthesis rate is too high to control particle size at high temperature. When reducing agent adds to precursor solution at 363 K, rate of growth and agglomeration as well as nucleation of copper nanoparticles accelerated almost coincidently. These phenomena result in the formation of copper nanoparticles were precipitated. Therefore moderate temperature (353 K) should be selected for synthesis of the copper nanoparticles with appropriate controlling on size.

3.1(d) Stability of nanoparticles dispersion

The stability of nanoparticles dispersion is key factor in their application. In this study L-ascorbic acid was used as both reducing and capping agent without any other special capping agent. The photographs of dispersion before and after the storage (2 months) are shown in

(Figure 5). The antioxidant properties of L-ascorbic acid come from its ability to scavenge free radicals and reactive oxygen molecules (Wu, *et al*, 2006) accompanying the donation of electrons to give semi-dehydroascorbate radical and dehydroascorbic acid and finally converted into polyhydroxyl structure through hydrolysis (Kerber, 2008). Therefore L-ascorbic acid plays dual role as reducing agent and antioxidant of copper nanoparticles. Thus reaction can complete without any protective gas.

Figure 5 The photos of dispersion of Cunps (A) before (B) after 2 months of storage

3.2 Stoichiometry

Attempts were made to determine the stoichiometry, the reaction mixture containing an excess of peroxodisulphate (PDS) over Alanine (Ala) were allowed for 24 hours to react is a temperature controlled water bath. The excess of PDS was determined iodometrically. The identification of product by IR (Infra red spectrum) and formation of 2, 4-dinitrophenyl hydrazone derivative indicate the stoichiometry as represented by equation (1).

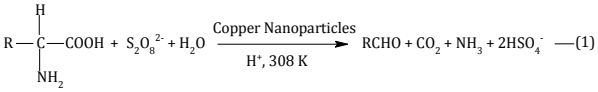

—(1)

Where R represents -CH_3

Ammonia identified by nessler's reagent, brownish colour was observed indicating deamination reaction, carbon dioxide was identified by freshly prepared lime water and the solution turned milky indicating decarboxylation reaction. The product aldehyde was identified by qualitative test and further 2, 4-dinitrophenyl hydrazone derivative was also obtained which is confirmed by FTIR spectrum in (Figure 6). The IR peaks at 3343 cm^{-1}, 2901 cm^{-1}, 1610 cm^{-1} are attributed to –NH, –CH and –C=N stretching respectively. The deamination of the L-Alanine by persulphate in presence of copper nanoparticles was shown in UV- Visible absorption spectrum (Figure 7).

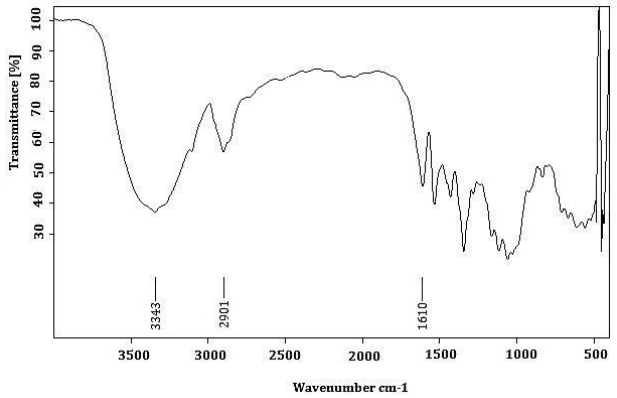

Figure 6 The FTIR Spectra of the oxidation product of alanine oxidation

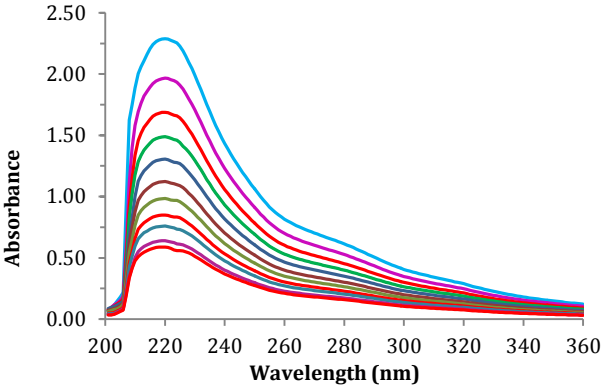

Figure 7 UV absorption spectra for the deamination of L-alanine (time 0-40 min.) in the presence of the copper nanoparticles

3.3 Peroxodisulphate dependence

Kinetic runs were carried out by varying concentration of peroxodisulphate from 1×10^{-3} – 7.5×10^{-3} mol L^{-1} at fixed concentration of [Ala] = 5×10^{-2} mol L^{-1}, [H^+] = 0.1 mol L^{-1}, I = 0.2 mol L^{-1}, [Cunps] = 1×10^{-5} mol L^{-1} at 308 K temperature. The plot of log [PDS] versus time was linear for each initial concentration of peroxodisulphate. The observed pseudo first order rate constant (k_{obs}) were independent of the concentration of peroxodisulphate which is given in Table-1.

3.4 Alanine dependence

Reaction were carried out at constant concentration of all reactants [PDS] = 5×10^{-3} mol L^{-1}, [Cunps] = 1×10^{-5} mol L^{-1}, [H^+] = 0.1 mol L^{-1}, I = 0.2 mol L^{-1} and by varying initial concentration of alanine from 1×10^{-2} – 7×10^{-2} mol L^{-1} at 308 K temperature. Plot of log k_{obs} versus log [Ala] gave straight line parallel to log [Ala] axis indicating zero order dependence with respect to alaine as shown in Table 1.

Table 1: Effects of variation of [PDS], [Ala], [Cunps], [H^+] on the oxidation of Alanine by Peroxodisulphate at fixed Ionic Strength (I) = 0.2 and Temperature 308 K

S. No.	10^3 [PDS] mol L^{-1}	10^2 [Ala] mol L^{-1}	10^5 [Cunps] mol L^{-1}	10^1 [H^+] mol L^{-1}	10^4 k_{obs} sec^{-1}
1	1	5	1	1	5.7
2	2	5	1	1	5.7
3	3	5	1	1	5.7
4	4	5	1	1	5.73
5	5	5	1	1	5.73
6	6	5	1	1	5.75
7	7.5	5	1	1	5.73
8	5	1	1	1	5.7
9	5	2	1	1	5.72
10	5	3	1	1	5.7
11	5	4	1	1	5.7
12	5	5	1	1	5.73
13	5	6	1	1	5.73
14	5	7	1	1	5.7
15	5	5	0	1	1.5
16	5	5	0.1	1	1.95
17	5	5	0.2	1	2.35
18	5	5	0.3	1	2.8
19	5	5	0.4	1	3.2
20	5	5	0.5	1	3.65
21	5	5	0.6	1	4.15
22	5	5	0.7	1	4.5
23	5	5	0.8	1	4.9
24	5	5	0.9	1	5.3
25	5	5	1	1	5.73
26	5	5	1	1.1	4.5
27	5	5	1	1.2	3.2
28	5	5	1	1.3	2.3
29	5	5	1	1.4	1.6
30	5	5	1	1.5	1.2
31	5	5	1	1.6	0.95
32	5	5	1	1.7	0.85
33	5	5	1	1.8	0.8
34	5	5	1	1.9	0.8
35	5	5	1	2	0.79

3.5 Copper Nanoparticles dependence

The concentration of copper nanoparticles were varied from 1×10^{-6} – 1×10^{-5} mol L^{-1} at fixed concentration of all reactants [PDS] = 5×10^{-3} mol L^{-1}, [Ala] = 5×10^{-2} mol L^{-1}, [H^+] = 0.1 mol L^{-1}, I = 0.2 mol L^{-1} at three temperature (303 K, 308 K, 313 K). The rate of reaction increases with increasing concentration of copper nanoparticles (Table-1). In order to show the catalytic activity, a graph is plotted between the concentration of copper nanoparticles and rate constants at different temperature. The plot obtained is straight lines showing direct dependence of reaction rate on copper nanoparticles concentration (Figure 8). As these straight lines do not pass through origin, it is evident that the uncatalysed oxidation of alanine by peroxodisulphate is also possible.

The activation parameters were also calculated from the observed constants at three temperatures (Table-2).

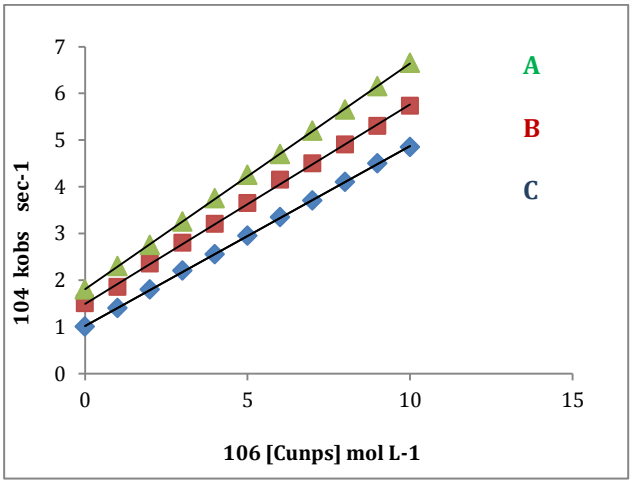

Figure 8 The effect of [Cunps] at different temperature (A) 303, (B)308, (C) 313 K at fixed [PDS] = 5.0×10^{-3} mol L^{-1}, [Ala] = 5.0×10^{-2} mol L^{-1}, [H^+] = 0.1 mol L^{-1}, I = 0.2 mol L^{-1}

Table-2 [PDS] = 5×10^{-3} mol L^{-1}, [Cunps] = 1×10^{-5} mol L^{-1}, [Ala] = 5×10^{-2} mol L^{-1}, [H^+] = 0.1 mol L^{-1}, I = 0.2 mol L^{-1}

Temperature (K)	10^4 K_{obs} (sec^{-1})	E_a (KJ/mol)	ΔS (J/K/mol)	ΔH (KJ/mol)	ΔG (KJ/mol)
303	4.85	23.846	-238.17	21.29	94.651
308	5.73				
313	6.65				

The high positive values of free energy of activation (ΔG) and enthalpy of activation (ΔH) indicated that the transition state was highly solvated while the negative values of entropy of activation (ΔS) suggested the formation of rigid transition state with reduction in the degree of freedom of molecules.

3.6 Hydrogen ion dependence

Hydrogen ion variation was made by varying the concentration of sulphuric acid from 0.1 to 0.2 mol L^{-1} at fixed concentration of [PDS] = 5×10^{-3} mol L^{-1}, [Ala] = 5×10^{-2} mol L^{-1}, [Cunps] = 1×10^{-5} mol L^{-1}, I = 0.2 mol L^{-1} and temperature 308 K. The rate of the reaction decreases with increasing concentration of H^+ and then tends towards a limiting value at higher concentration (Table-1). Since rate does not depend upon the concentration of alanine, hydrogen ion dependence cannot be related to the amino acid. However, decrease in rate with increasing H^+ concentration accounts for the higher reactivity of the molecular form of the acid.

3.7 Effect of ionic strength

The effect of ionic strength on the rate of reaction was studied by varying the concentration of potassium sulphate at constant concentration of reactants and conditions. The change in the k_{obs} with increase in the ionic strength is found to be very small. This indicates that unionized molecular forms are involved in the reaction.

3.8 Mechanism

The definite mechanism of the homogeneous metal nanoparticles catalysed oxidation is not clear. Although identify the formation of transition species through certain physical measurements but it is very difficult to isolate and characterize from homogeneous mixture. Since in the present study, the rate of reaction does not depend upon the concentration of alanine, oxidative deamination of alanine occurs in presence of peroxodisulphate only upon addition of copper nanoparticles while peroxodisulphate converted to hydrogen sulphate ion. The plausible mechanism in support of the observed kinetics is given in scheme-1.

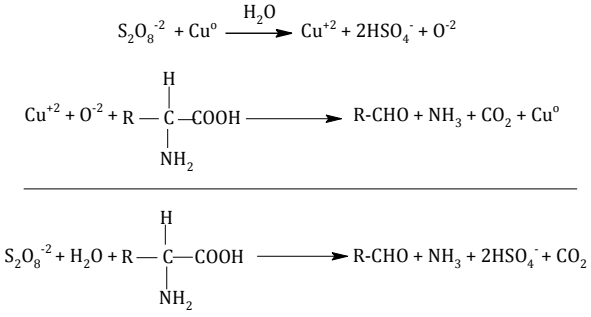

Scheme-I The plausible route of copper nanoparticles catalyzed oxidation of alanine

Conclusion

In the present work, highly stable dispersed copper nanoparticles were prepared by low cost, environment friendly and can be prepared in simple lab equipment in ambient condition. The synthesized nanoparticles are highly stable and do not show sedimentation even after storage for 2 months. The catalytic activity of copper nanoparticles was investigated through the oxidation of alanine in aqueous acid medium. The reaction is four times faster in the presence of very small copper nanoparticles concentration (10×10^{-6} mol L^{-1}). The results of the study indicate the reaction between alanine and peroxodisulphate in the presence of Cunps was first order. The study will be helpful in the biochemical and medical fields.

References

Berlett, B. S., Chock, P. B., Yim, M. B., Stadtman, E. R. (1990), Manganese(II) catalyzes the bicarbonate-dependent oxidation of amino acids by hydrogen peroxide and the amino acid-facilitated dismutation of hydrogen peroxide, *Proc. Natl. Acad. Sci.,* 87**,** 389-393.

Bilehal, D., Kulkarni, R., Nandibewoor, S. (2005), Comparative study of the chromium(III) catalysed oxidation of l-leucine and l-isoleucine by alkaline permanganate: A kinetic and mechanistic approach , *Journal of Molecular Catalysis A: Chemical,* 232, 21-28.

Bradley J. S., Scmided G. (1994), Clusters and Colloids: From Theory to Application VCH, New York *Cluster Colloids,* 459

Bruss A.S., Gelesky M.A., Machado G., Dupont. J. (2006), Rh(0) nanoparticles as catalyst precursors for the solventless hydroformylation of olefins*, J. Of Molecular Catalysis A: Chemical*, 252, 212-218.

Chandra, G. and Srivastava, S. N. (1971), Kinetics of Ag(I) ion catalyses oxidation of glycine by peroxy disulphate ion, *Bull. Chem. Soc.,* 44, 3000-3003.

Chandra, G. and Srivastava, S. N. (1973), Kinetics of Ag(I) catalysed peroxydisulphate oxidation of glycine, alanine and valine, *Ind. J. Chem.,* 11, 773-776.

Devra, V., Yadav, M. B. (2012), Kinetics and Mechanism of Osmium (VIII) Catalysed Oxidation of Valine by Hexacyanoferrate (III) in Alkaline Medium, *Rasayan J. Chem*., 5**,** 67-73.

Dang, T. M. D., Le, T. T. T., Fribourg-Blanc, E. and Dang, M. C. (2011), The Influence of Solvents and Surfactants on the Preparation of Copper Nanoparticles by a Chemical

reduction Method, *Adv. Nat. sci. Nanosci. Nanotechnol*., 2, 015009-015021.

Eastman, J. A., Choi, S. U. S., Li, S., Yu, W. and Thompson, L. (2001), Anomalously increased effective thermal conductivities of ethylene glycol based nano fluids containing copper nanoparticles, *J. Appl. Phy. Lett,* 78, 718-720.

Firooz A. A., Mahjoub A. R. and Khodadadi A. A. (2011), World Academy of Science,Engineering and Technology, 5, 118-120.

Hoover, N. N., Auten, B. J., Chandler, B. D. (2006), Tuning supported catalyst reactivity with dendrimer-templated Pt−Cu nanoparticles, *J. Phys. Chem. B*, 110**,** 8606-8612.

House, D. A. (1962), Kinetics and Mechanism of Oxidations by Peroxydisulfate, *Chem. Rev.,* 62, 185-203.

Huang, X., El-Sayed, I. H., Yi, X., El-Sayed, M. A. (2005), Gold nanoparticles: Catalyst for the oxidation of NADH to NAD^+, *J. Photochem. Photobiol. B*, 81, 76-83.

Jansat, S., Gomez, M., Philippot, K., Muller, G., Guiu, E., Claver, C., Castillon, S., Chaudret, B. (2004), A Case for Enantioselective Allylic Alkylation Catalyzed by Palladium Nanoparticles*, J. Am. Chem Soc.,* 126, 1592-1593.

Kapoor, S., Joshi, R., Mukherjee, T. (2002), Influence of I-anions on the formation and stabilization of copper nanoparticles, *Chemical Physics Letters***,** 354, 443-452.

Kerber, R. C. (2008), As simple as possible, but not simpler-the case of dehydroascorbic, *J. Chem. Educ.,* 85**,** 1237-1242.

Khalid, M. A. A. (2008), Oxidative Kinetics of Amino Acids by Peroxydisulphate: Effect of Dielectric Constant, *The Arabian Journal for Science and Engineering,* 33, 199-210.

Khalid, M. A., Kheir, A. M. (2008), Kinetics and Mechanisms of Amino Acids-Peroxodisulphate Reaction, Part I, *Sudan Journal of Basic Sciences*, 15, 69-83.

Liu, Q. M., Zhou, De-bi., Nishio, K., Ichino, R., Okido, M. (2010), Effect of Reaction Driving Force on Copper Nanoparticle Preparation by Aqueous Solution Reduction Method, *Materials Transactions*, 51**,** 1386-1389.

Niu, Y., Crooks, R. M. (2003), Preparation of dendrimer-encapsulated metal nanoparticles using organic solvents, *Chem. Mater.,* 15, 3463-3467.

Sanathanlakshmi, J., Vankatesan, P. (2012), Kinetic of oxidation of L-leucine by mono- and bimetallic gold and silver nanoparticles in hydrogen peroxide solution, *Chinese Journal of Catalysis*, 33, 1306-1311.

Seregar, V., Veeresh, T. M., Nandibewoor, S. T. (2007), Ruthenium (III) catalysed oxidation of L-leucine by a new oxidant, diperiodatoargentate(III) in aqueous alkaline medium, *Polyhedron*, 26**,** 1731-1739.

Singh, B. K., Singh, R. P. (1992), Mechanism of Rh(III) Catalysis in Oxidation of Glutamic Acid by Alkaline Solution of Hexacyanoferrate(III), *Asian J. of Chem.,* 4, 508-510.

Thomas, J. M., Johnson, B. F. G., Raja, R., Sankar, G., Midgley, P. A. (2003), High-Performance Nanocatalysts for Single-Step Hydrogenations, *Acc. Chem. Res*., 36, 20-30.

Wilmarth, W. K. & Haim, A. (1961), Mechanism of Oxidation by Peroxodisulphate ion, edited by J. O. Edwards (Interscience, London), 175.

Wu, C. W., Mosher, B. P., Zeng, T. F., Yin, Z. L. (2006), one step green route to narrowly dispersed copper nanocrystals, *J. Nanopart. Res.,* 8, 965-969.

Xiong, J., Wang, Y., Xue, Q. and Wu, X. (2011), Synthesis of highly stable dispersion of nanosized copper particles using L-ascorbic, *Green Chemistry***,** 13, 900 - 904.

Zhang, H. X., Siegert, U., Liu, R. and Cai, W. B. (2009), Facile fabrication of ultrafine copper nanoparticles in organic solvent, *Nanoscale Research Letter***,** 4, 705-708.

Zelechonok, Y. and Silverman, R. B. (1992), Silver(I)/Peroxydisulfate-Induced oxidative decarboxylation of aminoacids: A chemical model for a possible intermediate in the monoamine oxidize-catalysed oxidation of amine, *J. Org. Chem.,* 57, 5787-5790.

International Journal of Advanced Research in Engineering and Applied Sciences

ISSN: 2278-6252
Impact Factor: 4.817

A KINETIC STUDY ON COPPER NANOCATALYSIS IN THE OXIDATION OF SERINE BY PEROXOMONOSULPHATE

Shikha Jain*

Ankita Jain*

Vijay Devra*

Abstract: *Highly stable dispersion of nanosized copper nanoparticles (Cunps) was prepared successfully by chemical reduction method. The synthesized copper nanoparticles were characterized by UV-Visible spectrophotometer, Scanning Electron Microscopy (SEM), Transmission Electron Microscopy (TEM) analysis. The catalysis by colloidal copper nanoparticles was studied kinetically in the oxidation of L-serine by peroxomonosulphate (PMS) in acidic aqueous medium. The copper nanoparticles catalyst exhibited very good catalytic activity and the kinetics of the reaction was found to be first order with respect to serine and peroxomonosulphate. The effects of catalyst concentration, ionic strength and temperature on the reaction were also investigated.*

Keywords: *Copper nanoparticle, L-serine, Peroxomonosulphate, Perchloric acid, Oxidation, Kinetics.*

* Department Of Chemistry, J.D.B. Govt. P.G. Girls College, Kota, Rajasthan

1. INTRODUCTION

Amino acids act not only as the building blocks in the protein synthesis but they also play a significant role in metabolism. The specific metabolic role of amino acid includes the biosynthesis of polypeptides, proteins and synthesis of nucleotides [1]. Several kinetic studies on the oxidation of amino acids both in acid and alkaline medium and also in presence of metal and non-metal ions catalysts have been reported [2-5]. The study of amino acids becomes important of their biological significance and selectivity towards the oxidant to yield different product [6, 7]. Aqueous solutions of amino acids have been oxidized by Mn(II) [8], ($[Fe(CN)_6]^{3-}$) [9], Chloramines T [10], Peroxomonosulphate [11] etc. in both acid and alkaline media. Very few reports are available on the kinetics of oxidation of serine by peroxomonosulphate [12]. Peroxomonosulphate is a derivative of hydrogen peroxide, replacing one of the hydrogen atoms in H_2O_2 by sulphate group. Peroxomonosulphate is one of the strong oxidizing agents compared to other peroxo oxidants [13, 14]. The predominant reactive species of peroxomonosulphate in acidic medium is HSO_5^-. The HSO_5^- frequently act as a two electron oxidant in redox reactions that involve heterolytic cleavage of peroxo bond [15, 16], oxidative decarboxylation of amino acids is a known and documented in biochemical reaction. Kinetics and mechanism of decarboxylation of amino acids by peroxo oxidants is an area of intensive research because peroxo oxidants are environmentally benign oxidants and do not produce toxic compounds during their reduction.

Some selective oxidation reactions are reported involving transition metal ions of Ag, Rh, Cr, Ru, Mn etc. are reported to act as catalyst for amino acids oxidations [17-21], with the emergence of metal nanoparticles possessing appreciable stability and high surface area per particle, their potential use as catalyst for organic biochemical relevant reactions [22, 23]. Amongst them copper nanoparticles are paid more attention due to their low cost and easy availability. Copper nanoparticles have also been considered [24, 25] as an alternative for noble metals in many applications such as heat transfer and microelectronics [26]. In the present work, copper nanoparticles were prepared by chemical reduction method, in which L-ascorbic acid is used as reducing and capping agent in aqueous medium. The prepared copper nanoparticles are highly stable and do not show sedimentation even after storage for two months. Therefore, it is of great interest to study metal nanoparticle catalyzed

oxidation of serine using peroxomonosulphate. In this study, we demonstrate the efficiency of synthesized nanoparticles catalyst on the oxidation of serine under a range of different experimental conditions.

2. EXPERIMENTAL

2.1 Material

Peroxomonosulphate (PMS) was obtained from Sigma-Aldrich under the trend name "Oxone". The purity of the triple salt $2KHSO_5 \cdot KHSO_4 \cdot K_2SO_4$ was estimated by iodometry and found to be 98%. However, the presence of H_2O_2 in the oxone sample was tested and it shows negative results, thus eliminating the chances of hydrolysis of oxone. A fresh solution of oxone was prepared before starting the experiments. Copper Chloride dihydrate ($CuCl_2.2H_2O$-97%), L-ascorbic acid (vitamin C-98%), L-Serine and Perchloric acid were obtained from E. Merck. All other chemicals used in this study were of Analar grade and used as such without any further treatment. Double distilled water was employed throughout the study.

2.2 Synthesis of Copper Nanoparticles

In a synthetic procedure, copper nanoparticles were obtained via a wet chemical reduction route. $CuCl_2.2H_2O$ aqueous solution was prepared by dissolving $CuCl_2.2H_2O$ (0.02 mol L^{-1}) in 50 ml deionized water. The flask containing aqueous solution of $CuCl_2.2H_2O$ was heated to 353 K in oil bath with magnetic stirring. 50 ml of L-ascorbic acid aqueous solution (0.1 mol L^{-1}) was added drop wise into the flask while stirring. With the passage of time, the color of dispersion gradually changed from white, yellow, orange, brown finally dark brown with a number of intermediate stages. The appearance of yellow color followed by orange color indicated the formation of fine nanoscale copper particles from L-ascorbic acid assisted reduction. The resulting dispersion was centrifuged for 15 minutes. The supernatant was placed under ambient conditions for 2 months. Various optimization studies were performed to investigate the size and shapes of copper nanoparticles.

2.3 Characterization

UV-Visible spectroscopy from a double beam spectrophotometer (U.V. 3000^+ LABINDIA) was used for preliminary estimation of copper nanoparticles synthesis. FTIR (ALPHA-T –Bruker) provided information about oxidation product of the reaction. Morphological study of the copper nanoparticles was carried out with scanning electron microscope (SEM) (EVO 18

carlzeiss) and Transmission electron microscope (TEM) (FEI Techni G2S2 Twin). TEM and SEM images were recorded to confirm size distribution and shape homogeneity of synthesized copper nanoparticles.

2.4 Kinetic Measurements

The reaction were carried out with desired concentration of reactants in a 250 ml blackened iodine flask and kept in a thermostat at 308 K. A known volume of peroxomonosulphate solution, thermostatted at the same temperature separately, was pipetted out into the reaction mixture, and simultaneously a timer was started. Consumption of peroxomonosulphate was monitored by iodometric method [27]. The rate of the reaction was studied under pseudo first order condition i.e., [amino acid] » [PMS]. The rate of the reaction followed first order kinetics and the rate constant k_{obs} was calculated from the linear plots of log [PMS] versus time.

3. RESULTS AND DISCUSSION

3.1 Metal Nanoparticles Characterization Results

The UV-Visible absorbance spectrum of synthesis of copper nanoparticles was recorded at different interval of time at every color change as shown in Figure 1. The spectacular color change correlates with large shift of UV-Visible spectra. The first absorption peak of different curves is at 335 nm corresponding to oxidation product of L-ascorbic acid [28]. The second absorption peak is increasingly broadening with an increasing concentration of L-ascorbic acid. The absorption peak of copper nanoparticles has been reported at around 560 nm of UV-Visible wavelength which proves the formation of copper nanoparticles [29, 30].

The effect of initial concentration of precursor salt on synthesis of copper nanoparticles was studied at four different concentrations $CuCl_2.2H_20$ viz. 0.01, 0.015, 0.02, 0.03 mol L^{-1}. There are two stages in the synthesis of copper nanoparticles, the first stage is to generate copper nuclei and second stage is the growth of copper [31]. So it is important to control preparation process that copper nuclei must generate faster and grow up slower which requires better control of the initial concentration of Cu^{+2}. It can be seen that reaction rate increases with increases the concentration of Cu^{+2}. With the increasing reaction rate, the amount of copper nuclei rises and smaller particle size are obtained correspondingly which is shown in SEM images A, B, C of Figure 2 further increases the concentration of Cu^{+2}, the result is the agglomeration of the nuclei and growing the particle size as shown in SEM

ISSN: 2278-6252
Impact Factor: 4.817

image D of Figure 2. This may be due to collision between small particles, which leads to particle growth [32]. So the optimal concentration of precursor salt is 0.02 mol L^{-1} and 0.1 mol L^{-1} of L-ascorbic acid at 353 K. In this experimental condition, the TEM image of the synthesized copper nanoparticles is shown in Figure 3. It can be seen that the nanoparticles are spherical in shape and monodispersed with size 12 nm ± 0.5 nm.

The stability of nanoparticles dispersion is key factor in their application. In this study L-ascorbic acid was used as both reducing and capping agent without any other special capping agent. The antioxidant properties of L-ascorbic acid come from its ability to scavenge free radicals and reactive oxygen molecules [33], accompanying the donation of electrons to give semi-dehydroascorbate radical and dehydroascorbic acid. (Equation-1)

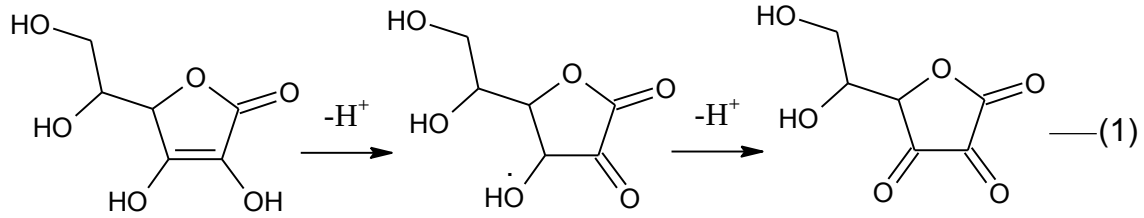

L-Ascorbic acid Semi-dehydroascorbate radical dehydroascorbic acid

The dehydroascorbic acid has three carbonyl groups in its structure. The 1, 2, 3 tricarbonyl is too electrophilic and finally converted into polyhydroxyl structure through hydrolysis [34]. (Equation-2)

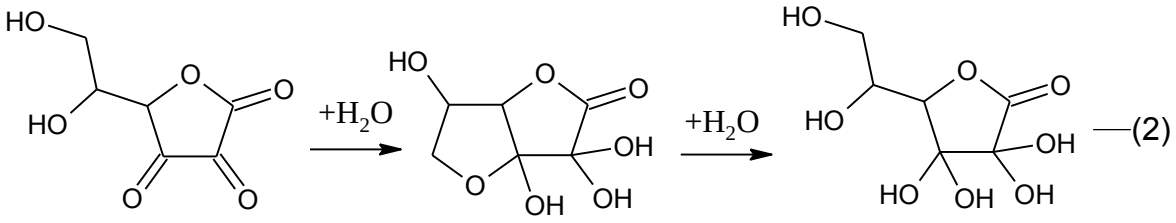

Hydrolysis of dehydroascorbic acid

Therefore L-ascorbic acid plays dual role as reducing agent and antioxidant of copper nanoparticles. Thus reaction can complete without any protective gas.

3.2 Stoichiometry

The Stoichiometry of the reaction was determined for copper nanoparticles catalyzed reaction mixtures containing a large excess of [PMS] over [amino acid]. The reaction mixtures were kept at 308 K for 48 hours and the excess of PMS was estimated iodometrically. The Stoichiometry of the oxidation of serine by an oxygen transfer from peroxomonosulphate in presence of copper nanoparticles was presented by equation (3).

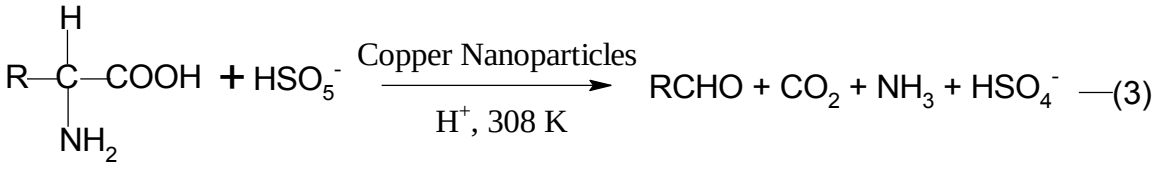

Where R represents -CH_2OH

The product aldehyde was identified by qualitative test and further 2, 4- dinitrophenyl hydrazone derivative was also obtained which is confirmed by FTIR spectrum in Figure 4. The IR peaks at 3367.24 cm^{-1}, 2936 cm^{-1} and 1618 cm^{-1} are attributed to –NH, –CH, –C=N stretching respectively. The deamination of the L-serine in presence of copper nanoparticles was shown in UV- Visible absorption spectrum which is presented in Figure 5.

3.3 Effect of Peroxomonosulphate Concentration

The copper nanoparticles catalyzed oxidation of serine was studied at different concentration of peroxomonosulphate varying from 1×10^{-3} - 7×10^{-3} mol L^{-1} at 308 K temperature, at fixed concentration of [Serine] = 5×10^{-2} mol L^{-1}, [H^+] = 0.01 mol L^{-1}, I = 0.02 mol L^{-1}, [Cunps] = 5×10^{-6} mol L^{-1}. The plot of log [PMS] versus time was linear which was shown in Figure 6, indicating that the reaction is first order with respect to [PMS]. The observed pseudo first order rate constant (k_{obs}) were independent of the concentration of peroxomonosulphate which is given in Table-1.

3.4 Effect of Serine Concentration

The effect of Serine concentration was studied by varying its concentration in the range of 2×10^{-2} – 7×10^{-2} mol L^{-1} at 308 K temperature, keeping all other reactant concentration and conditions constant. The rate of reaction increases with increasing concentration of serine is given in Table -1. Plot the graph between k_{obs} versus concentration of serine, straight line obtained with zero intercept confirm the first order with respect to serine as shown in Figure 7.

3.5 Effect of Copper Nanoparticles Concentration

The effect of copper nanoparticles on the oxidation of serine has been studied by varying its concentration from 1×10^{-6} – 1×10^{-5} mol L^{-1}. The result show the reaction rate increases as copper nanoparticles concentration increases as given in Table-1.

3.6 Effect of $[H^+]$ and Ionic Strength

The rate of reaction was decreases with increasing concentration of $[H^+]$ ion by the variation of concentration of $HClO_4$ at constant other reactants concentration and conditions as given in Table1. The rate of reaction was unaffected by the variation of ionic strength. The ionic strength adjusted by different concentration of $NaClO_4$, which indicates that in our experimental conditions, HSO_5^- and serine (Neutral) to be reactive form of peroxomonosulphate and serine respectively.

3.7 Effect of Temperature

The effect of temperature on the rate of reaction was studied at three temperature 303 K, 308 K, 313 K respectively at constant concentration of other reaction ingredients. A plot of log k_{obs} was made against 1/T, yielded a straight line which is shown in Figure 8. The energy of activation (E_a) was calculated from the slope of the line to be 21.02 $KJmol^{-1}$. The entropy of activation was calculated by employing the relationship [35],

$$k=\frac{k_B T}{h}\times e^{-\Delta H^{\neq}/RT}.e^{\Delta S^{\neq}/R}$$

Where $\Delta S^{\neq}$ is entropy of activation and other terms have their usual significance. Thus entropy of activation was calculated to be -240.67 JK^{-1} mol^{-1}.

3.8 Mechanism

Serine is neutral amino acid, the probability of initial interaction in between serine and peroxomonosulphate is weak. The deamination of the amino group in serine to NH_3 occurs in the presence of copper nanoparticles by peroxomonosulphate, while peroxomonosulphate is change into hydrogen sulphate ion. Although the definite mechanism of homogenous metal nanoparticles catalyzed oxidation of serine is not clear, based on previous report[12] and present observation the catalytic cycle shown in scheme-1.

ISSN: 2278-6252
Impact Factor: 4.817

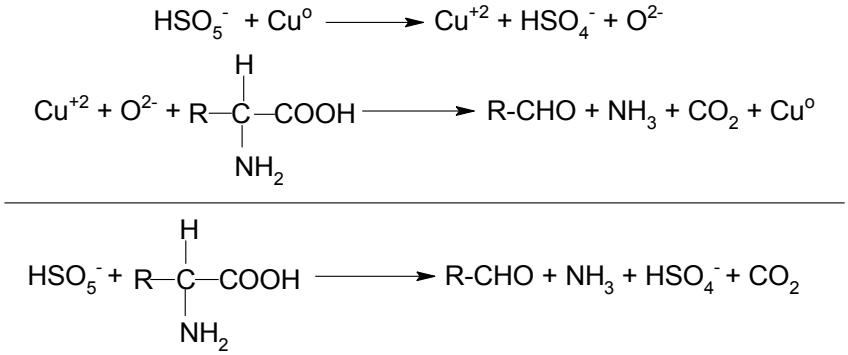

Scheme-I The plausible route of copper nanoparticles catalyzed oxidation of serine

4. CONCLUSION

The copper nanoparticles were prepared by low cost, environment friendly and can be prepared in simple lab, equipment in ambient condition. The synthesized nanoparticles are highly stable and do not show sedimentation even after storage for 2 months. The catalytic activity of copper nanoparticles was investigated through the oxidation of serine in aqueous acid medium. The reaction is 10 times faster in the presence of copper nanoparticles. The oxidation study revealed that the reaction was pseudo first order with respect to serine and peroxomonosulphate. The study will be helpful in the biochemical and medical fields.

FIGURES

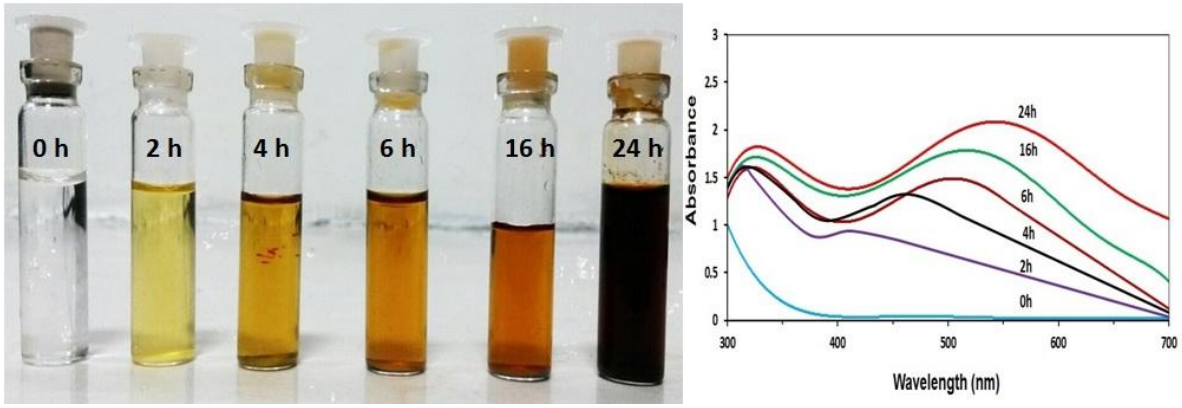

Figure 1. The time evolution of the dispersion photographs and the UV-Visible spectra

ISSN: 2278-6252
Impact Factor: 4.817

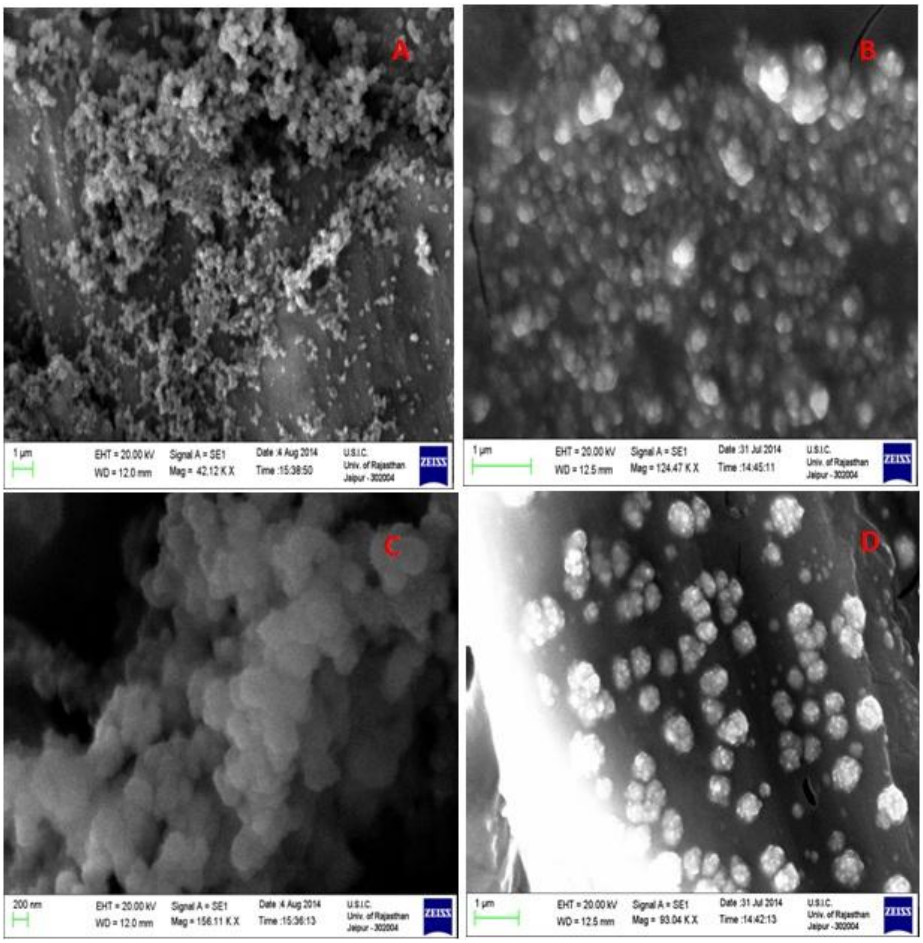

Figure 2. SEM images of the synthesized copper nanoparticles with various concentration of the precursor salt ($CuCl_2.2H_20$) (A) 0.01 mol L^{-1}, (B) 0.015 mol L^{-1}, (C) 0.02 mol L^{-1}, (D) 0.03 mol L^{-1}

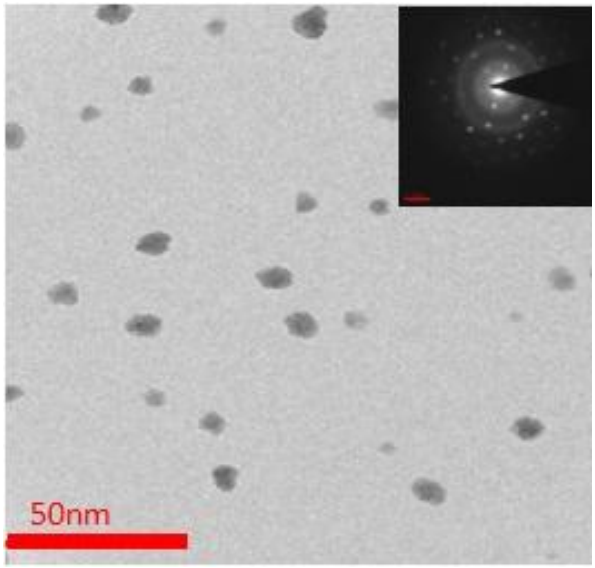

Figure 3. TEM image of synthesized copper nanoparticles At the optimal experimental conditions

ISSN: 2278-6252
Impact Factor: 4.817

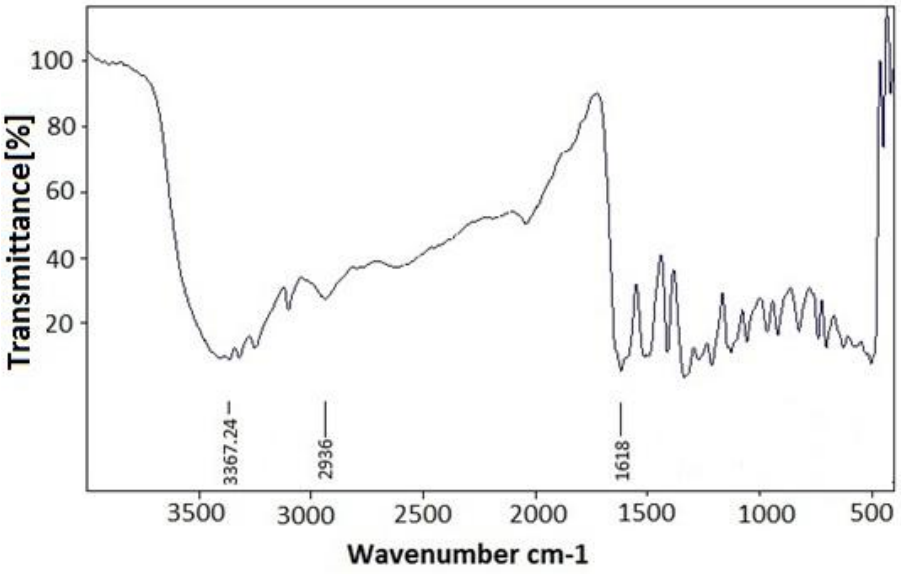

Figure 4. The FTIR Spectra of the oxidation product of serine oxidation

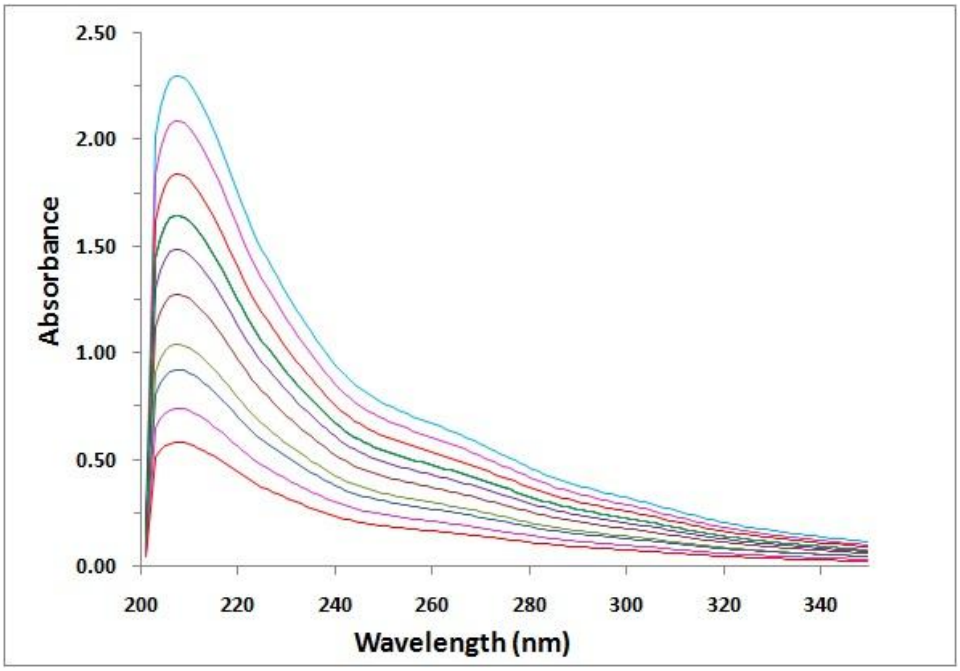

Figure 5. UV absorption spectra for the deamination of L-serine in the presence of the copper nanoparticles

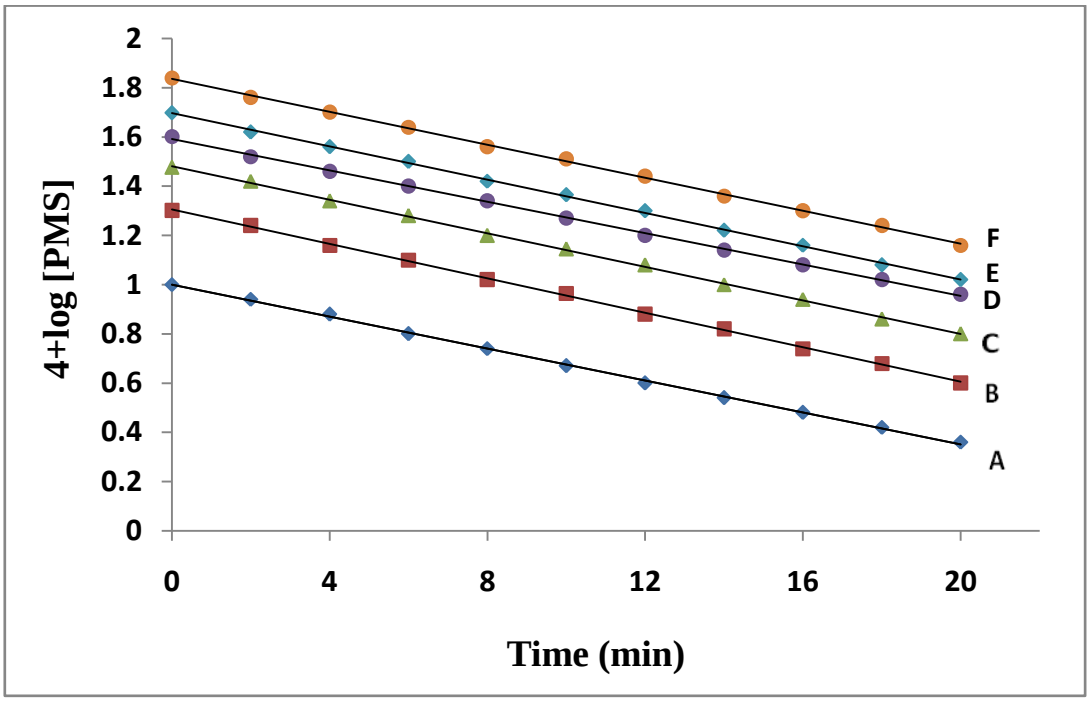

Figure 6. First order plots of the variation of Peroxomonosulphate concentration at 308 K [Serine]= 5.0×10^{-2} mol L^{-1}, [Cunps] = 5.0×10^{-6} mol L^{-1}, $[H^+]$ = 0.01 mol L^{-1}, I = 0.02 mol L^{-1}. [PMS]$\times10^{-3}$ mol L^{-1} = (A) 1.0, (B) 2.0, (C) 3.0, (D) 4.0, (E) 5.0, (F) 7.0

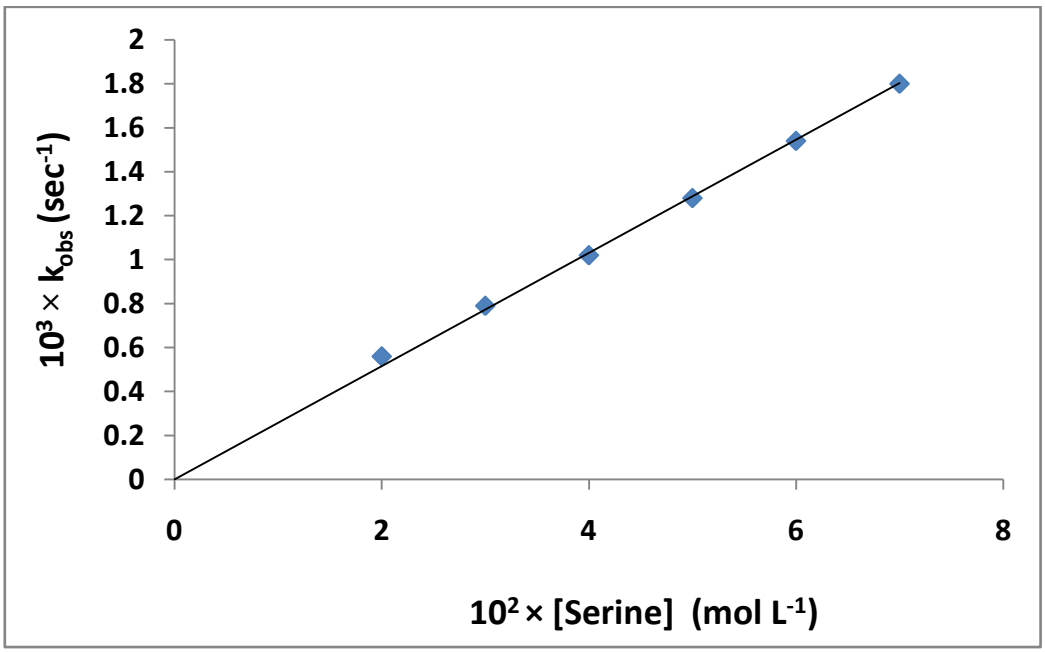

Figure 7. The variation of Serine concentration [PMS] = 5.0×10^{-3} mol L^{-1}, [Cunps] = 5.0×10^{-6} mol L^{-1}, $[H^+]$ = 0.01 mol L^{-1} and I = 0.02 mol L^{-1} at temperature 308K

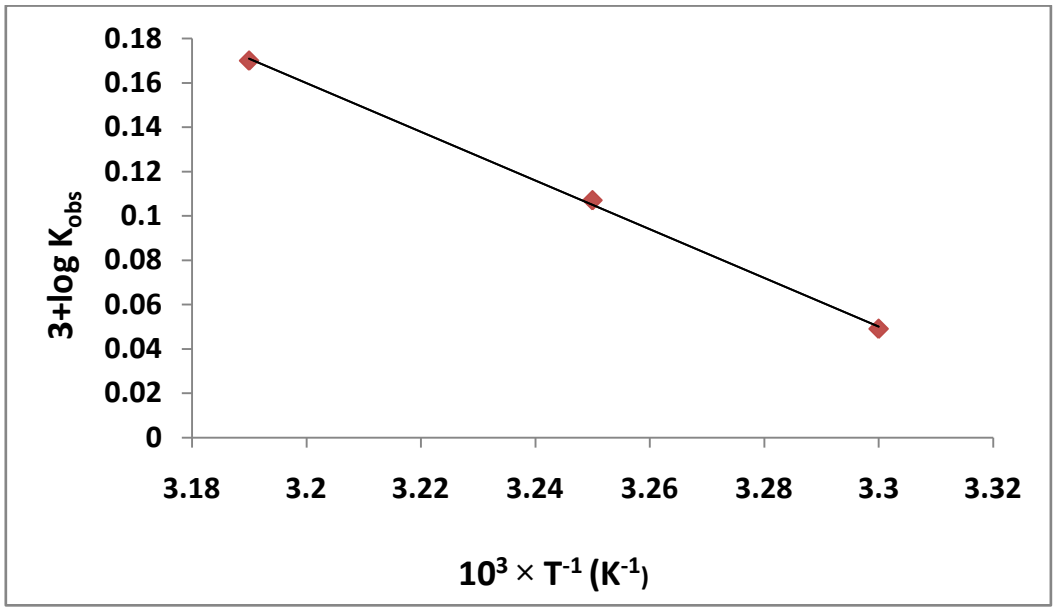

Figure 8. Plot of Temperature dependence

[PMS] = 5.0×10^{-3} mol L^{-1}, [Serine] = 5.0×10^{-2} mol L^{-1}, [Cunps] = 5.0×10^{-6} mol L^{-1}, $[H^+]$ = 0.01 mol L^{-1} and I = 0.02 mol L^{-1}

TABLE

Table 1: Effects of variation of [PMS], [Serine], [Cunps], $[H^+]$ on the oxidation of Serine by Peroxomonosulphate at fixed Ionic Strength (I) = 0.02 and Temperature 308 K.

S. No.	10^3 [PMS] (mol L^{-1})	10^2 [Serine] (mol L^{-1})	10^6 [Cunps] (mol L^{-1})	10^2 $[H^+]$ (mol L^{-1})	10^3 k_{obs} (s^{-1})
1.	1.0	5.0	5.0	1.0	1.26
2.	2.0	5.0	5.0	1.0	1.28
3.	3.0	5.0	5.0	1.0	1.27
4.	4.0	5.0	5.0	1.0	1.27
5.	5.0	5.0	5.0	1.0	1.28
6.	7.0	5.0	5.0	1.0	1.26
7.	5.0	2.0	5.0	1.0	0.56
8.	5.0	3.0	5.0	1.0	0.79
9.	5.0	4.0	5.0	1.0	1.02
10.	5.0	5.0	5.0	1.0	1.28
11.	5.0	6.0	5.0	1.0	1.54
12.	5.0	7.0	5.0	1.0	1.80
13.	5.0	5.0	1.0	1.0	0.40
14.	5.0	5.0	2.0	1.0	0.64
15.	5.0	5.0	3.0	1.0	0.84
16.	5.0	5.0	4.0	1.0	1.06
17.	5.0	5.0	5.0	1.0	1.28

18.	5.0	5.0	6.0	1.0	1.57
19.	5.0	5.0	7.5	1.0	1.83
20.	5.0	5.0	10.0	1.0	2.30
21.	5.0	5.0	5.0	1.0	1.52
22.	5.0	5.0	5.0	2.0	1.47
23.	5.0	5.0	5.0	4.0	1.38
24.	5.0	5.0	5.0	5.0	1.28
25.	5.0	5.0	5.0	7.0	1.22
26.	5.0	5.0	5.0	10.0	1.12

ACKNOWLEDGEMENT

This work was supported in part by University Grant Commission, New Delhi through Junior Research Fellowship and Department of Science and Technology sponsored FIST Laboratory of our institution for experimental work.

REFERENCES

1) Barrett, G. C., 1998, "Amino acids, peptides and proteins," Royal society of Chem., UK p. 29.
2) Hiraemath, R. C., Mayanna, S. M., Venkatasubramanian, N., 1987, "Chloride ion-catalysed oxidation of arginine, threonine, and glutamic acid by 1-chlorobenzotriazole: a kinetic and mechanistic study," J. Chem. Soc. Perkin Trans II, 2, pp.1569-1573.
3) Laloo, D., Mahanti, M. K., 1990, "Kinetics of oxidation of amino acids by alkaline hexacyanoferrate(III)," J. Chem. Soc. Dalton Trans, 1, pp. 311-313.
4) Gupta, D., Bhasin, M., Devra, V., Sharma, I., Sharma, P. D., 1996, "Kinetics and Mechanism of Electron Transfer Reactions in Aqueous Solutions: Silver (I) Catalyzed Oxidation of Glutamic Acid by Cerium (IV) in Acid Perchlorate Medium," Oxidation Communications, 19, pp. 242-250.
5) Yadav, M. B., Devra, V. and Rani, A. 2010, "Kinetics and mechanism of silver(I) catalyzed oxidation of valine by cerium(IV) in acid perchlorate medium," Indian journal of chemistry, 49A, pp. 442-447.
6) Chandraju, S., Rangappa, K. S., Made Gowda, N. M., 1999, "Manganese(III) oxidation of L-serine in aqueous sulfuric acid medium: Kinetics and mechanism," Int. J. Chem. Kinet., 31**,** pp. 525-530.

7) Mathur, S., Yadav, M. B., Devra, V., 2013, "Kinetics and Mechanism of Uncatalyzed and Ag (I) Catalyzed Oxidation of Hydroxylysine by Cerium (IV) in Acid Medium," J. Phys. Chem. Biophys., 3, pp.128-133.

8) Iloukhani, H., Bahrami, H., 1999, "Kinetic studies and mechanism on the permanganic oxidation of L-Glutamine in strong acid medium in the presence and absence of Silver (I)," Int. J. Chem. Kinet., 31, pp. 95-102.

9) Jose, T. P., Nandibewoor, S. T., Tuwar, S. M., 2006, "Kinetics and Mechanism of the Oxidation of Vanillin by Hexacyanoferrate(III) in Aqueous Alkaline Medium," J. Solution Chem., 35, pp. 51-62.

10) Grover, N., Kambo, N., Upadhyay, S. K., 2002, "Kinetics and mechanism of palladium(II) catalysed oxidation of some α-aminoacids by chloramine-T in perchloric acid," Indian J. Chem., 41A, pp. 2482-2488.

11) Rayappan, S. M., Easwaramurthy, D., Palanichamy, M., Murugesan, V., 2010, "Kinetics of Ag(I) catalyzed oxidation of amino acids by peroxomonosulphate," Inorgani. Chemistry Communications, 13, pp. 131-133.

12) Parimala, L., Santhanalakshmi, J., 2013, " Studies on the Oxidation of α-Amino acids by Peroxomonosulphate Catalysed by Biopolymers Stabilized Copper Nanoparticles – Effect of Stabilizers," Nanoscience and Nanotechnology: An International Journal, 3, pp. 4-11.

13) Sundar, M., Easwaramoorthy, D., Kutti Rani, S., Mohammed Bilal, I., 2008, "Mn(II) catalysed decomposition of peroxomonosulphate – Kinetic and mechanistic study," Catalysis Communication, 9, pp. 2340-2344.

14) Shailaja, S., Ramachandran, M. S., 2011, "Radical copolymerization of fullerene (C_{60}) and *n*-butyl methacrylate (BMA) using triphenylbismuthonium ylide and characterization of C_{60}–BMA copolymers," Inter. J. Chem. Kinet., 43, pp.620-630.

15) Gilbert, B. C., Stell, J. K., 1990, "Mechanisms of peroxide decomposition. An ESR study of the reactions of the peroxomonosulphate anion ($HOOSO_3^-$) with Ti^{III}, Fe^{II}, and α-oxygen-substituted radicals," J. Chem. Soc. Perkin Trans., 2, pp. 1281-1288.

16) Sayee Kannan, R., Easwaramoorthy, D., Vijaya, K., Ramachandran, M. S., 2008, "Autocatalytic oxidation of β-alanine by peroxomonosulfate in the presence of copper(II) ion," International Journal Chemical Kinetic, 40, pp. 44-49.

17) Devra, V., Yadav, M. B., 2012, "Kinetics and Mechanism of Osmium (VIII) Catalysed Oxidation of Valine by Hexacyanoferrate (III) in Alkaline Medium," Rasayan J. Chem., 5**,** pp. 67-73.

18) Singh, B. K., Singh, R. P., 1992, "Mechanism of Rh(III) Catalysis in Oxidation of Glutamic Acid by Alkaline Solution of Hexacyanoferrate(III)," Asian J. of Chem., 4 pp. 508-510.

19) Bilehal, D., Kulkarni, R., Nandibewoor, S., 2005, "Comparative study of the chromium(III) catalysed oxidation of L-leucine and L-isoleucine by alkaline permanganate: A kinetic and mechanistic approach ," Journal of Molecular Catalysis A: Chemical, 232, pp. 21-28.

20) Seregar, V., Veeresh, T. M., Nandibewoor, S. T., 2007, "Ruthenium(III) catalysed oxidation of L-leucine by a new oxidant, diperiodatoargentate(III) in aqueous alkaline medium," Polyhedron, 26**,** pp.1731-1739.

21) Berlett, B. S., Chock, P. B., Yim, M. B., Stadtman, E. R., 1990, "Manganese(II) catalyzes the bicarbonate-dependent oxidation of amino acids by hydrogen peroxide and the amino acid-facilitated dismutation of hydrogen peroxide," Proc. Natl. Acad. Sci., 87**,** pp. 389-393.

22) Sanathanlakshmi, J., Vankatesan, P., 2012, "Kinetic of oxidation of L-leucine by mono- and bimetallic gold and silver nanoparticles in hydrogen peroxide solution," Chinese Journal of Catalysis, 33, pp. 1306-1311.

23) Huang, X., El-Sayed, I. H., Yi, X., El-Sayed, M. A., 2005, "Gold nanoparticles: Catalyst for the oxidation of NADH to NAD^+," J. Photochem. Photobiol. B, 81, pp.76-83.

24) Hoover, N. N., Auten, B. J., Chandler, B. D., 2006, "Tuning supported catalyst reactivity with dendrimer-templated Pt–Cu nanoparticles," J. Phys. Chem. B, 110**,** pp. 8606-8612.

25) Niu, Y., Crooks, R. M., 2003, "Preparation of dendrimer-encapsulated metal nanoparticles using organic solvents," Chem. Mater., 15, pp. 3463-3467.

26) Eastman, J. A., Choi, S. U. S., Li, S., Yu, W. and Thompson, L., 2001, "Anomalously increased effective thermal conductivities of ethylene glycol based nano fluids containing copper nanoparticles," J. Appl. Phy. Lett*,* 78, pp. 718-720.

27) Mendham, J., Denney, R. C., Barnes, J. D., and Thomas, M. J. K., 2004, "Vogel's Textbook of Quantitative Chemical Analysis," 6th edition Pearson Education: Harlow, U.K p. 428.

28) Xiong, J., Wang, Y., Xue, Q. and Wu, X., 2011, "Synthesis of highly stable dispersion of nanosized copper particles using L-ascorbic," Green Chemistry**,** 13, pp. 900 - 904.

29) Kapoor, S., Joshi, R., Mukherjee, T., 2002, "Influence of I-anions on the formation and stabilization of copper nanoparticles," Chemical Physics Letters**,** 354, pp. 443-452.

30) Zhang, H. X., Siegert, U., Liu, R. and Cai, W. B., 2009, "Facile fabrication of ultrafine copper nanoparticles in organic solvent," Nanoscale Research Letter**,** 4, pp. 705-708.

31) Liu, Q. M., Zhou, De-bi., Nishio, K., Ichino, R., Okido, M., 2010, "Effect of Reaction Driving Force on Copper Nanoparticle Preparation by Aqueous Solution Reduction Method," Materials Transactions, 51**,** pp. 1386-1389.

32) Dang, T. M. D., Le, T. T. T., Fribourg-Blanc, E. and Dang, M. C., 2011, "The Influence of Solvents and Surfactants on the Preparation of Copper Nanoparticles by a Chemical reduction Method," Adv. Nat. sci. Nanosci. Nanotechnol., 2, pp. 015009-015021.

33) Wu, C. W., Mosher, B. P., Zeng, T. F., Yin, Z. L., 2006, "One step green route to narrowly dispersed copper nanocrystals," J. Nanopart. Res., 8, pp. 965-969.

34) Kerber, R. C., 2008, "As simple as possible, but not simpler- the case of dehydroascorbic," J. Chem. Educ., 85**,** pp. 1237-1242.

35) Laidler, K. J., 1983, "Reaction kinetics," pergamon press, oxford p. 86.

Experimental Investigation on The Synthesis of Copper Nanoparticles By Chemical Reduction Method

Shikha Jain*[1], Ankita Jain*[2], Vijay Devra*[3]

Abstract-Highly stable dispersion of nanosized copper particles was prepared by chemical reduction method. Chemical reduction of copper salts by L-ascorbic acid is a new and green approach in which L-ascorbic acid is used as reducing and capping agent in aqueous medium. This approach is the most effective and is also economical. The effects of reactant concentration and reaction temperature on morphology of dispersed copper nanoparticles were studied. The formation of copper nanoparticles in dispersion was monitored through the analysis of absorbance spectra by UV-Visible Spectrophotometer at different stages during the process of synthesis. The morphology of copper nanoparticles was characterized by Scanning Electron Microscopy (SEM) and Transmission Electron Microscopy (TEM). The product of adding L-ascorbic acid in copper salt was characterized by Fourier Transform Infrared (FTIR) Spectrophotometer. The study revealed that L-ascorbic acid plays an important role of protecting the copper nanoparticles to prevent oxidation and agglomeration and they have good stability for application.

Index Terms: Copper nanoparticles, Experimental Conditions, L-Ascorbic acid, Oxidation resistance, Chemical reduction.

1 INTRODUCTION

Nanotechnology is the most promising technology that can be applied almost all sphere of life, ranging from electronics, pharmaceuticals, defense, transportations heat transfer to sports and aesthetics. Metallic nanoparticles are of great interest due to their excellent physical and chemical properties such as high surface to volume ratio and high thermal conductivity. Amongst them copper nanoparticles are paid more attention due to their low cost and easy availability. Copper nanoparticles have also been considered [1], [2] as an alternative for noble metals in many applications such as heat transfer and micro electronics [3]. The micro fabrication of conductive features like inkjet technology is common. So for electronics devices have utilized noble metal like gold and silver for printing highly conductive element while cost of noble metals are very high, copper is low cost, conductive material, therefore it is economically attractive.

*Department of Chemistry
J.D.B. Govt. Girls P.G. College, University of Kota,
Kota -324001, India

- First author- shikhajain.rock@gmail .com
- Co-author-ankitajain.swm@gmail.com
- Corresponding author- v_devra1@rediffmail.com

Copper nanoparticles have been synthesized by different methods such as thermal reduction [4], thermal decomposition [5], [6], electrochemical reduction [7], mechano-chemical process [8], chemical reduction [7], [8], [9], [10], [11] have all been developed to prepare copper nanoparticles. Chemical reduction method is one of the most convenient methods for the synthesis of metallic nanoparticles because this synthesis process is simple, shape and size of nanoparticles can be controlled. The main question arises from the stability of copper nanoparticles including the extremely sensitive to oxygen and colloidal agglomeration. Therefore there are several approaches related to the dispersion and oxidation resistance that needs to be solved before application. Some study reveals that to protect copper nanoparticles against oxidation during preparation and storage, ascorbic acid is utilized as reductant and antioxidant of nanostructured Copper [12].

Despite that oxidation resistance and dispersion are of immense importance in several applications but few studies have been carried out in this area. So in the present study, the influence of L-ascorbic acid, different concentration of $CuCl_2.2H_2O$ and reaction temperature on the oxidation and dispersion of the aqueous copper nanoparticles were investigated. Copper nanoparticles were prepared with single reduction method without protective gas and synthesis was studied by UV-Visible Spectrophotometer, SEM and TEM and FTIR Spectrophotometer.

2 EXPERIMENTAL

2.1 Material

For the present work, we used analytical grade chemicals such as copper chloride dihydrate ($CuCl_2.2H_2O$-97%) and

L-ascorbic acid (vitamin C-98%) purchased from E. Merck. All chemicals were used as received without further purification. Double distilled water was employed throughout the study.

2.2 Synthesis of Copper Nanoparticles

In a synthetic procedure, copper nanoparticles were obtained via a wet chemical reduction route. $CuCl_2.2H_2O$ aqueous solution was prepared by dissolving $CuCl_2.2H_2O$ (0.02M) in 50 ml deionized water. The flask containing aqueous solution of $CuCl_2.2H_2O$ was heated to 80°c in oil bath with magnetic stirring. 50 ml of L-ascorbic acid aqueous solution (0.1M) was added drop wise into the flask while stirring. With the passage of time, the color of dispersion gradually changed from white, yellow, orange, brown finally dark brown with a number of intermediate stages. The appearance of yellow color followed by orange color indicated the formation of fine nanoscale copper particles from L-ascorbic acid assisted reduction. The resulting dispersion was centrifuged for 15 minutes. The supernatant was placed under ambient conditions for 2 months. Various optimization studies were performed to investigate the size and shapes of copper nanoparticles.

2.3 Characterization

UV-Visible spectroscopy from a double beam spectrophotometer (U.V. 3000+ LABINDIA, path length 1.0cm spectral range from 200 nm to 800 nm) was used for preliminary estimation of copper nanoparticles synthesis. FTIR (ALPHA-T –Bruker) provided information about the binding interactions of L-ascorbic acid with zero valent copper particles. Morphological study of the copper nanoparticles was carried out with scanning electron microscopy (SEM) (EVO 18 carlzeiss) image analysis, for which dispersed nanoparticles were centrifuged and ultrasonicated for 40 minutes. 30µl aliquots were then extracted and deposited on stub for SEM analysis. Transmission electron microscope (TEM) (FEI Techni G2S2 Twin) images were recorded to confirm size distribution and shape homogeneity of newly synthesized copper nanoparticles. Samples were prepared by taking small quantities of copper nanoparticles separated by centrifugation then ultrasonicated dispersed suspensions were mounted on carbon coated copper grids.

3 RESULTS AND DISCUSSION

3.1 Effect of L-ascorbic acid as reducing agent

UV-Visible absorbance spectroscopy has proved to be a very useful technique for studying metal nanoparticles because the peak position and shapes are sensitive to particle size. The syntheses of copper nanoparticles were recorded by UV-Visible spectra at every color change (Fig. 1.)

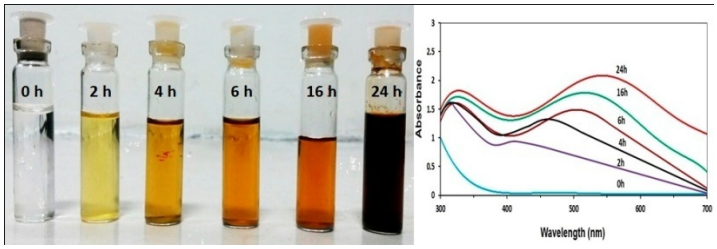

Fig.1. The time evolution of the dispersion photographs and the UV-Visible absorption spectra

The effect of L-ascorbic acid concentration (0.08M, 0.09M, and 0.1M) on the UV-Visible absorbance spectroscopy of the synthesized copper nanoparticles is shown in Fig. 2.

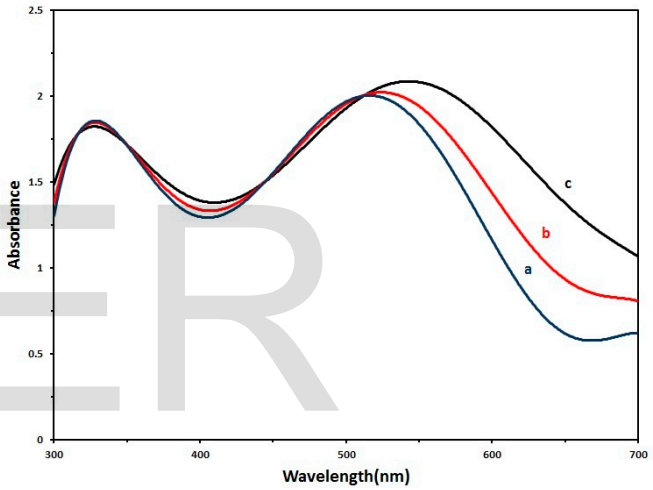

Fig.2. The UV-Visible absorption spectra of copper nanoparticles stabilized in L-ascorbic acid with various concentrations: (a) 0.08M, (b) 0.09M, (c) 0.10M

The first absorption peak of different curves is at 335 nm corresponding to oxidation product of L-ascorbic acid [13]. The second absorption peak is increasingly broadening with an increasing concentration of L-ascorbic acid. The absorption peak of copper nanoparticles has been reported at around 560 nm of UV-Visible wavelength which proves the formation of copper nanoparticles [14], [15]. In this work, the resulting copper nanoparticles did not show a peak at 560 nm but displayed a broadened peak at short wavelength, indicating the presence of small separated copper nanoparticles.

TEM images of the synthesized copper nanoparticles are shown in Fig. 3. at different concentration of L-ascorbic acid.

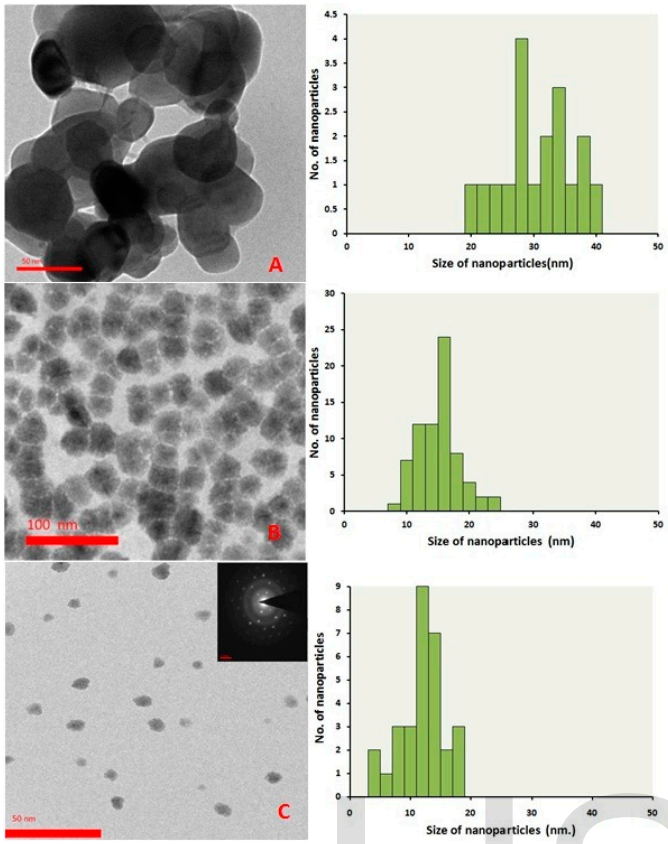

Fig.3. TEM images with histogram of copper nanoparticles with variable concentration of L-ascorbic acid ((A) 0.08M, (B) 0.09M, (C) 0.1M)

The histograms of copper nanoparticles size distribution are also presented in Fig. 3. The particles are spherical in shape. The histogram reveals a decrease in particle size with increase of L- ascorbic acid concentration. The size of the copper nanoparticles with various concentration of L-ascorbic acid are (0.08M, 0.09M, 0.10M) 28nm, 16nm, 12nm respectively. The reason is that the number of Cu^{+2} encapsulated in ascorbic acid molecules decreases with increasing concentration of L-ascorbic acid, leading to the formation of small copper nanoparticles.

3.2 The effect of initial concentration of precursor salt

There are two stages when copper nanoparticles generate in the solution. The first stage is to generate copper nuclei and second stage is the growth of copper [16]. So it is important to control preparation process that copper nuclei must generate faster and grow up slower which requires better control of the initial concentration of Cu^{+2}. In this experiment the concentration of precursor salt is varied from (0.01M to 0.03M). It can be seen that reaction rate increases with increases the concentration of Cu^{+2}. With the increasing reaction rate, the amount of copper nuclei rises and smaller particle size are obtained correspondingly. The SEM images of the synthesized copper nanoparticles are shown in Fig. 4. The SEM results indicate that an excess number of nuclei will be generated when the reactant concentration is too high. This result is the agglomeration of the nuclei and growing the particles size. This may be due to collision between small particles, which leads to particle growth [17]. So the optimal concentration of precursor salt is 0.02M.

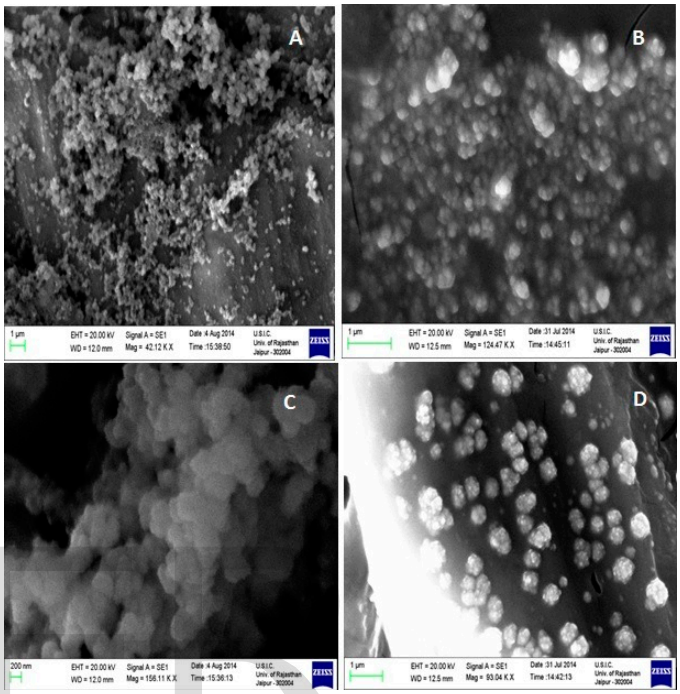

Fig. 4. SEM images of the synthesized copper nanoparticles with various concentration of the precursor salt ($CuCl_2.2H_20$) (A) 0.01M, (B) 0.015M, (C) 0.02M, (D) 0.03M

3.3 Effect of reaction temperature

The present investigation reveals that nanoparticles did not form below the temperature 60°c in any conditions. Therefore reaction temperature higher than 60°c with appropriate concentration of the reactants should be inserted to the synthesis of copper nanoparticles.

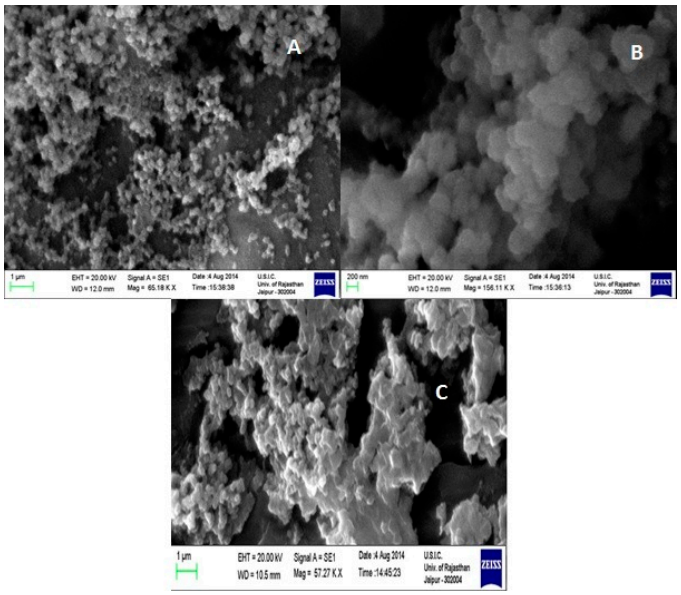

Fig.5. SEM images of synthesized copper nanoparticles with variation of temperature 70°c to 90°c (A) 70°c, (B) 80°c, (C) 90°c

In Fig. 5. SEM images of copper nanoparticles synthesized at 70°c, 80°c, 90°c respectively, shown that at higher temperature (90°c), the nanoparticles were agglomerated, while at 80°c are well dispersed with an average size at about 12 nm. Basically, the reduction of Cu^{+2} were increase by increasing the reaction temperature. Therefore the synthesis rate is too high to control particle size at high temperature. When reducing agent adds to precursor solution at 90°c, rate of growth and agglomeration as well as nucleation of copper nanoparticles accelerated almost coincidently. These phenomena result in the formation of copper nanoparticles were precipitated. Therefore moderate temperature (80°c) should be selected for synthesis of the copper nanoparticles with appropriate controlling on size.

3.4 The stability of copper nanoparticles

The stability of nanoparticles dispersion is key factor in their application. In this study L-ascorbic acid was used as both reducing and capping agent without any other special capping agent. The photographs of dispersion before and after the storage (2 months) are shown in Fig. 6.

(A) (B)

Fig.6. The photos of dispersion of copper nanoparticles (A) before and (B) after 2 months of storage

During the synthesis process, excessive L-ascorbic acid is essential to avoid the oxidation of copper nanoparticles. The antioxidant properties of L-ascorbic acid come from its ability to scavenge free radicals and reactive oxygen molecules [18], accompanying the donation of electrons to give semi-dehydroascorbate radical and dehydroascorbic acid .

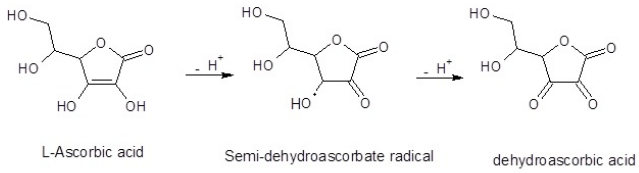

The dehydroascorbic acid has three carbonyl in its structure. The 1, 2, 3 tricarbonyl is too electrophilic to survive more than a few seconds in aqueous solution. Hydration of 2-carbonyl is also reported [19]. Finally the polyhydroxyl structure is obtained through hydrolysis [13].

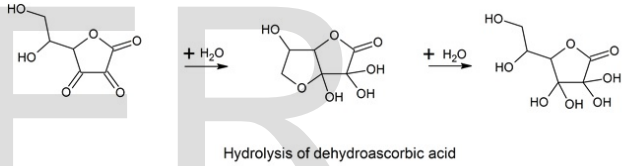

The excessive number of hydroxyl group can be facilitated the complexation of copper nanoparticles to the number of matrix by inter–intramolecular hydrogen bond and thus prevent the agglomeration of copper nanoparticles. The result is confirmed with FT-IR Spectrophotometer (Fig. 7.).

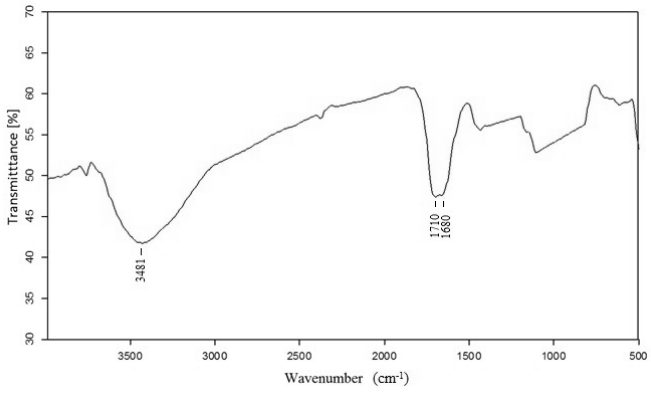

Fig.7. FTIR spectra of L-ascorbic acid stabilized copper nanoparticles

FTIR spectrum shows the peaks at 3481cm^{-1}, 1710cm^{-1} and 1680 cm^{-1}. These peaks corresponds to the hydroxyl, oxidated carbonyl group and conjugated carbonyl group

respectively. These results indicate the presence of polyhydroxyl structure on the surface of copper nanoparticles. Therefore L-ascorbic acid plays dual role as reducing agent and antioxidant of copper nanoparticles. Thus reaction can complete without any protective gas.

4 CONCLUSIONS

The study suggests that synthesis route is low cost, environmental friendly and can be prepared in simple laboratory equipment in ambient condition. By this method synthesized monodispersed copper nanoparticles (ranging from 12nm to 28nm) by employing different concentration of L-ascorbic acid as both reducing and capping agent. The prepared copper nanoparticles are highly stable and do not show sedimentation even after storage for 2 months. Moreover, it was clearly shown that the initial concentration of reactant and reaction temperature has a remarkable effect on particle size and agglomeration of the synthesized copper nanoparticles.

ACKNOWLEDGMENT

This work was supported in part by Department of Science and Technology sponsored FIST Laboratory of our institution for experimental work and University Grant Commission, New Delhi for financial support through Junior Research Fellowship.

REFERENCES

[1] N. N. Hoover, B. J. Auten and B. D. Chandler, Tuning Supported Catalyst Reactivity With Dendrimer Templated Pt-Cu Nanoparticles, J. Phys. Chem. B 110, 8606 (2006).

[2] Y. Niu and R. M. Crooks, Dendrimer-Encapsulated Metal Nanoparticles and Their Applications to Catalysis, Chem. Mater., 15, 3463 (2003).

[3] J. A. Eastman, S. U. S. Choi, S. Li, W. Yu and L. Thompson, Anomalously Increased Effective Thermal Conductivities of Ethylene Glycol Based Nano Fluids Containing Copper Nanoparticles, Appl. Phys. Lett., 78, 718 (2001).

[4] M. S. Niasari, Z. Fereshteh, and F. Davar, Synthesis of Oleylamine Capped Copper Nanocrystal via Thermal Reduction of a New Precursor, Polyhedron, 28, 126 (2009).

[5] M. S. Niasari and F. Davar, Synthesis of Copper and Copper (I) Oxide Nanoparticles by Thermal Decomposition of A New Precursor, Mater. Lett., 63, 441 (2009).

[6] Y. H. Kim, D. K. Lee, B. G. Jo, J. H. Jeong and Y. S. Kang, Synthesis of Oleate Capped Cu Nanoparticles by Thermal Decomposition, Physicochem. Eng. Asp., 284, 364 (2006).

[7] W. K. Han, J. W. Choi, G. H. Hwang, S. J. Hong, J. S. Lee and S. G. Kang, Fabrication of Cu Nanoparticles by Direct Electrochemical Reduction from CuO Nanoparticles, Appl. Surface Sci., 252, 2832 (2006).

[8] S. Sheibani, A. Ataie and S. Heshmati-Manesh, Role of Process Control Agent on Synthesis and Consolidation Behavior of Nano-crystalline Copper Produced by Mechano-Chemical Route, J. Alloys Compd., 465, 78 (2008).

[9] Q. Zhang, Z. Yang, B. Ding, X. Lan, Y. Guo, Preparation of Copper Nanoparticles by Chemical Reduction Method Using Potassium Borohydride, Transactions of Nonferrous Metals Society of China, 20, 240 (2010).

[10] P. Pulkkinen, J. Shan, K. Leppanen, A. Kansakoshi, A. Laiho, M. Jarn and H. Tenhu, Poly(Ethyleneimine) and Tetraethylenepentamines as Protecting Agent For Metallic Copper Nanoparticles, Appl. Mater. Interfaces, 2, 519 (2009).

[11] X. Cheng, X. Zhang, H. Yin, A. Wang and Y. Xu, Modifier effects on Chemical Reduction Synthesis of nanostructured Copper, Appl. Surface Sci., 253, 2727 (2006).

[12] W. Yu, H. Xie, L. Chen, Y. Li and C. Zhang, Synthesis and Characterization of Monodispersed Copper Colloids in Polar Solvents, Nanoscale Res. Lett., 4, 465(2009).

[13] Xiong, Ye Wang, Qunji Xue and Xuedong Wu, Synthesis of Highly Stable Dispersion of Nanosized Copper Particles Using L-Ascorbic Acid, Green Chemistry, 13, 900-904 Jing (2011).

[14] S. Kapoor, R. Joshi and T. Mukherjee, Influence of I-Anions on the Formation and Stabilization of Copper Nanoparticles, Chemical Physics Letters, 354, 443-448 (2002).

[15] H. X. Zhang, U. Siegert, R. Liu and W. B. Cai, Facile Fabrication of Ultrafine Copper Nanoparticles in Organic Solvent, Nanoscale Research Letter, 4, 705-708 (2009).

[16] Qing- Ming Liu, De-bi Zhou, K. Nishio, R. Ichino, M. Okido, Effect of Reaction Driving Force on Copper Nanoparticle Preparation by Aqueous Solution Reduction Method, Materials Transactions, 51, 1386 (2010).

[17] T. M. D. Dang, T. T. T. Le, E. Fribourg-Blanc and M. C. Dang, The Influence of Solvents and Surfactants on the Preparation of Copper Nanoparticles by a Chemical reduction Method, Adv. Nat. sci.: Nanosci. Nanotechnol. , 2, 015009 (2011).

[18] C.W. Wu, B. P. Mosher, T. F. Zeng, Z. L. Yin, One Step Green Route to Narrowly Dispersed Copper Nanocrystals, J. Nanopart Res. 8, 965 (2006).

[19] R. C. Kerber, As simple As Possible, But Not Simpler- The Case of Dehydroascorbic acid, J. Chem. Educ., 85, 1237-1242 (2008).